

Modulation of macrophage differentiation and activation by paracrine signals from cardiac progenitor cells

Sara Samari

C.I.D. 00873387

A thesis submitted to Imperial College London
for the degree of Doctor of Philosophy

National Heart and Lung Institute
Faculty of Medicine
Imperial College London

Declaration of Authenticity

I certify that this thesis, and the research to which it refers, are the product of my own work, conducted during the past five years of my PhD degree at Imperial College London. Any idea or quotations from the work of other people, published or otherwise, or from my own previous work are fully acknowledged in accordance with the standard referencing practices of the discipline. Some of the results contained here have been presented at conferences and seminars.

Copyright Declaration

“The copyright of this thesis rests with the author. Unless otherwise indicated, its contents are licensed under a Creative Commons Attribution-NonCommercial 4.0 International Licence (CC BY-NC).

Under this licence, you may copy and redistribute the material in any medium or format. You may also create and distribute modified versions of the work. This is on the condition that: you credit the author and do not use it, or any derivative works, for a commercial purpose.

When reusing or sharing this work, ensure you make the licence terms clear to others by naming the licence and linking to the licence text. Where a work has been adapted, you should indicate that the work has been changed and describe those changes. Please seek permission from the copyright holder for uses of this work that are not included in this licence or permitted under UK Copyright Law.”

Acknowledgements

I express my sincere gratitude to the British Heart Foundation (BHF) for awarding me the BHF 4-year PhD program. I want to also thank the BHF Centre for Research Excellence, the National Heart and Lung Institute (NHLI) and the Imperial College London for supporting my research project. I want to acknowledge my supervisors, Prof Michael D. Schneider, Prof Dorian Haskard and Dr Michela Nosedà, for their precious help, support and guidance during this exciting PhD degree. Besides, I would also like to thank the two examiners, Dr Jacques Behmoaras and Dr Gillian Gray.

I am grateful to have worked in an enriching and stimulating environment full of colleagues from different academic backgrounds and their contributions to this work. Thanks to the flow sorting technician, Patricia Chaves, for her help with the FACS data. Thanks to Dr Andrea Massaia, who developed the R script for single-cell analysis. Thanks to Dr Chrystalla Constantinou for her contribution to the development of the CSC-conditioned media. Thanks to Dr Antonio Miranda, who optimised the efferocytosis experiments. I would also like to thank all the members of Michael's and Dorian's groups for their help and support, especially Pelin, Mohamed, Cassie and Sam, who contributed to this project's success. I am indebted to them for their generous technical and academic support and their moral support, friendship, and words of wisdom.

A special thanks go to all my friends for five years of fun moments, especially Katie, Koval, Ari, Cinzia, Tom, Alex, Jini, the NHLI postgraduate committee, the BHF students, the 5th, the 4th and the 3rd floor of ICTEM building.

Finally, thanks to you, Nicole, for your love, encouragement and support (she even proofread this thesis). You never let me down; thanks, you are my family. Thank mom, brother, family, and Italian friends.

Thank you, Angelos. You make me smile every day.

Publications and Presentations

Publications

- M. Litviňuková, C. Talavera-López, H. Maatz, D. Reichart, C.L. Worth, E.L. Lindberg, M. Kanda, K. Polanski, M. Heinig, M. Lee, E.R. Nadelmann, K. Roberts, L. Tuck, E.S. Fasouli, D.M. DeLaughter, B. McDonough, H. Wakimoto, J.M. Gorham, **S. Samari**, K.T. Mahbubani, K. Saeb-Parsy, G. Patone, J.J. Boyle, H. Zhang, H. Zhang, A. Viveiros, G.Y. Oudit, O. Bayraktar, J.G. Seidman, C.E. Seidman, M. Nosedá, N. Hubner and S.A. Teichmann. **Cells and gene expression programs in the adult human heart.** *Nature*. 2020.
- S. Samari***, P. Chaves*, A. Massaia, A. Miranda, G. McLean, C. Constantinou, D. Haskard, M. Schneider and M. Nosedá. **Cardioprotective progenitor cells modulate differentiation and activation of macrophages at least in part via secretion of M-CSF.** *In preparation*.
- C. Constantinou, A.M.A. Miranda, P. Chaves, M. Bellahcene, A. Massaia, K. Cheng, **S. Samari**, S.M. Rothery, A. M. Chandler, R.P. Schwarz, S.E. Harding, P. Punjabi, M. Schneider and M. Nosedá. **Human pluripotent stem cell-derived cardiomyocytes as a target platform for paracrine protection.** *Sci. Rep.* 2020; 1-18.
- M. Nosedá*, **S. Samari***, P. Chaves, A. Massaia, D. Haskard and M. D. Schneider. **Modulation of macrophages differentiation and activation: paracrine signals from cardiac progenitor cells.** *Cardiovascular Drugs and Therapy*. 2019; 33:261-274. (Abstract)
- A. Massaia, P. Chaves, **S. Samari**, R.J. Miragaia, K. Meyer, S.A. Teichmann and M. Nosedá. **Sc gene expression to understand the dynamic architecture of the heart.** *Frontiers in Cardiovascular Biology*. 2018; 5, 167.
- M. Nosedá, C. Constantinou, **S. Samari**, P. Chaves, K. Cheng, C. Beretta, T. Rito, M. Abreu-Paiva, A. Pombo, and M.D. Schneider. **Paracrine impact of cardiac progenitor cells on macrophage phenotypes and human iP-s-derived cardiomyocytes survival.** *Circ. Res.* 2017; 121:A191 (Abstract).

Oral Presentations

- **BHF Centre of Regenerative Medicine – Work in Progress Meeting.** Imperial College London, May 2019
- **British Society For Cardiovasc. Res. (BSCR) - Autumn meeting 2018.**

University of Sheffield, September 2018

- **National Heart and Lung Institute (NHLI) - Postgraduate Day 2018.** Imperial College London, June 2018
- **5th British Heart Foundation (BHF) 4-Year Student Conference.** King's College London, April 2017

Poster Presentation

- **EMBO – The Molecular and Cellular Basis Of Regeneration And Tissue Repair.** Malta, September 2018
- **Joint BHF Regenerative Medicine Centres Symposium.** Queen's Medical Research Institute (QMRI), University of Edinburgh, June 2018
- **6th British Heart Foundation (BHF) 4-Year Student Conference.** University of Edinburgh, April 2018
- **National Heart and Lung Institute (NHLI) - Postgraduate Day 2017.** Imperial College London, June 2017
- **2017 Joint Symposium - The Heart: Models, Measurements, and Medicine.** Imperial College London, June 2017
- **BHF Centre of Research Excellence Annual Symposium - Cardiovascular target identification and drug discovery.** Imperial College London, July 2016
- **4th British Heart Foundation (BHF) 4-Year Student Conference.** University of Glasgow, April 2016
- **BHF Regenerative Medicine Centre Post-doc and PhD Students Annual Meeting.** Imperial College London, December 2015

Abstract

Myocardial infarction (MI) triggers an inflammatory response that contributes to cardiac remodelling in adult mice. In contrast, the heart of the post-MI neonatal mouse regenerates without scarring due to an anti-inflammatory macrophage-dependent process. Previously, Nosedá and colleagues demonstrated that intramyocardial injection of Lin⁻Sca1⁺CD31⁻PDGFR α ⁺SP⁺ cardiac progenitor/stem cells (CSCs) improved cardiac function. However, despite the lack of long-term engraftment, the cardiac improvement could be explained by paracrine factors released by CSCs. The paracrine effects of CSCs could affect several cell types in the heart, including macrophages. Therefore, this PhD thesis hypothesises that CSCs release paracrine factors that promote a subtype of anti-inflammatory macrophage phenotype to support cardiac regeneration.

After flow sorting, single F4/80⁺CD11b⁺ macrophages were analysed by single qRT-PCR. GM-CSF+LPS+IFN γ -driven M ϕ , identified as CX3CR1⁺CD11b⁺F4/80^{lo}CD206⁻, co-expressed pro-inflammatory genes, *Nos2*, *Cxcl9*, *Cxcl10* and *Il-6*. On the other hand, M-CSF+IL-4+IL-13-driven M ϕ , identified as CX3CR1⁺CD11b⁺F4/80⁺CD206⁺, upregulated anti-inflammatory genes, *Arg1*, *Angpt2*, and *Igf1*. Notably, CSCs conditioned media (CSC CondM)-driven macrophages were indistinguishable from M-CSF+IL-4+IL-13-M ϕ . Lastly, CSC CondM+IL4+IL13-driven M ϕ group was identified as CX3CR1⁺CD11b⁺F4/80⁺CD206⁺, expressing *Arg1*, *Angpt2*, *Igf1*, *Il1rl1*, and *Mrc1*, and showing a distinct subtype of anti-inflammatory macrophage phenotype compared to all prior reports of anti-inflammatory/M2-like macrophages.

After confirming that CSCs secrete M-CSF (20pg/mL) as the potential protective factor, the M-CSF/CSF1R pathway was inhibited by using first the pharmacological inhibitor BLZ945 and then a monoclonal antibody against CSF1R. These inhibitory experiments demonstrated that the inhibition of M-CSF activity reduced cell viability, the percentage of F4/80⁺CD11b⁺CX3CR1⁺CD206⁺ macrophages, expression of anti-inflammatory and pro-fibrotic genes (*Arg1*, *Angpt2*, *Igf1*, *Il1r1*, *Mrc1* and *Gdf15*), and phagocytosis activity. Multiplex bead-based flow immunoassays also showed that CSC CondM+LPS+IFN γ -M ϕ secrete IL-10 depending upon the M-CSF/CSF1R pathway.

In conclusion, CSC-secreted M-CSF is the indispensable paracrine factor that induces macrophages with an anti-inflammatory phenotype.

Table of contents

Declaration of Authenticity	2
Copyright Declaration.....	3
Acknowledgements	4
Abstract	8
Table of contents.....	10
List of Figures.....	14
List of Tables	15
List of abbreviations	16
Chapter 1 – Introduction	20
1.1 Cardiac repair: an urgent unmet clinical need	21
1.1.1 Cardiovascular diseases: the leading cause of mortality and healthcare cost worldwide	21
1.1.2 Cardiac remodelling following myocardial infarction and progression to heart failure	25
1.1.3 Heart transplant: the only available cure for advanced heart failure	29
1.2 The mammalian heart has a limited capacity for regeneration	30
1.2.1 Heart regeneration in zebrafish, amphibia and neonatal mice.....	30
1.2.2 Limitation in cardiac regeneration of adult mammals.....	35
1.3 Cardiac regeneration and repair: from cell therapy to “cell-free” therapy	39
1.3.1 Evolution of cardiac regenerative therapy over the past two decades	39
1.3.2 The first generation of cell therapy: non-cardiac cells in the adult mammalian heart.....	41
1.3.3 The second generation of cell therapy: cardiac stem/progenitor committed cells	42
1.3.3.1 Sca1 ⁺ CSCs.....	43
1.3.3.2 Subpopulations of Sca1 ⁺ CSCs.....	45
1.3.3.3 Human clinical trials using CSCs	50
1.3.4 The next-generation of cell therapy: the paracrine hypothesis	51
1.4 Mouse macrophages in the model of cardiac injury and regeneration	54
1.4.1 Mouse macrophages: from embryo to adulthood	54
1.4.2 Macrophages classification	59
1.4.2.1 Growth and survival factors.....	61
1.4.2.2 Activators and stimuli of M1-like and M2-like macrophages	64
1.4.2.3 Gene expression of <i>Nos2</i> and <i>Arg1</i>	65
1.4.2.4 M1-like macrophage secretome profile	67
1.4.2.5 M2-like macrophage secretome profile	73
1.4.2.6 Surface receptor expression pattern in M1-like and M2-like macrophages.....	78
1.4.3 Role of tissue-resident macrophages in the healthy heart.....	81
1.4.4 Role of macrophages in ischemic cardiac damage	82
1.4.5 Single-cell genomics to explore macrophage phenotypes.....	85
1.5 M-CSF promotes M2-like macrophages	90
1.5.1 Bulk RNAseq and single-cell qRT-PCR identified that Lin ⁻ Sca1 ⁺ CD31 ⁻ PDGFR α ⁺ SP ⁺ CSCs secreted M-CSF.....	90
1.5.2 M-CSF promotes anti-inflammatory-like macrophages via CSF1R	92
1.5.3 Preclinical and early clinical use of M-CSF	95
1.5.4 Inhibition of the M-CSF-CSF1R macrophage pathway.....	96
Chapter 2 - Hypothesis and aims	102
2.1 Hypothesis.....	103

2.2	Questions and corresponding objectives	104
Chapter 3 - Materials and Methods		105
3.1	Cell Culture	106
3.1.1	Cell lines	107
3.1.1.1	Mouse RAW 264.7 macrophages	107
3.1.1.2	Rat H9c2 cardiomyocytes	108
3.1.2	Primary cells	108
3.1.2.1	Animals.....	108
3.1.2.2	<i>In vitro</i> differentiation of BMDMs	109
3.1.2.3	Cardiac progenitors/stem/stromal-like cells (CSCs)	110
3.2	CSC conditioned media production and <i>in vitro</i> use	112
3.2.2	Production of CSC conditioned media (CSC CondM)	112
3.2.3	<i>In vitro</i> system for differentiating BMDMs with CSC's CondM	112
3.3	Chemical and antibody-based assays	114
3.3.1	Pharmacological inhibitor of CSF1R: BLZ945	114
3.3.2	Neutralising antibody against CSF1R (α CSF1R).....	114
3.4	Flow cytometry	115
3.5	Gene expression analysis.....	116
3.5.1	Single-cell quantitative reverse transcription-PCR (sc qRT-PCR).....	116
3.5.2	Methods of visualisation of the results of the sc qRT-PCR.....	119
3.6	Protein expression assays	122
3.6.1	Enzyme-linked immunosorbent assay (ELISA).....	122
3.6.2	Multiplex bead-based immunoassay (LEDENDplex)	122
3.7	Phagocytosis assays.....	125
3.8	Statistical analysis.....	127
3.9	Key resources.....	128
Chapter 4 – Result I		133
4	Result I: <i>In vitro</i> generation of M1- and M2-driven macrophages	134
4.1	Introduction and rationale	134
4.2	Results	136
4.2.1	<i>In vitro</i> system to study M1- and M2-driven-M ϕ	136
4.2.2	The immunophenotype of M1- and M2-driven-M ϕ	137
4.2.3	The single-cell gene expression profile of M1- and M2-driven-M ϕ	139
4.3	Discussion.....	146
4.3.1	<i>In vitro</i> differentiation of macrophages: advantages and limitations	146
4.3.2	Characterisation of the immunophenotype of macrophages by flow sorting: advantages and limitations.....	149
4.3.3	Single-cell qRT-PCR: advantages and limitations	151
4.3.4	The genes enriched in clusters 1 and 2	153
4.3.5	Gene expression profiles correlate with culture treatments but not with the F4/80 CD206 immunophenotype	155
4.4	Summary and Conclusion	157
Chapter 5 – Results II.....		159

5	Result II: Paracrine factor(s) released by CSCs modulate macrophage immunophenotypes, gene signatures and protein profiles	160
5.1	Introduction and rationale	160
5.2	Results	162
5.2.1	<i>In vitro</i> study of the paracrine effects of CSC CondM on BMDMs	162
5.2.2	The immunophenotype of CSC-driven M ϕ	164
5.2.3	Single-cell qRT-PCR analysis of the gene signatures of CondM+LPS+IFN γ -M ϕ	167
5.2.4	Single-cell qRT-PCR analysis of the gene signatures of CSC CondM+IL4+IL13-M ϕ	172
5.2.5	Evaluation of the secretion of 23 cytokines and chemokines in macrophages.....	176
5.3	Discussion	178
5.3.1	The choice of using Lin ⁻ Sca1 ⁺ CD31 ⁻ PDGFR α ⁺ SP CSCs	178
5.3.2	FACS analysis revealed an anti-inflammatory-like immunophenotype of CSC CondM-driven-M ϕ	180
5.3.3	CSC CondM+LSP+IFN γ -M ϕ and GM-CSF+LPS+IFN γ -M ϕ have different gene signatures ..	181
5.3.4	CSC CondM+IL4+IL13-M ϕ and M-CSF+IL4+IL13-M ϕ have similar gene signatures	182
5.3.5	CSC CondM+LSP+IFN γ -M ϕ and GM-CSF+LPS+IFN γ -M ϕ have different secretomes	183
5.4	Summary and Conclusion	184
Chapter 6 – Results III		187
6	Result III: Exploring whether CSC-secreted M-CSF promotes an anti-inflammatory macrophage phenotype	188
6.1	Introduction and rationale	188
6.2	Results	190
6.2.1	ELISA	190
6.2.2	Pharmacological inhibition of CSF1R with BLZ945	191
6.2.2.1	Pharmacological inhibition of CSF1R with BLZ945 to evaluate macrophage immunophenotypes	191
6.2.2.2	Single-cell qRT-PCR analysis of the effects of BLZ945 on macrophage gene signatures....	194
6.2.3	Inhibition of CSF1R with neutralising mAb (AFS98): α CSF1R	201
6.2.3.1	Inhibition of CSF1R with α CSF1R to evaluate macrophage immunophenotypes	201
6.2.3.2	Single-cell qRT-PCR analysis of the effects of α CSF1R on macrophage gene signatures ..	203
6.2.3.3	Inhibition of CSF1R with α CSF1R to evaluate the macrophage secretome.....	208
6.2.3.4	Inhibition of CSF1R with α CSF1R to evaluate macrophage phagocytosis.....	209
6.3	Discussion	211
6.3.1	CSC-secreted M-CSF promotes an anti-inflammatory-like macrophage phenotype.....	211
6.3.2	Pharmacological inhibition (BLZ945) of CSF1R suggested a compensatory effect CSC CondM+IL4+IL-M ϕ	212
6.3.3	\square CSF1R confirmed that CSC-secrete M-CSF induces a unique anti-inflammatory-like macrophage phenotype.....	213
6.4	Summary and Conclusion	216
Chapter 7 - General Discussion		218
7.1	General Discussion	219
7.1.1	CSC-secreted M-CSF induces a unique anti-inflammatory-like macrophage phenotype that may provide a therapeutic strategy to support post-MI heart repair and regeneration ..	219
7.1.2	Insight into CSC-driven phenotype	221
7.2	Study limitations and future implications	223

7.2.1	Model system and assay limitations.....	223
7.2.2	Identification of paracrine factors secreted by CSC that work in synergy with M-CSF.....	225
7.2.3	Therapeutic benefits of translation	226
7.3	Conclusive summary	228
	References.....	276
	Appendix	230

List of Figures

Figure 1.1 Cardiovascular diseases, particularly ischemic heart disease, are the leading global cause of mortality _____	24
Figure 1.2 Post-MI cardiac remodelling _____	28
Figure 1.3 Cardiac regeneration capacity in zebrafish, amphibians and mice _____	34
Figure 1.4 Illustration to summarise the evolution of cardiac regenerative therapy _____	40
Figure 1.5 PDGFR α delimits Sca1 ⁺ CSCs _____	49
Figure 1.6 Next-generation of cell therapy: the paracrine hypothesis _____	53
Figure 1.7 Developmental waves of mouse macrophages _____	57
Figure 1.8 <i>Nos2</i> and <i>Arginase 1</i> compete for the same substrate: L-Arginine _____	66
Figure 1.9 Phagocytosis of apoptotic CMs _____	85
Figure 1.10 Identification of M-CSF as a potential mediator of CSC anti-inflammatory effect _____	91
Figure 1.11 Schematic structure of CSF1R _____	93
Figure 3.1 An <i>in vitro</i> system to study M1- and M2-driven macrophages _____	110
Figure 3.2 Schematic representation of CSC CondM production _____	112
Figure 3.3 <i>In vitro</i> system for differentiating BMDMs with CSC CondM _____	113
Figure 3.4 The workflow of sc expression profiling by qRT-PCR _____	121
Figure 3.5 Schematic representation of LEGENDplex (BioLegend) protocol _____	124
Figure 4.1 Illustration of the four populations generated <i>in vitro</i> _____	136
Figure 4.2 Flow cytometry data of the four macrophage populations generated <i>in vitro</i> _____	138
Figure 4.3 Unbiased hierarchical clustering heatmap shows the single-cell gene expression profile of M1- and M2-driven-M ϕ _____	141
Figure 4.4 PCAs show the single-cell gene expression profile of M1- and M2-driven-M ϕ _____	143
Figure 4.5 Dot plots show the single-cell gene expression profile of M1- and M2-driven-M ϕ _____	145
Figure 4.6 <i>In vitro</i> generation of GM-CSF+LPS+IFN γ and M-CSF+IL4+IL13-M ϕ _____	158
Figure 5.1 Illustration of the seven populations generated with the integrated version of the <i>in vitro</i> system _____	163
Figure 5.2 Flow cytometry data from the seven culture conditions _____	166
Figure 5.3 An unbiased hierarchical clustering heatmap shows the effects of LPS+IFN γ on the gene signatures of macrophages _____	168
Figure 5.4 PCAs show the effects of LPS+IFN γ on the gene expression profiles of macrophages _____	170
Figure 5.5 Investigation of the effects of LPS+IFN γ on the gene expression of CSC-driven M ϕ by sc qRT-PCR: dot plot _____	171
Figure 5.6 An unbiased hierarchical clustering heatmap shows the effects of IL-4+IL-13 on the gene expression of CSC-driven M ϕ _____	173
Figure 5.7 PCAs show the effects of IL-4+IL-13 on the gene expression profiles of macrophages _____	174
Figure 5.8 Investigation of the effects of IL-4+IL-13 on the gene expression of CSC-driven M ϕ by sc qRT-PCR: dot plots _____	175
Figure 5.9 Heatmap of secretion levels of 23 cytokines and chemokines evaluated via a multi-analyte bead-based immunoassay _____	177
Figure 5.10 CSC CondM induces an anti-inflammatory macrophage phenotype _____	186
Figure 6.1 Lin ⁻ Sca1 ⁺ CD31 ⁻ PDGFR α ⁺ SP ⁺ CSCs secrete M-CSF _____	190
Figure 6.2 Pharmacological inhibition of CSF1R with BLZ945 to evaluate macrophage immunophenotype. _____	193
Figure 6.3 BLZ945 effects on <i>Arg1</i> and <i>Nos2</i> expression in activated macrophages _____	195
Figure 6.4 An unbiased hierarchical clustering heatmap shows the effects of BLZ945 on the gene signature of M-CSF+IL4+IL13-M ϕ _____	196
Figure 6.5 PCAs show the effects of BLZ945 on the M-CSF+IL4+IL13-M ϕ gene signature _____	197
Figure 6.6 Dot plots show the effects of BLZ945 on cluster 1 expression _____	198

Figure 6.7 An unbiased hierarchical clustering heatmap shows the effect of BLZ945 on the CSC CondM+IL4+IL13-M ϕ gene signature _____	199
Figure 6.8 Dot plots show the effects of BLZ945 on CSC CondM+IL4+IL13-M ϕ gene expression _	200
Figure 6.9 α CSF1R to evaluate macrophage immunophenotypes _____	202
Figure 6.10 The effects of α CSF1R on the pro-inflammatory gene signature _____	204
Figure 6.11 The effects of α CSF1R on the anti-inflammatory gene signature _____	206
Figure 6.12 α CSF1R effects on macrophage secretome _____	209
Figure 6.13 α CSF1R effects on phagocytosis _____	210
Figure 6.14 CSF1R inhibition disrupts the anti-inflammatory CSC-driven macrophage phenotype.	217
Figure 7.1 Conclusive summary _____	229
Figure A1. Result I: Full heatmap _____	278
Figure A2. Result I: p-values heatmap _____	279

List of Tables

Table 1.1 CSCs used in human clinical trials.....	50
Table 1.2 Identified pro- and anti-angiogenic factors secreted by BMDMs	76
Table 1.3 Preclinical and early clinical use of M-CSF listed	96
Table 1.4 Application of neutralising anti-M-CSF antibodies	98
Table 1.5 Key findings of M-CSF deficiency in different disease models via neutralising antibody against CSF1R (AFS98)	99
Table 3.1 Cell lines and primary cells used in this study.....	107
Table 3.2 Clonal Growth Medium	111
Table 3.3 Antibodies and staining used for FACS analyses.....	115
Table 3.4 RT-Mix (10 μ l/well)	116
Table 3.5 TaqMan probes used for sc qRT-PCR. All probes are conjugated to MGB-FAM dye (ThermoFisher).	117
Table 3.6 Pre-amplification RT-PCR thermal cycles	118
Table A1 Summary table of the key findings of these paper.....	276

List of abbreviations

AMP	Adenosine Monophosphate
ANGPT	Angiopoietin
Arg1	Arginase
ATP	Adenosine Triphosphate
BM	Bone Marrow
BMDMs	Bone Marrow-Derived Macrophages
BMMNC	Bone Marrow Mononuclear Cells
BMP	Bone Morphogenetic Protein
BMPER	Bmp Binding Endothelial Regulator
cCFU	Cardiac Colony Forming Units
CCL	C-C Motif Chemokine Ligand
<i>Ccr2</i>/CCR2	Chemokine Receptor 2
CDCs	Cardiospheres-Derived Cells
CDK	Cyclin-Dependent Kinase
CGM	Clonal Growth Medium
cKO	Conditional Knockout
CL₂MDP-L	Clodronate Liposome
CM	Cardiomyocytes
CNH	C-Terminal Citron Homology
CO₂	Carbon Dioxide
CondM	Csc's Conditioned Media
CPC	Cardiac Progenitor Cells
CSC	Cardiac Progenitor/Stem/Stromal-Like Cell
<i>Csf1</i>/CSF1	Csf1 Colony Stimulating Factor 1
<i>Csf2</i>/CSF2	Csf1 Colony Stimulating Factor 2
<i>Csf1r</i>/CSF1R	Csf1r Colony Stimulating Factor 1 Receptor
CT1	Cardiotrophin-1
CVD	Cardiovascular Disease
CXCL	C-X-C Chemokine Ligand
<i>Cx3cr1</i>/CX3CR1	C-X3-C Motif Chemokine Receptor-1

DAMPs	Danger-Associated Molecular Patterns
DMEM	Dulbecco's Modified Eagle's Medium
DNA	Deoxyribonucleic Acid
DCs	Dendritic Cells
DTR	Diphtheria Toxin Receptor
EC	Endothelial Cells
ECM	Extracellular Matrix
ERK	Extracellular Signal Regulated Kinase
eRNA	Extracellular RNA
ESC	Embryonic Stem Cell
FBS	Fetal Bovine Serum
FSC-A/W	Forward Scatter/Width
<i>Gata4</i>/GATA4	Gata-Binding Protein 4
<i>GFP</i>/GFP	Green Fluorescent Protein
G-CSF	Growth Colony Stimulating Factor
GDF15	Growth Differentiation Factor 15
GM-CSF	Granulocyte-Macrophage Colony-Stimulating Factor
GO	Gene Ontology
HF	Heart Failure
hiPSC	Human Induced Pluripotent Stem Cells
HSC	Hematopoietic Stem Cells
IFNγ	Interferon- γ
<i>Igf1</i>/IGF1	Insulin-Like Growth Factor 1
<i>Igf2</i>/IGF2	Insulin-Like Growth Factor 2
IL	Interleukin
<i>Inhba</i>/INHBA	Inhibin Subunit Beta A
iNOS	Inducible Nitric Oxide Synthase
I/R	Ischemia/Reperfusion
IRF-3, -5	Ifn Regulatory Factor- 3, -5
IZ	Ischemic Zone
JAK	Janus Kinase
KD	Knockdown

KO	Knockout
LPS	Lipopolysaccharides
LV	Left Ventricle
LVEF	Left Ventricular Ejection Fraction
Ly6a	Lymphocyte Activation Protein-6a
MAPK	Mitogen-Activated Protein Kinase
MCP1	Monocytes Chemoattractant Protein
M-CSF	Macrophage Colony-Stimulating Factor
MHC	Major Histocompatibility Complex
MI	Myocardial Infarct
MRC1	Mannose Receptor
MRI	Magnetic Resonance Tomography
MSC	Mesenchymal Stem/Stromal Cells
MyD88	Myeloid Differentiation Primary Response 88
Mϕ	Macrophages
NO	Nitric Oxide
Nos2	Nitric Oxide Synthase 2
PBS	Phosphate Buffered Saline
PDGFRα	Platelet-Derived Growth Factor Receptor Alpha
<i>Pecam1</i>/PECAM1	Platelet/Endothelial Cell Adhesion Molecule 1
PTGES	Prostaglandin E Synthase
RNA	Ribonucleic Acid
ROS	Reactive Oxygen Species
Sc	Single-cell
<i>Sca1</i>	Stem Cell Antigen-1
ScRNA-Seq	Sc RNA Sequencing
SEM	Standard Error of the Mean
siRNA	Small Interfering RNA
SMC	Smooth Muscle Cells
SP	Side Population Dye-Efflux Phenotype
SSC-A	Side-Scattered
STEMI	ST-Elevation MI

TBX	T-Box Transcription Factor
TGM2	Transglutaminase 2
Th1	Type 1 Helper T-Cell
Th2	Type 2 Helper T-Cell
TLRs	Toll-Like Receptors
<i>Tnfa</i>/TNFα	Tumour Necrosis Factor-Alpha
TRAF	Tnf Receptor-Associated Factors
TRIF	TIR-domain-containing adapter-inducing interferon- β
<i>Ubc</i>	Ubiquitin C
VEGF	Vascular Endothelial Growth Factor
<i>Wt1</i>	Wilm's Tumour 1

Chapter 1 – Introduction

1.1 Cardiac repair: an urgent unmet clinical need

1.1.1 Cardiovascular diseases: the leading cause of mortality and healthcare cost worldwide

The Global Burden of Disease study (2015) estimated that non-communicable diseases are the leading cause of death globally (~70%), followed by communicable, maternal, neonatal and nutritional diseases estimated at around 20%, and injuries at about 8%. Among the non-communicable diseases, cardiovascular disease (CVD) is the leading cause of mortality, with 17 million deaths globally reported in 2015 alone, nearly double the number of deaths caused by cancer (10 million) (Benjamin et al., 2019; Reddy, 2016; Roth et al., 2017; White & Chew, 2008; Wilkins et al., 2017) (Fig. 1.1 A). CVDs account for more than 4 million deaths annually in Europe, accounting for 45% of all-cause mortality (Townsend et al., 2016).

The most common form of CVD is myocardial infarction (MI), an acute ischemic injury resulting in widespread death of cardiomyocytes (CMs). MI has a global incidence of over 7 million per year for both genders, with over 70,000 cases in the United Kingdom alone (White & Chew, 2008; Wilkins et al., 2017) (Fig. 1.1 B). The prevalence of all CVDs is projected to increase as the population ages, reaching 25 million deaths annually by 2030, offsetting all advances in age-adjusted mortality (Moran et al., 2014). This is due to the direct correlation between increasing age and a higher incidence of common risk factors in Western countries, such as diabetes, obesity, tobacco smoking, physical inactivity, and even excess alcohol (Cook et al., 2014). The global population with a high body mass index (BMI) is increasing, with one-third

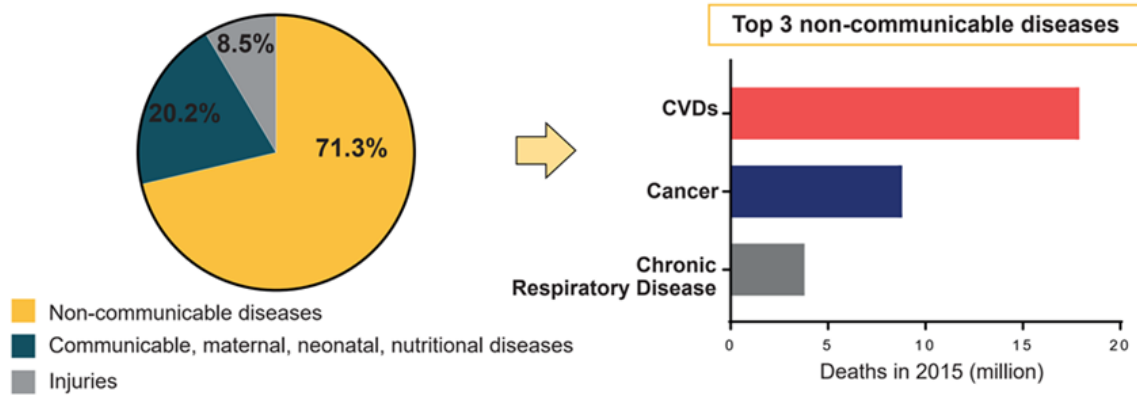
classified as overweight or obese (Forouzanfar et al., 2016). By 2025, 18% of men and 25% of women are expected to reach the BMI of obesity (Di Cesare et al., 2016). A high BMI is a risk factor for developing other conditions such as type 2 diabetes mellitus (T2D), hypertension and coronary diseases (Heidenreich et al., 2013; Manrique-Acevedo et al., 2020; Stone et al., 2016). On the other hand, the main risk factors for developing CVDs are rapid urbanisation, ageing, and population growth in low-income countries (Mensah et al., 2015).

Over the past 20 years, for post-MI patients, a breakthrough in cardiac care has been the urgent reperfusion therapy, which has improved prognosis by reducing infarct size and short-term mortality (Dorn, 2009; Opie et al., 2006). However, uncorrected ischemic injury, especially if the infarct area is large or following recurrent MI, predisposes to long-term heart failure (HF). HF is a severe deficiency in ventricular pump function that impairs ventricular filling or ejection of blood (Anderson & Morrow, 2017; Saleh & Ambrose, 2018). HF is expected to increase by 50% over the next ten years (Ambrosy et al., 2014; Braunwald, 2015; Moran et al., 2014; Vigen, Maddox, & Allen, 2012). Worldwide, 38 million people suffer from HF, and the survival rate is estimated to be 50% five years after diagnosis (Braunwald, 2015; Cahill et al., 2017). The only definitive therapy for advanced HF remains heart transplantation (Dark, 2009; Fraccarollo et al., 2012; Hoffman, 2005). However, heart transplantation has many limitations, such as the availability of suitable donors or factors related to the immune rejection of organs. In addition, it imposes a significant economic burden, estimated at over \$100 billion annually (Cook et al., 2014). Therefore, CVDs represent a socio-economic problem with a high financial burden. In Europe, the total annual cost of CVDs is approximately €210 billion, split among healthcare (53%), lost productivity

(26%) and informal after-care (21%) (Wilkins et al., 2017). Meanwhile, in the United States, the total cost is estimated to increase from \$318 billion (2015) to \$749 billion by 2035 (Benjamin et al., 2019).

In conclusion, understanding the clinical progression of HF following MI is essential to identify the most effective therapeutic approaches to prevent HF and promote cardiac regeneration.

A Global Causes of Death (2015)



B Ischemic heart disease: Foremost global cause of death & disability

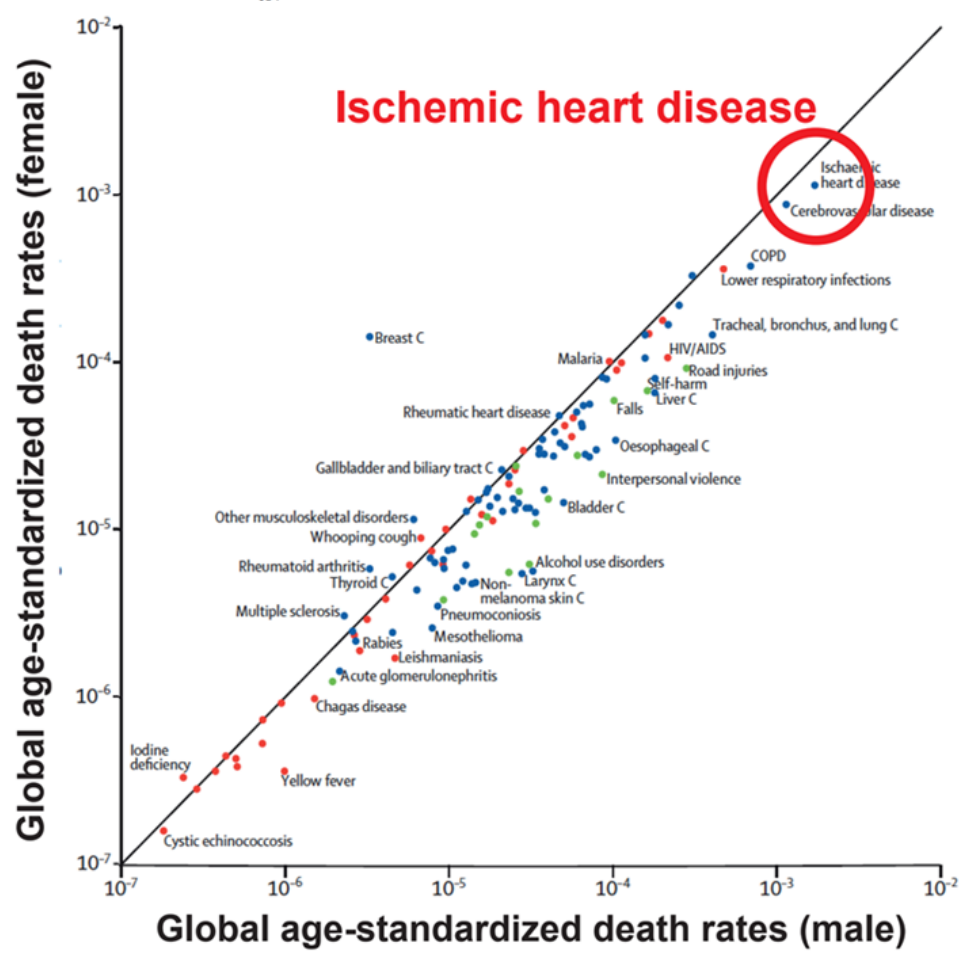


Figure 1.1 Cardiovascular diseases, particularly ischemic heart disease, are the leading global cause of mortality.

A, Non-communicable diseases were the most significant cause of death globally in 2015 (71.3%), while communicable, maternal, neonatal and nutritional diseases accounted for 20.2% and injuries only 8.5%. Among the non-communicable diseases, the top 3 are CVD (17 million), cancer (10 million) and chronic respiratory disease (less than one million). Therefore, ischemic heart disease is the leading global cause of death for both males and females (Modified from Reddy, 2016; Yeh et al., 2010).

1.1.2 Cardiac remodelling following myocardial infarction and progression to heart failure

MI occurs due to a lack of oxygenated blood flow supplied to the heart tissue. Typically, this event is due to a rupture of the atherosclerotic plaque, which causes ischemic damage resulting in loss of CM, estimated at around 1 billion cells (Lundy et al., 2014; Saleh & Ambrose, 2018).

Due to ischemic damage, the remaining CMs cannot perform their mechanical and structural function. The resulting cardiac damage triggers a repair process, replacing necrotic tissue and forming a non-contractile fibrous scar to avoid fatal heart rupture (Fraccarollo, Galuppo, & Bauersachs, 2012; Frangogiannis, 2006; Frangogiannis et al., 2002; Frangogiannis, 2014). The intrinsic ability of an adult mammalian heart to repair or regenerate is next to nil (Aurora & Olson, 2014; Braunwald, 2015; Bui, Horwich, & Fonarow, 2011; Mercola, Ruiz-Lozano, & Schneider, 2011; Schneider, 2016; Uygur & Lee, 2016; Zhang et al., 2016).

The cardiac repair depends on a complex and sequential series of inflammatory events that can be divided into three overlapping phases: first, the pro-inflammatory, second, the proliferative or regenerative, and finally, the resolution of inflammation with the remodelling of the left ventricle (LV) (Dobaczewski, Gonzalez-Quesada, & Frangogiannis, 2010; Frangogiannis, 2008; Frangogiannis et al., 2002).

Phase I: Pro-inflammatory phase

In the first few hours after MI, apoptotic and necrotic death of CMs triggers an inflammatory response. The initial inflammatory phase activates the pro-inflammatory pathways and cellular mediators. In this phase, immune cells are recruited, including monocytes, macrophages, neutrophils, and lymphocytes. Neutrophils and macrophages infiltrate the infarcted area to remove dead and necrotic cells and debris (Forbes & Rosenthal, 2014; Forte et al., 2018). Macrophages recognise and ingest apoptotic cells through a process known as efferocytosis (Harel-Adar et al., 2011; Huynh et al., 2002). During efferocytosis, macrophages suppress the production of pro-inflammatory mediators while inducing anti-inflammatory molecules (Harel-Adar et al., 2011; Huynh et al., 2002).

Phase II: Proliferative phase

The proliferative phase lasts from hours to days. It is characterised by the proliferation of endothelial cells (ECs) and fibroblasts and the formation of a microvascular network. The microvascular network provides oxygen and nutrients and facilitates the migration of fibroblasts to the new developing scar tissue. Cardiac fibroblasts differentiate into myofibroblasts that secrete extracellular matrix (ECM) proteins, such as collagen I, collagen III and fibronectin (Forbes & Rosenthal, 2014; Spinale, 2007).

Phase III: Resolution of inflammation with LV remodelling

The resolution of inflammation occurs within weeks or months with a progressive apoptotic death of fibroblast and vascular cells and the resulting formation of a non-contractile fibrotic scar that prevents cardiac rupture (de Couto et al., 2015; Frangogiannis, 2008). Preservation of the physiological cardiac structure is vital for

maintaining proper cardiac function (Frangogiannis, 2012). Prompt resolution of the inflammation is needed to prevent lesion extension and tissue damage. An overactive, dysregulated, temporally, or spatially prolonged inflammatory response can lead to disastrous consequences. For example, extensive fibrosis promotes adverse cardiac remodelling, leading to progressive cardiac dysfunction. Therefore, controlling the level and duration of inflammatory activity is both crucial in the natural history of MI and also gives rise to potential therapeutic targets to improve heart repair (Fildes et al., 2009; Frangogiannis, 2012; Frangogiannis, 2015; Frangogiannis, 2014; Prabhu, 2005; Sutton & Sharpe, 2000).

During the resolution of the inflammation phase, the LV undergoes a complex structural change in size, shape, and function, known as LV remodelling. The LV dilates due to myocyte hypertrophy to preserve the systolic strength by reducing the stress on the myocardial wall. The remaining functioning myocardium is forced to compensate for impaired heart function due to the loss of contractile strength caused by CM death. The extent of LV remodelling is influenced by the location and size of the infarct zone (Burchfield et al., 2013).

The initial physiological phase of LV remodelling can be beneficial because it preserves cardiac output. However, this is followed by a pathological phase, where an architectural rearrangement of the surviving myocardium is observed (Burchfield et al., 2013; Fraccarollo et al., 2012; Opie et al., 2006; Prabhu, 2005; Sutton & Sharpe, 2000). Fibroblasts near the MI region acquire the smooth muscle cell (SMC) characteristics that secrete collagen-based matrix. This form of reparative fibrosis is necessary to maintain the structural integrity of the heart and to avoid the rupture of

the LV. However, excessive ECM deposition increases myocardium stiffness because the fibrotic scar is not contractile. Reactive fibrosis leads to systolic and diastolic dysfunction, increasing the risk of arrhythmogenicity and progression towards HF (Ambrosy et al., 2014; Braunwald, 2015; Fraccarollo et al., 2012; Houser et al., 2012; Moran et al., 2014; Nosedá et al., 2015; Vigen et al., 2012) (Fig. 1.2).

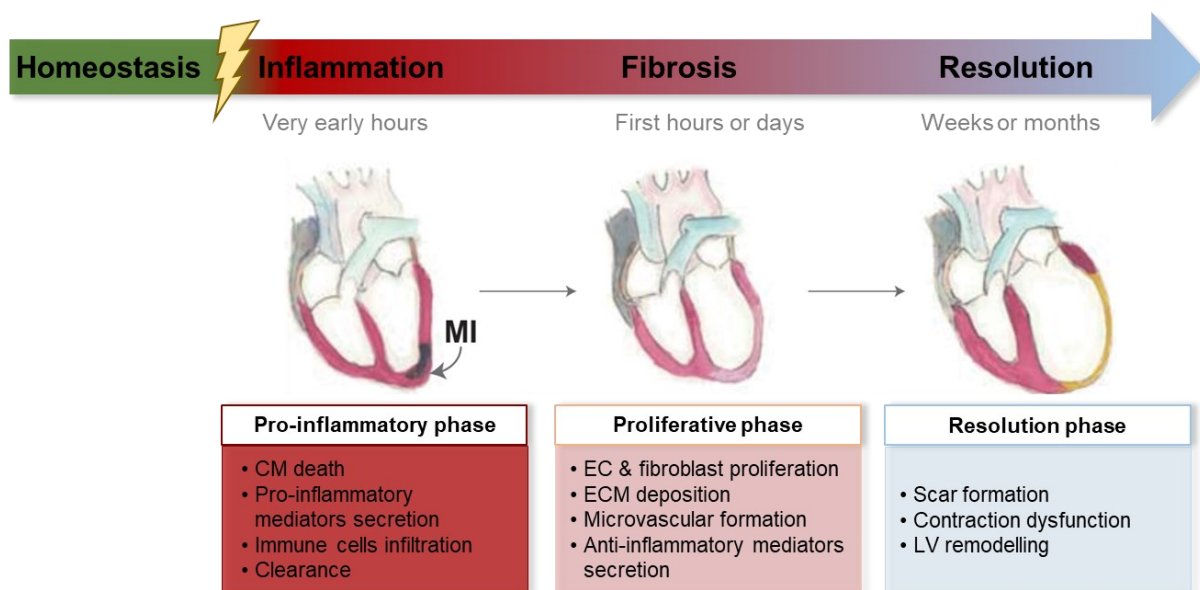


Figure 1.2 Post-MI cardiac remodelling

The lack of oxygen in the first few hours after MI leads to CM death and a pro-inflammatory response. In the following hours or days, a proliferative phase is mediated by anti-inflammatory cytokines stimulating ECM deposition and proliferation of EC and fibroblast. Finally, the formation of a non-contractile fibrotic scar indicates the resolution of inflammation. The fibrotic scar's appearance leads to remodelling of the LV, which can also evolve into general cardiac dysfunction, arrhythmogenicity, and even HF (Modified from Forte et al., 2018; Fraccarollo, Galuppo, & Bauersachs, 2012).

1.1.3 Heart transplant: the only available cure for advanced heart failure

Current treatments to protect against progression from MI to HF are early reperfusion therapy, angioplasty, stents, coronary artery bypass graft surgery and anticoagulant drugs (Braunwald, 2015; Han et al., 2018). All currently used reperfusion treatments can quickly restore blood flow, delaying the progression of the injury that has already occurred. However, they do not address the clinical need to repair or reverse the damaged tissue (Segers & Lee, 2008).

The goal of the scientific community is to reduce the incidence and severity of CVDs globally. A recent pooled patient-level analysis of ten randomised clinical trials of primary percutaneous coronary intervention demonstrated the strong link between infarct size and the likelihood of hospitalisation for HF within one year (Stone et al., 2016). The risk of developing HF increased by 20% for every 5% increase in infarct size, regardless of all other variables, such as age, gender, diabetes, hypertension, hyperlipidaemia, and smoking (Mozaffarian, 2016; Stone et al., 2016). Thus, although early reperfusion therapy improves premature mortality from MI, structural remodelling of the LV increases progression to HF by impairing the heart's pumping capacity. The only definitive therapy for advanced HF remains heart transplant, which cannot be considered a realistic long-term therapeutic option for the population at risk due to the markedly limited amount of available donors (Dark, 2009; Fracarro et al., 2012; Hoffman, 2005; Yacoub, 2015).

1.2 The mammalian heart has a limited capacity for regeneration

1.2.1 Heart regeneration in zebrafish, amphibia and neonatal mice

Regenerative capacity is defined as the complete recovery of the structure and function of an injured organ or part of the body and varies between species. Teleost fish and urodele amphibians are primary models for studying cardiac regeneration in vertebrates because they regenerate limbs, fins and organs after injury (Claycomb, 1992; Jopling et al., 2010; Kikuchi et al., 2010; Poss & Keating, 2002; Raya et al., 2003).

Danio rerio, also known as zebrafish, regenerates heart tissue without forming a fibrotic scar through a robust proliferation of pre-existing adult CMs that re-enter the cell cycle (González-Rosa et al., 2017). After surgical resection of approximately 20% of the ventricle, within 30-60 days, CM proliferation restored the ventricular myocardium (Poss, Wilson & Keating, 2002; Raya et al., 2003). After cryoinjury, the apoptotic response causes immune cell infiltration, fibrotic tissue deposition, and scar formation, which disappear within 3-4 months, indicating that fibrosis is a transient event (González-Rosa et al., 2011). Cardiac regeneration requires upregulation of the mitotic checkpoint kinase, *ttk* protein kinase (Poss, Wilson & Keating, 2002), and muscle segment homeobox 1b (*msx1b/msxB*) and 3 (*msx3/msxC*) (Raya et al., 2003). Genetically engineered CMs express the bacterial enzyme Nitroreductase (NTR), which triggers the prodrug metronidazole (Mtz) activation. Activated Mtz becomes a

cytotoxic DNA cross-linking agent. The controllable administration of Mtz into the water tank allows monitoring of CMs ablation in adult zebrafish (Curado et al., 2007). Finally, the hypoxia/reoxygenation (H/R) injury model showed a temporary reduction of ventricular function due to cardiac oxidative stress, CMs death, and inflammation response, followed by full functional recovery through CM proliferation (Parente et al., 2013). Despite there are still questions on how to translate these findings into therapeutic strategies, considerable work confirmed that adult zebrafish hearts regenerate through a robust proliferation of pre-existing CMs, which is maintained in adulthood (Jopling et al., 2010; Kikuchi et al., 2010; Mahmoud & Porrello, 2011) (Fig. 1.3 A).

In *Ambystoma mexicanum*, also known as axolotls, partial ventricular amputation resulted in CMs proliferation, tissue restoration, and contractile function recovery (Cano-Martínez et al., 2010). Ventricle wall cryoinjury resulted in the invasion of inflammatory leukocytes and activation of CM proliferation for healing, as monitored using Bromodeoxyuridine (BrdU) incorporation (Godwin et al., 2017). Interestingly, macrophage depletion experiments demonstrated that salamander cardiac regeneration is based on a macrophage-mediated mechanism. Macrophage depletion by clodronate liposomes (CL2MDP-L) failed cardiac regeneration after cryoinjury, while CM proliferation was maintained, indicating that CM proliferation is insufficient to prevent fibrotic scar progression (Godwin et al., 2017) (Fig. 1.3 B).

Following cardiac injuries, neonatal mice regenerate the heart without scar (Haubner et al., 2012; Lavine et al., 2018; Mahmoud et al., 2014; Porrello et al., 2011, Porrello et al., 2013; Xin et al., 2013). However, this regeneration capacity is retained only for

seven days after birth, and it is driven by CM proliferation and an angiogenic response (Aurora et al., 2014; Forbes & Rosenthal, 2014; Porrello et al., 2011, 2013).

Although the mechanisms involved in mouse neonatal cardiac regeneration remain unknown, immune cell infiltration plays a significant role, demonstrating that cardiac repair is a macrophage-dependent process (Aurora et al., 2014; Lavine et al., 2014). A permanent ligation model demonstrated a quantitative difference in immune response between postnatal day one mice (P1, defined as regenerative mice) and P14 mice (Aurora et al., 2014). Post-MI, fluorescence-activated cell sorting (FACS) and immunostaining localised macrophages around the ischemic zone (IZ). Macrophages were identified based on F4/80 expression, a widely used marker for mouse macrophages. Regenerative mice, P1, expressed a higher number of cardiac F4/80⁺ macrophages without injury and seven days post-MI (Aurora et al., 2014). Monocyte and macrophages were depleted from the heart of neonatal mice (P1) undergoing MI using CL2MDP-L to establish the role of macrophages in regeneration. Twenty-one days after MI, mice treated with CL2MDP-L showed increased collagen staining throughout the infarct area up to the apex, forming a fibrotic scar and leading to cardiac dysfunction, demonstrating that macrophages are essential for cardiac regenerative capacity (Aurora et al., 2014).

Crossing myosin light chain 2v (*Mlc2v*)-*Cre* with *Rosa26-DTR* mice and daily administration of diphtheria toxin caused a ventricular CM death bypassing the systemic inflammatory activity associated with a thoracotomy (Dewald et al., 2003; Lavine et al., 2014). Terminal deoxynucleotidyl transferase dUTP nick end labelling

staining (TUNEL) and cardiac troponin I (cTnI) serum concentration levels showed a reduction in age-related mortality (Lavine et al., 2014).

Surface marker chemokine (C–C motif) receptor 2 (CCR2) identifies circulation-derived macrophages (Epelman et al., 2014). Post-injury, two subsets of cardiac macrophages increase: in neonatal mice, CCR2⁻ resident macrophages, and in adult mice, CCR2⁺ recruited and monocyte-derived macrophages (Lavine et al., 2014). *In vitro*, neonatal CCR2⁻ macrophages stimulate CM proliferation, EC tube formation and angiogenesis. Therefore, CCR2⁻ macrophages were classified as reparative and non-inflammatory (Lavine et al., 2014). CCR2⁻ macrophages express high levels of pro-inflammatory genes, such as monocyte chemoattractant protein-1 (*Ccl2*) and -7 (*Ccl7*), chemokine (C-X-C motif) ligand 1 (*Cxcl1*), interleukin 6 (*Il6*), interleukin 1 β (*Il1 β*) and tumour necrosis factor-alpha (*Tnf α*). On the other hand, CCR2⁺ macrophages are considered pro-inflammatory with a limited restorative capacity. (Lavine et al., 2014) (Fig. 1.3 C).

Overall, injured cardiac tissue can regenerate without scar formation through a new proliferation of CMs in adult zebrafish, salamander, and neonatal mice (within 7-day after birth). The common feature of this regeneration is the ability of CMs to re-enter the cell cycle days after birth (Aguirre, Sancho-Martinez, Izpisua Belmonte, 2013; Yin & Poss, 2008), even if only temporarily, as shown in the first week of the life of mice (Porrello et al., 2011). Cardiac regeneration, at least in part, depends on a balance between monocyte-derived and tissue-resident macrophages. In amphibia and neonatal mice, macrophages are involved in cardiac tissue repair, suggesting that their role might be an evolutionarily conserved mechanism (Aurora et al., 2014).



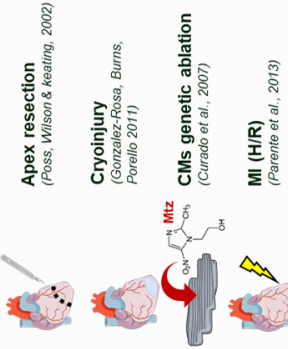









Animal Model	Regeneration capacity over time	Cardiac injury	Regeneration
 <p>Zebrafish (<i>Danio rerio</i>)</p>	 <p>Age: Embryo, New Born, Young, Adult</p> <p>Several organs, include the heart</p>	 <p>Apex resection (Poss, Wilson & Keating, 2002)</p> <p>Cryoinjury (Gonzalez-Rosa, Burns, Porello 2011)</p> <p>CMs genetic ablation (Curado et al., 2007)</p> <p>MI (H/R) (Parente et al., 2013)</p>	 <ul style="list-style-type: none"> • If formed, transient fibrotic scar • Proliferation of pre-existing adult CMs • CMs re-enter the cell-cycle • Upregulation of <i>mip1/ltk</i> • Upregulation of <i>msx1b</i> and <i>msx3</i>
 <p>Amphibians (Axolotls, <i>Ambystoma mexicanum</i>)</p>	 <p>Age: Embryo, New Born, Young, Adult</p> <p>Limbs & tail and the heart</p>	 <p>Ventricular amputation (Cano-Martinez et al., 2010)</p> <p>Cryoinjury & Mφ genetic ablation (Godwin et al., 2017)</p>	 <ul style="list-style-type: none"> • Proliferation of pre-existing adult CMs • CMs re-enter the cell-cycle • Invasion of inflammatory leukocytes • Macrophage-dependent • Fibroblast activation
 <p>Mouse (<i>Mus musculus</i>)</p>	 <p>Age: Embryo, New Born, Young, Adult</p> <p>Heart within 7 days after birth</p>	 <p>Permanent ligation (Aurora et al., 2014)</p> <p>Mφ genetic ablation & MI (Aurora et al., 2014)</p> <p>CMs genetic ablation (Devald et al., 2003; Lavine et al., 2014)</p>	 <ul style="list-style-type: none"> • Proliferation of pre-existing adult CMs • CMs re-enter the cell-cycle • Angiogenic response • M2-like macrophage-dependent

Figure 1 Error! No text of specified style in document. **3 Cardiac regeneration capacity in zebrafish, amphibians and mice**

(A) Zebrafish, (B) urodele amphibians (e.g. axolotls) and (C) mice are animal models used for cardiac regeneration. From embryos to adulthood, they regenerate their organs and body parts. Godwin (2017) and Aurora and Lavine (2014) demonstrated that scar-free heart tissue regeneration in mice depends on M2-like macrophages (Aurora et al., 2014; Godwin et al., 2017; Lavine et al., 2014) (Modified from Uygur & Lee, 2016b) (<https://smart.servier.com/>).

1.2.2 Limitation in cardiac regeneration of adult mammals

Unlike the neonatal mouse heart, the adult mammalian heart is a post-mitotic organ, unable to regenerate following myocardial damage. Mammalian embryonic and fetal CMs can undergo cell division; after birth, this ability is lost and never significantly recovered (Ali et al., 2020; Bergmann et al., 2009; Eulalio et al., 2012; Lázár et al., 2017; Lestuzzi, 2016). Consequently, due to cardiac damage in adult mice and human hearts, insufficient renewal of CMs results in a fibrotic scar (Bergmann et al., 2009, 2011; Hashimoto et al., 2019; Hsieh et al., 2007). Therefore, several studies have addressed this challenging topic to obtain a clinically meaningful result. Several studies aimed to understand the turnover rate of CM and whether post-ischemic damage, adult mammalian cardiac regeneration is driven by pre-existing CMs or by CMs derived from undifferentiated progenitor cells.

Sensitive methods retrospectively determine the age of CMs (Bergmann et al., 2009). A series of above-ground nuclear bomb tests during the Cold War, which ended in 1963, raised ^{14}C levels in the global atmosphere. Reacting with oxygen, ^{14}C formed $^{14}\text{CO}_2$. The average turnover of the CMs was determined by measuring the permanent internalisation of $^{14}\text{CO}_2$ into the DNA of CMs, which was around 1% in young people (~20 years old) and gradually decreased in adulthood (Bergmann et al., 2009; Bergmann et al., 2015; Eschenhagen et al., 2017). However, Bergmann's studies focused on the basal proliferation activity of CMs without addressing the more critical question related to the differentiation potential of post-injury CMs (Bergmann et al., 2009; Bergmann et al., 2015).

Cardiogenesis under homeostatic conditions and post-ischemic injury was studied using tamoxifen-inducible double-transgenic mice (*Cre-loxP* system). Here, CMs were labelled with a green fluorescent protein (GFP) and cardiogenesis was measured with the multi-isotope high-resolution imaging mass spectrometry (MIMS) (Senyo et al., 2013). MIMS quantified the two non-radioactive-isotopes-of-nitrogen-14 (^{14}N) and nitrogen-15 (^{15}N) (Steinhauser et al., 2012; Zhang et al., 2012). Adult mammalian CMs replicate without completing the cell cycle. Therefore, the measurement of the nuclear incorporation of ^{15}N in thymidine quantified age-related cardiogenesis. Under homeostatic conditions, the incorporation was 5.5%/year in young mice and 2.6%/year in older mice (Senyo et al., 2013).

On the other hand, tamoxifen induces GFP expression in CMs derived from pre-existing myocytes (labelled GFP^+ CM), while CMs derived from progenitor cells express a GFP^- phenotype. Eight weeks after MI, ^{15}N thymidine pulse labelling resulted in a similar frequency of the $^{15}\text{N}^+$ expression level in GFP^+ myocytes compared to $^{15}\text{N}^-$ CMs. This indicated that pre-existing CMs are the primary source of new myocyte replacement in adult mice in homeostasis and after MI (Senyo et al., 2013). Under homeostatic conditions, the proliferation of CM was about 0.76%/year in young adult mice while, after injury, it increased by four times (Senyo et al., 2013).

Visual cytokinetic analysis indicated that CMs maintain the ability to become polyploid post-MI but lose the capacity to undergo cell division (Hesse et al., 2012). Others argue for even lower division rates, suggesting that CMs withdraw entirely from the cell cycle after birth and attribute the higher percentage of CM division to binucleation. Microarray studies on neonatal DNA synthesis have credited the CM binucleation to

karyokinesis without cytokinesis (Walsh et al., 2010). Additionally, this was endorsed through a high spatiotemporal resolution system that visualises cell division in live native CMs. During the late mitotic phase of the cell cycle, scaffolding protein anillin, a specific component of both the contractile ring and the midbody, was fused with enhanced GFP (eGFP).

The genes required to induce efficient division of CM involving cytokinesis and karyokinesis are unknown. The ability to manipulate these genes is critical to regulating CM proliferation. Therefore, several studies have focused on the cell cycle regulation of CMs. A study screened a series of cell cycle regulators during proliferation in mouse, rat and human fetal CMs, identifying an overexpression of four cyclins: cyclin-dependent kinase 1 (CDK1), - 4 (CDK4), cyclin B1 and cyclin D1 (Mohamed et al., 2018). The combination of these regulators causes post-mitotic CMs to re-enter the cell cycle, promoting proliferation and survival and improving cardiac function after MI (Mohamed et al., 2018). A chromatin-immunoprecipitation study showed that two transcription factors inhibited the cell cycle of CMs: *Meis1* and *Hoxb13*. In postnatal mouse CMs, a member of the three amino acid loop extension (TALE) family, *Meis1*, is responsible for the loss of CM's ability to regenerate. *Meis1-Hoxb13* double knockout (KO) mice showed a reactive CM cell cycle (Nguyen et al., 2020).

Instead, some studies have shown that post-MI mouse cardiac regeneration did not occur via re-entering the pre-existing myocytes cell cycle but from new CMs. Therefore, it has been suggested that post-ischemic injury, CM replenishment is mediated by adult stem/progenitor cells (Hsieh et al., 2007; Hsueh et al., 2014; Uchida

et al., 2013). Genetic fate-mapping studies using tamoxifen-dependent irreversible GFP⁺ CMs provide evidence that the percentage of GFP⁺ CMs in the border zone of MI is 15% lower than in sham-treated mice, indicating a regeneration from de novo CMs (Hsieh et al., 2007). Based on these data, in the heart of adult mammals, this new population (up to about 10% of host myocytes) can be augmented by therapeutic grafting and defined agents (Bergmann et al., 2009; Hsieh et al., 2007; Hsueh et al., 2014; Johnston et al., 2009; Smart et al., 2011; Smith et al., 2017). Despite these findings, which make the regeneration of the dormant adult mammalian heart plausible, the post-injury source of the newly formed CMs is still uncertain. Of at least equal importance, the biological and technical obstacles to clinically workable self-regeneration of the heart, which most commonly requires genetic manipulations, give renewed emphasis to alternative means of reducing cardiac muscle cell loss, including cell transplantation and cardioprotective therapies.

1.3 Cardiac regeneration and repair: from cell therapy to “cell-free” therapy

1.3.1 Evolution of cardiac regenerative therapy over the past two decades

Cardiac regenerative medicine aims to overcome the challenges faced by current MI treatments. It focuses on finding alternative strategies to treat MI and restore pump function by encouraging cardiac regeneration preventing CM death, promoting CM regeneration, and inducing cardiac self-repair. Cardioprotective therapy aims to prevent the extension of heart damage, while cardio-restorative treatment aims to restore normal cardiac function (Aurora & Olson, 2014; Banerjee, Bolli, & Hare, 2018; Fiedler, Maifoshie, & Schneider, 2014; Mercola, Ruiz-Lozano, & Schneider, 2011; Schneider, 2016; Uygur & Lee, 2016; Zhang et al., 2016).

Cardiac regenerative medicine has evolved over the past 20 years (Fig.1.4). The first generation of cardiac regenerative therapy used non-cardiac cells, such as bone marrow mononuclear cells (BMMNC), endothelial progenitor cells (EPC) and mesenchymal stromal cells (MSC). Although some benefits were observed, there was an inconsistency between preclinical and clinical results. The second generation of cell therapy targeted organ cells. In the heart, they include cardiac progenitor cells (CPCs), cardiac stem cells (CSCs), and human pluripotent stem cell-derived CMs (hPSC-CMs). Compared to the first generation, a generic beneficial improvement was observed despite the poor long-term cell retention. The next generation introduced a

cell-free therapy approach, focusing on the paracrine effects of growth factors, cytokines, chemokines, non-coding RNAs and extracellular vesicles.

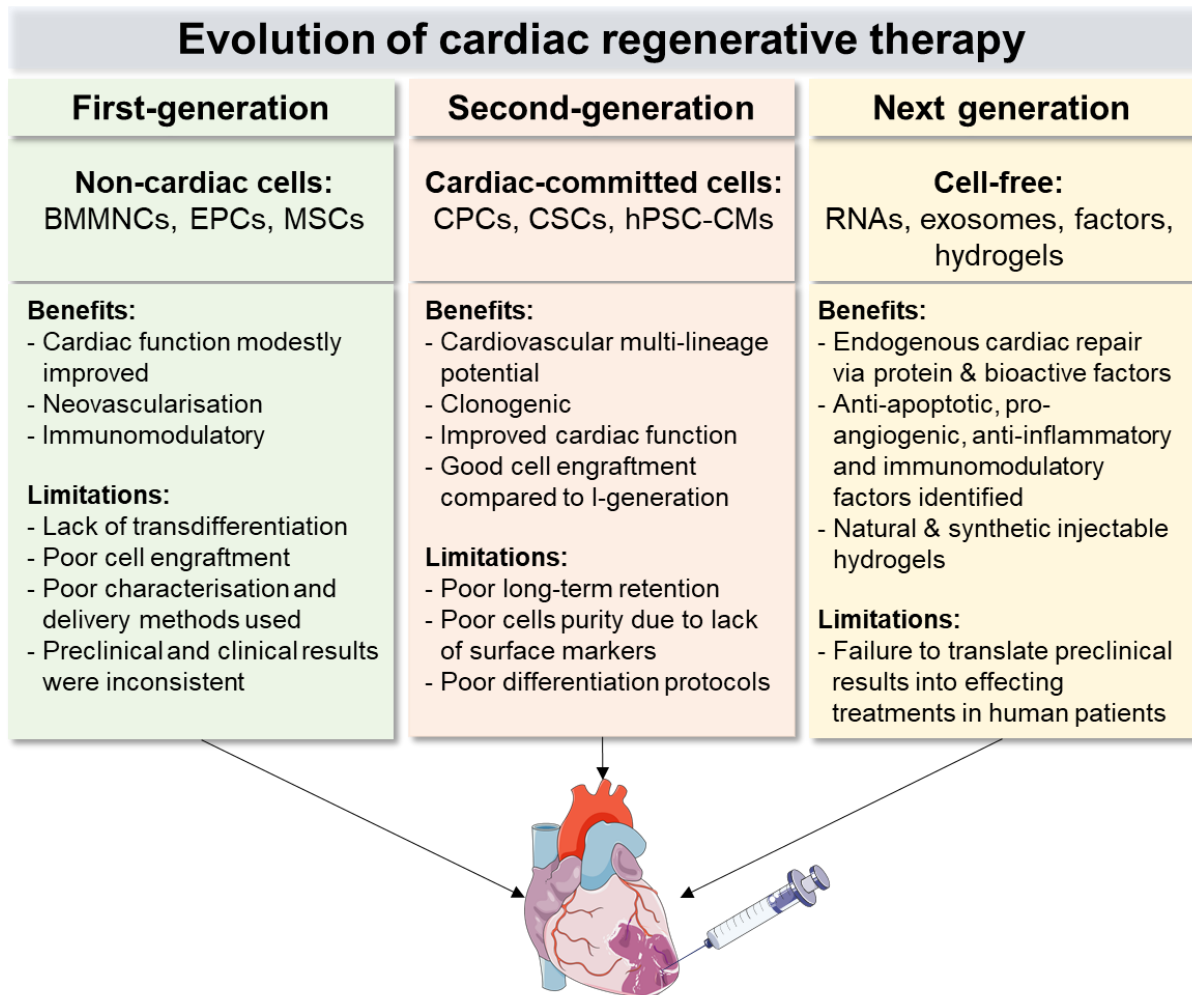


Figure 1.4 Illustration to summarise the evolution of cardiac regenerative therapy (Modified from (Le et al., 2017)) (<https://smart.servier.com/>).

1.3.2 The first generation of cell therapy: non-cardiac cells in the adult mammalian heart

The first generation of cell therapy using non-cardiac stem cells began with BMMNCs, demonstrating a modest improvement in heart function but without myocyte replacement, as first claimed (Jackson et al., 2001; Meyer et al., 2006; Orlic et al., 2002; Strauer et al., 2002). The results using BMMNCs, though likewise encouraging at first, were ultimately irreproducible by meta-analysis (Gyöngyösi et al., 2016; Kovacic & Fuster, 2001; Nguyen et al., 2016; Nowbar et al., 2014). Given this failure of the underlying therapeutic principle plus the lack of empirical benefit, the efficacy of other cell types was tested. After MI, a purified CD34⁺ population of ECP showed a beneficial impact on neovascularisation (Losordo et al., 2007, 2011; Mangi et al., 2003; Ruifrok et al., 2009; Van Ramshorst et al., 2009). In preclinical studies, MSCs transplantation was demonstrated to be beneficial. However, in the follow-up clinical trial (named POSEIDON), the negative correlation between MSC dosages and cardiac improvement raised concern in the scientific community (Hare et al., 2012; Hass et al., 2011; Huang et al., 2010; Williams & Hare, 2011). The main reasons for the negative results obtained in clinical trials were speculated to be how the non-cardiac/stem/progenitor cells were chosen, characterised, and delivered. Some of the observed limited benefits may be attributable to early spontaneous cardiac recovery post-MI (Behfar et al., 2014). Furthermore, the lack of standardised molecular markers or the formation of colony-forming units followed no practical standards. Therefore, it was impossible to guarantee these cells' uniform, efficient and functional power. (Dimmeler & Leri, 2008). In summary, the main challenges faced by the first generation of cell therapy were the lack of trans-differentiation capacity into cardiac myocytes and

the inconsistent cardiac benefits (Balsam et al., 2004; Chien et al., 2019; Mercola et al., 2011; Murry et al., 2004; Preda et al., 2014).

1.3.3 The second generation of cell therapy: cardiac stem/progenitor committed cells

In the second generation, the scientific community used cells that better resemble cardiac stem/progenitor cells to promote autologous regeneration. The main advantage of the second generation was the improved engraftment, albeit transiently, while the main challenge was identifying and characterising CSCs without knowing a specific and unique surface marker (Beltrami et al., 2001; Chong et al., 2011; Chong & Angeli, 2019; Martin et al., 2004; Matsuura et al., 2004; Messina et al., 2004; Nosedá et al., 2015; Nosedá et al., 2015; Oh et al., 2003; Oskouei et al., 2012; Oyama et al., 2007; Pfister et al., 2005; Smart et al., 2011).

The definition, origin, and complete molecular characterisation of dormant adult cardiac progenitor cells are unknown. Historically, these studies began with the use of the most well-known hematopoietic surface markers, such as the orphan receptor stem cell antigen 1 (Sca-1) (Hsueh et al., 2014; Matsuura et al., 2009; Oh et al., 2003; Uchida et al., 2013) and the receptor tyrosine kinase (c-kit) (Beltrami et al., 2003; Ellison et al., 2013; Kawaguchi et al., 2010). Then, various intracellular and functional markers followed, such as the side population (SP) dye-efflux phenotype but still without a definitive answer (Martin et al., 2004; Oyama et al., 2007; Pfister et al., 2005).

1.3.3.1 Sca1⁺ CSCs

Sca1 is one of the most investigated markers for defining mouse CSCs. The lymphocyte activation protein-6A (*Ly6a*) gene encodes for Sca1. *Sca1/Ly6a*-null mice studies showed that Sca1 regulates the developmental and self-renewal of hematopoietic stem cells (HSC) (Ito et al., 2003). *Ly6a* ablation experiments showed that Sca1 plays an essential role in HSCs and MSCs differentiation, migration, and proliferation (Bradfute et al., 2005; Holmes & Stanford, 2007; Ito et al., 2003; Stanford et al., 1997).

In 2003, Professor Michael Schneider's team isolated Sca1⁺ MSCs from adult mouse myocardium. Following treatment with 5'-azacytidine, cultured Sca1⁺ MSCs showed cardiomyocytes lineage potential by producing sarcomeric α -actin and cTnI and expressing Homeobox protein *Nkx-2.5*, α - and β -myosin heavy chain (α MHC and β MHC), and bone morphogenetic protein receptor type-1A (*Bmpr1a*). Furthermore, intravenous injections of cardiac Sca1⁺ cells in *Cre/loxP* (α MHC-*Cre/R26R*) mice undergoing ischemia/reperfusion (I/R) showed homing, differentiation and fusion of Sca1⁺ cells in the injured myocardium (Oh et al., 2003).

Engrafting experiments using lineage-tracing tools demonstrated that Sca1⁺ CSCs transplanted post-MI in mouse hearts delayed functional decline, attenuated LV remodelling, and increased neo-vascularisation (Bailey et al., 2012; Hsueh et al., 2014; Matsuura et al., 2009; Rosenblatt-Velin et al., 2011; Uchida et al., 2013; X. Wang et al., 2006; Ye et al., 2012). However, there are still questions about the mechanism

and role (if there is one) of Sca1⁺ cells in myocardial development, renewal and repair (Zhang et al., 2019).

Circulation has published five independent studies discussing the role of Sca1⁺ CSCs in cardiac repair. These studies showed that Sca1⁺ CSCs injected into the heart do not differentiate into CMs but towards the endothelial lineage. A table summarising the key findings in Table A1 (Appendix) (Lee, 2018). These five studies present three main limitations. First, none of these five studies worked with the same subpopulation of CSCs characterised by Nosedá and colleagues. Nosedá's CSCs expressed Sca1⁺ and the platelet-derived growth factor receptor alpha (PDGFR α ⁺) but did not express the endothelial marker platelet/endothelial cell adhesion molecule 1 (PECAM1, also known as CD31) (Nosedá et al., 2015). The Sca1/*Cre* deleter line and conventional *Rosa26*-driven, *Cre*-dependent reporter systematically fail to capture the entire population of Sca1⁺ CSCs in the heart. Instead, it skewed toward PDGFR α ⁻CD31⁺ endothelial precursors and omitted nearly all the PDGFR α ⁺CD31⁻ cells, the relevant sub-population expressing cardiogenic transcription factors. Secondly, although they questioned whether endogenous Sca1⁺ CSCs generate new CMs, these five studies did not claim to answer whether manipulation, expansion, and injection of these cells into the injured heart could lead to Sca1⁺-derived CMs. Finally, *in vivo* studies did not consider the possible adjustments Sca1⁺ cells could undergo following therapeutic stimulation. As discussed below, the developmental plasticity of CSCs, whether or not they have the potential to become CMs or ECs, is irrelevant, as this PhD thesis focuses on the beneficial effects that secreted paracrine factors might have. Therefore, this PhD thesis moved away from the idea that CSCs need to become CMs to enhance cardiac regeneration and repair.

1.3.3.2 Subpopulations of Sca1⁺ CSCs

The side-population (SP) dye-efflux phenotype: SP Sca1⁺CSCs

Ly6a lacks the human counterpart (Loughner et al., 2016), so other markers have been used to identify CSCs. The SP population is enriched in different tissues, but the mouse heart is 100-time richer than non-myocytes (Asakura & Rudnicki, 2002; Kim & Morshead, 2003; Montanaro et al., 2003; Summer et al., 2003; Wulf et al., 2003). Cardiac SP Sca1⁺ CSCs differentiate and proliferate, forming hematopoietic and cardiac lineages demonstrating multi-potency differentiation (Martin et al., 2004; Nosedá et al., 2015; Pfister et al., 2005).

CD31: SP Sca1⁺CD31⁻CSCs

A specific subpopulation of cardiac SP Sca1⁺ CSCs does not express CD31, SP Sca1⁺CD31⁻ CSCs can differentiate into SMCs, ECs and CMs (Martin et al., 2004; Matsuura et al., 2009; Nosedá et al., 2015; Oh et al., 2003; Oyama et al., 2007; Pfister et al., 2005). SP Sca1⁺CD31⁻ CSCs treated with single factors (e.g. oxytocin or trichostatin) formed sarcomere and differentiated into beating CMs. On the other hand, under osteogenic inducers, SP Sca1⁺CD31⁻ CSCs showed positivity for early osteocyte markers, while under adipogenic activators, they accumulated oil droplets in the cytoplasm, indicating differentiation into adipocytes (Oyama et al., 2007; Pfister et al., 2005).

The cardiac-resident colony-forming units-fibroblast (cCFU-Fs)

The third subpopulation of Sca1⁺ CSCs consists of adult cardiac-resident colony-forming units-fibroblast (cCFU-Fs) enriched for PDGFR α (Chong et al., 2011). During

embryogenesis and differentiation of ESCs, transcription factors of the heart (e.g. *Wt1* or *Isl1*) were used to identify CSCs (Laugwitz et al., 2008; Moretti et al., 2006; Smart et al., 2011). After MI, embryonic *Wt1* is re-expressed and activated via thymosin β 4 peptide, generating CMs *de novo* (Bock-Marquette et al., 2004; Smart et al., 2011).

Lin⁻*Sca1*⁺*CD31*⁻*PDGFR* α ⁺*SP*⁺ CSCs

Nosedá and colleagues combined two approaches to investigate CSCs heterogeneity using single-cell flow cytometry and clonal study (Nosedá et al., 2015). Flow cytometry allowed the purification of negative hematopoietic lineage (*Lin*) non-myocytes based on the expression of *Sca1* in adult mouse myocardium. The *Sca1*⁺ CSC population was then divided based on the *SP* phenotype and the mutually exclusive expression of *PDGFR* α against *CD31*. Therefore, *Lin*⁻*Sca1*⁺ CSCs were distinguished into two subpopulations: 25% were in *PDGFR* α ⁺*CD31*⁻ cells, while the rest were *PDGFR* α ⁻*CD31*⁺ cells (Nosedá et al., 2015) (Fig. 1.5 A).

Single-cell (sc) quantitative reverse transcription real-time PCR (sc qRT-PCR) revealed a mosaic of subsets of unknown genes using bulk analysis (Nosedá et al., 2015). *SP* cells represented 1-3% of the whole *Sca1*⁺ population, encompassing these two subpopulations (Nosedá et al., 2015; Oh et al., 2003; Oyama et al., 2007; Pfister et al., 2005). *PDGFR* α ⁺ cells do not express endothelial lineage markers, such as kinase insert domain protein receptor (*Kdr*), cadherin 5 (*Cdh5*), Von Willebrand factor (*Vwf*), or sarcomeric gene markers. On the other hand, *PDGFR* α ⁺ cells are enriched with genes encoding cardiogenic factors, including GATA-binding proteins 4 and 6 (*Gata4* and *Gata6*), myocyte enhancer factor 2A and C (*Mef2a* and *Mefc*), T-box 5 and 20 (*Tbx5* and *Tbx20*), and heart and neural crest derivatives expressed 2 (*Hand2*)

(Nosedá et al., 2015; Olson, 2006). CD31⁺ cells show opposite gene signature devoid of cardiogenic genes while expressing endothelial lineage markers (e.g. *Kdr*, *Cdh5*) (Nosedá et al., 2015). The CSCs described by Nosedá showed a divergent cardiogenic potential compared to previously described Sca1⁺ CSCs (Pfister et al., 2005) (Fig. 1.5 B).

Functionally, the double-positive phenotype SP and PDGFR α delimits a population of Lin⁻Sca1⁺ cells with an efficient clonogenic capacity of 30%. One year of culture propagation of Lin⁻Sca1⁺CD31⁻PDGFR α ⁺SP⁺ CSCs maintained a cardiogenic gene signature and lacked replicative senescence, as shown by senescence-associated β -galactosidase activity (Nosedá et al., 2015). Subsequently, 250,000 rigorously characterised mOrange-labelled Lin⁻Sca1⁺CD31⁻PDGFR α ⁺SP⁺ CSCs were injected intramurally at infarction. These engrafted cells showed trilineage EC, SMC and CM capabilities, presenting typical CM features, such as a rod shape, bi-nucleation and striation. Cell retention dropped dramatically from about 10% (day 1) to 0.1-0.5% (day 14), with only 10-20 cells persisting in the heart twelve weeks later (Nosedá et al., 2015).

As discussed above, recent fate-mapping studies have challenged the ability of endogenous CSCs to differentiate into new CMs (Lee, 2018). This PhD thesis considers these results, although the limitations of the experimental design call these conclusions into question. For these reasons, this specific subpopulation is referred to in this thesis most accurately as cardiac stromal cells (CSCs). This terminology is agnostic regarding cell fate as an endogenous population. After cardiac grafting, these cells demonstrate a cardiogenic potential while improving cardiac function (Fig. 1.5 C).

A series of magnetic resonance tomography (MRI) measurements demonstrated that CSCs delivery improved cardiac structure and function, with an increase in LVEF, reduction of LV remodelling, and an overall reduction of the infarct size from 45% to 35% (Nosedá et al., 2015). Paradoxically, in contrast to these enormous organ-level benefits, lasting engraftment was incredibly rare (0.002%). Subsequent studies using transwell co-culture and CSC's conditioned media experiments confirmed that CSCs secrete sufficient paracrine factors to protect mouse and human CMs from I/R injury and oxidative stress in culture, respectively (Constantinou et al., 2020). Together, these results suggest a potential early paracrine signal for cardioprotection mediates the organ-level benefit conferred by CSCs.

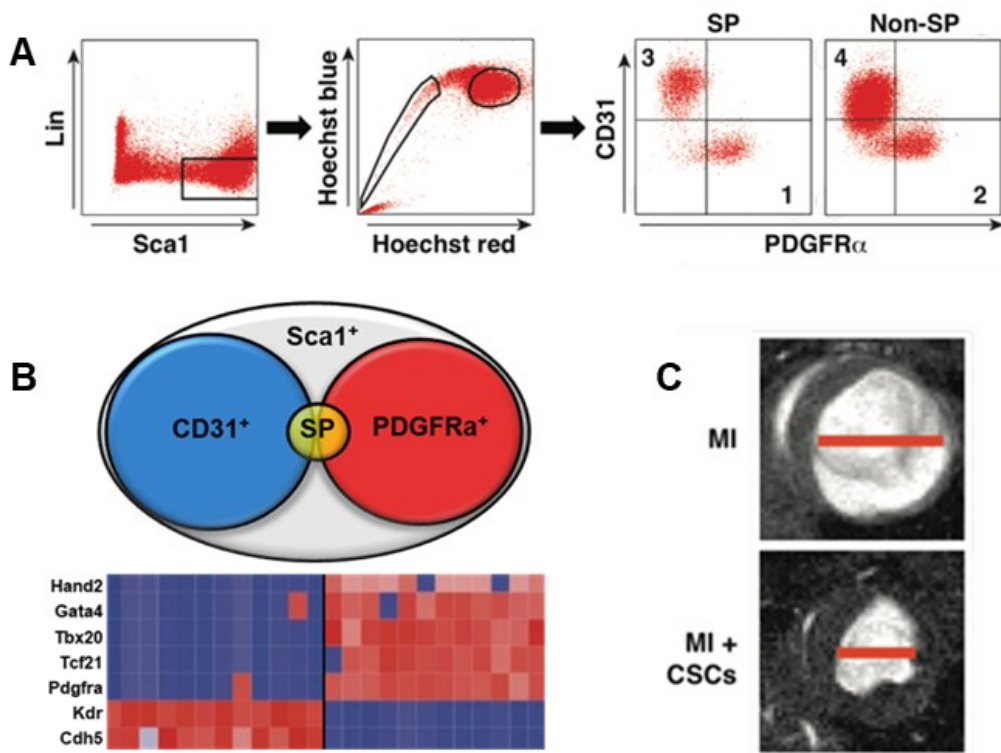


Figure 1.5 PDGFR α delimits Sca1⁺ CSCs.

A, Flow cytometry gating strategy to identify Lin⁻Sca1⁺CD31⁻PDGFR α ⁺SP⁺ CSCs. Mouse cardiac non-myocytes can be divided into four populations as indicated 1-4. **B**, Venn diagram maps Sca1⁺PDGFR α ⁺ versus Sca1⁺CD31⁺ (section 1-4 from **A**) shows that regardless of the SP classification, PDGFR α ⁺CD31⁻ cells are highly clonogenic. Sc qRT-PCR heatmap shows PDGFR α ⁺CD31⁻ cells express cardiogenic genes, while PDGFR α ⁻CD31⁺ cells are enriched for EC lineage markers. **C**, Twelve weeks later, CSCs injection into the infarct size, MRI showed prevented wall thinning, chamber dilation, double post-infarct ejection fraction, and reduced infarct size over time by 9.4 Tesla MRI (Modified from Nosedá et al., 2015).

1.3.3.3 Human clinical trials using CSCs

CSCs began to be used in human clinical trials, although their characterisation was not completed. As reviewed by Ptaszek and colleagues, early human clinical trials using CSCs transplants showed poor cardiac functional improvement due to poor cell retention of the transplanted cells (Ptaszek et al., 2012) (Table 1.1).

Table 1.1 **CSCs used in human clinical trials**

Clinical Trial	Patients	Autologous CSC	Administration method	Results	Issue	Reference
SCIPIO	16	c-kit, Atrial	Intracoronary injection	Scar reduction: 30% (at 1 year)	Retracted	(Bolli et al., 2011; Lancet, 2015)
CADUCEUS	17	Sca1, LV	Intracoronary injection	Scar reduction: 11% (at 1 year)	Negative effectiveness	(Makkar et al., 2012)
TICAP	14 ≤6-year	Atrial	Intracoronary injection	LVEF: 9%	PERSEUS (Phase 2)	(Ishigami et al., 2015)
ALCADIA	6	CD105 ⁺ CD90 ⁺	Transepicaldial	LVEF: 12.1±4.9%	No results posted	(Takehara et al., 2012)

Due to the limited number of participants in these studies, it was difficult to conclude the ability of the transplanted CSCs to improve cardiac function. Virtually all the proposed cell types lacked graft persistence in animal testing. This highlights the limitation in the conditions for cell delivery. Hence, preclinical studies show that cardiac functional improvements are more plausibly attributable to early paracrine effects rather than grafted cells becoming new myocytes. Therefore, finding appropriate approaches to regenerate CM lost after an injury is ongoing (Chimenti et al., 2010; de Couto et al., 2015; Hong et al., 2014; Li et al., 2012; Malliaras et al., 2013; Ong et al., 2015; Tachibana et al., 2017; Tang et al., 2016; Wang et al., 2006).

1.3.4 The next-generation of cell therapy: the paracrine hypothesis

The next generation of cell therapy moved toward a cell-free approach based on the hypothesis that paracrine mechanisms mediated functional effects. Despite low long-term cell retention, several studies have found similar beneficial improvements through the paracrine effects of transplanted CSCs. These studies used differently: animal models (e.g. mouse, rat, dog, sheep, pig, monkey and even work with human tissues); methods of administration (e.g. intramyocardial, intracoronary, and intravenous injection); and, types of donor cells (e.g. BMMNCs, CD34⁺ enriched BMMNCs, adipose-derived stem cells, Sca1⁺, c-kit⁺, SP Sca1⁺, CDCs, MSCs, and others). Cardiac functional recoveries with improvements in LVEF and LV function were observed in all of these studies (Chimenti et al., 2010; Gnechi et al., 2005; Hong et al., 2014; Kinnaird et al., 2004; Li et al., 2012; Malliaras et al., 2013; Nosedá et al., 2015; Wang et al., 2006).

CSCs differentiated into CMs showed secretion and induction of several molecules, including the soluble vascular cell adhesion protein 1 (sVCAM-1). Inhibition of its receptor, integrin $\alpha 4\beta 1$ (very late antigen-4) (VLA-4), induces EC and CSC migration, CM survival and amelioration of cardiac dysfunction (Matsuura et al., 2009). This is accompanied by improved cardiac function and the activation of endogenous progenitor CMs via secretion of stromal cell-derived factor 1 (SDF-1) (Malliaras et al., 2014). Post-MI, the paracrine effects from CSCs inhibit neutrophil infiltration, excess inflammation and oxidative stress via the junctional adhesion molecule-A (JAM-A) (Liu et al., 2014). Injection of exogenous CSCs into the mouse heart stimulates the heart to produce paracrine factors, such as angiopoietin-2 (ANGPT2), basic fibroblast

growth factor (bFGF), hepatocyte growth factor (HGF), insulin-like growth factor 1 (IGF-1), stromal cell-derived factor 1 (SDF-1) and vascular endothelial growth factor (VEGF) (Li et al., 2012). CSCs also secrete extracellular vesicles (EVs) containing microRNAs (miRNAs) (Barile et al., 2014; Gray et al., 2015; Ibrahim et al., 2014).

Sca1⁺ CSC and cardiosphere-derived stem cells (CDCs) compared to BM cells, and non-cardiac MSCs are functionally superior due to their paracrine potency (Li et al., 2012; Liu et al., 2014). Although long-term retention of CSCs in the recipient's heart is lacking, at least in the pre-clinical settings, cell transplant has been reported to improve cardiac function with significant benefits. Therefore, a strong consensus has emerged that the long-term benefits are likely to be mediated by early secretory mechanisms. The paracrine effects of transplanted cells have been reported to benefit several aspects of cardiac repair. The most relevant cardiac benefit elements are the following: CM's survival and proliferation, wound healing, angiogenesis, infarct regression, immunomodulation, activation of endogenous cardiac progenitor cells and enhancement of contractile function (Chimenti et al., 2010; Chong et al., 2011; de Couto, 2019; de Couto et al., 2015; den Haan et al., 2012; Gallet et al., 2017; Hong et al., 2014; Ibrahim et al., 2014; Kawaguchi et al., 2010; Li et al., 2012; Liu et al., 2014; Malliaras et al., 2014; Matsuura et al., 2004, 2009; Nie et al., 2018; Nosedá et al., 2015; Wollert & Drexler, 2010; Wysoczynski et al., 2017).

In conclusion, cell therapy for heart repair has undergone a recent paradigm shift. These emerging consensuses have created a new way to address cardiac regeneration from cell therapy to a 'cell-free' therapy. Paracrine factors secreted by CSCs could influence the fate of all cardiac cells. The cells shown to be affected by

CSCs are the following: CMs, resident cardiac stem cells, leucocytes, vascular cells, fibroblasts, conduction system, and immune cells, including monocytes and macrophages (Figure 1.6). Thus, early paracrine signals to the host milieu likely explain the extensive findings observed on the heart at the organ level. Among these potential targets, the specific role of macrophages in the heart will be discussed below.

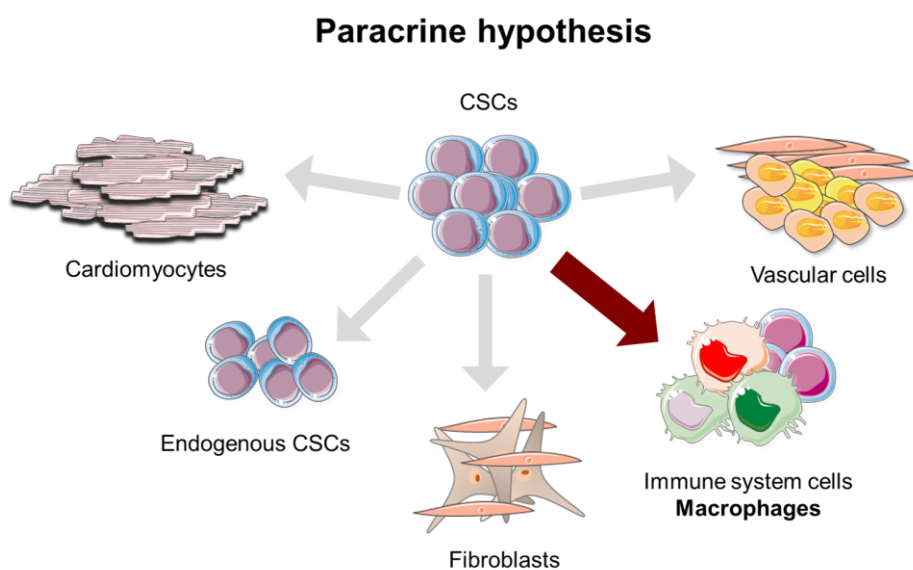


Figure 1.6 Next-generation of cell therapy: the paracrine hypothesis.

CSCs secrete many factors, such as growth factors, chemokines, cytokines, miRNAs, vesicles, etc., which modulate several functions, such as proliferation, differentiation, angiogenesis, and inflammation. Despite poor long-term retention, transplanted CSCs interact with heart cell types, CMs, ECs, endogenous CSCs, fibroblast, and immune cells, including monocytes and macrophages. (<https://smart.servier.com/>).

1.4 Mouse macrophages in the model of cardiac injury and regeneration

1.4.1 Mouse macrophages: from embryo to adulthood

Macrophages perform various functions, from maintaining tissue homeostasis to invading pathogens to tissue repair and remodelling (Biswas & Mantovani, 2012; Ensan et al., 2016; Gordon & Martinez, 2010; Mantovani et al., 2004; Sica & Mantovani, 2012). The classification of macrophages is complex and constantly evolving due to discoveries. The heterogeneity of macrophage phenotypes reflects the diversity of the tissue environment in which they reside (Gautiar et al., 2012). Knowing the origin of macrophages could help understand their functions.

Two distinct lineages classify tissue-resident macrophages, one derived from circulating monocytes and the other established during development (Ensan et al., 2016; Epelman et al., 2014; Lavine et al., 2014). In the late 1960s, van Furth and Cohn proposed that the primary sources of mouse tissue-resident macrophages were the circulating bone marrow-derived monocytes (BMDMs) (Furth & Cohn, 1968).

More recently, mouse embryonic studies revealed adult HSCs are the primary source of self-renewal-maintained macrophages. Embryonic established mouse resident macrophages derive from yolk-sac macrophages and foetal monocyte progenitors before forming HSC (Epelman et al., 2014; Morris, Graham, & Gordon, 1991; Pinto et al., 2012). Yolk-sac-derived macrophages grow independently, contributing to the

development of erythroblasts and megakaryocytes (Palis et al., 1999; Tober et al., 2006).

Embryonic progenitors transiently populate tissues during development in “development waves”. The first wave of development occurs between embryonic day 7 (E7) and day 9 (E9). Between E8 and E8.5, the first macrophages or primitive progenitors arise from erythro-myeloid progenitors (EMP) with myeloid lineage potential (Frame et al., 2013; Mass et al., 2016; Palis & Yoder, 2001). The foetal liver receives two consecutive progenitors during the second wave of development: EMPs at E9.5 and HSCs at E10.5/E11. At E9, EMPs begin to populate the foetus and liver following the onset of blood circulation and differentiate into monocytes (Hoeffel et al., 2015).

During development, the heart is enriched with two resident macrophage types: the first at E11.5, carrying primitive yolk-sac progenitors expressing low levels of CCR2 and low levels of major histocompatibility complex class II (MHC-II): CCR2^{lo}MHC-II^{lo}. The second wave at E14.5 is enriched for CCR2⁺MHC-II^{lo} macrophages (Ginhoux et al., 2010; Leid et al., 2016).

Studies using *Ccr2*^{-/-} embryos demonstrated the critical functional role in the coronary system development for CCR2⁻MHC-II^{low} macrophages related to epicardium, epicardial-derived cells and coronary endothelium (Leid et al., 2016; Stevens et al., 2016). CCR2⁻ macrophages express insulin-like growth factors 1 and 2 (*Igf1*, *Igf2*), potential macrophage-derived effector molecules that mediate coronary development (Leid et al., 2016). Moreover, CCR2⁻MHC-II^{lo} macrophages exist independently of the

circulating monocytes maintained during local proliferation (Stevens et al., 2016). On the other hand, the maintenance of CCR2⁺MHC-II^{low} macrophages depends on monocytes, which are associated with the endocardial surface (Leid et al., 2016).

Subsequently (around E15), through the newly developed blood vascular system, macrophages transit to the foetal liver, populating the BM, which is, therefore, the primary source of subsequent populations of monocyte and macrophage (Hoeffel et al., 2015; Stremmel et al., 2018). Between approximately E11 and E17.5, the primary source of tissue macrophages is foetal liver monocyte-progenitor cells up to the development of BM (Hoeffel et al., 2015). During the third wave of development, from about E17.5 to adulthood, haematopoiesis is the primary source of macrophage lineages in the tissues (Fig. 1.7).

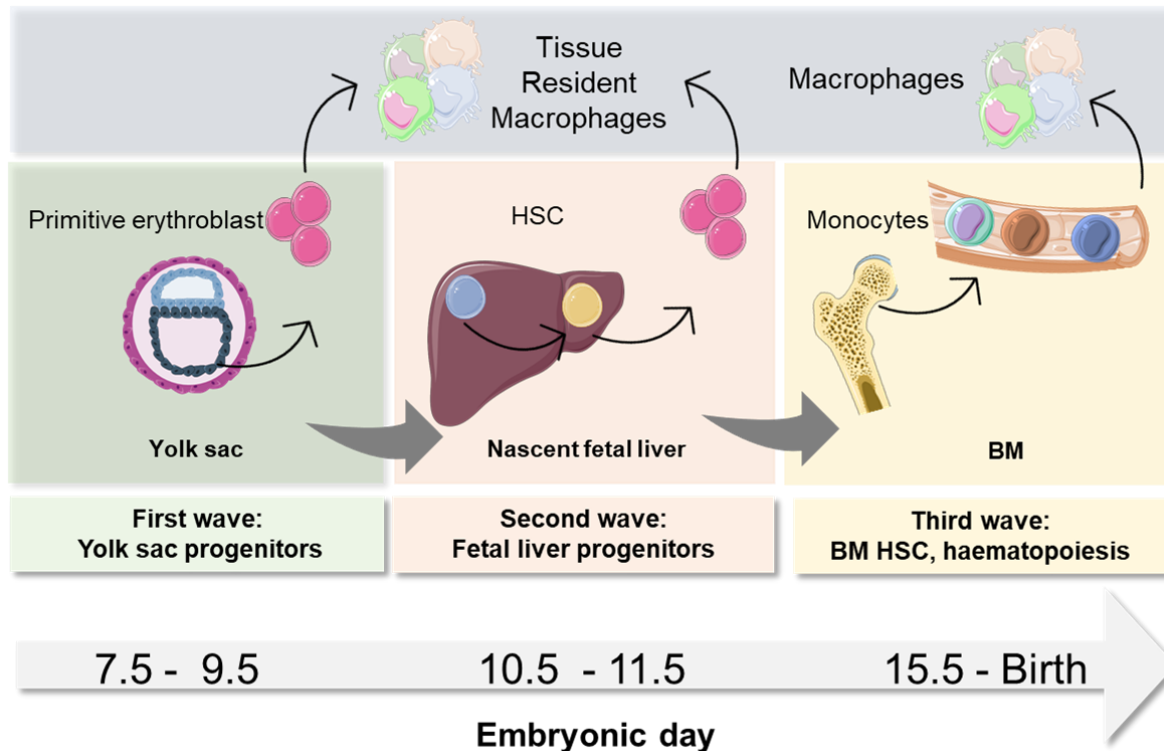


Figure 1.7 Developmental waves of mouse macrophages

Three waves of progenitor cells are responsible for seeding macrophages into the tissue: the first wave, yolk sac progenitors between E7 and E9. Monocyte-like cells populate the fetal liver (E11-17.5). The third wave begins around E15.5/E17.5 and continues into adulthood (haematopoiesis) (Modified from Williams et al., 2018) (<https://smart.servier.com/>).

After birth, the heart of the neonatal mouse exhibits two populations of CCR2⁻ macrophages. Within the first week, through embryogenesis, the “primitive” population deriving from the yolk sac is established (Lavine et al., 2014). Next, the “definitive” population expressing FMS-like tyrosine kinase three receptors (*Flk3*) is established (Boyer et al., 2011). The upregulation of *Flk3* results in a lack of self-renewal in the HSC. Hence, a lineage tracing study using *Flt3-Cre* mice demonstrated that HSC derived from *Flk3*⁺ progenitors (Boyer et al., 2011). In the arteries, embryonic yolk-sac macrophages arise from precursors expressing the fractalkine receptor called C-X3-C motif chemokine receptor-1- (CX3CR1) (Molawi et al., 2014; Pinto et al., 2012). The

survival of arterial macrophages is maintained by the interaction between CX3CR1 and its fractalkine ligand, C-X3-C motif chemokine ligand-1 (CX3CL-1) (Ensan et al., 2016). These interactions also promote survival in other organs and systems such as the brain (Boehme et al., 2000), kidneys (Lionakis et al., 2013), and even circulating monocytes (Landsman et al., 2009). Using tamoxifen-inducible recombinase Cre mice (CX3CR1^{Cre}) crossed with *R26-yfp* reporter mice, the genetic fate-mapping study showed that embryonic CX3CR1⁺ cardiac macrophages persist even in adulthood (Molawi et al., 2014).

In homeostasis, the primary source of adult cardiac resident macrophages is local proliferation rather than recruitment of circulating monocytes (Ensan et al., 2016; Epelman et al., 2014; Ginhoux et al., 2010; Guilliams et al., 2013; Hashimoto et al., 2013; Jakubzick et al., 2013). On the other hand, some studies have shown that HSCs (in the BM) differentiate into monocytes and are the source of the turnover of resident macrophages (Davies et al., 2013; Epelman et al., 2014; Hashimoto et al., 2013; Jenkins et al., 2011; Molawi et al., 2014). Interestingly, in adulthood, the sympathetic nervous system also regulates the proliferation of cardiac resident macrophages. The β 3-adrenergic receptors improve the re-entry into the cell cycle of extra-medullary haematopoiesis (Sager et al., 2016).

Macrophages have significant heterogeneity in origin, functions, molecular markers, and classification. Hence, understanding the similarities and differences of macrophage populations in more excellent resolution could help study them.

1.4.2 Macrophages classification

Macrophages are highly heterogeneous, with different functions based on microenvironmental stimulation. Therefore, their classification can be challenging. Originally, macrophages were classified according to the two activation pathways of type 1 and type 2 helper T-cells (Gordon, 2003). Hence, the separation into a pro-inflammatory pathway of “classical” activation with M1 macrophages, and an “alternative” anti-inflammatory pathway, with M2 macrophages. However, *in vivo*, macrophages are in continuous plasticity; they are subject to change depending on the surrounding environment, modifying their phenotypes in response to endogenous and exogenous signals, to the point that the M1 and M2 dichotomy does not possibly describe the phenotypes of macrophages (Becker et al., 2014; Kratochvill et al., 2015; Stables et al., 2017).

Classifying macrophages as M1 and M2 is a recognised oversimplification (Ginhoux et al., 2016; Xue et al., 2014) since they have been often classified using subtypes (e.g. M1a, M1b, M2a, M2b, M2c) (Ben-Mordechai et al., 2015). However, their classification is still contentions and partially confusing. The current challenge is to find a way to classify macrophages reflecting their multidimensional activation system, function (in development, homeostasis, diseases, inflammation and repair), and location (tissue organ specific versus circulating macrophages) (Ginhoux et al., 2016; Mosser & Edwards, 2008; Okabe & Medzhitov, 2016; Wynn et al., 2013).

Therefore, acknowledging that macrophages classification is moving away from a

dichotomy model toward a multi-dimensional description, this PhD thesis, in line with others (Ginhoux et al., 2016; Murray et al., 2014), proposes classifying macrophage phenotypes using the specific stimuli nomenclature.

The M1/pro-inflammatory and M2/anti-inflammatory macrophages should be interpreted as the two extremes of a continuum spectrum of possible phenotypes that macrophages assume. In line with previous publications, this system helps interpret macrophage activity when the focus is on studying the effects of macrophages' subpopulations *in vitro* (Biswas et al., 2012; de Couto, 2019; Frangogiannis, 2007; Gordon, 2003; Gordon & Taylor, 2005; Mantovani et al., 2004; Martinez & Gordon, 2014; Murray et al., 2014; Parisi et al., 2018; Sica & Mantovani, 2012; Xue et al., 2014).

The following paragraphs detail the environmental cues most responsible for altering the physiology of macrophages: growth and survival factors, activators and stimuli, gene expression signatures, secretome profiles, and surface receptor patterns.

1.4.2.1 Growth and survival factors

Growth and survival factors play a crucial role in the development and regeneration of the heart. Several cardiac cells secrete growth and survival factors, including CMs and immune cells. During an ischemic event, CMs secrete growth factors to improve cardiac remodelling and repair, promoting angiogenesis (Ellison et al., 2011; Hausenloy & Yellon, 2009; Ranganath et al., 2012).

Colony-stimulating factors (CSFs)

The most relevant growth factors implicated in the differentiation of monocytes into macrophages are the colony-stimulating factors (CSFs). There are three colony-stimulating factors, and they can be defined by their ability to differentiate BM progenitor cells into distinct types of myeloid cells. They have different roles during haematopoiesis, homeostasis and inflammation.

Monocyte-CSF (M-CSF/CSF1) is a hemopoietic growth factor implicated in the differentiation, proliferation, and survival of M2-like macrophages. On the other hand, granulocyte-macrophage-CSF (GM-CSF/CSF2) promotes neutrophils and eosinophils survival and monocytes differentiation into M1-like macrophages. Finally, granulocyte-CSF (G-CSF) regulates the differentiation and survival of neutrophils (Bonecchi et al., 2000; Chitu & Stanley, 2006; Delneste et al., 2003; Fleetwood et al., 2007, 2009; Frangogiannis et al., 2003; Hamilton, 2008; McLaren et al., 2011; Pixley & Stanley, 2004; Pollard et al., 1987; Smith et al., 1998; Stanley et al., 1978; Verreck et al., 2004).

CSFs are critical therapeutic targets for intervention in inflammatory, autoinflammatory, and autoimmune diseases. Data from cDNA microarray demonstrated that *in vitro* M-CSF stimulation of human BMDMs promotes macrophage differentiation. Microarrays meta-analysis confirmed that GM-CSF and M-CSF induce BM-derived cells to differentiate into the phagocytes system cells, opposite to dendritic cells (DCs) (Mabbott et al., 2010). The following paragraph (1.5) will further discuss the role of M-CSF on macrophages.

GM-CSF alone promotes the survival and proliferation of the hematopoietic lineage, including BMDMs (Hercus et al., 2009). Circulating GM-CSF levels are low until the onset of inflammatory stimuli. Studies on GM-CSF^{-/-} deficient mice confirmed that the hematopoietic cellular composition is unchanged in homeostasis, indicating that GM-CSF is not involved in their survival and maturation within this condition (Cebon et al., 1994; Cheers et al., 1988). Some exceptions include alveolar macrophages, whose functions are hampered in GM-CSF^{-/-} mice, indicating a specific interaction between GM-CSF activity and these subsets of macrophages (Paine et al., 2001). Peritoneal macrophages were also affected in these conditions, indicating a general role of GM-CSF in inflammation (L. Becker et al., 2012; Fleetwood et al., 2009).

Insulin-Like Growth Factor 1 (IGF1)

IGF1 is an anti-inflammatory polypeptide whose beneficial effects on cardiac development and disease have been extensively studied (Chao et al., 2003; Duerr et al., 1995; Gallego-Colon et al., 2015; Qiong Li et al., 1997). Following acute cardiac injury, IGF1 protects the ischemic myocardium, as demonstrated by reducing the death of CMs and necrosis induced by polymorphonuclear leukocytes (Buerke et al.,

1995). Several preclinical cell culture and animal models (e.g. MI mice, I/R rat, and culture rat myocytes) have demonstrated that IGF1 improves cardiac function. This occurs by preventing CMs apoptosis, inducing CMs survival and improving contractility (Buerke et al., 1995; Fabbi et al., 2015; Kawaguchi et al., 2010; Rupert & Coulombe, 2017; Troncoso et al., 2014).

IGF1 can reduce the expression of pro-inflammatory cytokines, such as IL-1 β and IL-6, while promoting anti-inflammatory molecules, such as IL-4 and IL-10 (Santini et al., 2007). IGF1 also shows the ability to promote: the regeneration of myocytes by inducing DNA synthesis in post-injury adult ventricular rat myocytes (Reiss et al., 1997); survival of CSCs, delaying cellular ageing by improving telomerase activity (Torella et al., 2004); MSCs survive, accelerating their growth when injected using an injectable hydrogel (Wang et al., 2010).

Clinical trials have shown that low plasma levels of IGF1 in chronic HF patients have deleterious effects, such as severe ventricular dysfunction, due to increased apoptosis of skeletal muscle cells (Anker et al., 2001; Niebauer et al., 1998). A rabbit model study of MI demonstrated that injection of BM stem cells (BMSC) and biotinylated IGF1 promotes cell therapy inhibiting CMs apoptosis while inducing specific cardiac proteins (Zhang et al., 2017). Thus, a pilot trial called RESUS-AMI demonstrated that despite a low dose of IGF1 injected intracoronary in ST-elevation myocardial infarction (STEMI) patients did not improve LVEF, a beneficial dose-related effect was observed (Caplice et al., 2018).

Growth differentiation factor 15 (GDF15)

Growth differentiation factor 15 (GDF15) is a biomarker of cardiometabolic risk (Blankenberg & Zeller, 2017). Serum levels of GDF15 are used to predict the progression of cardiac disease (Xu et al., 2006). In hypertrophic and dilated cardiomyopathies, GDF15 upregulation prevents CM apoptosis by various agents, including oxidative stress (Heger et al., 2010; Kempf et al., 2006; Xu et al., 2006; Zhang et al., 2015). Gene expression analysis demonstrated that GDF15 inhibits the M1-like phenotype of macrophages downregulating M1-related genes such as *Il6*, *Tnf α* and *Ccl2*. On the other hand, GDF15 promotes, through paracrine and autocrine effects, the M2-like phenotype of macrophages. In brown adipocytes, GDF15 upregulates the mannose receptor (*Mrc1*) and arginase (*Arg1*) (Campderrós et al., 2019; Jung et al., 2018).

1.4.2.2 Activators and stimuli of M1-like and M2-like macrophages

Lipopolysaccharide (LPS), interferon-gamma (IFN γ) and TNF α are standard stimuli to induce an M1-like macrophage phenotype (Bosisio et al., 2002; Frasca et al., 2008; Guha & Mackman, 2002; Mackman et al., 1991; Verreck et al., 2004). The main characteristics of the phenotype of M1-like macrophages are the following: the high ability to present the antigen, high levels of IL-12 and IL-23 expression, low level of IL-10 expression, opsonic receptors expression; reactive oxygen species production; and high levels of Toll-like receptor 4 (TLR4) expression.

On the other hand, the M2-like macrophage phenotype is characterised by low IL-12 and IL-23 expression levels and high levels of IL-10 and non-opsonic receptors. M2-like anti-inflammatory macrophages can be divided into three subtypes based on specific activation stimuli, pathways and functions. First, the M2a macrophages, activated by IL-4 and IL-13, correlate with the type II inflammatory response that promotes wound-healing and pathogen elimination. Single-use of IL-4 and IL-13 induce similar and partially overlapping gene expression signatures. Second, immune-regulatory M2b macrophages are considered the newest macrophage subtypes. They are activated by the exposure to IL-10 – via STAT3/IL-10R pathways, immune complexes (IC), or TLR ligands (e.g. LPS). They have generic anti-inflammatory characteristics but also pro-fibrotic activities. Finally, M2c macrophages are activated by IL-10 or glucocorticoids. They also correlate with immunoregulation, deposition of ECM, phagocytosis capacity and post-injury tissue remodelling (Gordon, 2002; Mantovani et al., 2004; Martinez et al., 2008; Scotton et al., 2005; Stein et al., 1992).

1.4.2.3 Gene expression of *Nos2* and *Arg1*

The best-established genes used as markers to distinguish M1-like and M2-like macrophages are nitric oxide synthase 2 (*Nos2*) and *Arg1*. These two enzymes compete for the same substrate, L-arginine. NOS2 metabolises L-arginine to nitric oxide (NO) and citrulline. NO is then further metabolised to reactive nitrogen species, while citrulline is reused in the citrulline-NO cycle for NO synthesis. Alternatively, Arginase 1 hydrolyses L-arginine to ornithine and urea. The arginase pathway limits the arginine available for NO synthesis. Moreover, ornithine can be used downstream

of polyamine and proline syntheses to maintain cellular proliferation and tissue repair pathway activity (Rath et al., 2014) (Fig. 1.8).

Macrophages change phenotypes by modifying arginine metabolism from ornithine production to NO, moving from tissue repair to engulfment activities. (Mills et al., 2000). The preference toward one of these two pathways polarises macrophages as M1-like or M2-like. Cytokines, such as IL-4 and IL-13, induce *Arg1* gene expression (Pauleau et al., 2004), while pro-inflammatory stimuli, such as IFN γ , induce *Nos2* (Pesce et al., 2009). Thus, there are higher levels of *Nos2* in M1-like macrophages and of *Arg1* in M2-like macrophages (Bronte & Zanovello, 2005; Das et al., 2010; Lawrence & Natoli, 2011).

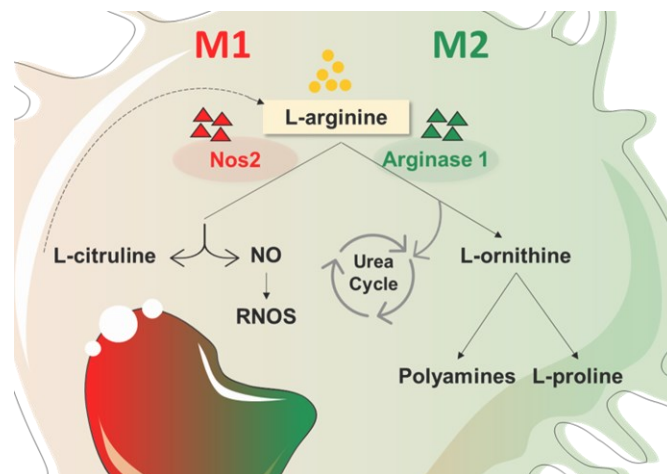


Figure 1.8 *Nos2* and *Arginase 1* compete for the same substrate: L-Arginine

Nos2 metabolises L-arginine and produces L-citrulline and NO, which leads to reactive nitrogen species (RNOS). Alternatively, *Arginase 1* metabolises L-Arginine to urea, which enters the urea cycle, and L-ornithine. The final products are L-proline and polyamines to support fibrosis and tissue remodelling (Modified from Bronte & Zanovello, 2005).

1.4.2.4 M1-like macrophage secretome profile

Macrophages secrete a series of molecules based on their phenotype. M1-like macrophages secrete pro-inflammatory cytokines, chemokines, growth factors, and metabolites (Gordon et al., 2014).

Cytokines are small proteins responsible for cell signalling interactions, including chemokines, interferons, and interleukins (ILs). Cytokines are secreted by immune cells and play a crucial role as modulators of the post-MI inflammatory response (Zhang & An, 2007). Chemokines are a family of over 50 small chemotactic cytokines (8-12kDa), characterised by their highly conserved four-cysteine motifs. All cytokines and chemokines can be grouped based on their functions. There are four subfamilies based on their N-terminal cysteine residues (Rollins, 1997; Szentes et al., 2018). CXC, or α -chemokines with the CXC chemokine receptors (CXCR); CC, or β -chemokines, with the CC receptors (CCR); C, or γ -chemokines; and CX3C chemokines with a single ligand, CX3CL1, and a receptor CX3CR1.

Pro-inflammatory cytokines and chemokines

LPS-stimulated M1-like macrophages activate the nuclear factor kappa-light-chain-enhancer of activated B cells (NF- κ B)-dependent transcription pathway. This induces the production of inflammatory chemokines, including C-X-C motif chemokine (CXCL) -1, 2, 3, 5, 8, 9, 19 and C-C chemokine ligand (CCL) -2, 3, 4, 5, 7, 11, 17 and 22 (Richmond, 2002).

LPS-stimulated macrophages release high levels of CXCL1 and CXCL2. CXCL2 and CXCL3 are angiogenic chemokines acting through their common receptor, CXCR2, attracting neutrophils into the inflammatory site (Frangogiannis, 2006; Sarmiento et al., 2011). CXCL1 and CXCL2 show 65% identical amino acid sequences, and their syntheses depend on TLR-dependent through the myeloid differentiation primary response 88 (MyD88). However, CXCL2 is also synthesised through an alternative pathway that uses the TIR-domain-containing adapter-inducing interferon- β (TRIF) (De Filippo et al., 2008). CXCL2 is important in neutrophil adhesion guidance through the MyD88 pathway, as demonstrated in the MyD88-deficient heart grafts study, in which WT/CCR2⁺ mice express higher levels of CXCL2 than MyD88 deficient mice (Li et al., 2016).

IFN γ plays an essential role in the innate and adaptive immune response, expressed by Th1 cells, NK, B cells and macrophages. The IFN γ molecular pathway includes activation of its receptor, followed by the phosphorylation of JAK-1 and -2, which then bind with STAT-1 activating STAT-2, inducing transcription interferon-stimulated responsive elements in its promoter region (Corbera-Bellalta et al., 2016). Blockade of IFN γ is linked with selective inhibition of CXCL9, CXCL10, and CXCL11 (Corbera-Bellalta et al., 2016). Interestingly, a study demonstrated that blocking IFN γ in macrophages did not impair the expression of *Nos2* – a primary M1 gene marker – identifying an IFN γ -independent pathway that can compensate for inducing an M1 gene signature (Corbera-Bellalta et al., 2016).

When LPS is combined with IFN γ , it induces the upregulation of CXCL9, -10 and CCL5 via activation of IRF-3 (Ito et al., 1999; Ohmori & Hamilton, 2001; Akira, 2003). CXCL-

9 and CXCL10, and CXCL11 bind to the same receptor, CXCR3. The CXCL9, -10, -11/CXCR3 axis regulates Th1 cells leading to migration, differentiation and activation of immune cells (Farber, 1997; Lee, Lee, & Song, 2009; Qian et al., 2015; Tannenbaum et al., 1998).

Pro-inflammatory cytokines and chemokines are also biomarkers of inflammation in advanced HF (Altara et al., 2016). Following ischemic/reperfusion, M1-like macrophages and Th1 cells are recruited to the site of inflammation and release CXCL10, which regulates the reparative response. CXCL10 expression is transient. CXCL10 is upregulated until dead cells and debris are cleared, while 24 hours after reperfusion, CXCL10 is downregulated to promote angiogenesis (Frangogiannis et al., 2001).

Interleukin-6 (IL-6)

IL-6 is a pleiotropic pro-inflammatory cytokine in cardiac disease. After MI, macrophages and CMs secrete IL-6, which affects the gene expression profiles of many other cardiac cells.

In the short-term post-acute cardiac damage, the primary roles of IL-6 are the promotion of inflammation, protection against CMs death, and modulation of tissue repair (Frangogiannis et al., 1998; Gwechenberger et al., 1999). However, long-term circulating levels of IL-6 are related to pathophysiological conditions, such as hypertrophy or reduction of the contractile function (Fontes et al., 2015; Rosen et al., 2014; Wollert et al., 1996). Hence, the duration of IL-6 signalling determines the final clinical outcome, shifting the role of IL-6 from protective to pathogenic (Tsutamoto et

al., 1998). Chronic exposure of IL-6 to the heart appears deleterious, while its activity in acute conditions showed beneficial effects on CMs. A clinical study with HF patients, BIOSTAT-CHEF, showed that elevated IL-6 levels are associated with a better clinical outcome, such as reduced LVEF, atrial fibrillation and iron deficiency (Markousis-Mavrogenis et al., 2019).

Interestingly, a study in IL-6-deficient mice demonstrated that IL-6 absence is unrelated to long-term MI size or LV function (Fuchs et al., 2003). IL-6 works through homodimerisation of the glycoprotein 130 receptor (gp130), initiating signal transduction through phosphorylation and activation of three main pathways: JAK/STAT3, SHP2/Gab/MAPK and the Phosphoinositide 3-kinase (PI3K) (Akira et al., 1990; Fukada et al., 1996; Ohtani et al., 2000; Su et al., 2017). Hence, in IL-6-null mice, these pathways may have been activated via alternative mediators. In neonatal rat studies, following acute injury, the cardioprotective capacity of IL-6 functions through both PI3K and NO-dependent signalling pathways. It regulates the concentration of Ca^{2+} in mitochondria, inhibits the mitochondrial membrane's depolarisation and protects the mitochondria's structural integrity (Smart et al., 2006).

Inhibin subunit beta A (Inhba) - Activin A

Inhibin subunit beta A (*Inhba*) encodes a preproprotein belonging to the TGF β superfamily: Activin A. Following a proteolytic cleavage, the preproprotein produces a subunit shared between the activin and inhibin protein complex. Activin A/Inhibin are factors with a pluripotent capacity (Sierra-Filardi et al., 2011). When stimulated with pro-inflammatory mediators stimuli, Activin A modulates the innate immunity, promoting the inflammatory response (K. L. Jones et al., 2007; Phillips et al., 2009;

Robson et al., 2008), increasing migration of mast cells, expression of mast cell protease 1 (mMCP1) (Funaba et al., 2003), and matrix metalloprotease-2 in peritoneal macrophages (Ogawa et al., 2000).

Activin A is also induced in monocytes via CD40 and T cell-derived cytokines (Abe et al., 2002). Interestingly, studies on Th cells demonstrated that Activin A activation produces Arginase1 (Ogawa et al., 2006). Hence, Activin A, which triggers Arginase 1 production, promotes an anti-inflammatory response while inhibiting the gene expression profile of IFN γ (Ogawa et al., 2006), indicating the critical role of Activin A in the polarisation of macrophages.

Mitogen-activated protein kinase kinase kinase kinase-4 (MAP4K4) and Tissue Factor (TF)

The mitogen-activated protein kinase kinase kinase kinase-4 (MAP4K4) is a ubiquitously expressed protein enriched in CMs, and its functions are cell-type dependent (Chuang et al., 2014; Fiedler et al., 2019). In mice and human CMs, MAP4K4 activates the transforming growth factor β -activated kinase-1 (TAK1, also known as MAP3K7) - c-Jun N-terminal kinase (JNK) pathway, which mediates cardiac muscle cell death or apoptosis (Fiedler et al., 2019; Xie et al., 2006). The involvement of MAP4K4 in immune responses, insulin resistance, and TNF- α activation has already been demonstrated in T-cell-specific conditional knockout (cKO) Map4k4 mice, where MAP4K4 deficiency induces upregulation of TRAF2 and IL-6 (Chuang et al., 2014; Mack et al., 2005).

Little is known about the role of MAP4K4 in macrophages. A study on mouse macrophages used a system for delivering small interfering RNA against MAP4K4

based on a glucan-based encapsulation. The selective silencing of the *Map4k4* gene and mRNA led to a decrease of 50% in TNF α and IL-1 β production. A new pathway of MAP4K4 has been discovered, which is insulin sensitive related to and independent of p38, JNK or ERK pathways (Aouadi et al., 2010). In M1-like macrophages, LPS is recognised by a transmembrane complex formed by TLR4 and the lipid-binding accessory protein MD-2 (TLR4-MD2) (Park et al., 2009), which recruits the TNF receptor-associated factors 2 and 6 (TRAF2 and TRAF6) leading to MAP4K4 activation (Poltorak et al., 1998). Inhibition of TAK1 in macrophages activated with LPS and IFN γ reduced the pro-inflammatory cytokines milieu, including TNF α (Scarneo et al., 2018). LPS – via MAP4K4 – induces the expression of several pro-inflammatory cytokines (e.g. TNF α , IL-1 β , IL-6, IL-10, IL-12) (Adams & Czuprynski, 1994; Gessani et al., 1989; Lee et al., 2000).

Tissue factor (TF, also known as factor III or F3) is a highly conserved transmembrane glycoprotein expressed in vascular and extra-vascular cells (Mackman et al., 1989; Wilcox et al., 1989). TF activates the extrinsic pathway of the coagulation cascade, which results in the production of thrombin (Iqbal et al., 2014; Steffel et al., 2006). In monocytes and macrophages, LPS, PDGF α , angiotensin II (Ang II), TNF α and oxidative low-density lipoprotein (oxLDL) can be used as inflammatory mediators to induce TF/F3 expression (Chung et al., 2007; Ernofsson & Siegbahn, 1996; Guha & Mackman, 2002; He et al., 2006; Lewis et al., 1995; Mackman et al., 1991).

After LPS stimulation, *TF* mRNA exhibits 2-hour stability, followed by a drastic decrease in mRNA levels (Brand et al., 1991; Crossman et al., 1990; Iqbal et al., 2014). The major protein involved in TF mRNA stability is Tristetraprolin (TTP). TTP exists in

two forms: phosphorylated (inactive) and dephosphorylated (active) (Iqbal et al., 2014; Iqbal, 2013). The critical equilibrium between these two forms of TTP is regulated upstream by the MAPK p38. The p38 pathway can be activated via different stimuli; among these, there are also pro-inflammatory mediators, such as LPS (Iqbal et al., 2014; Kagan et al., 2008; Keshet & Seger, 2010; Park et al., 2009; Poltorak et al., 1998; Sandler & Stoecklin, 2008). Although p38 is known to be a kinase downstream of MAP4K4, the signalling pathway linking MAP4K4 to p38 in *TF* regulation has not yet been characterised.

1.4.2.5 M2-like macrophage secretome profile

M2-like macrophages induce an anti-inflammatory protein profile while inhibiting the pro-inflammatory (Bonecchi et al., 1998; Cao et al., 2002; de Couto et al., 2015; Gordon & Martinez, 2010; Horner et al., 2000; Lumeng et al., 2007).

Interleukin-10 (IL-10)

In inflammation, IL-10 regulates different pathways to preserve damaged tissue. In LPS- or immune cell-activated macrophages, IL-10 strongly inhibits pro-inflammatory cytokines and chemokines production (Moore et al., 2001; Perrier et al., 2004; Sozzani et al., 1998). IL-10 downregulates the NF- κ B pathway and the activities of the signal transducer and activator of transcription 1 (STAT1) and STAT3. By inhibiting STAT1 phosphorylation, IL-10 prevents the production of two primary pro-inflammatory proteins whose expression is LPS-dependent, CXCL9 and CXCL10 (Ito et al., 2003; Ito et al., 1999; Lang et al., 2002; Li & Verma, 2002; Riley et al., 1999). Interestingly, M2b macrophages stimulated with LPS assume an antitoxic protective role of LPS by

expressing high levels of IL-10 and low levels of IL-12 (Mosser, 2003; Mosser & Karp, 1999).

A genome-wide analysis demonstrated that the IL-10 role is more than just an LPS inhibitor of macrophages and DCs function (Perrier et al., 2004). Human monocyte-derived DCs stimulated with IL-10 alone or combined with LPS express four different transcriptional programs, including a unique cluster expressed by combining these stimuli. The analysis of these IL-10/LPS induced or suppressed genes revealed inflammation inhibition by promoting tissue remodelling (Perrier et al., 2004).

Monocyte chemoattractant protein-2 (CCL2)

CCR2 expressed on the surface of circulating monocytes binds CCL2. The CCR2-CCL2 axis is responsible for migrating monocytes to the site of inflammation. However, oxygen availability is a critical factor in regulating chemotactic activities, and following MI, necrotic cardiac tissue has less than 1% oxygen. This hypoxia condition directly affects the production of the *Ccl2* transcript and its encoded protein (Bosco et al., 2004; Grimshaw & Balkwill, 2001; Turner et al., 1999). Excessive activity of CCL2⁺ monocytes has undesirable effects on cardiac tissue repair (Morimoto & Takahashi, 2007). Therapeutic studies on siRNA silencing in inflammatory mouse monocytes demonstrated a reduction in infarct size due to the degradation of CCR2 (Leuschner et al., 2011). However, cell culture experiments showed that CCL2 protects mouse myocytes from hypoxia by inhibiting myocyte apoptosis (Morimoto et al., 2008; Tarzami et al., 2005).

Interestingly, the CXCR4 receptor increases its chemotactic activities in a hypoxia-

dependent pathway. There is a reciprocal modulation between CCL2 and CXCR4 in monocytes trafficking within hypoxic tissues (Schioppa et al., 2003).

Transglutaminase 2 TGM2

Transglutaminase 2 (TGM2) is a multifunctional enzyme implicated in several cell functions. TGM2 regulates the migration of macrophages through β 3-integrins and syndecans and promotes their differentiation (Akimov et al., 2000; Akimov & Belkin, 2001; Nadella et al., 2015; Scarpellini et al., 2009; Telci et al., 2008; Thomas-Ecker et al., 2007; Wang et al., 2010, 2012; Wang & Griffin, 2012). TGM2 also regulates the ability of macrophages to engulf apoptotic cells. Following the engulfment of an apoptotic cell, macrophages release anti-inflammatory cytokines while hindering the pro-inflammatory response to avoid an autoimmune reaction (Gregory & Devitt, 2004; Grimsley & Ravichandran, 2003; Hochreiter-Hufford & Ravichandran, 2013; Martinez & Gordon, 2014; Röszer et al., 2011; Savill et al., 2002).

Vascular endothelial growth factor A (VEGFA) and Angiopoietin 2 (ANGPT2)

Angiogenesis and lymphangiogenesis are crucial in cardiac repair, regeneration, and remodelling after MI (Frangogiannis, 2008). Neovascularization supplies nutrients and oxygen to the infarcted site; however, pathophysiological vessel growth has an adverse clinical outcome (Jetten et al., 2014). Circulating monocytes infiltrate damaged heart tissue via post-capillary venules and release pro-and anti-angiogenic growth factors (Bruce et al., 2014) (Table 1.2).

At the infarcted site, BMDMs secrete the vascular endothelial growth factor A (VEGFA) to induce angiogenesis (Stockmann et al., 2011) (Table 1.2). M1- and M2-like

macrophages are present in the early phase of tissue repair, while in the late stage, M2-like macrophages are predominant (Willenborg et al., 2012). A tissue engineering study implanted collagen scaffolds in the tissue of mice for ten days and confirmed that both M1- and M2-like macrophages are needed to achieve vascularisation. M1-like macrophages coordinate capillary growth while M2-like macrophages stabilise the vessels (Spiller et al., 2014). Additionally, a study tested the combined use of tissue engineering with the paracrine effects of co-delivering M-CSF and VEGFA-A. The results demonstrated an improvement in angiogenesis and pericytes recruitment. Thus, promoting M2-like macrophages via M-CSF stabilises vascularisation (Hsu et al., 2015).

Table 1.2 Identified pro- and anti-angiogenic factors secreted by BMDMs

Pro-angiogenic factors	
Ang-2	(Felcht et al., 2012; Hubbard et al., 2005; Zheng et al., 2014)
Angiotropin	(Hockel et al., 1987, 1988)
CCL2/MCP1	(Deshmane et al., 2009; Jung et al., 2015; Stamatovic et al., 2006)
GM-CSF G-CSF	(Kuwahara et al., 2014; Lee et al., 2005; Natori et al., 2002; Root & Dale, 1999; Shi et al., 2006; Tura et al., 2010)
IGF-1, -2	(Björndahl et al., 2005; Suh et al., 2013; Sunderkötter et al., 1991)
IL-1α, -β	(Voronov et al., 2003; Watari et al., 2014)
IL-6	(Bryant-Hudson et al., 2014; Fan et al., 2008)
PDGF	(Sato et al., 1993)
TGF-α, -β	(Ferrari et al., 2009; Sunderkötter et al., 1991)
TNF-α	(Leibovich et al., 1987; Riabov et al., 2014)
VEGF A	(Nowak et al., 2008; Wu et al., 2010)
Anti-angiogenic factors	
Angiostatin	(Falcone et al., 1998; Matsunaga et al., 2002)
IL-10	(Wu et al., 2010)
TSP-1, -2	(Cursiefen et al., 2011; Ferrari et al., 2009; Fordham et al., 2012)
VEGF Ab	(Nowak et al., 2008)

Within the first few hours post-MI, macrophages release angiopoietins that regulate the maturation and stability of the neovascular system. Angiopoietin 1 and 2 (ANGPT1 and ANGPT2) are antagonists. ANGPT1 inhibits angiogenesis, while ANGPT2 promotes angiogenesis by activating ECs and inducing the expression of angiogenic factors, such as VEGF α (Augustin & Koh, 2017; Felcht et al., 2012; Kim et al., 2007). During inflammation and hypoxia, ANGPT2, VEGF α and other angiogenic chemokines (CD206, IL8, CXCL10, TGF β) work in synergy (Fiedler et al., 2006; Frangogiannis et al., 2001; Lee et al., 2000).

Only M2-like anti-inflammatory and pro-reparative macrophages secrete angiogenic-related factors (Ferraro et al., 2019; Jetten et al., 2014). Therefore, ANGPT2 is considered an attractive therapeutic target in CVDs due to its ability to ameliorate hypoxia and inflammation following cardiac damage (Lee et al., 2018).

Prostaglandin E Synthase (PTGES)

Prostaglandin E Synthase (PTGES) is an immunomodulator for cardiac injury. In cultured human DCs, PTGES works synergistically with TNF α , inducing elevated IL-12 and IL-23 levels. IL-23 induces the release of other pro-inflammatory cytokines (e.g. IL-17), showing the pro-inflammatory capacity of PTGES (Rieser et al., 1997). However, whole blood culture experiments demonstrated that PTGES inhibits IL-12 produced by LPS stimulation. In contrast with its pro-inflammatory activities, PTGES disrupts IL-6 production while doubling IL-10 levels (van der Pouw Kraan et al., 1995). Similarly, in a mouse study in which macrophages were treated with LPS, PTGES inhibited the production of TNF α and IL-6. Reduced TNF α and IL-6 expression levels were inversely proportional to IL-10 immunoreactivity levels. These results indicate

that PTGES plays an anti-inflammatory role in LPS-stimulated macrophages and produces, throughout an autocrine pathway, high levels of IL-10 (Strassmann et al., 1994). PTGES also inhibits the production of CCL3 and CCL4 in DCs treated with LPS (Jing et al., 2003), reinforcing the bivalent activity of PTGES as an anti-inflammatory molecule. In the early stage of MI, a balanced number of macrophages is essential for resolving cardiac inflammation and healing. The role of PTGES as an immunomodulator is crucial in regulating levels of both pro-inflammatory and anti-inflammatory macrophages.

1.4.2.6 Surface receptor expression pattern in M1-like and M2-like macrophages

Macrophages express different receptors based on their function and phenotype. The CCR2-CCL2 axis is involved in the initial recruitment and migration of blood monocytes in inflammation (Mantovani et al., 2004). There are two populations of monocytes: CX3CR1^{hi}CCR2^{lo} monocytes, precursors of tissue-resident macrophages, in the non-inflamed tissue, while CX3CR1^{lo}CCR2^{hi} monocytes are enriched in the inflamed tissues (Geissmann et al., 2003).

M1-like macrophages express low CCR1, CCR2 and CCR5 and high levels of opsonic receptors (Mantovani, 1999; Mantovani et al., 2001; Sica et al., 1997). GM-CSF activates a series of proteins involved in other M1-like pathways, such as STAT5, extracellular signal-regulated kinase (ERK), V-Akt murine thymoma viral oncogene homolog 1 (AKT) and NF-κB and the transcription factor IFN regulatory factor-5 (IRF5)

(Hansen et al., 2008; Krausgruber et al., 2011).

Following MI and cardiomyopathy, the expression of cardiac TLRs increases (Frantz et al., 1999). TLRs are a family of type I transmembrane receptors characterised by an extracellular amino terminus involved in pro-inflammatory pathways. To date, ten receptors have been identified in humans (TLR1-TLR10) and thirteen in mice (TLR1-TLR13) (Nie et al., 2018; Tabeta et al., 2004). TLR2 and TLR4 are the primary mediators of infarction signals (Arslan et al., 2010; Oyama et al., 2004; Timmers et al., 2008). Surgical ligation of the left anterior descending coronary artery on TLR2 KO mice demonstrated that TLR2 modulates fibrotic tissue deposition and remodelling of the LV (Shishido et al., 2003). LPS activation can be regulated by a TLR4-dependent and independent pathway, leading to inflammasome activation (Hagar et al., 2013; Kayagaki et al., 2013). An I/R study in mice demonstrated that TLR4 mediates the pro-inflammatory response of macrophages, indicating that TLR4-deficient mice reduce infarct size and have a lower inflammatory response to heart damage (Oyama et al., 2004).

On the other hand, M2-like macrophages have abundant non-opsonic receptors (e.g. CD206) and IL-1RII and IL-1Ra. Mouse and human resident macrophages, including cardiac resident macrophages, express elevated levels of CD206 (Dupasquier et al., 2006; Murray, Allen, Biswas, Fisher, Gilroy, Goerdt, Gordon, Hamilton, Ivashkiv, Lawrence, Locati, Mantovani, Martinez, Mege, Mosser, Natoli, Saeij, et al., 2014; Porcheray et al., 2005; Svensson-Arvelund et al., 2015; Titos et al., 2011; Zeyda et al., 2007). CD206 levels are elevated without anti-inflammatory stimulation, indicating that the tissue environment promotes its expression (Dupasquier et al., 2006).

A study of *Cd206*^{-/-} mice in lung inflammation demonstrated that the absence of CD206 induced migration of circulating monocytes to the inflammatory site and increased serum pro-inflammatory cytokine levels. Lee and colleagues interpreted this finding as showing a critical role for CD206 in controlling inflammation through the clearance of pro-inflammatory mediators (Kambara et al., 2015; Lee et al., 2002). Interestingly, human CD206⁺ macrophages also promote fibrosis, producing TGFβ and CCL18 (Bellón et al., 2011).

The IL-1 receptor (IL-1R) and TLR family regulate inflammation by producing a broad spectrum of cytokines and chemokines. Interleukin 1 receptor-like 1 (IL-1RL1)/IL-33 signalling activates M2-like macrophages and the production of Th2-related cytokines and chemokines, indicating their role in Th2-associated immunological response. Administration of IL-33 promotes an increase in IL-4 and IL-13 (Kurowska-Stolarska et al., 2009; Schmitz et al., 2005). Compared to M1-like macrophages, M2-like macrophages inhibit the production of IL-1 and TLR4 (Bosisio et al., 2002; Dinarello, 1991; Mantovani et al., 2002). M1-like macrophages upregulate the IL1R1 (Mantovani et al., 2002), while M2-like macrophages upregulate IL-1RII and IL-1ra and inhibit IL-1. Hence, the IL-1 system components are differentially regulated by the M1-like and M2-like macrophages.

1.4.3 Role of tissue-resident macrophages in the healthy heart

Cardiac resident macrophages, accounting for 6-8% of the total population of non-myocyte in the heart, contributes to cardiac homeostasis. Primarily, macrophages regulate immune surveillance through phagocytosis and activate the adaptive immune system through the MHC class II (Aurora et al., 2014; Epelman, Lavine, et al., 2014; Epelman et al., 2014; Frangogiannis, 2015; Perdiguero et al., 2015; Hashimoto et al., 2013; Heidt et al., 2014; Italiani & Boraschi, 2014; Murray & Wynn, 2011; Pinto et al., 2016, 2012; Yona et al., 2013).

Furthermore, optogenetic methods showed that connexin 43-expressing macrophages also contribute to electrical conduction in the heart. Connexin 43-expressing macrophages were found around the atrioventricular node, where they depolarise in synchrony with the CMs, accelerating the repolarisation of CMs and facilitating electrical conduction (Hulsmans et al., 2017).

Recently, single-cell technology identified new transcriptional profiles of macrophages (Buenrostro et al., 2018; Gorman et al., 2018; Lavin et al., 2017; Winkels et al., 2018). Single-cell RNA sequencing (scRNA-seq) identified two key surface markers, CCR2 and MHC-II, to distinguish adult macrophage populations. Adult mouse macrophages are classified accordingly to the expression levels of CCR2 and MHC-II into three populations: CCR2⁻MHC-II^{low}, CCR2⁻MHC-II^{high}, CCR2⁺MHC-II^{high} (Epelman et al., 2014; Heidt et al., 2014; Hulsmans et al., 2017; Lavine et al., 2014). The proliferation of embryonic CCR2⁻ macrophages is independent of circulating monocytes. On the

contrary, the proliferation of CCR2⁺ macrophages depends on circulating monocytes (Lavine et al., 2014; Molawi et al., 2014),

The role of CCR2⁻ macrophages during development is well defined, while their function is still unclear in the healthy adult heart. Overall, both CCR2⁻MHC-II^{low} and CCR2⁻MHC-II^{high} macrophages are considered reparative cells. They express low levels of inflammatory molecules and exhibit phagocytosis and pro-angiogenic characteristics including the expression of pro-angiogenic molecules, e.g. IGF 1 (Epelmann et al., 2014; Lavine et al., 2014; Leid et al., 2016). Conversely, in post-MI inflammation, CCR2⁺ macrophages expressing pro-inflammatory molecules regulate immune cell infiltration (Lavine et al., 2014; Ridker et al., 2017).

1.4.4 Role of macrophages in ischemic cardiac damage

In the early post-MI phase, the heart produces danger-associated molecular patterns (DAMPs) and pro-inflammatory molecules to recruit and activate the innate immune system (Arslan et al., 2011; Bianchi, 2007; Cekic & Linden, 2016; Crowther et al., 2001; Dobaczewski et al., 2010; Huebener et al., 2008; Lewis & Pollard, 2006; Osterloh et al., 2007; Sager et al., 2015; Sunderkotter et al., 1994; Timmers et al., 2012). The immune system recognises DAMPs through TLRs, mannose, purinergic and scavenger receptors (Lavine et al., 2018; Osterloh et al., 2007; Silverstein & Febbraio, 2009). Highly potent monocyte-chemoattractants are overexpressed within the first 24 hours, including CCL2 (Dewald et al., 2005). CCL2^{-/-} mice showed reduced infiltration of monocytes in the infarcted tissue (Dewald et al., 2005; Heidt et al., 2014; Hilgendorf

et al., 2014). Circulating monocytes migrate across the endothelium to the infarcted site to proliferate and differentiate into BMDMs (Nahrendorf & Swirski, 2013). The early phase is dominated by monocytes expressing Ly6C and CCR2 and low levels of CX3CR1 (Ly6C^{hi}CCR2⁺CX3CR1^{lo}) (Hilgendorf et al., 2014). Although BM and blood are the primary reservoirs of monocytes, Swirski *et al.* demonstrated that spleen monocytes accumulate in damaged tissue during ischemic injury and contribute to healing (Swirski, 2009). Experiments using MI as a disease model showed that the presence of Ly6C^{hi}-monocytes induces an increase in pro-inflammatory cytokines, such as IL-1 α , IL-6, and TNF- α (Nahrendorf et al., 2007).

In the later phase of post-MI inflammation (between days 4 and 7), anti-inflammatory or reparative monocytes were observed expressing low levels of Ly6C and CCR2 and high levels of CX3CR1 (Ly6C^{lo}CCR2⁻CX3CR1^{hi}) (Troidl et al., 2009). However it has not been determined whether Ly6C^{lo} monocytes are derived directly from Ly6C^{hi} monocytes or independently recruited via CX3CR1 (Frangogiannis, 2015; Hilgendorf et al., 2014; Nahrendorf et al., 2007).

During inflammation, the leading role of BMDMs is the clearance of debris and dead cells. Macrophages-depleted mouse models showed that macrophages use a specific form of phagocytosis, called efferocytosis, to remove necrotic and apoptotic CMs (Aurora et al., 2014; Frantz et al., 2013; Van Amerongen et al., 2007). There are three signals and processes involved in efferocytosis: the "find me" signals released by the apoptotic cells, the "eat me" signals exposed on the surface of the apoptotic cells, and the formation of the efferosome, a specific form of the phagosome used to internalise apoptotic cells. CMs undergoing apoptosis expose phosphatidylserine (PtdSer) as an

“eat me” signal on the outer leaflet of the cell membrane (Abdolmaleki et al., 2018; Grimsley & Ravichandran, 2003) (Fig. 1.9). Enhanced efferocytosis of apoptotic CMs demonstrated that tissue clearance is an essential step in inflammation resolution and cardiac healing (DeBerge et al., 2017; Howangyin et al., 2016; Wan et al., 2013). IL-4 is responsible for macrophage fusion and decreases phagocytic capacity (Martinez et al., 2013). IL-4 also induces the expression of *Tgm2*, a novel M2-like macrophage marker that controls efferocytosis (Martinez et al., 2013). Inhibition of TGM2 blocks phagocytosis and promotes the pro-inflammatory phenotype of macrophages (Eligini et al., 2020).

Overall, the repair of damaged heart tissue is a time-dependent process. In the early post-MI phase, M1-like macrophages are more abundant, promoting inflammation, clearance of necrotic cells and ECM debris (Frangogiannis, 2015; Hart et al., 1989), while during the later phase of inflammation, there is a shift towards a higher proportion of M2-like macrophages (Frantz et al., 2013). This shift promotes ECM reconstruction and scar formation by stimulating cell proliferation and angiogenesis (Song et al., 2000; Sunderkötter et al., 1991).

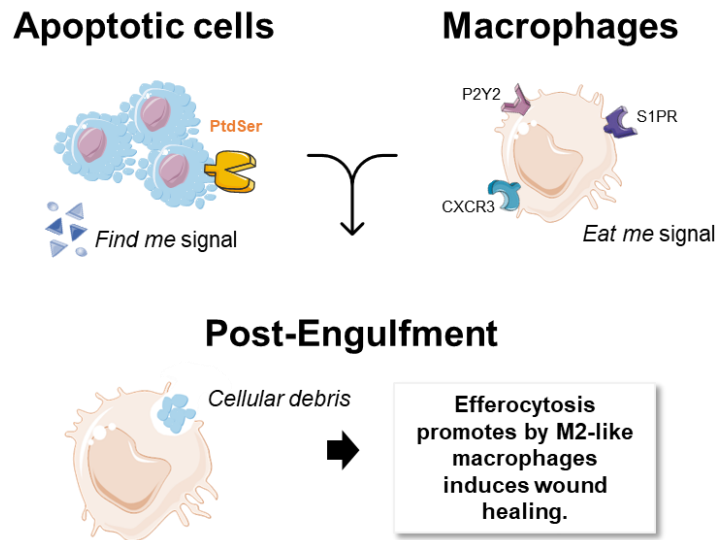


Figure 1.9 Phagocytosis of apoptotic CMs

Apoptotic cells release “find me” signals recognised by the “eat me” signals exposed on the surface of macrophages. Their binding induces apoptotic cells’ internalisation through efferosome formation (Modified from Asare et al., 2020) (<https://smart.servier.com/>).

1.4.5 Single-cell genomics to explore macrophage phenotypes

Gene expression has traditionally been studied using Northern blotting and quantitative PCR for pre-selected genes and microarrays or bulk RNA sequencing for unbiased, transcriptome-wide coverage. However, bulk analysis obscured populations with high levels of heterogeneity (Paik et al., 2020). The new era of gene expression is cell-centred, as observed by many studies using a single-cell point of view. The single-cell approach began with transcript analysing using qRT-PCR (Bengtsson et al., 2005; Eberwine et al., 1992; Warren et al., 2007). The first studies that employed a single-cell approach focused on the development and solid cancers (Dalerba et al., 2011; Deng et al., 2014; Hashimshony et al., 2012, 2016; Jaitin et al., 2014; Kroehne et al., 2011; Ramsköld et al., 2012; Shalek et al., 2013; Tang et al., 2009, 2010). Later, this technology evolved to reduce noise by improving sensitivity (Grün & Van

Oudenaarden, 2015; Islam et al., 2014; Kolodziejczyk et al., 2015; Picelli et al., 2013; Ramsköld et al., 2012; Wilson et al., 2015). In particular, gene expression profiles studied in bulk are now explored using higher sensitivity methods, such as scRNA-seq or single-nucleus RNA-seq (Litviňuková et al., 2020; Massaia et al., 2018). The single-cell approach has also entered the cardiac field, studying cardiac development and disease models (DeLaughter et al., 2016; Farbehi et al., 2019; Gladka et al., 2018; Li et al., 2015; Litviňuková et al., 2020; Martini et al., 2019; Nosedá et al., 2015; Schafer et al., 2017; Skelly et al., 2018). ScRNA-seq resolution allows for the deconvolution of more complex cellular functions and ambiguous network interactions in bulk analysis. ScRNA-seq represents the most advanced technology for exploring heterogeneities and identifying new and rare cells or cell states in complex tissues, which is true even in the heart. Therefore, scRNA-seq uses unsupervised clustering to deconvolve cellular tissue composition and even reconstruct lineage fates (Bendall et al., 2014; Durruthy-Durruthy & Heller, 2015; Grün et al., 2016; Llorens-Bobadilla et al., 2015; Treutlein et al., 2014).

The heart comprises several cell types in addition to CMs, including fibroblasts, and vascular and immune cells, whose interactions and communications are still poorly characterised (Farbehi et al., 2019). Following isolation of single cells and single nuclei, performing scRNA-seq and single-nucleus RNA-seq highlighted the distribution of the cell landscape of a healthy human heart (Litviňuková et al., 2020). Immune cells (myeloid and lymphoid), mainly distributed in the atrial tissue (10.4% versus 5.3% of the ventricular tissue), are divided into 21 clusters. Thirteen clusters represent myeloid cells, including different subtypes of macrophages, monocytes, and DCs; the other eight groups are lymphoid cells (Litviňuková et al., 2020). Macrophages were divided

into three populations based on the expression of the Lymphatic Vessel Endothelial Hyaluronan Receptor 1 (LYVE1) (Litviňuková et al., 2020). LYVE1⁺ macrophages have previously been described as perivascular cells in human and mouse vessels. They maintain arterial stiffness and regulate collagen expression by SMCs (Lim et al., 2018). Spatial mapping revealed that LYVE1⁺ macrophages interact with CMs and fibroblasts expressing *POSTN* and *TNC*, genes related to the TGF β signalling pathway. Interactions between immune cells, CMs and fibroblasts suggest a tissue-specific paracrine signalling pathway to maintain homeostasis (Litviňuková et al., 2020). Among the bioinformatics platforms for scRNA-seq, cell-cell interactions analysis (CellPhoneDB) elucidates biological mechanisms and interactions between all cardiac cells during homeostasis and disease (Farbehi et al., 2019; Yamada & Nomura, 2020). Cell-cell interactions identified that POSTN⁺TNC⁺ fibroblasts interact with macrophages that express the migration inhibitory factor (MIF). MIF is a pleiotropic inflammatory cytokine with a high affinity for the receptor CD74. Hence, this interaction has antifibrotic and tissue reparative activity (Heinrichs et al., 2021; Litviňuková et al., 2020).

To better understand the interactions between immune and stromal (non-CMs) cells during post-MI inflammation, more than 30,000 single cells from post-MI mouse hearts (day 3 and 7 versus sham) were analysed by scRNA-seq, revealing more than 30 different cell populations in the heart (Farbehi et al., 2019). ScRNA-seq of cardiac CD45⁺ cells identified many immune cells in the inflammatory process, including neutrophils, T-cells, mast cells, monocytes and macrophages (Martini et al., 2019). As critical cells in promoting post-MI inflammation and regeneration, monocytes and macrophages have been extensively characterised in several studies (Aurora et al.,

2014; Dick et al., 2019; Farbehi et al., 2019; Hulsmans et al., 2017; Lavine et al., 2014; Leid et al., 2016; Litviňuková et al., 2020; Martini et al., 2019; Nahrendorf et al., 2007). The t-SNE projection allowed for classifying cardiac residents and recruiting monocytes and macrophages into four clusters. They confirmed, as described above, that CCR2⁻ are resident macrophages, while CCR2⁺ monocytes expressing pro-inflammatory characteristics are recruited from the bloodstream (Dick et al., 2019; Epelman et al., 2014; Farbehi et al., 2019). The analysis of the lineage trajectory confirmed that macrophage phenotypes are in a continuum state. From day three post-MI, M1-like pro-inflammatory macrophages change to an M2-like anti-inflammatory phenotype on day seven post-MI (Farbehi et al., 2019; Lavine et al., 2018; Nahrendorf & Swirski, 2016). M2-like anti-inflammatory macrophages also merge with cardiac resident macrophages (Farbehi et al., 2019). More recently, this continuum has been observed in the gene expression gradient in macrophages following ischemic cardiac injury (Molenaar et al., 2021). Alongside monocytes and macrophages, CD4⁺ and CD8⁺ T-cells and neutrophils are expanded in response to the HF disease model (Transverse aortic constriction-operated mice) (Farbehi et al., 2019; Martini et al., 2019).

Building an *in vitro* model of macrophages is a practical approach that can be used to classify disease macrophages *in vivo*. The *in vitro* study of macrophages is considered a helpful tool for characterising gene expression profiles because it can also explore the role of macrophages during disease. Several studies have been performed using microarrays and bulk RNA-sequencing datasets (Chen et al., 2019). Meta-analyses based on a computational model of eight publicly available transcriptomic datasets investigated different phenotypes and functional states of differentiated macrophages

in vitro (Chen et al., 2019). This can be considered a practical platform for deconvolving macrophage heterogeneity *in vitro*. They identified both novel and well-established markers of activated macrophages, including pro-inflammatory cytokines (e.g. $\text{TNF}\alpha$, CXCL9) expressed by macrophages activated by LPS (Chen et al., 2019).

1.5 M-CSF promotes M2-like macrophages

1.5.1 Bulk RNAseq and single-cell qRT-PCR identified that Lin⁻ Sca1⁺CD31⁻PDGFR α ⁺SP⁺ CSCs secreted M-CSF

Dr Nosedá and Prof Schneider used a systematic complementary approach of bulk RNA-Seq and single-cell technologies to investigate the secretome of the Lin⁻ Sca1⁺CD31⁻PDGFR α ⁺SP⁺ CSCs.

Bulk RNA-Seq of the starting (large, unfractionated) population of Sca1⁺ CSCs was compared with the transcriptomics of ESC and neonatal CMs (neoCMs). Data mining was performed using the ToppFun function in the ToppGene Suite tool to identify categories of Gene Ontologies (GO, “Biological process”). The GO analysis of the identified genes encoding for soluble proteins relevant to regeneration, repair and paracrine pathways. To further study the transcriptomes of CSCs, the top genes determined with GO were mapped, including *Csf1*, to the freshly isolated Sca1⁺PDGFR α ⁺ fraction by sc qRT-PCR (Nosedá et al., 2015 and *unpublished data*) (Fig. 1. 10 A).

Secondly, mouse and human CSCs resemble each other in molecular signatures. Nosedá isolated and expanded human CSCs (hCSC) from several patients. The gene expression of the same top genes identified from the bulk RNA-seq in mice was analysed by sc qRT-PCR, confirming an enrichment for *Csf1* even in hCSC (*unpublished data*) (Fig. 1.10 B).

Lastly, human and mouse data sets were analysed for overlapping hits as a route to initial prioritisation. It was found that mouse and human CSCs secreted eighteen paracrine factors in common, *Csf1* among them. The Venn diagram below uses circles to visualise these similarities (overlapping region) and differences (non-overlapping regions) (*unpublished data*) (Fig. 1.10 C).

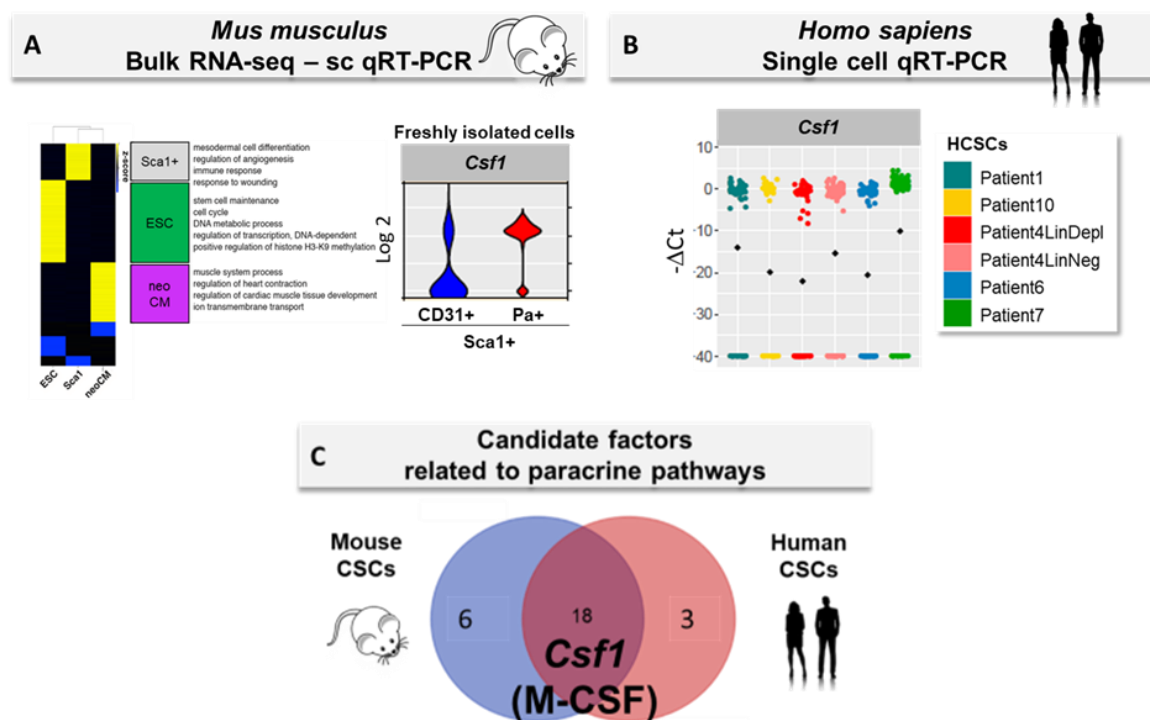


Figure 1.10 Identification of M-CSF as a potential mediator of CSC anti-inflammatory effect

A, (LEFT) Bulk RNAseq of ESC, Sca1⁺ CSCs and neonatal CM (neoCM), gene ontology (GO) category. (RIGHT) Sc qRT-PCR tested the expression of paracrine genes in populations of interest, including Sca1⁺ PDGFR α ⁺ versus Sca1⁺CD31⁺. **B**, hCSC derived from five patients were analysed by sc gene expression profile. **C**, Venn diagram visualisation of 18 candidate factors expressed in mouse and human CSCs, M-CSF among them. Dr Nosedá generated **A**, **B**, and **C** (*unpublished data*).

1.5.2 M-CSF promotes anti-inflammatory-like macrophages via CSF1R

M-CSF regulates monocyte survival and differentiation into a reparative macrophage phenotype expressing phagocytic characteristics (Hume & MacDonald, 2012; Lin et al., 2008; Ma et al., 2012; Pollard, 2009; Rae et al., 2007). M-CSF has a high affinity for its colony-stimulating factor 1 receptor (CSF1R).

CSF1R is a homodimeric tyrosine kinase protein containing an extracellular and an intracellular domain (Rovida & Sbarba, 2015; Sherr et al., 1988). The extracellular domain presents five immunoglobulin (Ig)-like domains and the binding sites of CSF1R ligands. The intracellular domain contains two tyrosine kinases domains: the juxtamembrane in the proximity of the cellular membrane, one in the middle and one at the C-terminus tail. The activation of CSF1R occurs through the autophosphorylation of 8 intracellular tyrosine (Tyr): juxtamembrane domain (Tyr-559 and Tyr-544), kinase insert domain (Tyr-697, Tyr-706 and Tyr-721) and C-terminus domain (Tyr-807, Tyr-721 and Tyr-974). Phosphorylation of these tyrosine leads to the activation of specific signalling pathways (Stanley & Chitu, 2014) (Fig. 1.11).

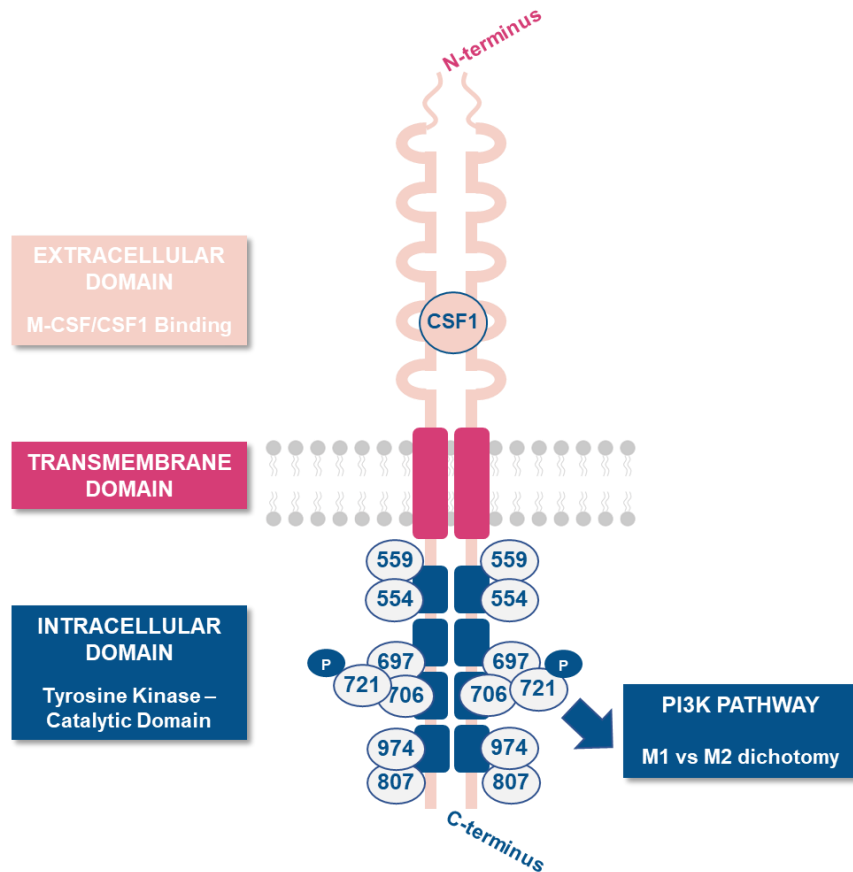


Figure 1.11 Schematic structure of CSF1R

CSF1R is a homodimeric tyrosine kinase protein with an extracellular (pink) and an intracellular domain (blue), which contains a juxtamembrane region in proximity to the cellular membrane and a catalytic domain at the C-terminus. Eight tyrosine residues undergo autophosphorylation following M-CSF binding. Tyr-721 phosphorylation activates a PI3K pathway, regulating the M1 and M2 dichotomy (Modified from Mun et al., 2020).

CSF1R is expressed mainly on the surface of monocytes, macrophages, myeloid DCs, microglia and osteoclasts (El-Gamal et al., 2018). *In vivo* studies conducted in *Csf1r^{-/-}* mice showed that the absence of CSF1R leads to developmental defects, such as skeletal and neurological growth problems, and a reduced amount of tissue macrophages (Dai et al., 2002; Okamura et al., 2003; Wiktor-Jedrzejczak et al., 1990).

M-CSF competes for the CSF1R with another ligand called IL-34 (Lin et al., 2008). The primary roles of IL-34 are in brain development, microglia homeostasis in adult mice and promoting macrophages survival and proliferation (Lin et al., 2008; Greter et al., 2012; Wei et al., 2010). Levels of M-CSF are detectable, being approximately 10ng/mL in the blood and tens of picograms per milligram in tissues, such as the liver, lung, spleen, kidney, intestine and heart (Roth et al., 1997). On the other hand, IL-34 is only detectable locally when released (Rovida & Sbarba, 2015). M-CSF and IL-34 do not have a homologous sequence; they bind CSF1R in the extracellular domain but at two different sites (Chihara et al., 2010).

The phosphorylation of Tyr-721 activates the PI3K/Akt pathway, which regulates the polarisation of M1-like and M2-like macrophages (López-Peláez et al., 2011; Martinez, 2011; Weichhart & Säemann, 2008; Weisser et al., 2011). In particular, Tyr-721 phosphorylation improves the phenotype of M2-like macrophages by inhibiting the pro-inflammatory M1-like macrophages (Caescu et al., 2015). Hence, the M-CSF-CSF1R pathway regulates the expression of genes related to the survival, proliferation and differentiation of primary macrophages, either by decreasing the expression of the anti-apoptotic protein Bcl-xL (Sevilla et al., 2001) or by blocking the expression of the CSF1-induced G1 cyclin, cyclin D (Dey et al., 2000; Sherr et al., 1992).

The modulation of macrophage populations through pharmacological disruptions of the M-CSF-CSF1R pathway can have various therapeutic applications, such as inflammatory, autoimmune diseases or cancer.

1.5.3 Preclinical and early clinical use of M-CSF

Since macrophages often regulate chronic inflammatory diseases, modulation of the M-CSF-CSF1R pathway has a potential clinical use. Monocytes need constant exposure to M-CSF to re-enter the S phase of the cell cycle and improve differentiation into BMDMs (Tushinski & Stanley, 1985). Pharmacokinetics and renal clearance of a higher molecular weight recombinant M-CSF protein are slower, allowing a more prolonged exposure of monocytes to the cytokine (Bauer et al., 1994; Wong et al., 1987). Repeated and prolonged treatment of M-CSFS yields more macrophages (Hume et al., 1988; Munn et al., 1990; Stoudemire & Garnick, 1991). In mice, 4-day administration of recombinant human M-CSF (rhM-CSF) increased circulating mature monocytes, tissue-resident macrophages (liver, peritoneal cavity and peritoneum) and levels of F4/80 by 10-fold (Hume et al., 1988). In non-human primates, continuous intravenous or subcutaneous injection of rhM-CSF increased the number of CD16⁺ and F4/80⁺ M2-like resident macrophages by five times (Munn et al., 1990). In contrast, a single intravenous injection in rats resulted in a peak of resident M2-like macrophages within 24 hours, followed by a return to baseline after 36 hours (Ulich et al., 1990). The first preclinical and clinical studies using M-CSF are summarised in Table 1.3.

Table 1.3 Preclinical and early clinical use of M-CSF listed (chronological order)

Phase	Patients	Dose	Duration	Key Results	Reference
III	Randomised double-blind (59)	2x10 ⁵ units/kg	Daily; 14 days post -BMT	Increased granulocytes recovery time (0.5x10 ⁹ /L); survival (120 days post-BMT)	(Masaoka et al., 1990)
I	Metastatic (42)	0.1-25.6mg /m ² /d	A subcutaneous injection every 28 days; days: 1-5; 8-12	Monocytes-LPS treated enhanced secretion of TNF α and IL1 β . Lower blood levels of M-CSF due to an increase in renal clearance rate	(Bukowski et al., 1994)
I	Metastatic (18)	Escalation: 50-150 μ g/kg/d	Continuous infusion; two 14-day cycles; 2 weeks of rest.	Adverse effect: rapidly reversible thrombocytopenia	(Cole et al., 1994)
I	Non-randomised; metastatic melanoma (24)	Escalation: 10-160 μ g/kg/d	Continuous infusion; two 7-day cycles; 2 weeks rest.	Increased macrophages: proliferation; differentiation; activation. Adverse effect: rapidly reversible thrombocytopenia	(Jakubowski et al., 1996)
-	Randomised double-blind; ovarian cancer (44)	8M units/body	Daily for 60min; 7 days 24hrs post-chemotherapy (course II)	Improvement of: NK-cell function; granulocyte function; T-cell maturation	(Hidaka et al., 2003)

1.5.4 Inhibition of the M-CSF-CSF1R macrophage pathway

Multiple, highly promising therapeutic applications have shown that M-CSF has a trophic and autocrine action (Gow et al., 2010; Irvine et al., 2006; Pollard, 2009). Before examining the latest therapeutic approaches for M-CSF, it is necessary to discuss three aspects inhibiting the M-CSF-CSF1R pathway (Hume & MacDonald, 2012).

First, there are two main approaches for inhibiting the M-CSF pathway: blocking the kinase activity of M-CSF or hindering the binding of M-CSF to CSF1R using antagonist

agents. Secondly, as mentioned above, IL-34 is the second ligand of CSF1R. M-CSF and IL-34 bind CSF1R at two different binding sites. However, specific antibodies against CSF1R must be designed considering whether or not they will inhibit both the M-CSF and IL-34 pathways. Due to the role of M-CSF in macrophage differentiation, selective monoclonal antibodies have been developed primarily for the M-CSF binding site (Ovchinnikov et al., 2010). Finally, the most commonly used inhibitor to block M-CSF activity over the past decade has been GW2580 due to the high specificity for CSF1R (Burns & Wilks, 2011). However, in the clinical setting, it should be considered that the blockade of CSF1R induces an increase in circulating levels of M-CSF (Bartocci et al., 1987).

According to the literature, only a few studies have used an antibody to inhibit M-CSF. This drawback can be circumvented by using CSF1R inhibitors that target the kinase domain of the receptor rather than the M-CSF-CSF1R binding site (Irvine et al., 2006). A summary of the most relevant studies using anti-CSF1 antibodies is shown in Table 1.4.

Table 1.4 Application of neutralising anti-M-CSF antibodies (chronological order) (i.p., intraperitoneal injection)

Antibody	Study model	Administration	Key Results & Conclusion	Reference
Rat anti-CSF1 mAb (5A1)	Mouse model of collagen-induced arthritis	Daily; 20/24 days post immunisation	Endogenous M-CSF macrophages exacerbate inflammation – collagen-induced arthritis	(Campbell et al., 2000; Lokeshwar & Lin, 1988)
	4-month old ovx mice	Weekly i.p of 0.5mh	M-CSF mediates ovariectomy-induced bone loss	(Cenci et al., 2000; Lokeshwar & Lin, 1988)
Anti-mouse CSF1 Ab	Post-natal mice; 0.5-57.5 days old	Subcutaneous injections	M-CSF is essential for organ maturation and somatic growth	(Wei et al., 2005)
Human mAb (PD-0360324)	Female nonhuman primates; 3 to 5 years old; 7/7 monkey dose-placebo	Bi-weekly intravenous injection of 100mg/kg; for 29 days	Serum M-CSF levels increase CD14 ⁺ CD16 ⁺ macrophages in Kupffer cells and skeletal muscle without injury	(Radi et al., 2011)
Anti-human CSF1 Ab (26730)	Rheumatoid arthritis (RA)	5µg/ml	Suppression of inflammatory activity of RA	(Garcia et al., 2016)
Anti-mouse CSF1 Ab	Mouse model of inflammatory pain induced by intraarticular injections of zymosan	Two and one days before zymosan injection: i.p. of 200µl	Inhibition of acute inflammatory pain induced by zymosan, GM-CSF and TNF α	(Saleh et al., 2018)
Anti-mouse CSF1 Ab (5A1)	Mouse model of cytokines storm syndrome induced by CpG injection	1mg 2 days before infection 0.5mg 48 and 96hrs later	Cytokine storm syndrome development reduced mortality and inflammatory cytokines levels.	(Mahajan et al., 2019)

The other option to hamper the M-CSF pathway is targeting CSF1R directly. To inhibit CSF1R is possible to use either monoclonal antibodies or kinase inhibitors.

Two studies developed neutralising antibodies against CSF1R: AFS98 (Sudo et al., 1995) and M279 (MacDonald et al., 2010). Tumour studies reported that the monoclonal antibody M279 has a higher affinity for CSF1R than AFS98 (MacDonald et al., 2010). Lenzo and colleagues found that M279 has no protective effect on

inflammation patterns, including post-tissue damage or regulation of monocytes and macrophages (Lenzo et al., 2012). The most relevant applications of AFS98 in the post-MI inflammatory response are in Table 1.5.

Table 1.5 Key findings of M-CSF deficiency in different disease models via neutralising antibody against CSF1R (AFS98) (chronological order)

Disease model	Study model	Administration	Key Results	Reference
Atherosclerosis	6-week old <i>apoE</i> ^{-/-} mice; High-fat diet	I.p. of 2mg; alternate days for 6-week	<ul style="list-style-type: none"> - Decreased circulating monocytes - 70% fewer macrophage-derived foam cells indicating the essential role of macrophages in the protection of early atherogenesis 	(Murayama et al., 1999)
Acute rejection post renal allograft	C57BL6 or BALB/c kidneys transplanted into BALB/c mice	I.p. of 50mg/kg/d; for 5-day	CD68 ⁺ macrophages: reduced proliferation (82%), interstitial accumulation (53%), glomerular accumulation (71%)	(Jose et al., 2003)
Skeletal muscle fibrosis post-injury	C3H/HeN mice Injected with 75µl cardiotoxin into TA muscle	I.p. of 4mg/0.4ml PBS. 3-time every 2-day	<ul style="list-style-type: none"> - Inhibition of skeletal muscle regeneration - Increased adipogenesis - Increased fibrosis (collagen deposition) - Reduced macrophages infiltration 	(Segawa et al., 2008)
Diabetic nephropathy	Obese (<i>db/db</i>) mice with type 2 diabetic	I.p. of 25mg/Kg; Alternate days for 6-week	<ul style="list-style-type: none"> - Inhibited glomerular macrophages accumulation, proliferation, and activation - Suppressed diabetic nephropathy progression 	(A. K. H. Lim et al., 2009)
Pathological angiogenesis & lymphangiogenesis (ischemic retinopathy; mouse osteosarcoma)	Osteopetrotic (<i>op/op</i>) mice	Subcutaneous injection of 50mg/kg/d. P8-11 and P11-16	<ul style="list-style-type: none"> - Reduce LYVE1⁺ and LYVE1⁻ macrophages - Reduced tumour angiogenesis and lymphangiogenesis 	(Kubota et al., 2009)
Lung and peritoneal inflammation	Peritonitis mice (5mg/ml of <i>M. tuberculosis</i>). Lung infection mice (10µg of LPS for 72hrs)	Subcutaneous injection, 300µg. Four days	<ul style="list-style-type: none"> - Reduce the accumulation of Ly6C^{lo} macrophages - CSF1R controls macrophages lineage development 	(Lenzo et al., 2012)

Several small molecules have been developed to target CSF1R directly. Among the kinase inhibitors used *in vivo*, GW2580 (Conway et al., 2005), Ki20227 (Kubota et al.,

2009) and BLZ945 (Beckmann et al., 2018; Pyonteck et al., 2014) have the most significant results and have shown greater specificity for CSF1R than other kinases.

A study in rats showed that the activity of GW2580 increased the circulating monocytes under homeostatic conditions (Conway et al., 2008), while the recruitment of macrophages into tumours or arthritis was not affected despite an increase in the dose of GW2580 (Conway et al., 2008; Priceman et al., 2010). Interestingly, a mouse model of acute graft-versus-host disease (GVHD) demonstrated an increase in resident macrophages at a lower dose of GW2580 (60mg/kg versus 160mg/kg used by Priceman and colleagues) (Hashimoto et al., 2011; Priceman et al., 2010).

Compared to CSF1R^{-/-} mice (Dai et al., 2002), Ki20227 had a minimum effect on the circulating concentration of M-CSF (Kubota et al., 2009) and a more significant effect on the reduction of Ly6G⁺ granulocytes, indicating that this inhibitor may have a lower affinity for CSF1R-expressing macrophages. It is worth mentioning that imatinib (Glivec, STI-571) was initially developed as an inhibitor to target the tyrosine kinase bcr-abl. Hence, it has been used to inhibit the expression of PDGFR α/β and c-kit in myeloid leukaemia cells. Finally, imatinib efficiently obstructs the cytokine-dependent pathways of CSF1R (Dewar et al., 2005).

The pharmacological compound BLZ945 has been described as 1,000-fold more selective against CSF1R than other chemical inhibitors (Pyonteck et al., 2014). BLZ945 has been used in several studies to induce pharmacological inhibition of CSF1R as a treatment to regulate inflammation (El-Gamal et al., 2018). In the mouse model of glioblastoma, 67nM of BLZ945 led to tumour regression and increased

survival of M2-like macrophages (Pyonteck et al., 2014). BLZ945 is used in an ongoing first-in-human (FIH) clinical trial (Phase I/II -NCT02829723).

Cannarile and colleagues have summarised the current clinical development of CSF1R inhibitors (Cannarile et al., 2017). A recent study identified M-CSF as an essential mediator of human coronary artery disease (CAD). Mendelian randomisation (MR) analysis was used based on the Outcome Reduction With Initial Glargine Intervention (ORIGIN, NCT00069784) trial of 4,147 participants combined with the CARDIoGRAM consortium dataset (Sjaarda et al., 2018). This study concluded that high levels of M-CSF concentration in the blood correlate with cardiovascular events (Sjaarda et al., 2018). These results add to previous studies that have shown a relation between M-CSF and atherosclerosis (Rajavashisth et al., 1998; Rajavashisth et al., 1990; Rosenfeld et al., 1992; Shaposhnik et al., 2010); and in ischemic stroke, as discovered by a targeted proteomics study based on two independent cohorts studies (PIVUS and ULSAM) (Lind et al., 2015).

Manipulating circulating monocytes and tissue-resident macrophages via the M-CSF-CSF1R pathway has clear therapeutic potential in tumour studies. Therefore, many monotherapy clinical trial studies have developed pharmacological inhibitors of CSF1R.

In summary, diverse investigations have implicated the M-CSF/CSF1R pathway in cardiovascular disease, inflammation, and cancer. For the present thesis, the relevance of the cited inhibitors is their straightforward utility in testing the potential contribution of CSC-secreted M-CSF to cardiomyocyte protection.

Chapter 2 - Hypothesis and aims

2.1 Hypothesis

Studies using zebrafish, amphibians, and neonatal mice as animal models demonstrated that the resolution of post-MI inflammation and cardiac regeneration without scar formation is a macrophage-dependent mechanism. Macrophages with an M2-like, anti-inflammatory, and pro-reparative phenotype orchestrate regeneration (Aurora et al., 2014; Dutta & Nahrendorf, 2015; Frangogiannis, 2015; Lavine et al., 2014). Furthermore, the paracrine signals released by adult mouse Lin⁻Sca1⁺CD31⁻PDGFR α ⁺SP⁺ CSCs could explain the reduction in infarct size despite the lack of durable engraftment (Nosedá et al., 2015). Thus, Lin⁻Sca1⁺CD31⁻PDGFR α ⁺SP⁺ CSCs could release paracrine factors beneficially affecting different cell types in the heart, including macrophages.

The overarching hypothesis of this dissertation is that **paracrine signals released by adult mouse Lin⁻Sca1⁺CD31⁻PDGFR α ⁺SP⁺ CSCs could promote an anti-inflammatory-like and reparative macrophage phenotype**. To investigate this hypothesis, (1) an *in vitro* model system was established to generate dichotomous populations of pro- and anti-/reparative macrophages, including the use of sc qRT-PCR to profile gene expression at the single-cell level; (2) the impact of CSC-conditioned medium (CondM) was assessed, using that model; and (3) a candidate factor found to be expressed by CSCs was tested, using complementary inhibitors of its signalling pathway. These specific questions and the related objectives are detailed immediately below.

2.2 Questions and corresponding objectives

Objective 1. Design an *in vitro* system that can generate pure populations of macrophages with unique and distinctive features of the two extremes of the macrophages spectrum.

- Establish a system that allow BMDMs to differentiate into macrophages and activate them using cocktails of growth factors and pro-, and anti-inflammatory stimuli;
- Demonstrate macrophages' distinctive immunophenotype using multi-parametric flow sorting;
- Demonstrate macrophages' distinctive gene expression signature using single-cell qRT-PCR.

Objective 2. CSC CondM is sufficient to differentiate BMDMs into macrophages and if yes, is it able to promote an anti-inflammatory-like phenotype of macrophages

- Establish *in vitro* whether CSC CondM is sufficient to differentiate BMDMs into macrophages;
- Demonstrate whether CSC CondM induces an anti-inflammatory-like immunophenotype of macrophages, tested via multi-parametric flow sorting, and based on secretome analysis;
- Demonstrate whether CSC CondM induces also an anti-inflammatory-like gene expression signature, investigated thoroughly through single-cell qRT-PCR.

Objective 3. CSC-secreted M-CSF is the potential factor that mediates the anti-inflammatory-like phenotype of macrophages

- Assess the effects of the inhibition of CSC-secreted M-CSF on macrophages survival, differentiation and activation towards an anti-inflammatory-like phenotype of macrophages using:
 - the pharmacological inhibitor of CSF1R, BLZ945;
 - the neutralising monoclonal antibody against CSF1R.

Chapter 3 - Materials and Methods

3.1 Cell Culture

Cell culture was carried out under standard sterile conditions in a Biomat 2 class II microbial safety cabinet. Cells were incubated in a CO₂ incubator (Sanyo; MC0-5M) in a humidified atmosphere at 37°C and 5% CO₂. All cells were maintained in vented T75cm² cell culture flasks or 6-well plates (Corning). At ≥80% confluence, cells were detached from flasks/plates by (1) scraping using a cell scraper (TPP) or (2) incubation with 1mL per 75cm²·0.25% Trypsin-Ethylenediaminetetraacetic acid (EDTA) diluted in phosphate-buffered saline (PBS), incubated at 37°C for 5 minutes and subsequently inactivated by adding 11mL fresh culture media to stop the enzymatic activity of Trypsin. Cells were then collected and centrifuged at 330 relative centrifugal forces (RCF) for 5 minutes at 4°C. The pellet was reconstituted using cultural media. Cell number and viability were determined using a Vi-CELL Cell Viability Analyser (Beckman Coulter), an automated cell counter, based on the Trypan Blue Dye Exclusion method, allowing nine samples to be loaded at once with automated cell analysis. Primary cells and cell lines used in this study are listed below and subsequently detailed (Table 3.1).

Table 3.1 Cell lines and primary cells used in this study

	Name	Cell type	Organism	Tissue origin or transformation method	Source
Cell Lines	RAW 264.7	Macrophages	<i>Mus musculus</i> (mouse)	Abelson murine leukaemia virus-transformed (Raschke et al., 1978)	ATCC, TIB-71
	H9c2	Cardiomyocytes	<i>Rattus norvegicus</i> (rat)	Embryonic rat heart tissue	ATCC, CRL-1446
Primary Cells	BMDMs	Macrophages	<i>Mus musculus</i> (mouse)	Bone marrow-derived from tibias and femurs of an adult mouse	In-house
	Lin ⁻ Sca1 ⁺ CD31 ⁻ PDGFR α ⁺ S P ⁺	Cardiac progenitors/stem/stromal-like cells	<i>Mus musculus</i> (mouse)	Adult mouse heart, derived from a pool of freshly isolated cells	(Nosedá et al., 2015)

3.1.1 Cell lines

3.1.1.1 Mouse RAW 264.7 macrophages

The mouse macrophage RAW 264.7 cell line was purchased from American Type Culture Collection (ATCC, TIB-71). RAW 264.7 cells were cultured in a macrophage medium, comprising Dulbecco's Modified Eagle's Medium (DMEM, Invitrogen), 10% heat-inactivated (56°C, 30 min) foetal bovine serum (FBS; Gibco), 2 mM L-glutamine (Thermo Fischer) and 1x antibiotic-antimitotic (100 U/ml penicillin, 0.1 g/ml streptomycin, 0.25 mg/ml amphotericin B; Invitrogen). They were plated at 10,000/cm², passaged every three days by scraping and used at a maximum of 30 passages.

3.1.1.2 Rat H9c2 cardiomyocytes

Rat cardiomyocyte H9c2 cell line was obtained from ATCC (CRL-1446) and cultured in ATCC-30-2002 media, which contained glucose (4500 mg/L), 4 mM L-glutamine, 1 mM sodium pyruvate, and 1500 mg/L sodium bicarbonate, supplemented with 10% FBS (Gibco) and 1x antibiotic-antimitotic as above. H9c2 were passaged every three days using trypsin-0.25% EDTA and maintained by plating at 5,000 cells/cm².

3.1.2 Primary cells

3.1.2.1 Animals

All animal procedures were performed with UK Home Office approval (PL 70/6806, 70/7880, 35/9318) and conformed to the UK Animals (Scientific Procedures) Act, 1986, incorporating Directive 2010/63/EU of the European Parliament. Procedures for the husbandry and housing of animals follow the recommendations of the Association for Assessment and Accreditation of Laboratory Animal Care and the UK Code of Practice for the Housing and Care of Animals Bred, Supplied or Used for Scientific Purposes. The Imperial Hammersmith campus animal facilities comprise an SPF animal breeding facility (H2) and a clean facility for experimental surgery and physiology (H1). Biosecurity and pathogen exclusions are taken from the Federation of European Laboratory Animal Science Associations (FELASA) health monitoring guidelines, and all animals are screened four times per year. Mice were housed in Allentown XJ individually ventilated cages, with Datas and bedding (ECO2) and a 12:12 light: dark cycle. Environmental enrichments included small tunnels, chew

blocks, and facial tissues. The maximum housing density was 7 per cage if < 25 g and 5 per cage if R 25 g. C57BL/6 adult mice (8-12 weeks old; Charles River) were sacrificed using methods of killing that are acceptable and humane, carried out by a competent person and set out in Schedule 1 to the UK Animals (Scientific Procedures) Act, 1986. Mice were sacrificed using increasing concentrations of CO₂, followed by cervical dislocation.

3.1.2.2 *In vitro* differentiation of BMDMs

After the humane killing, tibias and femur of 9-12-week-old male C57BL/6 mice were removed, cleaned out from skin and muscle, and immediately immersed in cold PBS (Gibco) and kept on ice until the isolation phase. BM was extracted by flushing tibias and femurs three times with 2 mL of cold DMEM (Invitrogen) using a 2 mL syringe and 23-gauge needle and was filtered through a 70- μ m mesh (BD Falcon). After counting, the unfractionated BM cells were centrifuged at 300 x g for 5 min at 4°C. Cells were then plated for 6 d at a density of 66,000 cells/cm² in macrophage media supplemented with recombinant mouse GM-CSF (10 ng/mL, Peprotech) or recombinant mouse M-CSF (10 ng/mL, Peprotech) to induce BMDMs differentiation. After 6 d, half of the GM-CSF-M ϕ and M-CSF-M ϕ were activated for 24 hr with either pro-inflammatory or anti-inflammatory stimuli (de Couto et al., 2015; Zhang, Goncalves, & Mosser, 2008). GM-CSF-M ϕ were activated with 100 ng/mL LPS (Sigma) and 50 ng/mL recombinant murine IFN- γ (Peprotech). M-CSF-M ϕ were activated with 10 ng/mL recombinant murine IL-13 and IL-4 (Peprotech) (Fig. 3.1).

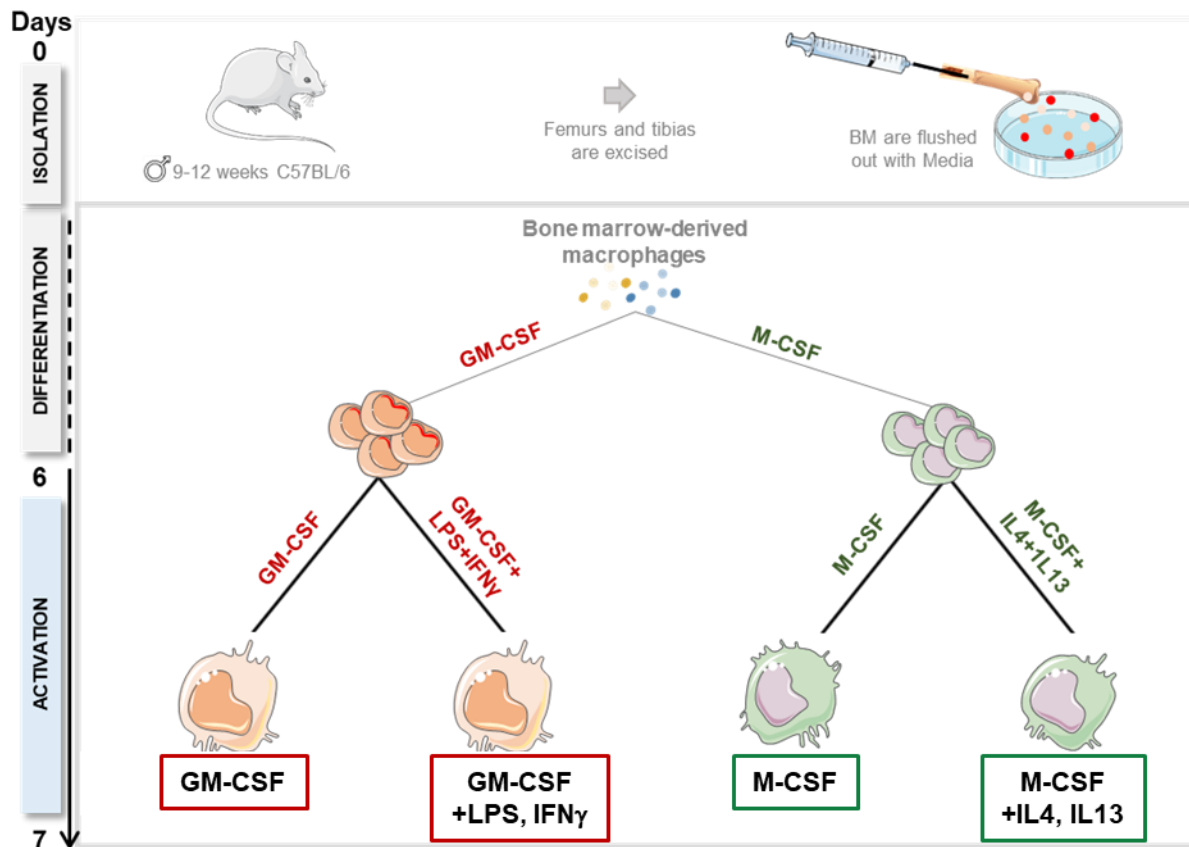


Figure 3.1 An in vitro system to study M1- and M2-driven macrophages.

Sequential chemokines differentiate and activate BMDMs into M1- or M2-driven macrophages. Unfractionated BM cells were isolated and cultured for six days in media enriched with either GM-CSF (10 ng/mL) or M-CSF (10 ng/mL) to differentiate M1-driven and M2-driven-M ϕ , respectively. On day 6, half of the cultures were also activated for 24 hr with either LPS (100 ng/mL) and IFN γ (50 ng/mL) or with IL-4 (10 ng/mL) and IL-13 (10 ng/mL).

3.1.2.3 Cardiac progenitors/stem/stromal-like cells (CSCs)

Adult mouse Lin⁻Sca1⁺CD31⁻PDGFR α ⁺SP⁺ cardiac progenitors/stem/stromal-like cell (CSCs) population were previously generated in our lab as described in Nosedá et al., 2015 and maintained in Clonal Growth Medium (CGM) (Table 3.2) on collagen-coated plates, seeded at 5,000 cells/cm², passaged every 2-3 days using Trypsin-0.25% EDTA, and used until passage 25-30.

Table 3.2 Clonal Growth Medium

DMEM/Ham F-12	65%
Iscove's Modified Dulbecco's Medium (IMDM)	35%
Bovine growth serum (BGS)	3.5%
Antibiotics-Antimycotics	100U/mL
L-Glutamine	2mM
β -mercaptoethanol	0.1mM
B27 media supplement	1.3%
Recombinant human epidermal growth factor (EGF)	6.5ng/mL
Recombinant human fibroblast growth factor (hFGF)	13ng/mL
Thrombin	0.0005 U/mL
Human cardiotrophin-1 (CT-1)	0.345 /mL

3.2 CSC conditioned media production and *in vitro* use

3.2.2 Production of CSC conditioned media (CSC CondM)

To generate CSC conditioned media (CSC CondM), CSC were seeded onto collagen-coated 6-well plates at high density (100,000 cells/cm²) in CGM for 24 hr. At 24 hr, the CGM was aspirated, plates washed twice with DMEM, and CGM replaced with new macrophage media. CSC CondM was collected 20-24 hr later, filtered through a 0.22µm syringe filter (GE Healthcare), further diluted 1:2 with macrophage media, and added to the BMDMs (Fig. 3.2).

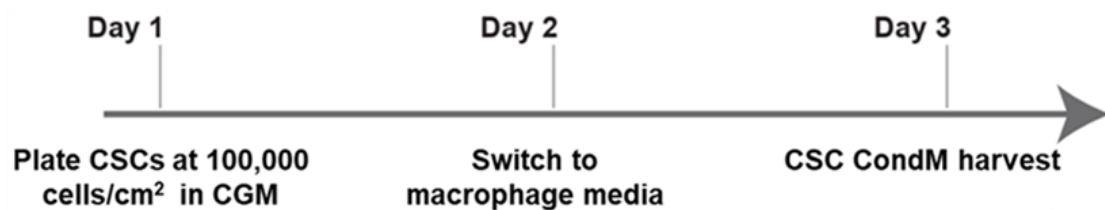


Figure 3.2 Schematic representation of CSC CondM production.

3.2.3 *In vitro* system for differentiating BMDMs with CSC's CondM

Unfractionated BMDMs were isolated, counted and cultured, as explained above. In this integrated version of the *in vitro* system, BMDMs were differentiated over six days in CSC CondM at 50% final concentration. After six days, BMDMs were then activated with the M1 stimuli (LPS and IFN γ) or the M2 stimuli (IL-4 and IL-13), as described above (Fig. 3.3).

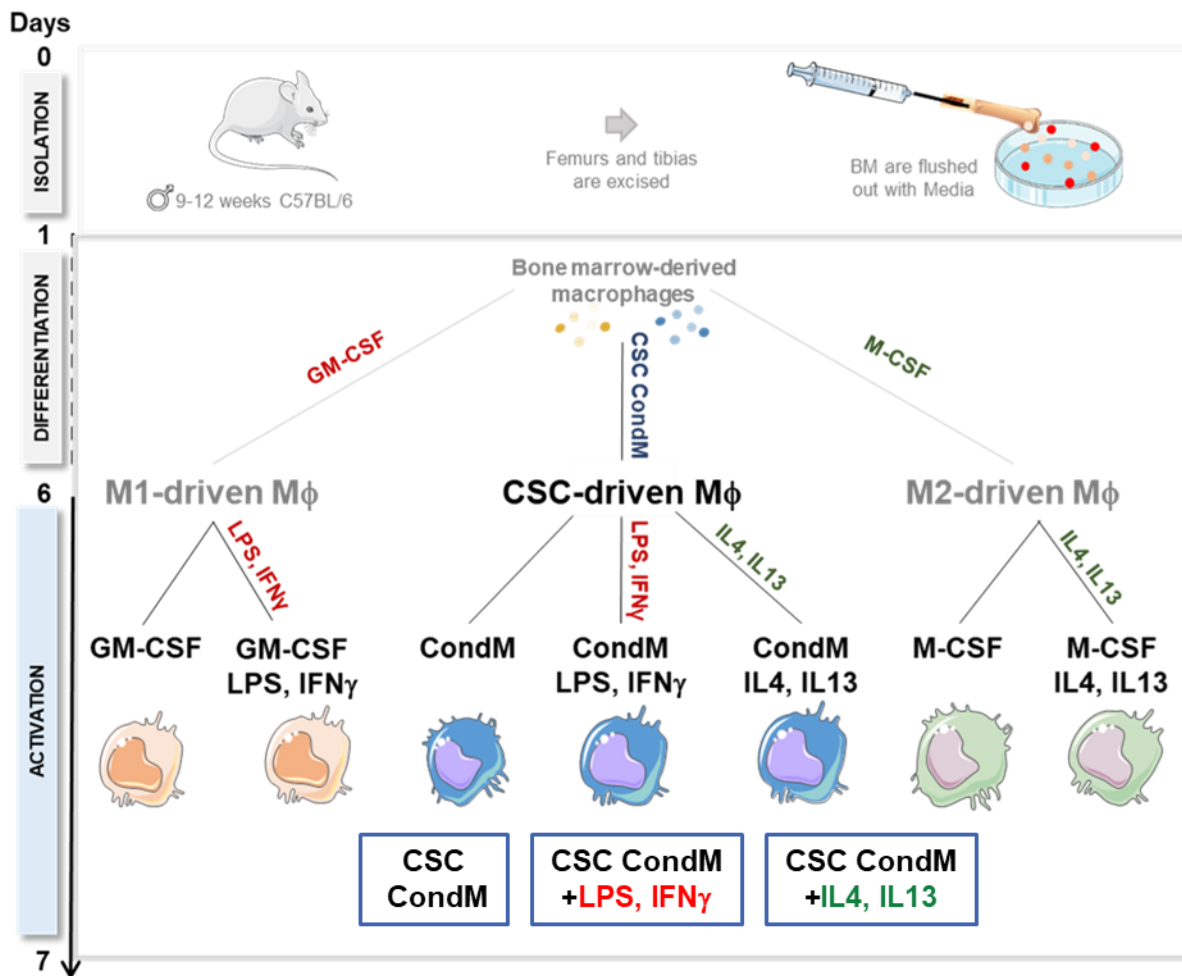


Figure 3.3 *In vitro* system for differentiating BMDMs with CSC CondM

Three new treatment conditions were added to the original *in vitro* system (Fig. 3.2). BMDMs were differentiated over six days in CSC CondM at 50% final concentration. At day 6, they were activated (18/20hrs) either with M1 stimuli, LPS (100 ng/mL) and IFN γ (50 ng/mL), or with M2 stimuli, IL-4 (10 ng/mL) and IL-13 (10 ng/mL).

3.3 Chemical and antibody-based assays

3.3.1 Pharmacological inhibitor of CSF1R: BLZ945

4-[[2-[[[(1R,2R)-2-hydroxycyclohexyl]amino]-6-benzothiazolyl]oxy]-N-methyl-2-pyridinecarboxamide (BLZ945) (Pyonteck et al., 2014) was supplied as a crystalline solid. A stock solution 10x was made by dissolving BLZ945 in dimethylsulfoxide (DMSO). On day 0, BLZ945 was added at two final concentrations: 67nM and 370nM. It was maintained during the duration of both the differentiation and activation phases of the *in vitro* system. DMSO at the highest concentration was used as vehicle control.

3.3.2 Neutralising antibody against CSF1R (α CSF1R)

The neutralising antibody CD115 (c-fms) Monoclonal Antibody (AFS98), Functional Grade, eBioscience (α CSF1R) was added at a final concentration of 1 μ g/100 μ l at day 0 of the *in vitro* system and maintained during the duration of both differentiation and activation. As the relevant control, rat IgG2a kappa Isotype Control (eBR2a), Functional Grade (eBioscience) was added at the same final concentration.

3.4 Flow cytometry

Cells were labelled with antibodies listed in Table 3.3, and to discriminate viable cells, Sytox Blue was added before the acquisition. Flow cytometry and sorting were performed using Ariallu flow sorter (Becton Dickinson) equipped with 355 nm ultraviolet, 405 nm violet, 488 nm blue, 561 nm yellow-green and 640 nm red lasers. FACS data were analysed using FlowJo v10.

Table 3.3 Antibodies and staining used for FACS analyses

Antibody	Conjugate	Dilution	Isotype
Mouse monoclonal anti-F4/80	AF647	1:100	Rat monoclonal anti-IgG2a
Mouse monoclonal anti-CD11b	AF700	1:100	Rat monoclonal anti-IgG2b
Mouse monoclonal anti-CD206	biotin	1:200	Rat monoclonal anti-IgG2a
Mouse monoclonal anti-CX3CR1	PE	1:100	Mouse monoclonal anti-IgG2a
Mouse monoclonal anti-CSF1R	PE/Cy7	1:100	Rat monoclonal anti-IgG2a
Staining	Conjugate	Dilution	Isotype
Streptavidin	BV605	1:50	N/A
Sytox Blue	N/A	1:1000	N/A

3.5 Gene expression analysis

3.5.1 Single-cell quantitative reverse transcription-PCR (sc qRT-PCR)

Multi-parametric FACS (Ariallu flow sorter, Becton Dickinson) directly sorted viable single-cells into 96-well plates containing the reaction mixture (RT-Mix, 10 μ L/well). Here, single cells were pre-amplified using a modified protocol based on CellDirect One-Step qRT-PCR Kits (Invitrogen) (Table 3.4), as previously described (Nosedá et al., 2015) (Fig. 3.4 – Step1).

Table 3.4 RT-Mix (10 μ l/well)

Reagent	
CellsDirect 2x Reaction Mix	5 μ l
SUPERase-In RNase Inhibitor	0.1 μ l
TE buffer	1.2 μ l
0.2x Assay Mix	2.5 μ l
RT/Taq mix	1.2 μ l
Total per reaction	10μl

RT-Mix contains a mix of prechosen TaqMan primer/probe (Thermo Fisher), listed in Table 3.5. TaqMan-MGB probes include a 5' reporter (R) and a 3' non-fluorescent quencher (Q), with the minor groove binding (MGB) moiety attached to the quencher molecule. FAM (6-carboxyfluorescein) was used as the 5' R dye.

Table 3.5 TaqMan probes used for sc qRT-PCR. All probes are conjugated to MGB-FAM dye (ThermoFisher).

The listed probes were used as two panels, designed in-house, as indicated in each experiment.

Gene	Panel	Gene	Panel
<i>Ang</i>	1, 2	<i>Il6</i>	1, 2
<i>Angpt1</i>	1, 2	<i>Il10</i>	2
<i>Angpt4</i>	1, 2	<i>Il11</i>	1, 2
<i>Angptl2</i>	1, 2	<i>Il13</i>	2
<i>Angptl4</i>	1, 2	<i>Il34</i>	2
<i>Angptl7</i>	1, 2	<i>Inhba</i>	2
<i>Arg1</i>	1, 2	<i>Kdr</i>	1
<i>Bmper</i>	1	<i>Ly6a</i>	1
<i>Bmp2</i>	1, 2	<i>Map4k4 Isf. 1</i>	2
<i>Bmp4</i>	1, 2	<i>Map4k4 Isf. 2</i>	2
<i>Ccl2</i>	1, 2	<i>Map4k4 Isf. 3</i>	2
<i>Ccl7</i>	1, 2	<i>Map4k4 Isf. 4</i>	2
<i>Ccl19</i>	1, 2	<i>Mrc1</i>	2
<i>Cdh5</i>	1, 2	<i>Myh6</i>	1, 2
<i>Cd31/pecam</i>	1	<i>Myh11</i>	2
<i>Clec3b</i>	1	<i>Myl2</i>	1, 2
<i>Csf1</i>	1, 2	<i>mPGES1</i>	1
<i>Csf1r</i>	2	<i>Ngf</i>	1
<i>Csf2</i>	1, 2	<i>Nos2</i>	1, 2
<i>Cx3cr1</i>	2	<i>Pecam1</i>	2
<i>Cxcl1</i>	1, 2	<i>Pdgfra</i>	1, 2
<i>Cxcl2</i>	1, 2	<i>Pi16</i>	1
<i>Cxcl3</i>	1, 2	<i>Ptch2</i>	1
<i>Cxcl5</i>	1, 2	<i>Ptges</i>	2
<i>Cxcl9</i>	1, 2	<i>Sod3</i>	1, 2
<i>Cxcl10</i>	2	<i>Tbx20</i>	1, 2
<i>Cxcl12</i>	1, 2	<i>Tcf21</i>	1
<i>Ereg</i>	1	<i>Tgfb1</i>	2
<i>F3</i>	2	<i>Tgfb2</i>	2
<i>Gata4</i>	1	<i>Tgfb3</i>	2
<i>Gdf15</i>	2	<i>Tgm2</i>	2
<i>Hand2</i>	1	<i>Tnfa</i>	2
<i>Igf1</i>	1, 2	<i>Vegfa</i>	2
<i>Igf2</i>	2	<i>Vegfb</i>	2
<i>Il1b</i>	2	<i>Vegfc</i>	2
<i>Il1r1</i>	2	<i>Wt1</i>	1
<i>Il1r2</i>	2	Controls	
<i>Il1r1</i>	1, 2	<i>Ubc</i>	1, 2
<i>Il4</i>	2	<i>Hmbs</i>	1, 2

The 22 cycles for the pre-amplification were performed in a Veriti Thermal Cycler (Applied Biosystems, Thermo Fisher) using specific thermal conditions as indicated in Table 3.6 (Fig. 3.4 – Step 2).

Table 3.6 Pre-amplification RT-PCR thermal cycles

	Step 1	Step 2	Step 3 22 cycles	Step 4
Temperature (°C)	50	95	95	60
Time (min)	15	2	15	4

As negative controls, at least three non-template control (NTC) samples were included in each run at the pre-amplification stage. Two to three wells per chip were used as positive controls containing ten cells/well.

A microfluidic technology performs high throughput gene expression using Dynamic Array chips (Fluidigm), the BioMark real-time PCR system (Fluidigm) and TaqMan probes to analyse the expression of 48 genes x 48 samples using the BioMark HD system (Fluidigm). This allows for the analysis of 42 single cells for each experiment/Dynamic Array chip (plus three wells used as a negative control and three wells used as a positive control as explained above) (Fig. 3.4 – Step 3 and 4). This system allows running 2,304 reactions simultaneously. The instrument's software for gene expression analysis generates a family of PCR curves representing the Cycle threshold (Ct) values for each reaction. Ct values were calculated and exported using Fluidigm Real-Time PCR Analysis software (v4.3.1, Fluidigm) and visualised as a heatmap (Fig. 3.4 – Step 5).

Data analysis was performed using an R script developed in-house by Dr Nosedá's team. Outliers were identified from quantile-quantile plots of Ct values for an internal control gene, Ubiquitin C (*Ubc*), using a quality control step based on robust, standardised expression fractions and expression levels (McDavid et al., 2013).

Ct values were normalised on a per-sample basis, using *Ubc* as a ubiquitous control,

$$\Delta Ct_{\text{sample, gene}} = Ct_{\text{sample, gene}} - Ct_{\text{sample, Ubc}}$$

ΔCt values were subsequently centred on the sample mean:

$$\Delta Ct_{\text{centred}} = \Delta Ct_{\text{sample, gene}} - Ct_{\text{sample mean}}$$

Opposite values ($-\Delta Ct_{\text{centred}}$) were used for visualisation and further analyses..

3.5.2 Methods of visualisation of the results of the sc qRT-PCR

There are different visualisation methods or plotting techniques for sc qRT-PCR data interpretation, such as unbiased hierarchical heatmap, principal component analysis (PCA), and dot plot (Fig. 3.4 – Step 6).

Unbiased hierarchical heatmap: An unbiased hierarchical heatmap visualises gene expression data by plotting the expression of every gene as $-\Delta Ct$ values (row) for every cell (column). An unbiased hierarchical heatmap is colour-coded to facilitate the visualisation of expression levels. Every unbiased hierarchical heatmap reported here includes a horizontal colour key for $-\Delta Ct$ values. Here, red means a high level of expression of a gene ($-\Delta Ct$ value >0), and blue means low expression or no expression

of a gene ($-\Delta\text{Ct}$ value <0). Hierarchical clustering also generated two dendrograms to reveal patterns among the rows and the columns: one of the genes (vertical) and one of the samples (horizontal).

Principal component analysis (PCA): Principal component analysis (PCA) using FactoMineR performs dimensionality reduction (Lê et al., 2008). PCA applies multiple linear transformations (singular value decomposition) to individual samples' expression profiles (PC - score plot) and identifies a series of PCs that elucidate the most distinguishing features between the samples. The coefficients of the linear transformations (PC - loading plot) measure the underlying variability of the genes associated with each component. All plotting was performed using R base graphics and ggplot2.

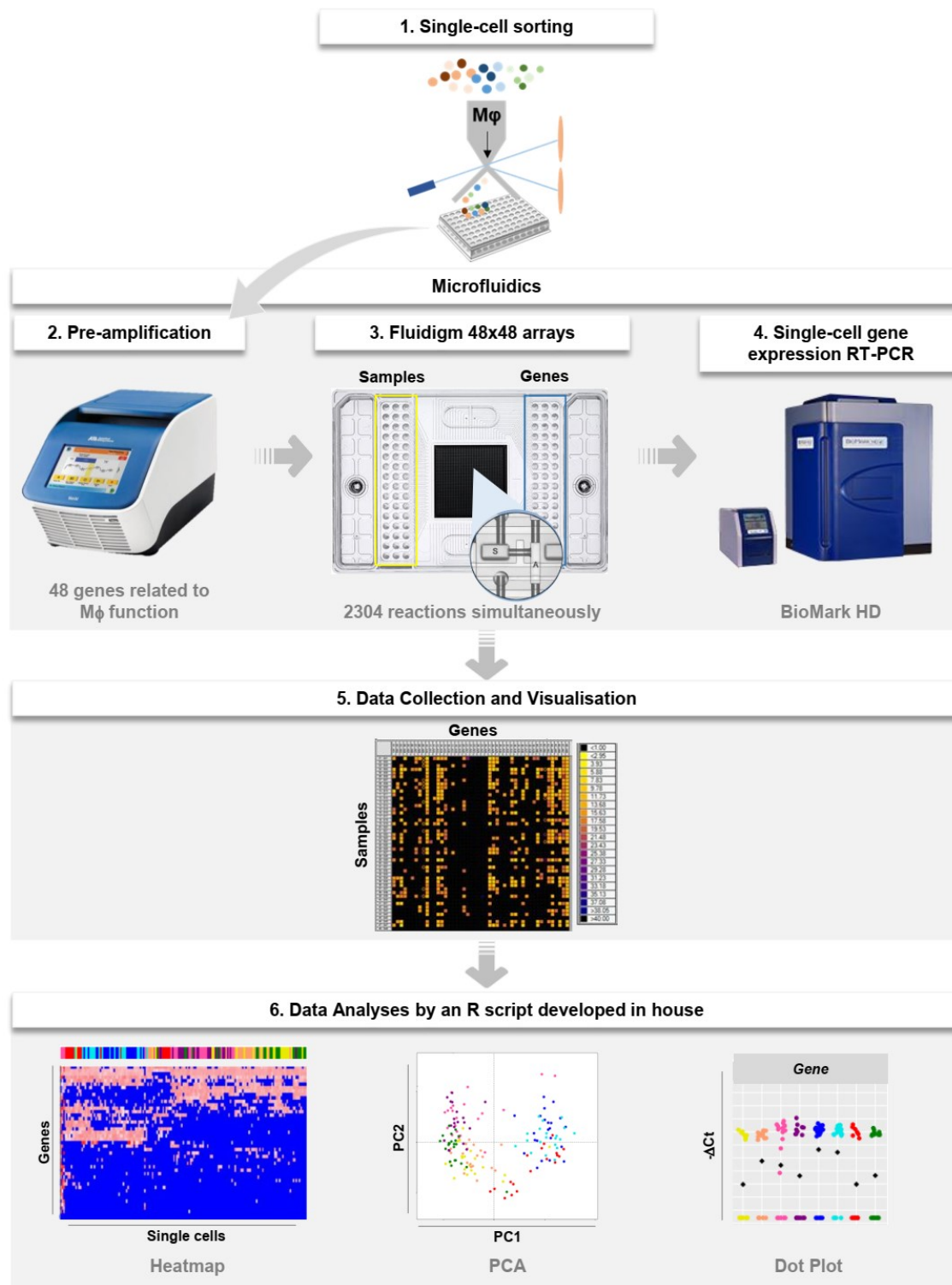


Figure 3.4 The workflow of sc expression profiling by qRT-PCR

1, By preparative sc flow sorting, individual cells were deposited into a 96-well plate. **2**, Pre-amplification for 48 target genes. **3**, Microfluidic arrays (Fluidigm) allow simultaneously analysing the expression of 48 genes in 48 single macrophages (2,304 reactions). **4**, qRT-PCR was then performed using the BioMark HD. **5**, Visualising the Ct values by Fluidigm Real-Time PCR analysis software as a heatmap. **6**, Final analysis was performed using an R-script developed in-house.

3.6 Protein expression assays

3.6.1 Enzyme-linked immunosorbent assay (ELISA)

To test M-CSF secretion levels in CSCs, an ELISA was performed using the M-CSF DuoSet kit (R&D systems) for manufacturing instructions. Briefly, 96-well microplates (Corning) were coated with 100 μ l/well diluted Capture Antibody overnight at room temperature. The following day, plates were washed three times with 400 μ l/well of Wash buffer, blocked using 300 μ l/well of Reagent Diluent, incubated at room temperature for 1 hr, washed three times as above, and 100 μ l/well of sample or standards in Reagent Diluent were added to the plate. The plates were then covered, incubated for 2 hr at room temperature, washed three times, and treated with 100 μ l/well of Detection Antibody for M-CSF (1:1000) for 2 hr at room temperature. For the detection step, 100 μ l/well Streptavidin-HRP was added for 20 min at room temperature, washed, and followed by 100 μ l/well of Substrate solution for 20 min, then 50 μ l/well of Stop Solution. Each well's absorbance was measured immediately using a plate reader (Beckman Coulter Paradigm Detection Platform) at 450 nm.

3.6.2 Multiplex bead-based immunoassay (LEDENDplex)

Supernatant from each cultured condition was collected on day 7 of the *in vitro* protocol. The experiments were always carried out in biological triplicate, including media-only conditions for each of the seven populations of macrophages generated. The supernatant was analysed using a bead-based multiplex immunoassay

LEGENDplex (BioLegend). This immunoassay uses two sizes of beads, designated A (big) and B (small), having different levels of Allophycocyanin (APC) fluorescence (Fig. 3.5 A), each combination of size and level being conjugated with a specific antibody to one of the 13 cytokines/chemokine of the panel. The bead-antibody-capture analyte is then detected using biotin. Therefore, the sandwich is made by capturing bead-(Ab)-analyte of interest-detection biotin. In the last step, Streptavidin-phycoerythrin (SA-PE) recognises a biotinylated antibody (Fig. 3.5 B). The fluorescent signal intensity is proportional to the analyte present in the supernatant. Flow cytometry (FACS Diva, Becton Dickinson) was then used to quantify PE signal fluorescence intensity, and the analyte concentration was obtained using LEGENDplex data analysis software (version 8.0.0.0, BioLegend).

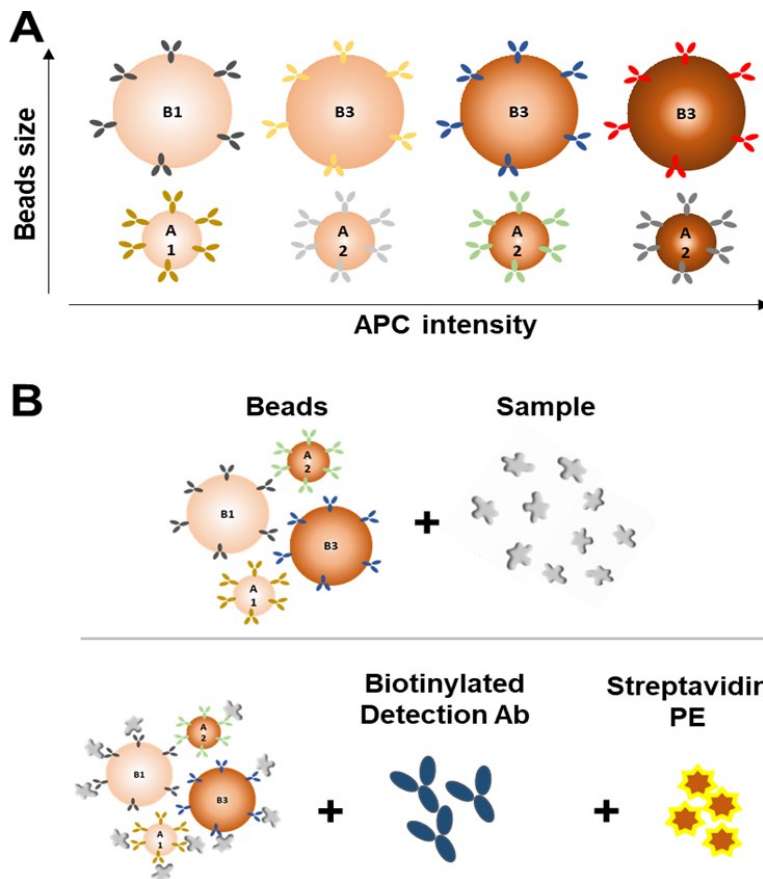


Figure 3.5 Schematic representation of LEGENDplex (BioLegend) protocol

A, The beads have two sizes (A-small and B-big) and different levels of APC intensities. Each bead is conjugated with an antibody against a specific analyte from the selected panel. **B**, Schematic representation of the three-step staining protocol accordingly to manufacturer instructions.

Cytokine/chemokine content was assessed using three 13-plex LEGENDPLEX panels, called (1) Mouse Inflammation panel; (2) Mouse Proinflammatory Chemokine panel; (3) Mouse Cytokine Panel 2; and a 6-plex panel, called Mouse Th2 Panel (6-plex), together with targeting the following chemokines:

1. Inflammation	2. Chemokine	3. Cytokines	4. Th2
Target	Target	Target	Target
CCL2 (MCP-1)	CCL2 (MCP-1)	IL-1 α	IL-5
GM-CSF	CCL3 (MIP-1 α)	IL-1 β	IL-13
IFN- β	CCL4 (MIP-1 β)	IL-3	IL-6
IFN- γ	CCL5 (RANTES)	IL-12p40	IL-10
IL-1 α	CCL11 (Eotaxin)	IL-12p70	TNF- α
IL-1 β	CCL17 (TARC)	IL-23	IL-4
IL-6	CCL20 (MIP-3 α)	IL-7	N/A
IL-10	CCL22 (MDC)	IL-11	N/A
IL-12p70	CXCL1 (KC)	IL-27	N/A
IL-17A	CXCL5 (LIX)	IL-33	N/A
IL-23	CXCL9 (MIG)	IFN- β	N/A
IL-27	CXCL10 (IP-10)	GM-CSF	N/A
TNF- α	CXCL13 (BLC)	TSLP	N/A

The concentration levels of three independent experiments for each secreted protein were normalised per analytes and visualised using an unbiased hierarchical clustering heatmap.

3.7 Phagocytosis assays

RAW 264.7 macrophages were plated on a 96-well half-area plate (Corning) at 27000 cells/cm² and incubated for 1 hour, left to attach to the plate before starting both phagocytosis assays. RAW 264.7 macrophages were fed with pHrodo™ Red *E. coli* BioParticles™ Conjugate (Thermo Fisher) prepared according to manufacturer instructions. Alternatively, RAW 264.7 macrophages were fed with apoptotic rat cardiomyocytes (H9c2). H9c2 cells were incubated with 80 μ M of Menadione (Sigma-

Aldrich) for 24 hours to induce apoptosis (Fiedler et al., 2019). Loss of H9c2 rat cardiomyocyte viability was confirmed using trypan blue exclusion (Vi-CELL Cell Viability Analyser). Dead H9c2 rat cardiomyocytes were resuspended at a concentration of 0.54×10^6 cells/mL. Subsequently, dead H9c2 cells were incubated with 5 μ M pHrodo™ Red, succinimidyl ester (pHrodo™ Red, SE, Invitrogen) for 1 hour at room temperature in dark conditions. Cells were centrifuged for 3 minutes at 160RCF to collect the pellet and gently resuspended in fresh media. Apoptotic H9c2 rat cardiomyocytes were passed through a 26G syringe and resuspended at a concentration of 0.27×10^6 cells/mL in the following media: control media (untreated), 50% CSC CondM, 50% CSC CondM + α CSF1R or 50% CSC CondM + 5 μ m Cytochalasin D. Cytochalasin D was used as a negative control as it inhibits actin polymerization and vacuole formation (Gardai et al. 2005; Ravichandran & Lorenz 2007; Santulli-Marotto et al. 2015).

Finally, RAW 264.7 macrophages were fed with media containing *E.coli* bioparticles or apoptotic H9c2 cells and incubated for 12 hours. The following day, media was aspirated, and RAW 264.7 macrophages were washed 3x with the respective media without bioparticles or apoptotic cells. RAW 264.7 macrophages were stained with Hoechst 33342 (Sigma-Aldrich) (1:2000) for 20 min.

Phagocytosis assays were then imaged using an AxioObserver Z1 inverted fluorescence microscope with a 10x objective (Zeiss). The percentage of pHrodo Red-positive cells was obtained by counting the total number of RAW 264.7 macrophages (Hoechst +) and pHrodo Red positive cells using Fiji (Schindelin et al., 2012).

3.8 Statistical analysis

GraphPad Prism (version 7.04) was used to perform statistical analysis. Data are reported as the mean, \pm standard error (SEM) with $p < 0.05$, unless otherwise stated in the legend of the Figures.

Flo cytometry, ELISA and multiplex immunoassays (Legendplex) have been performed at least three times independently, with at least three technical triplicates per experiment. Data reported from the FACS were analysed using one-way or two-way ANOVA followed by the Kruskal-Wallis/Dunn test ($p < 0.005$) or by Bonferroni's test for multiple comparisons ($p < 0.0001$). ELISA and Multiplex immunoassay (LegendPlex) data were analysed using a two-way ANOVA test, followed by Bonferroni's test ($p < 0.0001$).

The statistical analysis shown in the dot plots is based on the Kruskal-Wallis/Dunn test ($p < 0.005$) done using the R script developed in-house. Differential expression was determined using a non-parametric Kruskal-Wallis/Dunn test. Euclidean distances among samples and genes were used to compute hierarchical clustering using the complete linkage method and integrated into data visualization based on heatmaps.

3.9 Key resources

REAGENT	SOURCE	IDENTIFIER
Antibodies and other staining reagents		
Armenian Hamster monoclonal anti-IgG, PE/Cy7-conjugated	BioLegend	400921
Monoclonal Antibody (AFS98), CD115 (c-fms) Functional Grade, eBioscience	ThermoFisher	16-1152-82
Mouse anti-IgG, HRP-linked	Cell Signalling	7076
Mouse monoclonal anti-CD11b, Alexa Fluor 700-conjugated	BioLegend	M1/70:101222
Mouse monoclonal anti-CD206, biotin-conjugated	Invitrogen	MR5D3: MA516869
Mouse monoclonal anti-CX3CR1, PE-conjugated	BioLegend	SA011F11:149005
Mouse monoclonal anti-CSF1R, PE/Cy7-conjugated	BioLegend	AFS98:135524
Mouse monoclonal anti-F4/80, Alexa Fluor 647-conjugated	BioLegend	BM8:123121
Mouse monoclonal anti- β -actin	Cell Signalling	3700S
Mouse monoclonal anti-IgG2a, PE-conjugated	BioLegend	400211
Rabbit anti-IgG, HRP-linked	Cell Signalling	7074
Rat IgG2a kappa Isotype Control (Ebr2A), Functional Grade, eBioscience	ThermoFisher	16-4321-82
Rat monoclonal anti-IgG2a, Alexa Fluor 647-conjugated	BioLegend	400526
Rat monoclonal anti-IgG2b, Alexa Fluor 700-conjugated	BioLegend	400628
Rat monoclonal anti-IgG2a, biotin-conjugated	Invitrogen	PA533213
Rat monoclonal anti-IgG2b, BV510-conjugated	BioLegend	400645
Rat monoclonal anti-IgG2a, PE/Cy7-conjugated	BioLegend	400521
Rabbit polyclonal anti-HGK	Cell Signalling	3485S
Streptavidin, BV510-conjugated	BioLegend	405229
Sytox Blue	Invitrogen	S34857
Chemicals, Peptides, and Recombinant Proteins		

Antibiotic-antimycotic	Invitrogen	15240-096
BLZ-945	Cayman Chemical	953769-46-5
Bovine growth serum (BGS)	Hyclone	SH30541
B27 Supplement	Invitrogen	17504-044
Cardiotrophin-1	Cell Sciences	CRC700B
Collagen type I	BD Bioscience	354236
Dulbecco's Modified Eagle's Medium (DMEM)	Invitrogen	11965-092
Fetal Bovine Serum (FBS)	Gibco	10270
Gelatine solution	Sigma-Aldrich	G1393-100ML
Glycine	Sigma-Aldrich	G7126
Ham's F12	Invitrogen	11765-054
Human cardiotrophin-1 (CT-1)	Cell Sciences	CRC700A
Human epidermal growth factor	Peptotech	AF-100-15
Human fibroblast growth factor-basic	Peptotech	100-18B
Iscove's modified Dulbecco's medium (IMDM)	Invitrogen	12440-046
L-Glutamine (200mM)	ThermoFisher	25030-024
Lipopolysaccharides (LPS)	Sigma-Aldrich	L4391
Methanol	ThermoFisher	34860
ON-TARGETplus Mouse Map4k4 siRNA – smartpool	Dharmacon	J-040100-05, 06, 07, 08
Phosphate Buffered Saline (PBS) pH7.2 (1x)	Gibco	20012-019
Recombinant Human epidermal growth factor (EGF)	Miltenyi Biotec	130-097-749
Recombinant Human fibroblast growth factor (hFGF)	Peptotech	100-18B
Recombinant Murine GM-CSF	Peptotech	315-03
Recombinant Murine IFN- γ	Peptotech	315-05
Recombinant Murine IL-13	Peptotech	210-13
Recombinant Murine IL-4	Peptotech	214-14
Recombinant Murine M-CSF	Peptotech	315-02
Thrombin	Sigma-Aldrich	10602400001
Tris-Base	ThermoFisher	17926
Trypsin-EDTA 0.25% Phenol red	Gibco	25200-056
β -mercaptoethanol	Sigma-Aldrich	M3148
Critical Commercial Assays		
CellDirect One-Step qRT-PCR kits	Invitrogen	11753500
Mouse M-CSF DuoSet ELISA	R&D System	DY416
PureLink® RNA Micro Scale Kit	Invitrogen	12183016

LEGENDplex Mouse Inflammation Panel (13-plex) with V-bottom Plate	BioLegend	740150
LEGENDplex Mouse Proinflammatory Chemokine Panel (13-plex) with V-bottom Plate	BioLegend	740451
LEGENDplex Mouse Cytokine Panel 2 (13-plex)	BioLegend	740134
LEGENDplex Mouse Th2 Panel	BioLegend	741043
Experimental Models: Organisms/Strains		
C57BL/6 mice	Charles River	C57BL/6NCrl
Oligonucleotides (TaqMan probe)		
<i>Ang</i>	ThermoFisher	Mm01316661_m1
<i>Angpt1</i>	ThermoFisher	Mm00456503_m1
<i>Angpt4</i>	ThermoFisher	Mm00507766_m1
<i>Angptl2</i>	ThermoFisher	Mm00507897_m1
<i>Angptl4</i>	ThermoFisher	Mm00480431_m1
<i>Angptl7</i>	ThermoFisher	Mm01256626_m1
<i>Arg1</i>	ThermoFisher	Mm00475988_m1
<i>Bmper</i>	ThermoFisher	Mm01175806_m1
<i>Bmp2</i>	ThermoFisher	Mm01340178_m1
<i>Bmp4</i>	ThermoFisher	Mm00432087_m1
<i>Ccl2</i>	ThermoFisher	Mm00441242_m1
<i>Ccl7</i>	ThermoFisher	Mm00443113_m1
<i>Ccl19</i>	ThermoFisher	Mm00839967_g1
<i>Cdh5</i>	ThermoFisher	Mm00486938_m1
<i>Cd31/pecam</i>	ThermoFisher	Mm01242584_m1
<i>Clec3b</i>	ThermoFisher	Mm00495657_m1
<i>Csf1</i>	ThermoFisher	Mm00432686_m1
<i>Csf1r</i>	ThermoFisher	Mm01266652_m1
<i>Csf2</i>	ThermoFisher	Mm01290062_m1
<i>Cx3cr1</i>	ThermoFisher	Mm00438354_m1
<i>Cxcl1</i>	ThermoFisher	Mm04207460_m1
<i>Cxcl2</i>	ThermoFisher	Mm00436450_m1
<i>Cxcl3</i>	ThermoFisher	Mm01701838_m1
<i>Cxcl5</i>	ThermoFisher	Mm00436451_g1
<i>Cxcl9</i>	ThermoFisher	Mm00434946_m1
<i>Cxcl10</i>	ThermoFisher	Mm00445235_m1
<i>Cxcl12</i>	ThermoFisher	Mm00445553_m1
<i>Ereg</i>	ThermoFisher	Mm00514794_m1
<i>F3</i>	ThermoFisher	Mm00438855_m1

<i>Gata4</i>	ThermoFisher	Mm00484689_m1
<i>Gdf15</i>	ThermoFisher	Mm00442228_m1
<i>Hand2</i>	ThermoFisher	Mm00439247_m1
<i>Hmbs</i>	ThermoFisher	Mm01143545_m1
<i>Igf1</i>	ThermoFisher	Mm00439560_m1
<i>Igf2</i>	ThermoFisher	Mm00439564_m1
<i>Il1b</i>	ThermoFisher	Mm00434228_m1
<i>Il1r1</i>	ThermoFisher	Mm00434237_m1
<i>Il1r2</i>	ThermoFisher	Mm00439629_m1
<i>Il1rl1</i>	ThermoFisher	Mm00516117_m1
<i>Il4</i>	ThermoFisher	Mm00445259_m1
<i>Il6</i>	ThermoFisher	Mm00446190_m1
<i>Il10</i>	ThermoFisher	Mm01288386_m1
<i>Il11</i>	ThermoFisher	Mm00434162_m1
<i>Il13</i>	ThermoFisher	Mm00434204_m1
<i>Il34</i>	ThermoFisher	Mm01243248_m1
<i>Inhba</i>	ThermoFisher	Mm00434339_m1
<i>Kdr</i>	ThermoFisher	Mm00440111_m1
<i>Ly6a</i>	ThermoFisher	Mm00726565_g1
<i>Map4k4 Isf. 1</i>	ThermoFisher	AJKL180
<i>Map4k4 Isf. 2</i>	ThermoFisher	Mm00500808_m1
<i>Map4k4 Isf. 3</i>	ThermoFisher	AJKAK25
<i>Map4k4 Isf. 4</i>	ThermoFisher	AJIMWK
<i>Mrc1</i>	ThermoFisher	Mm01329362_m1
<i>Myh6</i>	ThermoFisher	Mm00440359_m1
<i>Myh11</i>	ThermoFisher	Mm00443013_m1
<i>Myl2</i>	ThermoFisher	Mm00440384_m1
<i>mPGES1</i>	ThermoFisher	Mm00452105_m1
<i>Ngf</i>	ThermoFisher	Mm00443039_m1
<i>Nos2</i>	ThermoFisher	Mm00440502_m1
<i>Pecam1</i>	ThermoFisher	Mm01242576_m1
<i>Pdgfra</i>	ThermoFisher	Mm01211685_m1
<i>Pi16</i>	ThermoFisher	Mm00470084_m1
<i>Ptch2</i>	ThermoFisher	Mm00436047_m1
<i>Ptges</i>	ThermoFisher	Mm00452105_m1
<i>Sod3</i>	ThermoFisher	Mm01213380_s1
<i>Tbx20</i>	ThermoFisher	Mm00451515_m1
<i>Tcf21</i>	ThermoFisher	Mm00448961_m1
<i>Tgfb1</i>	ThermoFisher	Mm01178820_m1
<i>Tgfb2</i>	ThermoFisher	Mm00436955_m1
<i>Tgfb3</i>	ThermoFisher	Mm00436960_m1

<i>Tgm2</i>	ThermoFisher	Mm00436987_m1
<i>Tnfa</i>	ThermoFisher	Mm00443258_m1
<i>Ubc</i>	ThermoFisher	Mm01201237_m1
<i>Vegfa</i>	ThermoFisher	Mm00437306_m1
<i>Vegfb</i>	ThermoFisher	Mm00442102_m1
<i>Vegfc</i>	ThermoFisher	Mm00437310_m1
<i>Wt1</i>	ThermoFisher	Mm00460570_m1
Software and Algorithms		
FlowJo Version 10	FlowJo	N/A
Fluidigm software Version 4	Fluidigm	N/A
Prism Versions 6 and 7	GraphPad Software Inc	http://www.graphpad.com/scientific-software/prism/
R software environment	The R Foundation	https://cran.r-project.org
Other		
Array chips for 48 assays x 48 samples	Fluidigm	BMK-M10-48.48
BioMark HD system	Fluidigm	N/A
Cell strainer mesh 70 µm	BD Falcon	352350
0.2 µm filter units FP30/0.2 CA-S	GE Healthcare	10462200
Veriti Thermal Cycler	ABI ThermoFisher	N/A

Chapter 4 – Result I

4 Result I: *In vitro* generation of M1- and M2-driven macrophages

4.1 Introduction and rationale

Macrophages are in a continuous spectrum of phenotypes ranging from one pro-inflammatory end to the opposite anti-inflammatory end. Over the past two decades, several definitions tried to identify, characterise and classify macrophage phenotypes. However, due to the complexity of these phenotypes, with overlapping characteristics, there is no consensus on the best way to define them (Anderson & Mosser, 2002; de Couto, 2019; Gleissner et al., 2010; Kadl et al., 2010; Mantovani et al., 2002, 2004; Martinez & Gordon, 2014; Mills et al., 2000; Parisi et al., 2018; Stein et al., 1992). Therefore, this PhD thesis considered the best way to name macrophages based on the stimulation used for their differentiation and activation.

Hence, the first objective of this PhD thesis was to design an *in vitro* system to generate pure populations of macrophages that formally express the opposite phenotypes of macrophage's spectrum. Therefore, this Chapter describes the experiments conducted to achieve the first aim of this PhD thesis addressing the following points:

- (i) Establish an *in vitro* system to differentiate BMDMs into macrophages and activate them using cocktails of growth factors and pro- and anti-

inflammatory stimuli towards the opposite extreme of the macrophages' phenotypic spectrum.

- (ii) Demonstrate their distinctive immunophenotype using multi-parametric flow sorting.
- (iii) Demonstrate their distinctive gene expression signature at the single-cell level, information lacking in the field at the time of this dissertation research.

4.2 Results

4.2.1 *In vitro* system to study M1- and M2-driven-M ϕ

The *in vitro* system designed in this PhD thesis uses a combination of growth factors and stimuli to generate four populations of macrophages, named according to the culture treatment used.

First, GM-CSF and M-CSF differentiated unfractionated BM progenitor cells into GM-CSF-M ϕ and M-CSF-M ϕ , respectively. Then, half of the GM-CSF-M ϕ were activated with the pro-inflammatory stimuli, LPS and IFN γ and named GM-CSF+LPS+IFN γ -M ϕ . Similarly, half of the M-CSF-M ϕ were activated with the anti-inflammatory stimuli, IL-4 and IL-13, and named M-CSF+IL4+IL13-M ϕ . M1-driven M ϕ includes GM-CSF-M ϕ and GM-CSF+LPS+IFN γ -M ϕ , while the M2-driven M ϕ includes M-CSF-M ϕ and M-CSF+IL4+IL13-M ϕ (Fig. 4.1).

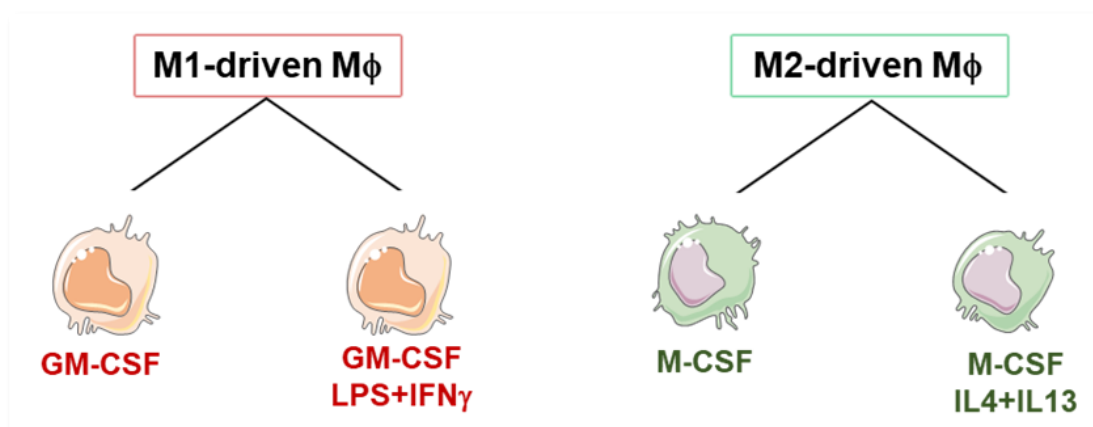


Figure 4.1 Illustration of the four populations generated *in vitro*

4.2.2 The immunophenotype of M1- and M2-driven-M ϕ

Sequential combinations of growth factors and stimuli used in the culture treatments induced distinctive immunophenotypes of macrophages. Multiparametric flow cytometry enriched a uniform population of resident cardiac macrophages using the resident cardiac marker CX3CR1 and the pan-macrophage marker CD11b, followed by a step to discern between M1- and M2-driven-M ϕ immunophenotypes using the pan-macrophage marker F4/80 and the anti-inflammatory macrophage marker, CD206 (Ensan et al., 2016; Gordon & Plüddemann, 2017; Jablonski et al., 2015; Lin et al., 2003; Molawi et al., 2014; Morris et al., 1991; Petty & Todd, 1996; Pinto et al., 2012; Shintani et al., 2016; Stewart et al., 1995).

Live single cells were gated on the Sytox™ Blue dead cell exclusion assay using side (SSC-A) and forward scatter(FSC-A). The expression levels of CX3CR1 and CD11b were evaluated to enrich resident cardiac macrophages (Ensan et al., 2016; Molawi et al., 2014; Pinto et al., 2012). The distribution of CX3CR1⁺CD11b⁺ in M1- and M2-driven-M ϕ was unequal, 80% and 50%, respectively ($p < 0.0001$) (Fig. 4.2 A, B). Within the CX3CR1⁺CD11b⁺ cells, F4/80 and CD206 expression levels were measured (Fig. 4.2 A, B). FACS data showed that approximately 40% of CX3CR1⁺CD11b⁺F4/80⁺CD206⁺ macrophages were found within the M2-driven-M ϕ (39% in M-CSF+IL4+IL13-M ϕ ; 18% in M-CSF-M ϕ). Conversely, less than 10% of CX3CR1⁺CD11b⁺F4/80⁺CD206⁺ macrophages were found within the M1-driven-M ϕ group, which was instead enriched for CX3CR1⁺CD11b⁺F4/80^{lo}CD206⁻ macrophages (58% in GM-CSF+LPS+IFN γ -M ϕ ; 43% in GM-CSF-M ϕ) ($p < 0.0001$) (Fig.

4.2 A, B). The unbalanced distribution of CX3CR1⁺CD11b⁺ among the generated populations did not meet the expectations of this experimental approach.

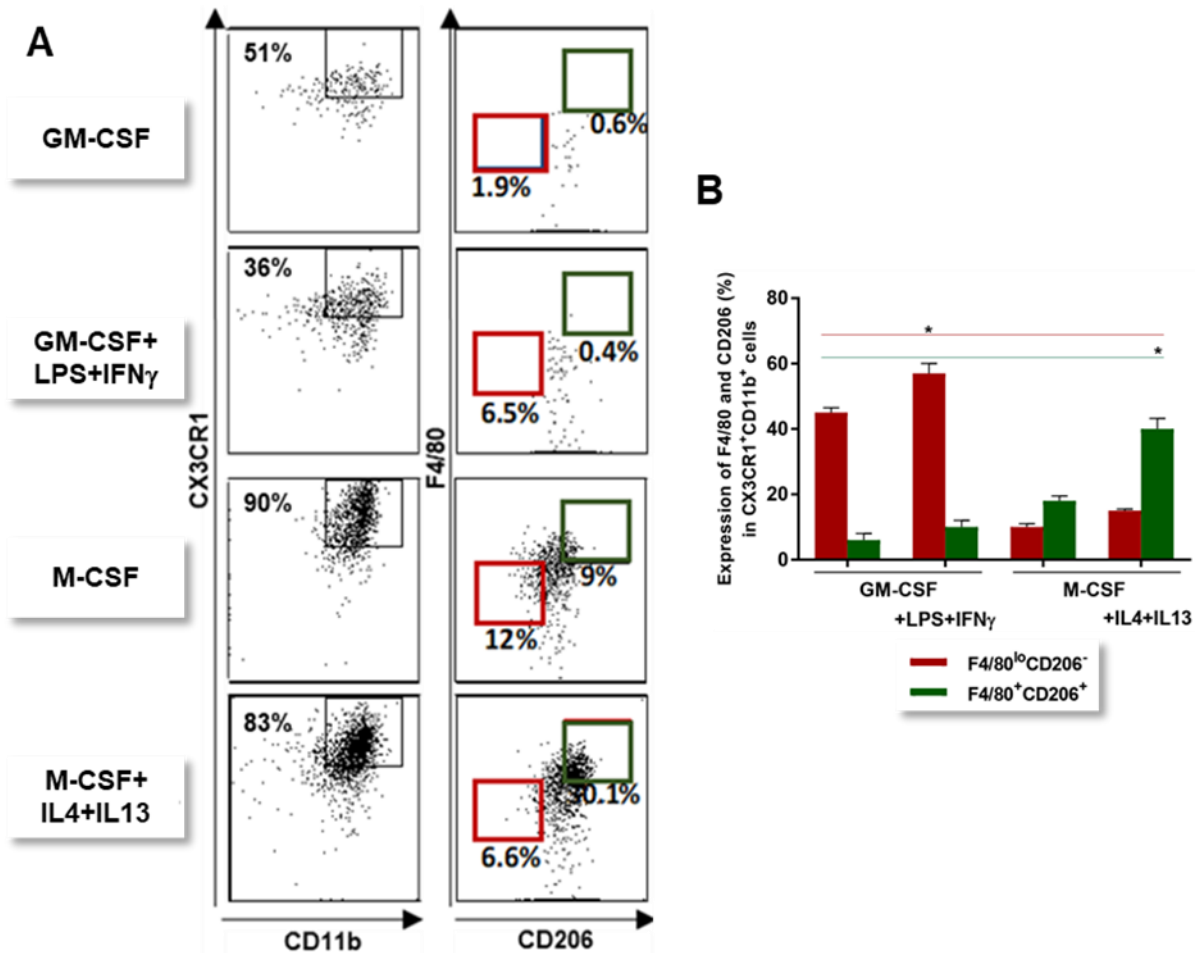


Figure 4.2 Flow cytometry data of the four macrophage populations generated *in vitro*

A, Representative flow cytometry plots of the four culture conditions. The first column shows the expressions CX3CR1 and CD11b. The second column shows the expressions F4/80 and CD206. The red gates are on the CX3CR1⁺CD11b⁺F4/80^{lo}CD206⁻ macrophages, while the green gates are on CX3CR1⁺CD11b⁺F4/80⁺CD206⁺ macrophages. **B**, Bar graph of the percentage of CX3CR1⁺CD11b⁺F4/80^{lo}CD206⁻ (red) and CX3CR1⁺CD11b⁺F4/80⁺CD206⁺ (green) cells in the four culture conditions. (±SEM, N=3). Two-way ANOVA test with Bonferroni's correction (*, p<0.0001).

4.2.3 The single-cell gene expression profile of M1- and M2-driven-M ϕ

Next, the gene expression profiles of GM-CSF+LPS+IFN γ -M ϕ and M-CSF+IL4+IL13-M ϕ were analysed using the state-of-the-art single-cell qRT-PCR technology.

For this analysis, 84 single cells were flow-sorted, as follows: 42 from the GM-CSF+LPS+IFN γ -M ϕ group: 21 CX3CR1⁺CD11b⁺F4/80^{lo}CD206⁻ and 21 CX3CR1⁺CD11b⁺F4/80⁺CD206⁺ cells. Similarly, the other 42 single cells were sorted from the M-CSF+IL4+IL13-M ϕ group: 21 CX3CR1⁺CD11b⁺F4/80^{lo}CD206⁻ and 21 CX3CR1⁺CD11b⁺F4/80⁺CD206⁺ cells. These 84 single cells were preamplified using 48 preselected genes related to paracrine functions (Table 3.5, Panel 1). Single-cell qRT-PCR data were analysed and visualised using the in-house developed R script. Due to the complexity of the data generated by sc qRT-PCR, three visualisation methods were used to interpret the biological meaning of the data better: unbiased hierarchical clustering heatmaps, principal component analysis (PCA), and dot plots.

An unbiased hierarchical clustering heatmap is the first method to visualise single-cell gene expression data. The heatmap showed the gene expression profile of all the sorted 84 cells, revealing two main clusters reflecting the two culture conditions. All 42 single cells sorted from GM-CSF+LPS+IFN γ -M ϕ grouped in cluster 1, while all 42 single cells sorted from M-CSF+IL4+IL13-M ϕ grouped in cluster 2. Thus, the selected panel of genes successfully resolved the two populations with no overlap. The heatmap highlighted seven genes responsible for forming these two clusters. Cluster 1 was enriched for *Ly6a*, *Il6*, *Nos2*, and *Cxcl9*, while cluster 2 for *Angptl2*, *Igf1*, and

Arg1. Consistent with the complementary instructive signals used, *Ly6a*, *Il6*, *Nos2*, and *Cxcl9* are pro-inflammatory genes, while *Angptl2*, *Igf1*, and *Arg1* are anti-inflammatory genes (Bashir et al., 2016; Bronte & Zanovello, 2005; De Couto et al., 2015; Guha & Mackman, 2002; Lewis & Pollard, 2006; Locati et al., 2013; Lumeng et al., 2007; Mackman et al., 1991; Mantovani et al., 2004; Murray et al., 2014). The sc qRT-PCR analysis confirmed a mutually exclusive expression of *Nos2* and *Arg1*, considered the best gene markers to distinguish pro- and anti-inflammatory macrophages. *Nos2* was expressed exclusively by the GM-CSF+LPS+IFN γ -M ϕ , while *Arg1* by the M-CSF+IL4+IL13-M ϕ . However, the expression of these two clusters did not correlate with the cells' immunophenotype based on the expression of F4/80 and CD206. Together with the heterogeneous markers under the two conditions tested, this suggests that the transcriptomic signature, although limited in scope, identifies macrophage features better, at least in this setting.

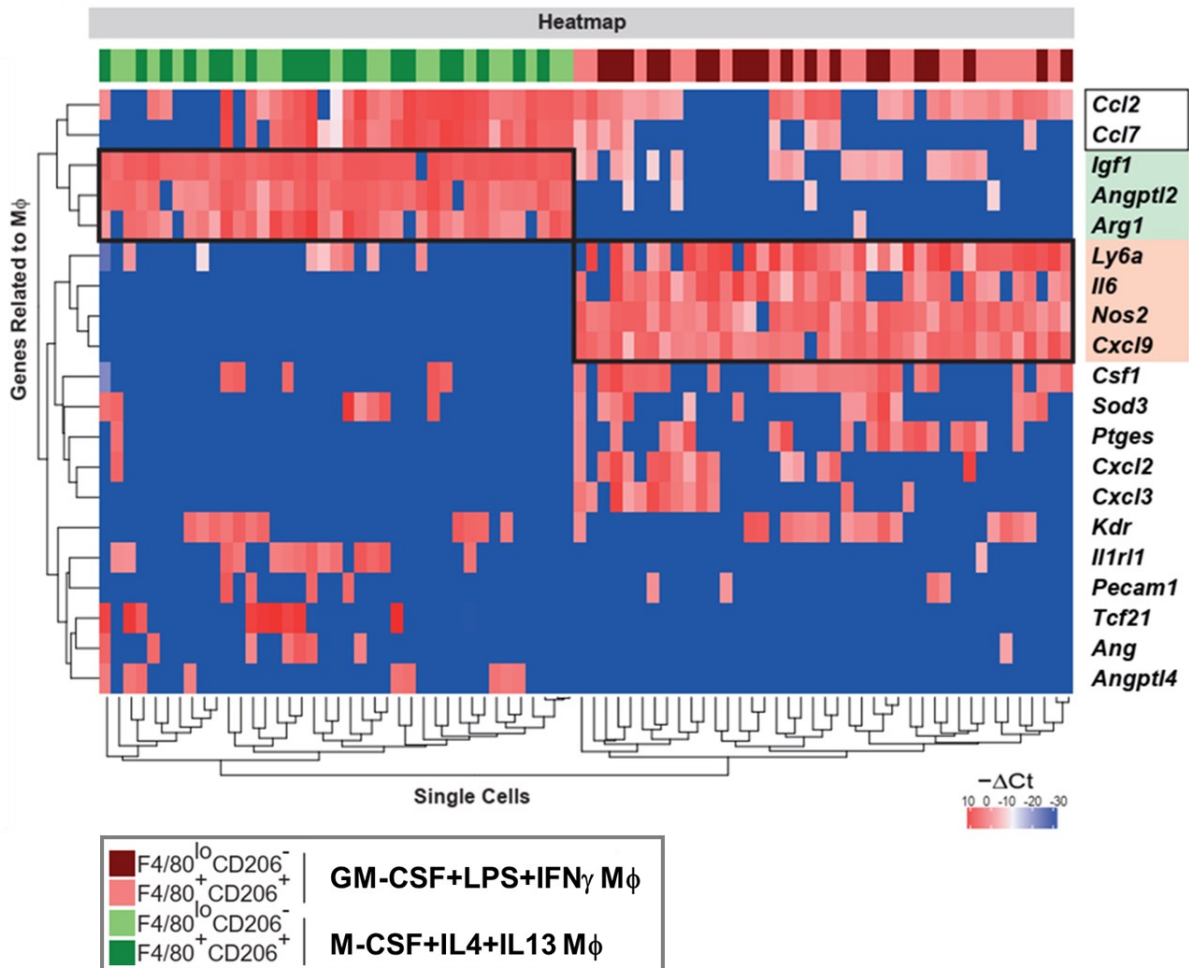


Figure 4.3 Unbiased hierarchical clustering heatmap shows the single-cell gene expression profile of M1- and M2-driven macrophages

Single-cell qRT-PCR analysis of 84 cells: from GM-CSF+LPS+IFN γ -M ϕ , 21 CX3CR1⁺CD11b⁺F4/80^{lo}CD206⁻ (red), 21 CX3CR1⁺CD11b⁺F4/80⁺CD206⁺ cells (pink), while from M-CSF+IL4+IL13-M ϕ , 21 CX3CR1⁺CD11b⁺F4/80^{lo}CD206⁻ (green) and 21 CX3CR1⁺CD11b⁺F4/80⁺CD206⁺ cells (dark green). The heatmap shows Δ Ct values (blue, low or absent; red, high). Not expressed genes were omitted to increase visualisation quality (Fig. A1).

The second visualisation method to further explore sc qRT-PCR data was the PCA. PCA shows how the data distribution can highlight variability, similarities and gene co-expression between single cells (Massaia et al., 2018). The difference between the first two principal components (PC1 and PC2) measures the variation of the data.

PCA of the samples showed that with approximately 40% variability, PC1 separates GM-CSF+LPS+IFN γ -M ϕ and M-CSF+IL4+IL13-M ϕ into two well-resolved non-overlapping groups based on their unique gene expression profiles. This visualisation method confirmed that the populations clustered based on their culture conditions rather than their immunophenotypes, as demonstrated with the heat map. PCA of the genes shows three clusters. At the top right, cluster 1 includes the pro-inflammatory genes *Nos2*, *Ly6a*, *Il6*, *Csf1*, and *Ptges*, and the chemokines *Cxcl2*, *Cxcl3*, and *Cxcl9*. PC1 separates clusters 1 from 2 and 3. Cluster 2 includes three anti-inflammatory genes, *Arg1*, *Ig1*, and *Angptl2*, and cluster 3 includes the migration-related genes, *Ccl2* and *Ccl7*. Clusters 1 and 2 define the main gene differences between GM-CSF+LPS+IFN γ -M ϕ and M-CSF+IL4+IL13-M ϕ , while the migration cluster is expressed in both macrophages subpopulations as they do not discriminate between these two states (Fig. 4.4).

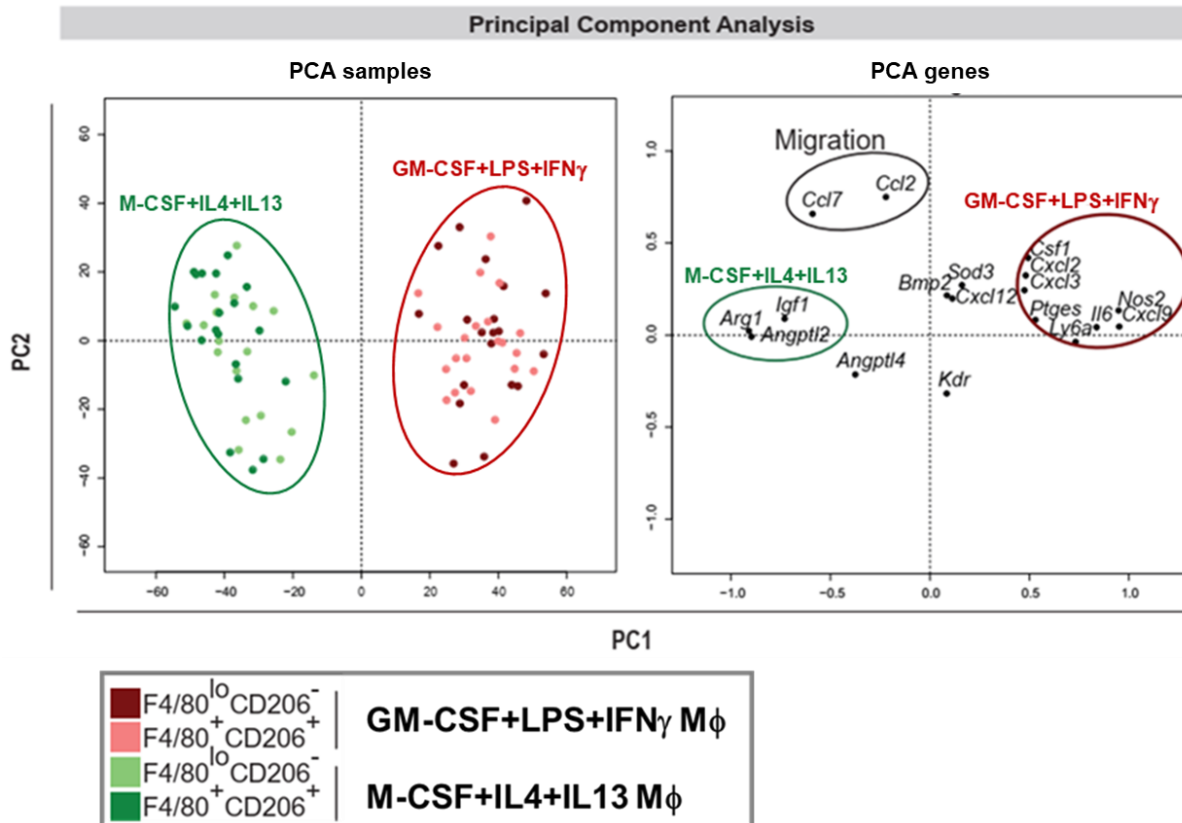


Figure 4.4 PCAs show the single-cell gene expression profile of M1- and M2-driven-M ϕ PCA of the sample. PC1 separates GM-CSF+LPS+IFN γ -M ϕ and M-CSF+IL4+IL13-M ϕ into two groups. By contrast, no difference was conferred by the immunophenotype. PCA of genes indicates three clusters defining the pro-inflammatory, the anti-inflammatory and the migration-related genes.

Finally, the dot plots were the third method for displaying the sc qRT-PCR data. Dot plots show a quantitative difference in the gene expression levels. The expression levels of *Csf1*, *Cxcl2*, *Cxcl3*, *Cxcl9*, *Il6*, *Nos2*, *Ly6a* and *Ptges* were significantly higher in GM-CSF+LPS+IFN γ -M ϕ than M-CSF+IL4+IL13-M ϕ ($p < 0.005$) (p -values in Fig. A2). However, within the GM-CSF+LPS+IFN γ -M ϕ , no differences were observed based on their immunophenotype. Similarly, M-CSF+IL4+IL13-M ϕ were enriched for *Igf1*, *Angptl2*, *Arg1*, *Il1r1* and *Tcf21*, regardless of their immunophenotypes ($p < 0.005$) (p -values in Fig. A2). (Fig. 4.5). Thus, single-cell gene expressions indicated that the *in*

vitro system generates two populations of macrophages with opposite gene patterns near to the two ends of the macrophage's phenotypic spectrum.

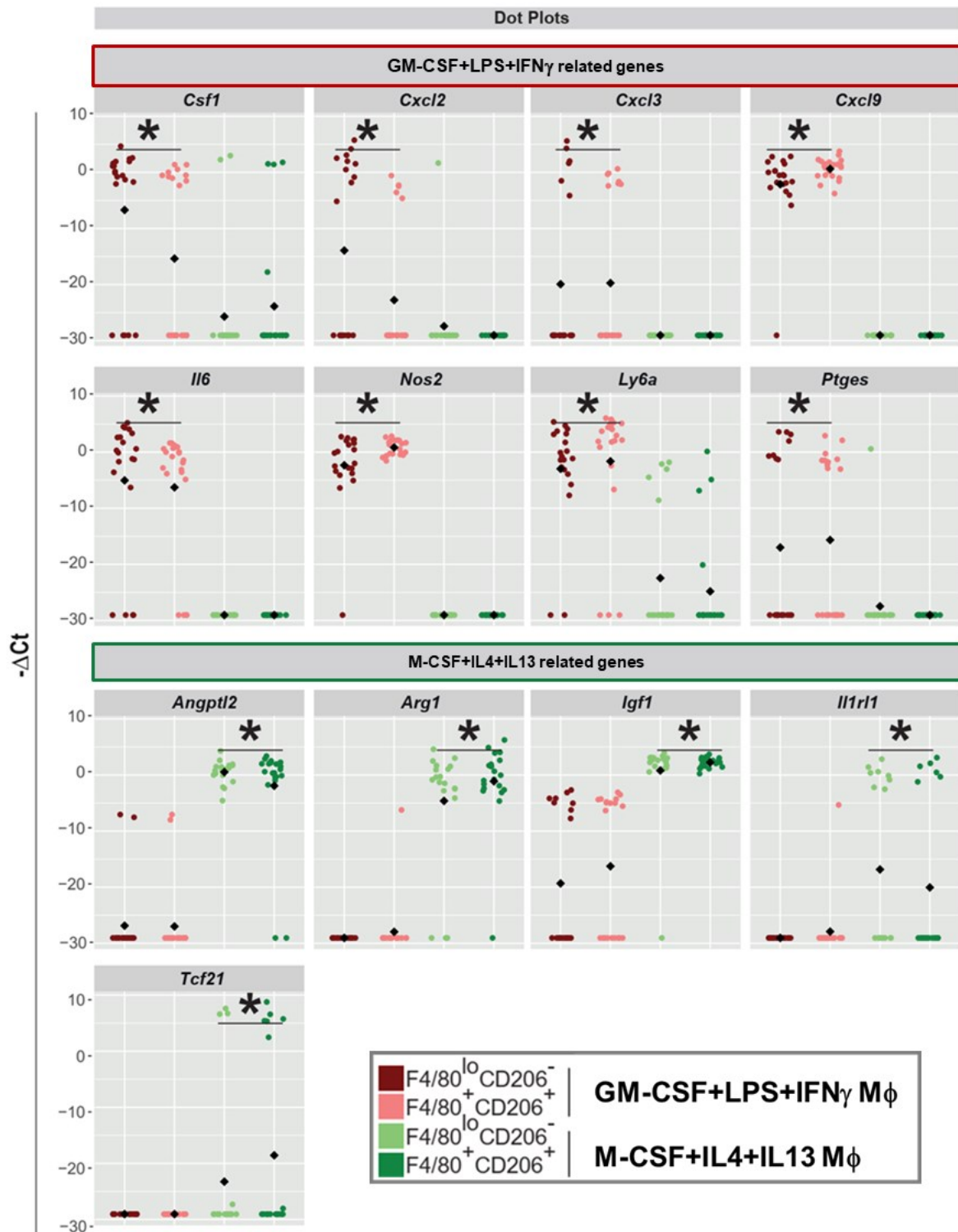


Figure 4.5 Dot plots show the single-cell gene expression profile of M1- and M2-driven macrophages

Dot plots complement the sc qRT-PCR analysis of genes scored statistically different between GM-CSF+LPS+IFN γ (TOP) and M-CSF+IL4+IL13-M ϕ (BOTTOM). *, $p < 0.005$ for GM-CSF+LPS+IFN γ versus M-CSF+IL4+IL13-M ϕ (Kruskal-Wallis/Dunn test). Full heatmap of the p-values (Fig. A2).

4.3 Discussion

4.3.1 *In vitro* differentiation of macrophages: advantages and limitations

The characterisation of signalling and transcription pathways to classify macrophage phenotypes *in vivo* is highly complex due to their spectrum variation. Therefore, *in vitro* studies provide a picture of the extremes of this spectrum (Martinez et al., 2008; Sica & Mantovani, 2012). Several *in vitro* protocols are currently available to differentiate BMDMs into macrophages. However, there is a general lack of consensus in the scientific community on the best protocol for generating distinct macrophage populations. This inconsistency could obscure comparing the results generated in various studies (Lee & Hu, 2013; Xu et al., 2007). Therefore, the first objective of this PhD thesis was to develop a robust, highly reproducible, and easy-to-use system for differentiating BMDMs into macrophages with distinct phenotypes that resemble the two extremes of the macrophages spectrum.

The main advantages of this in vitro system

First of all, the choice of BMDMs as a macrophage source is justifiable from the adequate number of monocytes and macrophages obtained compared to other methods, such as the isolation of the myeloid progenitor cells from the BM (Francke et al., 2011; Marim et al., 2010; Orecchioni et al., 2019). Secondly, the selected factors and stimuli generated macrophages with opposite phenotypes. This system is a two-step protocol that includes a 6-day differentiation phase using a single growth factor, either GM-CSF or M-CSF, followed by a short 24-hour activation phase using a

cocktail of stimuli. The two-step protocol was crucial in pushing the generated populations towards opposite ends of the spectrum of macrophage phenotypes. Another advantage of this system is its permutability, which allows studying macrophages' plasticity and responses to the local environment. It was designed to be easily adaptable and test how factors or conditioned media from different cell types or any other perturbation could modulate the phenotypic fate of monocytes/macrophages.

The advantage of using two growth factors during the differentiation phase

Considering that the first goal of this PhD thesis was to obtain macrophages with opposite phenotypes, research was conducted throughout the literature to find those factors that could produce the most diverse phenotypes of macrophages. Therefore, the two growth factors, GM-CSF and M-CSF, were selected and added into the culture as early as day zero (Fleetwood et al., 2007). Flow cytometry showed that differentiating BM progenitor cells with either GM-CSF or M-CSF produced macrophages already driven to opposite ends of the spectrum before the activation phase. M-CSF is widely used to differentiate BMDMs into macrophages with cardiac resident characteristics. In the next chapter, there is an in-depth discussion of the role of M-CSF in differentiation.

Several *in vitro* studies have used GM-CSF as a growth factor to differentiate DCs (Dong et al., 2016; Na et al., 2016). Therefore, in developing this *in vitro* system, two primary considerations were made to ensure BM cells differentiate into macrophages rather than DCs. First, macrophages have a strong adherent ability to attach to the tissue culture dish compared to DCs. Hence, during the 6-day differentiation phase,

the monocytes were allowed to adhere to the plastic surface, becoming monocyte-derived macrophages. Before starting any analysis or adding any stimuli, the cells were washed twice, and the media replaced. Non-strongly adherent cells were washed away during this step, leaving only well-differentiated macrophages on the bottom of the plastic culture dish. This is an easy, cost-effective step of differentiation that ensures a superior enrichment of macrophages. There are other forms of BMDMs isolation, such as positive beads isolation, cold-aggregation, Percoll gradient or immunomagnetic purification (Chometon et al., 2020). However, these various techniques are limited by the duration of their processes. They could cause a reduction in cell viability, in some cases due to increased toxicity, such as by using Percoll reagents (Oliveira et al., 2012). They can also alter gene and protein expression profiles and functional states (Chometon et al., 2020). Lastly, bioinformatics analysis confirmed that the M1-driven M ϕ generated here exhibit a gene expression profile resembling pro-inflammatory macrophages more closely than DCs (Croizat et al., 2010; Robbins et al., 2008).

The main limitations of this in vitro system

In vitro studies also have limitations. Several studies have reported that macrophage transcriptomes can vary drastically, increasing and decreasing hundreds of genes when transferred from their residential tissue to a tissue culture environment (Gosselin et al., 2017). Single-cell RT-PCR identifies genes enriched in a specific culture condition. Identification of these clusters of genes can be used as a reference for any experimental perturbation studies. Furthermore, mouse models are commonly used to study post-MI inflammation. However, the translation of mouse work into the clinic has its limitations. First, the number of circulating monocytes between mice and

humans is different, creating a functional difference in their pathophysiology. Second, these two species' gene expression profiles differ, as monocytes and macrophages function in healthy and pathological environments. Finally, the protein profile is varied enough that the results in mice may not be transferable to human studies.

4.3.2 Characterisation of the immunophenotype of macrophages by flow sorting: advantages and limitations

The main advantages of flow cytometry

Following the development of the *in vitro* system, the four macrophage populations were analysed by flow sorting. Flow cytometry is the gold standard for validating and characterising cell surface markers. Monitoring surface marker expression using FACS helps compare different macrophage populations and understand similarities and differences in a complex population. Therefore, the expression levels of four surface markers were used to determine their unique and distinctive immunophenotypes and classify these four populations in one of the two extremes of the spectrum.

Expressions of CX3CR1 and CD11b were used to obtain a much more homogeneous population of macrophages with characteristics of tissue-resident macrophages. The original assumption was that the percentage of CX3CR1⁺CD11b⁺ cells was similar in M1-driven and M2-driven macrophages. The chemokine receptor CX3CR1 is widely present in the mononuclear phagocytes system. As reported by Pinto and colleagues, CX3CR1 is expressed by cardiac-resident macrophages and in macrophages resident

in different tissues such as BM, brain, lung, liver, and gut (Pinto et al., 2012). The role of CX3CR1-expressing macrophages is to regulate homeostasis (Lee et al., 2018).

Flow cytometry analysis revealed an unequal proportion of CX3CR1⁺CD11b⁺ cells in M1-driven and M2-driven macrophages. The M1-driven M ϕ group has half as many CX3CR1⁺CD11b⁺ cells as the M2-driven M ϕ . This difference suggests a discrepancy in the distribution of cardiac-resident macrophages in the two generated populations. Therefore, these findings revealed a limitation in the proposed choice of surface markers for analysing these macrophage populations. The reason why a lower percentage of CX3CR1⁺CD11b⁺ cells was observed in the M1-driven M ϕ could be explained by some studies that have reported CX3CR1 primarily as a marker of anti-inflammatory monocytes/macrophages rather than a specific tissue-resident macrophage marker (Biagioli et al., 2017; Burgess et al., 2019; Olingy et al., 2017; Pinto et al., 2012). Therefore, the M2-driven M ϕ were enriched for CX3CR1⁺CD11b⁺ macrophages because CX3CR1 is related to anti-inflammatory macrophages.

The second step evaluated the expression levels of F4/80 and CD206 into CX3CR1⁺CD11b⁺ macrophages in each of the four generated populations. F4/80 is used to identify macrophages in organs and tissues due to its specificity (Epelman, Mann, et al., 2014; Morris et al., 1991). In contrast, CD206 targets anti-inflammatory macrophages (Bosisio et al., 2002; Dinarello, 1991; Jablonski et al., 2015; Mantovani et al., 2002; Shintani et al., 2016). As expected, the percentage of F4/80⁺CD206⁺ macrophages in the M2-driven M ϕ was five times higher than in the M1-driven M ϕ .

The limitation of this two-step gating strategy

Altogether, the four cocktails of factors and stimuli enabled the generation of four macrophage populations expressing contrasting immunophenotypes based on the analysis of surface marker levels. However, the main limitation of this strategy was using CX3CR1 and CD11b as markers to enrich a homogenous population of cardiac macrophages. The unbalanced proportion of CX3CR1⁺CD11b⁺ macrophages detected between M1-driven-M ϕ and M2-driven-M ϕ can be explained by previous investigations that have reported CX3CR1 as a primarily M2-related surface marker rather than a tissue-resident marker for macrophages (Biagioli et al., 2017; Olingy et al., 2017; Pinto et al., 2012). FACS data from this PhD thesis confirmed that CX3CR1 resembles an anti-inflammatory macrophage marker rather than a resident cardiac marker, explaining this unbalanced distribution. These findings were still valuable because they allowed for a better strategic approach used in Chapter 5.

4.3.3 Single-cell qRT-PCR: advantages and limitations

The main advantages of sc qRT-PCR

Single-cell investigation to resolve heterogeneity and complexity in specific cell populations remains a significant challenge in many scientific areas. The single-cell approach has been primarily used in the cardiac field to study development and target transcripts. It has only recently been applied to identify pathways related to disease models (Bengtsson et al., 2005; DeLaughter et al., 2016; Eberwine et al., 1992; Gladka et al., 2018; Li et al., 2015; Massaia et al., 2018; Nosedá et al., 2015; Schafer et al., 2017; Skelly et al., 2018; Warren et al., 2007).

At the beginning of this research dissertation, sc qRT-PCR was one of the most advanced methods for single-cell profiling and was considered the gold standard of gene expression analysis. This precise and rapid tool offers the main advantage of an unprecedented resolution of the single cells, revealing mRNA levels, prevalence, co-expression, and heterogeneities to be studied more subtly than in bulk cell populations (Massaia et al., 2018; Nosedà et al., 2015). Therefore, the advantage of the sc qRT-PCR is the ability to simultaneously detect and measure the expression of dozens of genes from hundreds of single cells (Bengtsson et al., 2005; DeLaughter et al., 2016; Eberwine et al., 1992; Gladka et al., 2018; Li et al., 2015; Massaia et al., 2018; Nosedà et al., 2015; Schafer et al., 2017; Skelly et al., 2018; Warren et al., 2007).

There already are clear reasons why sc qRT-PCR significantly impacts immune cell research. First, it studies rare cells that would be obscured in the bulk RNA approach. Secondly, it refines the co-expression models of several immune genes. Finally, it decodes signalling pathways that could be regulated differently (Diercks et al., 2009).

Limitations of sc qRT-PCR

On the other hand, the main limitation of sc qRT-PCR is the use of a preselected gene panel. However large the panel may be, the number of genes is still limited and is based on prior knowledge. Therefore, it is not possible to design a hypothesis-free experiment. The challenge is the ability to preselect genes based on the specific questions, acknowledging that other aspects or questions will be left out. For example, this case did not include transcriptional and epigenetic genes crucial in switching macrophage phenotypes (Chen et al., 2020; Ivashkiv, 2013; Kuznetsova et al., 2020).

Finally, another recognised limitation is the later and most recent development of single-cell or single-nucleus RNA-sequencing, which allows the entire transcriptome to be analysed at single-cell resolution with no a priori bias (Ding et al., 2020; Massaia et al., 2018). Regardless, future single-cell qRT-PCR experiments are likely to be informed by the findings of scRNA-seq, where hundreds or thousands of new gene and protein markers are likely to emerge. Indeed, selected examples will be explored in the Discussion.

4.3.4 The genes enriched in clusters 1 and 2

To recapitulate, the single-cell qRT-PCR analysis revealed that GM-CSF+LPS+IFN γ -M ϕ were enriched for *Csf1*, *Cxcl2*, *Cxcl3*, *Cxcl9*, *Il6*, *Nos2*, *Ly6a* and *Ptges* (cluster 1), while M-CSF+IL4+IL13-M ϕ were enriched for *Igf1*, *Angptl2*, *Arg1*, *Il1rl1* and *Tcf21* (cluster 2). Here, there is a discussion of the most relevant genes expressed in these two clusters.

Nos2 and Arg1

Among all the genes selected for the sc qRT-PCR, *Nos2* and *Arg1* are the best gene markers for discerning macrophages with pro-inflammatory-like and anti-inflammatory-like phenotypes. The divergent phenotypes of macrophages involve the common metabolic pathway of L-arginine, converted by either *Nos2* or *Arg1* (Bronte & Zanovello, 2005; Pesce et al., 2009). The *Arg1* pathway promotes cardiac healing and fibrosis, while *Nos2* promotes a strong microbicidal effect (Gordon, 2003; Mantovani et al., 2004). GM-CSF+LPS+IFN γ -M ϕ and M-CSF+IL4+IL13-M ϕ

exclusively expressed *Nos2* or *Arg1*, respectively. Therefore, *Nos2* and *Arg1* are the gene markers used in this PhD thesis to refer to the full activation of the macrophages.

Pro-inflammatory chemokine

Induction of cytokines and chemokines is a hallmark of the post-MI pro-inflammatory response because they can influence the clinical outcome (Frangogiannis, 2006; Power & Proudfoot, 2001). Macrophages treated with LPS express pro-inflammatory protein profiles, including the chemoattractants CXCL9 and CXCL10 (Corbera-Bellalta et al., 2016). Similarly, activating macrophages with the pro-atherogenic cytokine IFN γ induces a local expression of the adhesion molecules CXCL9, CXCL10 and CXCL11. IFN γ also regulates CXCL9/10 receptor expression, known as CXCR3 (Szentés et al., 2018).

Csf1 interacts synergically with LPS

The expression of *Csf1*, the gene encoded for M-CSF, was interestingly upregulated in GM-CSF+LPS+IFN γ -M ϕ . The baseline levels of circulating M-CSF are detectable in tens of nanograms per millilitre; however, after exposure to LPS, these levels are significantly increased. A counter-intuitive conclusion suggested a synergic interaction between endogenous *Csf1* in LPS-treated macrophages (François et al., 1997; Roth et al., 1997). Furthermore, GM-CSF induces M-CSF but quantitatively less than LPS (Martinez & Gordon, 2014). The synergism between higher levels of endogenous *Csf1* in GM-CSF+LPS+IFN γ -M ϕ than in M-CSF+IL4+IL13-M ϕ is explained by Evans and colleagues. Macrophages treated with M-CSF and LPS upregulated inflammatory molecules (e.g. IL-6, IL-12 and TNF α) (Evans et al., 1998).

M-CSF works synergistically with GM-CSF and IL-6, promoting the proliferation of macrophage colonies from human BM progenitor cells (Akira & Kishimoto, 1996). The increased production of these proteins may involve a GM-CSF autocrine effect or transcriptional mechanisms. For example, the IL-12p40 promoter is activated through Ets-2, which responds to M-CSF (Fowles et al., 1998; Ma et al., 1997). However, an exploratory approach would investigate whether M-CSF or *Csf1* produced under M1 stimulation contributes to the pro-inflammatory gene and protein profile observed in the GM-CSF+LPS+IFN γ -M ϕ or whether it is instead a harmless bystander. This aspect was not considered during this PhD thesis, but its role could have been tested under pro-inflammatory conditions using a neutralising mAb or a chemical inhibitor.

4.3.5 Gene expression profiles correlate with culture treatments but not with the F4/80 CD206 immunophenotype

The single-cell qRT-PCR data confirmed that the chosen culture treatments induced two unique and distinct gene expression profiles in GM-CSF+LPS+IFN γ -M ϕ and M-CSF+IL4+IL13-M ϕ . Despite the limitation of the chosen gene panel tested, GM-CSF+LPS+IFN γ -M ϕ and M-CSF+IL4+IL13-M ϕ expressed a homogenous genetic set. These uniformities in gene expression profiles were not a priority certainty. Therefore, while two distinct clusters enriched with mutually exclusive paracrine genes were expected, the unexpected side was that each cluster included an equal number of CX3CR1⁺CD11b⁺F4/80^{lo}CD206⁻ and CX3CR1⁺CD11b⁺F4/80⁺CD206⁺ cells.

Single-cell gene expression analysis revealed no difference between the two immunophenotypes in their gene expression signature, indicating a discrepancy between the culture treatments for activating macrophages and the expression levels of CX3CR1, CD11b, F4/80 and CD206.

This section's unexpected lack of correlation of the immunophenotypes is a limitation. Hence, the gene signatures of GM-CSF+LPS+IFN γ -M ϕ and M-CSF+IL4+IL13-M ϕ only reflect the respective culture treatments without correlating with the immunophenotypes evaluated by the initial markers used. Therefore, in the further set of experiments described in Chapter 5, it was necessary to re-evaluate the gating strategy to better discriminate between the pro- and anti-inflammatory-like macrophages, even if losing the goal of enriching resident cardiac macrophages.

4.4 Summary and Conclusion

The first objective of this PhD thesis was achieved by designing an *in vitro* system that proved to be easy to use and highly reproducible in differentiating BM into macrophages as expected, with unique immunophenotypes and gene expression profiles. M1-driven-M ϕ were identified as CX3CR1⁺CD11b⁺F4/80^{lo}CD206⁻, while the M2-driven-M ϕ as CX3CR1⁺CD11b⁺F4/80⁺CD206⁺ ($p < 0.0001$). However, the unbalanced distribution of CX3CR1⁺CD11b⁺ macrophages in M1-driven-M ϕ and M2-driven-M ϕ suggested that CX3CR1 is enriched in anti-inflammatory macrophage immunophenotype rather than tissue-resident macrophages. Therefore, the following experiments aim to enrich populations with distinct immunophenotypes rather than macrophages with tissue-resident features.

Discriminating better than immunophenotype between the culture treatment groups, single-cell qRT-PCR revealed two main clusters. Cluster 1 (enriched for *Ly6a*, *Il6*, *Nos2*, *Cxcl2*, *Cxcl3*, *Cxcl9*, *Csf1*, and *Ptges*) correlates with the GM-CSF+LPS+IFN γ -M ϕ ($p < 0.005$). Cluster 2 (enriched for *Igf1*, *Angpt2*, *Arg1*, *Il11rl1*, and *Tcf21*) correlates with the M-CSF+IL4+IL13-M ϕ group ($p < 0.005$).

In conclusion, these results indicated that these *in vitro* generated macrophage populations exhibit dichotomous phenotypes as ascertained by single-cell gene expression, one near the pro-inflammatory end of the spectrum of possible macrophage phenotypes, the other at the opposite anti-inflammatory end (Fig. 4.6).

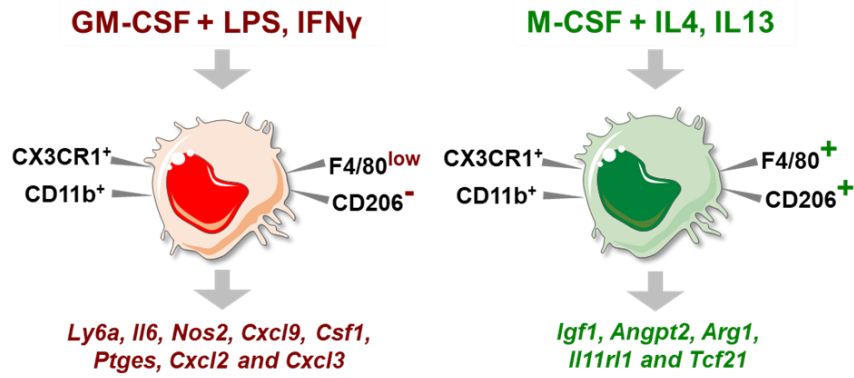


Figure 4.6 *In vitro* generation of GM-CSF+LPS+IFN γ -M ϕ and M-CSF+IL4+IL13-M ϕ
 The figure indicates which factors and stimuli have been used to differentiate and activate macrophages. Following these culture treatments, flow cytometry and sc qRT-PCR detected the expression of crucial surface markers and genes, as indicated.

Chapter 5 – Results II

5 Result II: Paracrine factor(s) released by CSCs modulate macrophage immunophenotypes, gene signatures and protein profiles

5.1 Introduction and rationale

The rare subset of CSCs used in this PhD thesis has been characterised and strictly defined as Lin⁻Sca1⁺CD31⁻PDGFR α ⁺SP⁺ (Nosedá et al., 2015). After grafting, Lin⁻Sca1⁺CD31⁻PDGFR α ⁺SP⁺ CSCs reduced infarcted size and improved cardiac function through lasting engraftment was extremely rare (Nosedá et al., 2015), as in related studies by others. (Chimenti et al., 2010; Chong et al., 2011; de Couto et al., 2015; Hong et al., 2014; Li et al., 2012; Malliaras et al., 2013; Matsuura et al., 2009; Ong et al., 2015; Tang et al., 2016; Wang et al., 2006). Based on this cardiac improvement without durable engraftment, the benefits might derive from an early paracrine effect of injected CSCs. The full range of factors released by CSCs is still under investigation. However, this PhD thesis postulated that CSCs could affect several types of heart cells beyond just cardiomyocytes, including macrophages. Focusing here on the paracrine effects of CSCs on macrophages is based on the critical role that anti-inflammatory and pro-reparative macrophages play in the repair and regeneration of heart tissue (Aurora et al., 2014; Godwin et al., 2017; Lavine et al., 2014).

Therefore, the overall hypothesis of this PhD thesis states that the paracrine signals secreted by Lin⁻Sca1⁺CD31⁻PDGFR α ⁺SP⁺ CSCs could modulate the phenotype of

macrophages towards the anti-inflammatory and reparative side of the phenotypic spectrum (Aurora et al., 2014; Danenberg et al., 2002; Dutta & Nahrendorf, 2015; Espinosa-Heidmann et al., 2003; Frangogiannis, 2015; Lambert et al., 2008; Lavine et al., 2014; Leor et al., 2006; Ong et al., 2018; Takayama et al., 2000).

The effects of the paracrine signals of CSCs on macrophages were evaluated using a cell-free approach based on CSCs' Conditioned Media (CSC CondM). Therefore, this Chapter describes the experiments conducted to achieve the second objective of this PhD thesis addressing the following points:

- (i) Establish *in vitro* whether CSC CondM is sufficient to promote survival and differentiation of BMDMs into macrophages.
- (ii) Demonstrate whether CSC CondM induces a phenotypic state similar to pro-inflammatory-like or anti-inflammatory-like macrophages.
- (iii) CSC CondM can do both (i) and (ii).

5.2 Results

5.2.1 *In vitro* study of the paracrine effects of CSC CondM on BMDMs

One of the advantages of the *in vitro* system developed here is its easy expansion to a broader range of samples, precisely, versatility in integrating different culture conditions while using M1-driven M ϕ and M2-driven M ϕ groups as a reference for the two extremes of the macrophage's spectrum. Here, three new culture conditions were included, testing for the differentiation of BMDMs using CSC CondM (instead of GM-CSF or M-CSF), followed by 24-hours stimulation with either LPS+IFN γ or IL-4+IL-13, the pro- and anti-inflammatory factors used for the previous results. Thus, the CSC-driven M ϕ consist of three culture conditions: BMDMs differentiated with CSC CondM, named CSC CondM-M ϕ ; CSC CondM-M ϕ activated with LPS+IFN γ , named CSC CondM+LPS+IFN γ -M ϕ ; and CSC CondM-M ϕ activated with IL-4+IL-13, named CSC CondM+IL4+IL13-M ϕ (Fig. 5.1).

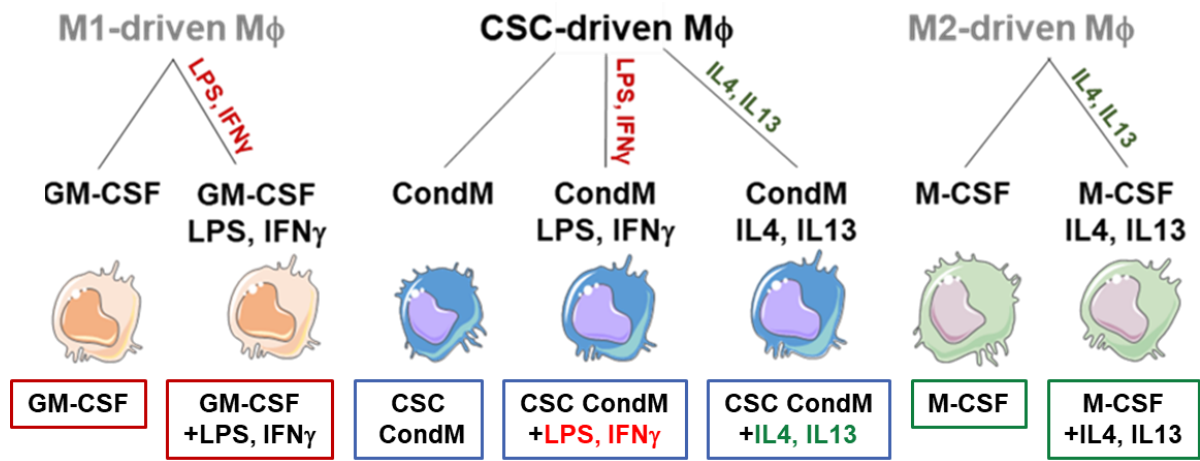


Figure 5.1 Illustration of the seven populations generated with the integrated version of the *in vitro* system

The modified version of the *in vitro* system includes the CSC-driven Mφ (blue): CSC CondM-Mφ, CSC CondM+LPS+IFN γ -Mφ, and CSC CondM+IL4+IL13-Mφ. As the reference extremes, M1-driven Mφ (red, left) and M2-driven Mφ (green, right) are used, as detailed in Chapter 4.

5.2.2 The immunophenotype of CSC-driven M ϕ

The results described in Chapter 4 showed that CX3CR1⁺CD11b⁺ macrophages were not uniformly distributed between the M1- and M2-driven M ϕ , confirming that high CX3CR1 and CD206 correlate more with an M2-like macrophage phenotype (Ensan et al., 2016; Molawi et al., 2014; Pinto et al., 2012).

Here, F4/80 and CD11b were used for better-balanced macrophage populations in M1-, M2-, and CSC-driven M ϕ . Analysis of 6 independent experiments showed that in each of the seven conditions tested, at least 70% were F4/80⁺CD11b⁺ cells. Thus, this change in the starting markers selects a more evenly balanced set of macrophages for more detailed analyses. This also includes the CSC-driven M ϕ groups, indicating that BM cells cultured in CSC CondM differentiate into a heterogeneous population comparable with M1-driven and M2-driven M ϕ ($p < 0.0001$) (Fig. 5.2 A, B).

Subsequently, within the F4/80⁺CD11b⁺ macrophage populations, the expression levels of CX3CR1 and CD206 were used to distinguish between pro- and anti-inflammatory immunophenotypes. The FACS data confirmed the mutually exclusive induction pattern of CX3CR1 and CD206. The M1-driven-M ϕ group expresses significantly lower CX3CR1 and CD206 ($< 10\%$; $p < 0.0001$) than M2-driven M ϕ , in which approximately 60% of cells were F4/80⁺CD11b⁺CX3CR1⁺CD206⁺. Interestingly, in the CSC-driven M ϕ , approximately 60% of the cells were F4/80⁺CD11b⁺CX3CR1⁺CD206⁺.

Hence, the percentage of F4/80⁺CD11b⁺CX3CR1⁺CD206⁺ cells in CSC-driven-M ϕ and M2-driven-M ϕ were analogous, indicating that macrophages generated with CSC CondM showed an anti-inflammatory-like macrophage immunophenotype, as judged by the best existing surface markers of this class (Fig. 5.2 A, C).

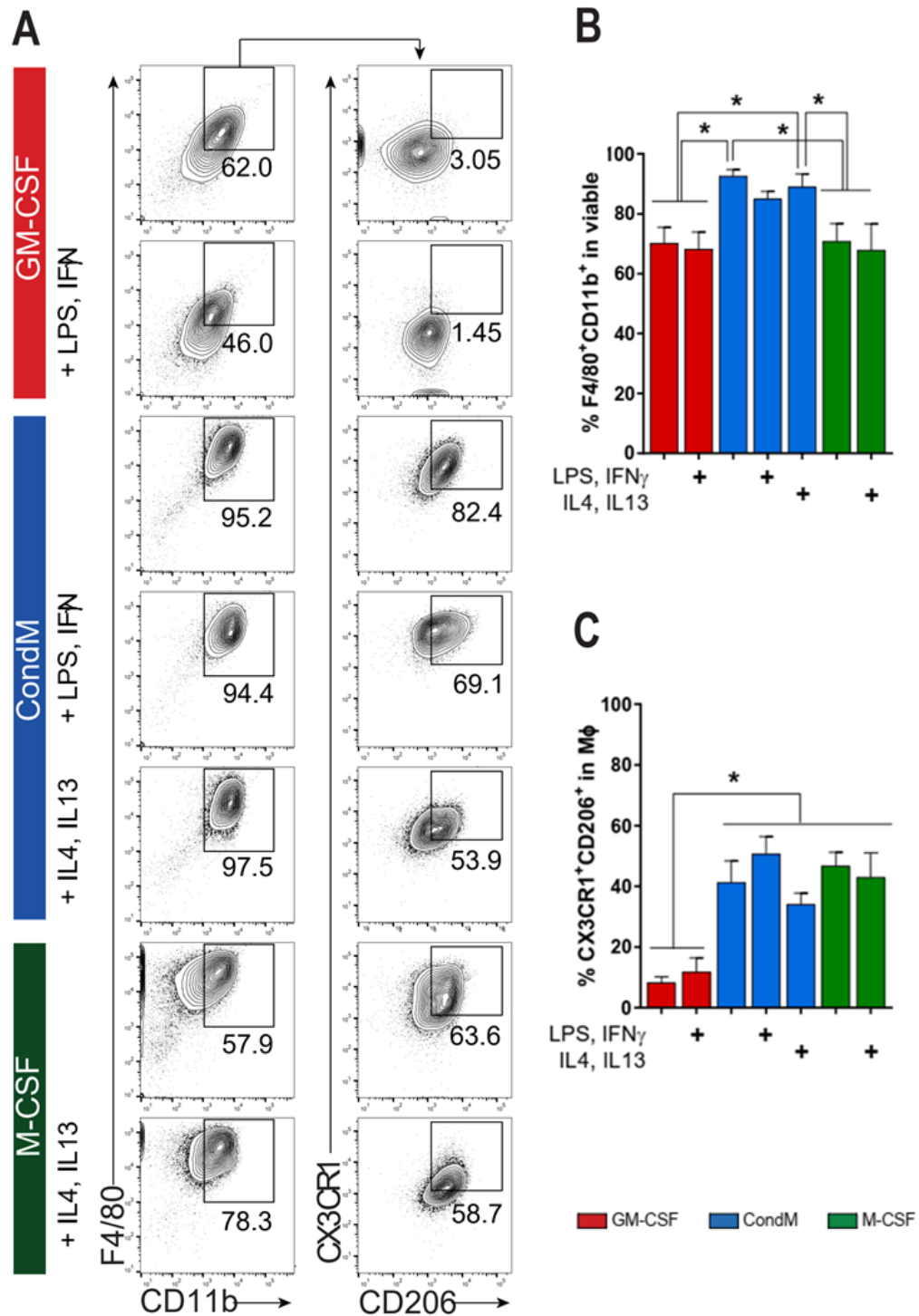


Figure 5.2 Flow cytometry data from the seven culture conditions.

A, Representative flow cytometry contour plots of the seven culture conditions analysed: M1-driven M ϕ (red); CSC-driven M ϕ (blue); M2-driven M ϕ (green). **B**, A bar graph of the percentage of F4/80⁺CD11b⁺ cells in the viable cells. **C**, A bar graph of the percentage of CX3CR1⁺CD206⁺ cells in F4/80⁺CD11b⁺ cells. (\pm SEM, N=6). Two-way ANOVA test with Bonferroni's correction (*, $p < 0.0001$).

5.2.3 Single-cell qRT-PCR analysis of the gene signatures of CondM+LPS+IFN γ -M ϕ

After FACS analysis, the gene expression profiles of the seven populations generated *in vitro* were explored by sc qRT-PCR (Table 3.5, panel 2). Single-cell qRT-PCR analyses were visualised and discussed in two aspects for clarity. First, the four pro-inflammatory-related populations were analysed, followed by the four anti-inflammatory-related populations.

The first analysis investigated how the gene expression profiles of macrophages were influenced by differentiation with GM-CSF or CSC CondM differentiation and by the activation with LPS and IFN γ . At least 60 single F4/80⁺CD11b⁺ macrophages were flow-sorted from the following cultural conditions and analysed by sc qRT-PCR: GM-CSF-M ϕ , GM-CSF+LPS+IFN γ -M ϕ , CSC CondM-M ϕ , and CondM+LPS+IFN γ -M ϕ .

The first method to visualise the sc qRT-PCR data was an unsupervised hierarchical clustering heatmap (Fig. 5.3). The dendrogram of the genes showed four main bifurcations. The first bifurcation determined the formation of cluster 1, enriched for the following twelve transcripts: *Cxcl1*, *Cxcl3*, *Cxcl9*, *Cxcl10*, *Il6*, *Inhba*, *Map4k4 Isoform 2*, *Map4k4 Isoform 3*, *Nos2*, *F3*, *Tgm2* and *Vegfa*. The population enriched in cluster 1 was GM-CSF+LPS+IFN γ -M ϕ . The second bifurcation formed cluster 2, enriched for just 4 of the 12 mentioned: *Cxcl9*, *Cxcl10*, *Nos2* and *Tgm2*. The population of cells in cluster 2 was CSC CondM+LPS+IFN γ -M ϕ . The last two bifurcations resolved the differentiated cells in two clusters, clusters 3 (CSC CondM-M ϕ) and 4 (GM-CSF-M ϕ).

Genes enriched in clusters 1 and 2 showed unique co-variation and upregulation patterns; however, they slightly overlap because cluster 2 contains four out of 12 genes of cluster 1. Based on these observations, cluster 1 was named the “M1-activated related genes” because the expression of these genes was influenced (hampered by CSC CondM or promoted by GM-CSF) by the differentiation medium used. In contrast, cluster 2 was named the “core pro-inflammatory genes” because these were induced by LPS+IFN γ regardless of the differentiation media (Fig. 5.3).

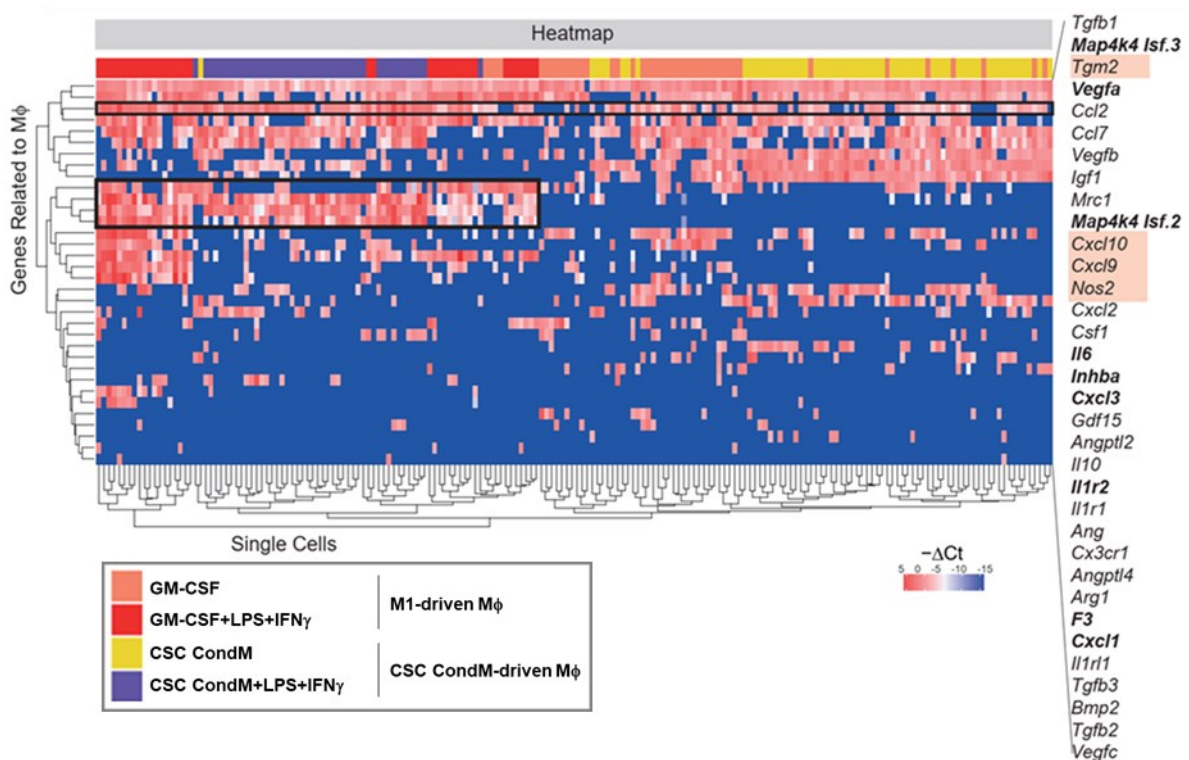


Figure 5.3 An unbiased hierarchical clustering heatmap shows the effects of LPS+IFN γ on the gene signatures of macrophages

~60 single F4/80⁺CD11b⁺ cells from GM-CSF-M ϕ (coral), GM-CSF+LPS+IFN γ -M ϕ (red), CSC CondM-M ϕ (yellow), and CondM+LPS+IFN γ -M ϕ (purple) were analysed by qRT-PCR. Unbiased hierarchical clustering reveals four genes (pink box) upregulated in GM-CSF+LPS+IFN γ -M ϕ and CSC CondM+LPS+IFN γ -M ϕ (cluster 2). In bold, genes of cluster 1. The heatmap shows Δ Ct values (blue, low or absent; red, high).

The PCA of the samples visualised four clusters corresponding to the four populations tested. PC1, accounting for 25% of the variation, divided differentiated and activated macrophages. In contrast, PC2, with a variability of 10%, separated M1-driven-M ϕ and CSC-driven-M ϕ (Fig. 5.4). Thus, CSC CondM-treated cells largely overlapped those differentiated by GM-CSF. In both cases, activation by LPS+IFN γ gave rise to a distinct population, although the overlap was less complete between CSC CondM+LPS+IFN γ and GM-CSF+LPS+IFN γ -M ϕ .

Next, the PCA of the genes showed the top differentially expressed genes identified within the four clusters. PC1 (~ 12% variability), separating the genes upregulated following LPS and IFN γ -stimulation. In comparison, PC2 (~10% variability) divided cluster 1 (“M1-activated related genes”) and cluster 2 (“core pro-inflammatory genes”). Interestingly, compared to the heatmap, PCA allowed even better visualisation of the genes enriched in clusters 3 (*Il10*, *Mrc1*, *Angptl2*, *Vegfb*, and *Igf1*), corresponding to the macrophages differentiated with CSC CondM on the PCA of the sample. Therefore, this group of genes was called the “differentiation” cluster. The last cluster identified in the PCA of the genes enriched for the migration-related genes *Ccl2* and *Ccl7*. *Ccl2* and *Ccl7* expressions were homogeneous under tested conditions (Fig. 5.4).

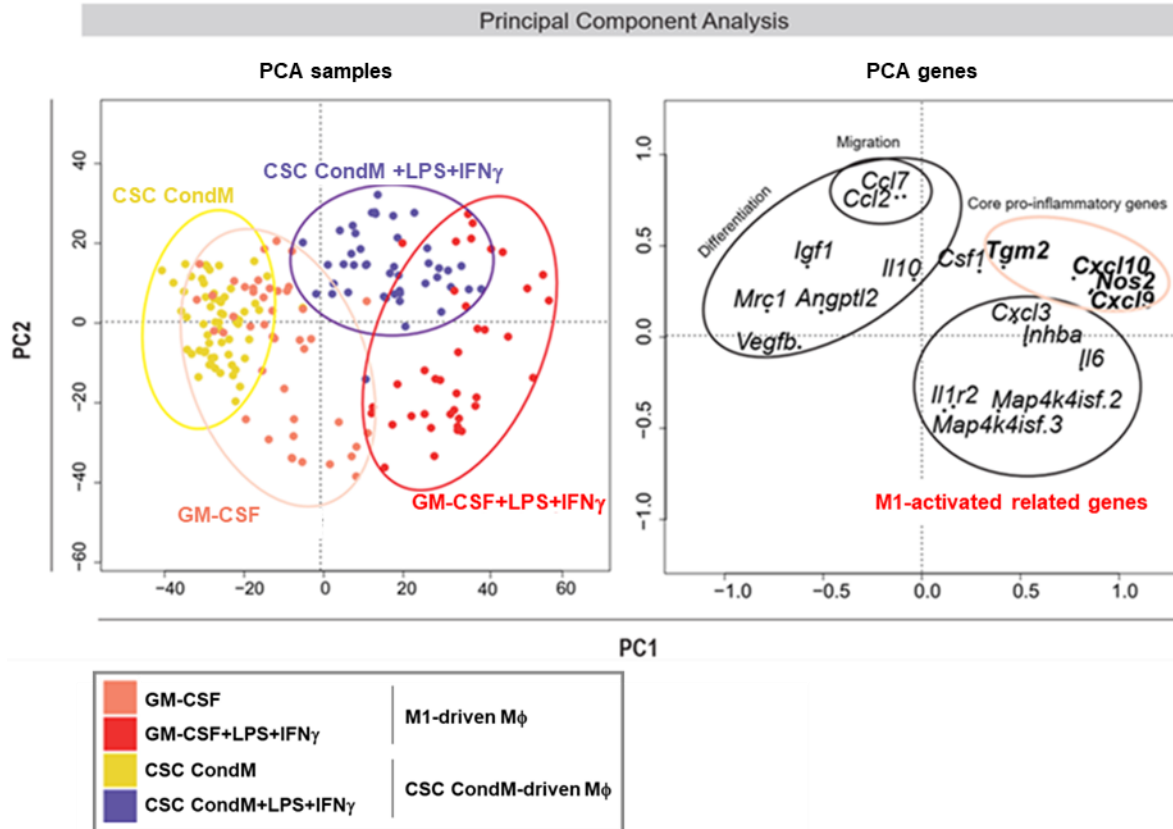


Figure 5.4 PCAs show the effects of LPS+IFN γ on the gene expression profiles of macrophages

PCA of the samples shows that PC1 separated LPS+IFN γ -stimulated cells from differentiated cells, while PC2 divided CSC CondM+LPS+IFN γ -M ϕ from GM-CSF+LPS+IFN γ -M ϕ . PCA of the genes indicates four clusters: Cluster 1, M1-activated related genes; Cluster 2, the core of pro-inflammatory genes; Cluster 3, differentiation genes; Cluster 4, genes related to migration.

The expression of the genes in cluster 2 appeared to depend on the activation with LPS+IFN γ because no significant difference was observed according to the differentiation media used (Fig. 5.5 A, top). On the other hand, the expression levels of the remaining eight genes enriched solely in cluster 1 suggested that their expression depends on the differentiation media used (Fig. 5.5 A, bottom). The heatmap based on the Kruskal-Wallis/Dunn test reports the complete set of p -values for each comparison made (Fig. 5.5 B).

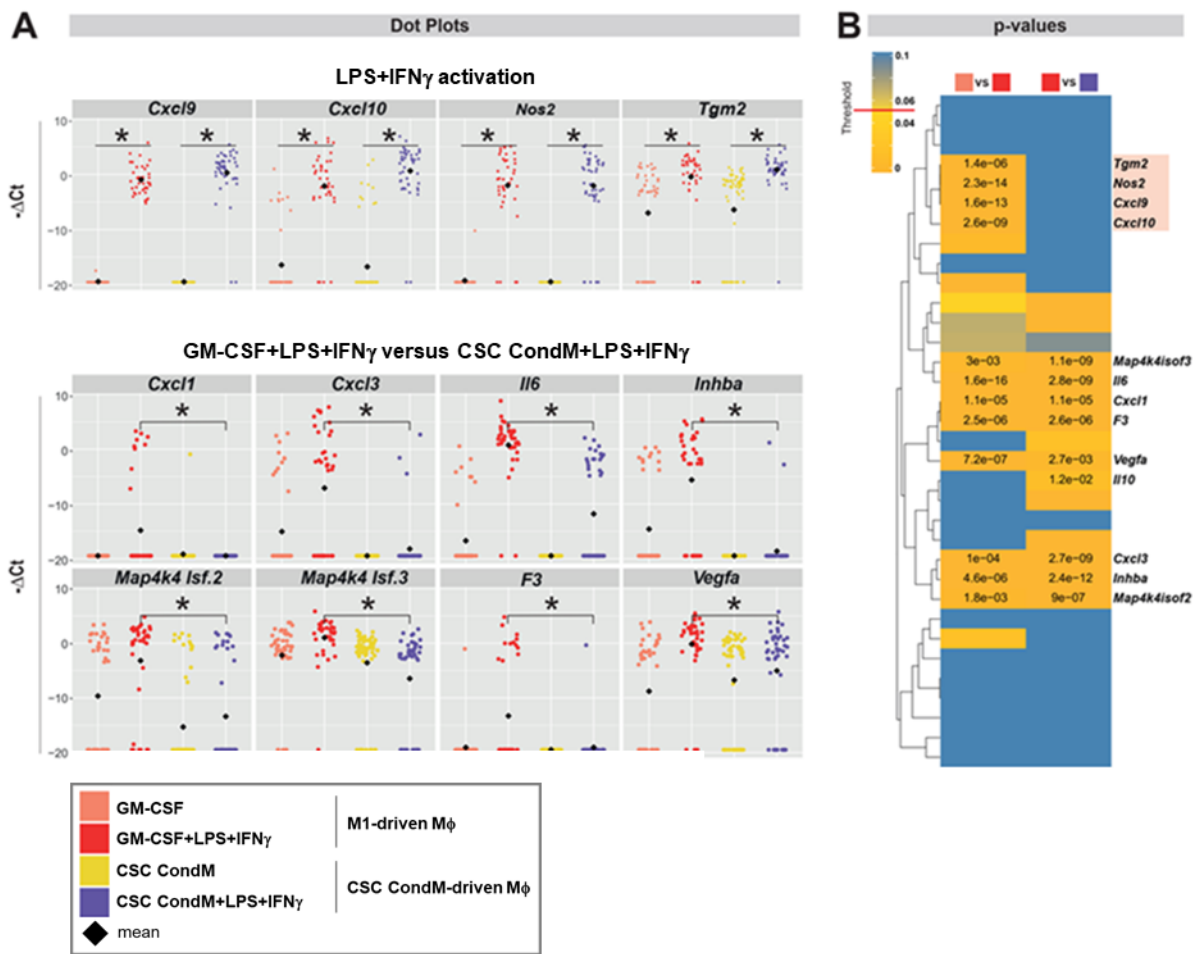


Figure 5.5 Investigation of the effects of LPS+IFN γ on the gene expression of CSC-driven M ϕ by sc qRT-PCR: dot plot

A, Dot plots show (TOP) the four core pro-inflammatory genes (cluster 2) upregulated in both GM-CSF+LPS+IFN γ -M ϕ (red) and CSC CondM+LPS+IFN γ -M ϕ (purple), and (BOTTOM) the remaining eight samples of the cluster 1, more expressed in GM-CSF+LPS+IFN γ (red) than CondM+LPS+IFN γ (purple). **B**, p-values heatmap based on the Kruskal-Wallis/Dunn test (*, $p < 0.005$).

Thus, these data suggest that the paracrine effects of CSCs could interfere with the pro-inflammatory gene expression signatures promoted by LPS and IFN γ .

5.2.4 Single-cell qRT-PCR analysis of the gene signatures of CSC

CondM+IL4+IL13-M ϕ

The second aspect of the sc qRT-PCR analysis compared the gene expression profiles of at least 60 F4/80⁺CD11b⁺ macrophages from each of the following culture conditions: M-CSF-M ϕ , M-CSF+IL4+IL13-M ϕ , CSC CondM-M ϕ , and CSC CondM+IL4+IL13-M ϕ .

In the unsupervised hierarchical clustering heatmap, the dendrogram of the genes showed two main bifurcations separating activated and differentiated macrophages. The genes expressed in M-CSF+IL4+IL13-M ϕ and CSC CondM+IL4+IL13-M ϕ overlapped to form a single cluster (cluster 1). The five genes upregulated in cluster 1 were *Arg1*, *Angptl2*, *Igf1*, *Il1rl1* and *Mrc1*. Therefore, cluster 1 was named the “M2-like activation cluster”. On the other hand, a third bifurcation separated M-CSF-M ϕ (cluster 2) from CSC CondM-M ϕ (cluster 3) within the differentiated group. However, due to the similarity between M-CSF-M ϕ and CSC CondM-M ϕ , the unsupervised hierarchical heatmap did not allow visualising the genes responsible for separating these clusters (Fig. 5.6).

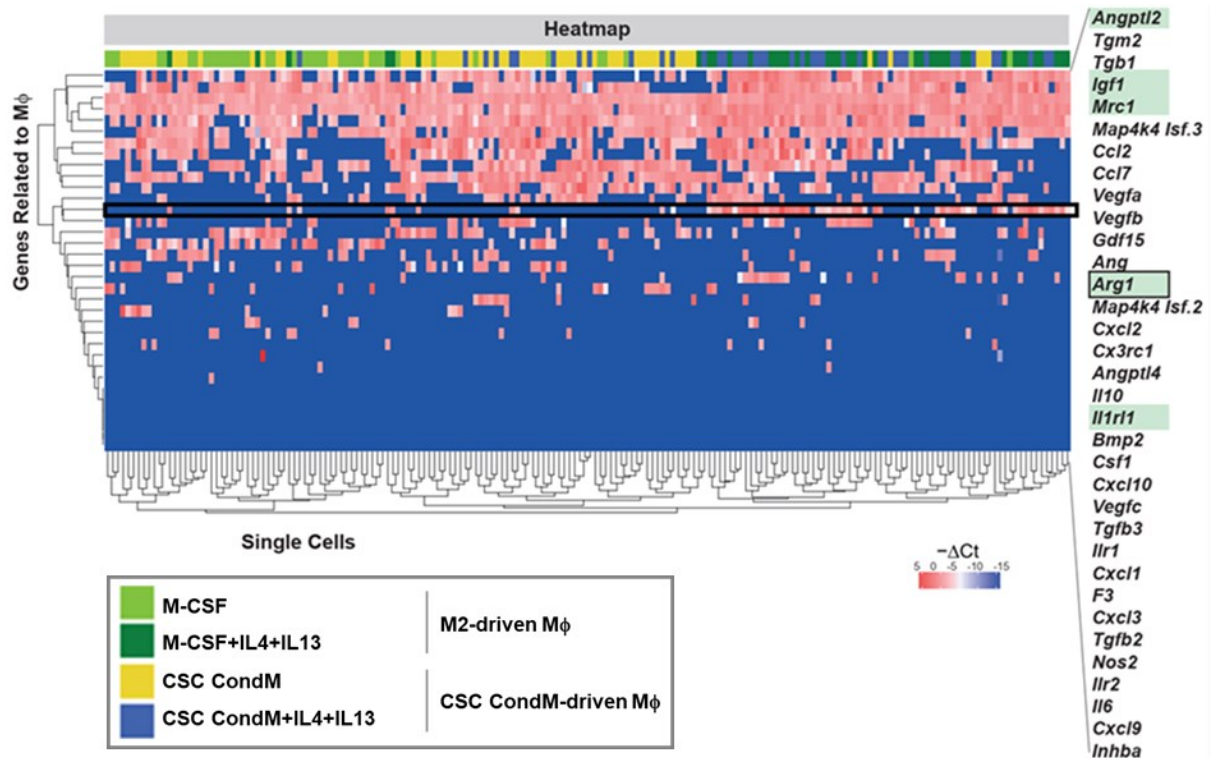


Figure 5.6 An unbiased hierarchical clustering heatmap shows the effects of IL-4+IL-13 on the gene expression of CSC-driven M ϕ

~60 single F4/80⁺CD11b⁺ cells from CSC CondM (yellow), CSC CondM+IL4+IL13 (blue), M-CSF (light green), M-CSF+IL4+IL13 (dark green) were analysed by qRT-PCR. M-CSF+IL4+IL13 and CSC CondM+IL4+IL13 upregulate 5 genes (green box) forming cluster 1. The heatmap shows ΔCt values (blue, low or absent; red, high).

PCA of the samples highlighted the separation between the IL4+IL13-activated macrophages (cluster 1), M-CSF-M ϕ (cluster 2) and CSC CondM-M ϕ (cluster 3), mirroring the three clusters observed with the unsupervised hierarchical clustering heatmap. PC1, with a variability of 15%, separated clusters 1 and 2, while PC2 (10% variability) separated cluster 3 from the other two. PCA of the genes identified the genes enriched in three clusters: *Arg1*, *Angptl2*, *Il1rl1* and *Mrc1* (cluster 1, the M2-like activation genes); *Cx3cr1*, *Cxcl2*, *Il10* and *Tgm2* (cluster 2); *Vegfb* and *Gdf15* (cluster 3) (Fig. 5.7). Thus, macrophages following activation with IL-4 and IL-13 express a

very similar gene expression signature regardless of the media used for the differentiation.

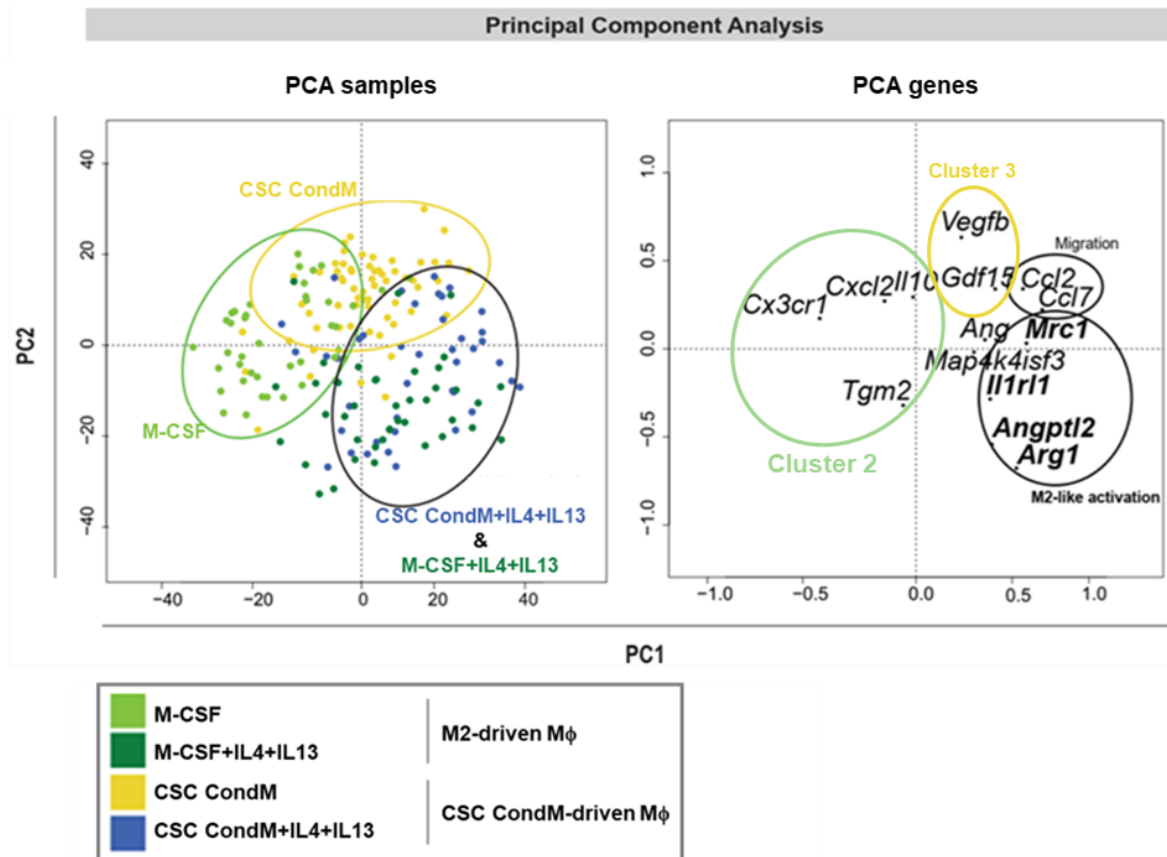


Figure 5.7 PCAs show the effects of IL-4+IL-13 on the gene expression profiles of macrophages

PCA of the samples shows that PC1 separated M-CSF-Mφ from M-CSF+IL4+IL13-Mφ, while PC2 CSC CondM-Mφ from M-CSF+IL4+IL13-Mφ and CSC CondM+IL4+IL13-Mφ. The PCA of the gene indicates that the M2-like activated anti-inflammatory genes (*Arg1*, *Angpt2*, *Il1r1* and *Mrc1*) clustered together.

Dot plots, paired with a p-values heatmap, confirmed that the expression of the five in the M2-like activation cluster depends on the IL-4+IL-13-stimulation (Fig. 5.8 A, top). However, there is a difference in the expression levels of *Tgm2*, *Gdf15* and *Mrc1* between M-CSF+IL4+IL13-Mφ and CSC CondM+IL4+IL13-Mφ (Fig. 5.9 A, bottom).

CSC CondM+IL4+IL13-M ϕ presented a higher expression level of *Mrc1* ($p=0.012$) and *Gdf15* ($p=0.001$) and a lower expression of *Tgm2* ($p=0.0016$) (Fig. 5.8 B).

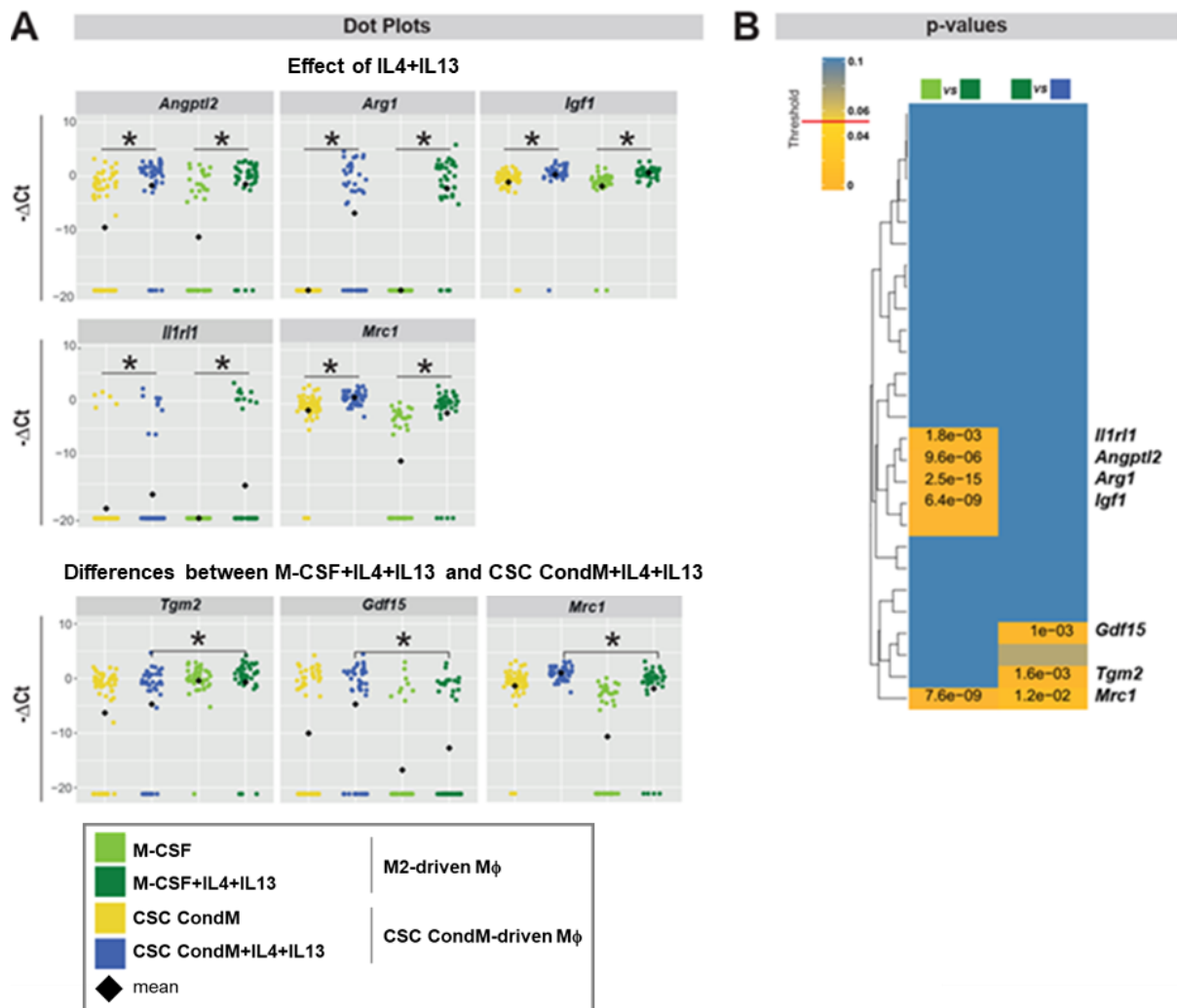


Figure 5.8 Investigation of the effects of IL-4+IL-13 on the gene expression of CSC-driven M ϕ by sc qRT-PCR: dot plots

A, (TOP) Dot plots showed the expression of genes in cluster 1 depends on IL-4+IL13-stimulation. (BOTTOM) The three genes whose expression levels differed between the two activated groups. **B**, p-values heatmap based on Kruskal-Wallis/Dunn test (*, $p<0.005$).

5.2.5 Evaluation of the secretion of 23 cytokines and chemokines in macrophages

The secretion levels of 23 cytokines and chemokines were analysed using a multi-analytical bead-based flow immunoassay to explore the potential CSC paracrine factors affecting the macrophage phenotypes.

GM-CSF+LPS+IFN γ -M ϕ secreted the highest levels of the inflammatory cytokines and chemokines tested: IL-23, IL-1 α , TNF α , CCL2, IL12p70, IL-1 β , IL-6, IL-27, IL17A, IFN- β , CCL5, CCL20, CCL11, CCL17, CXCL1, CXCL9, CXCL10, CCL3, CCL4, CXCL13, CXCL5 and CCL22 ($p < 0.0001$ for each analyte). On the other hand, CSC CondM+LPS+IFN γ -M ϕ showed a different secretome profile, secreting only 10 of these analytes: IL-6, IL-17A, CCL20, CXCL1, CCL2, CXCL10, CCL3, CCL4, CXCL13 and CXCL5. Of at least equal importance, these ten analytes were also five to 10 times less expressed in CSC CondM+LPS+IFN γ -M ϕ than GM-CSF+LPS+IFN γ -M ϕ ($p < 0.0001$ for each). Of all the analytes tested, CSC CondM+LPS+IFN γ -M ϕ secreted the highest levels of the immunoregulatory/anti-inflammatory protein IL-10, which was not expressed at all by GM-CSF+LPS+IFN γ -M ϕ ($p < 0.0001$) (Fig. 5.9).

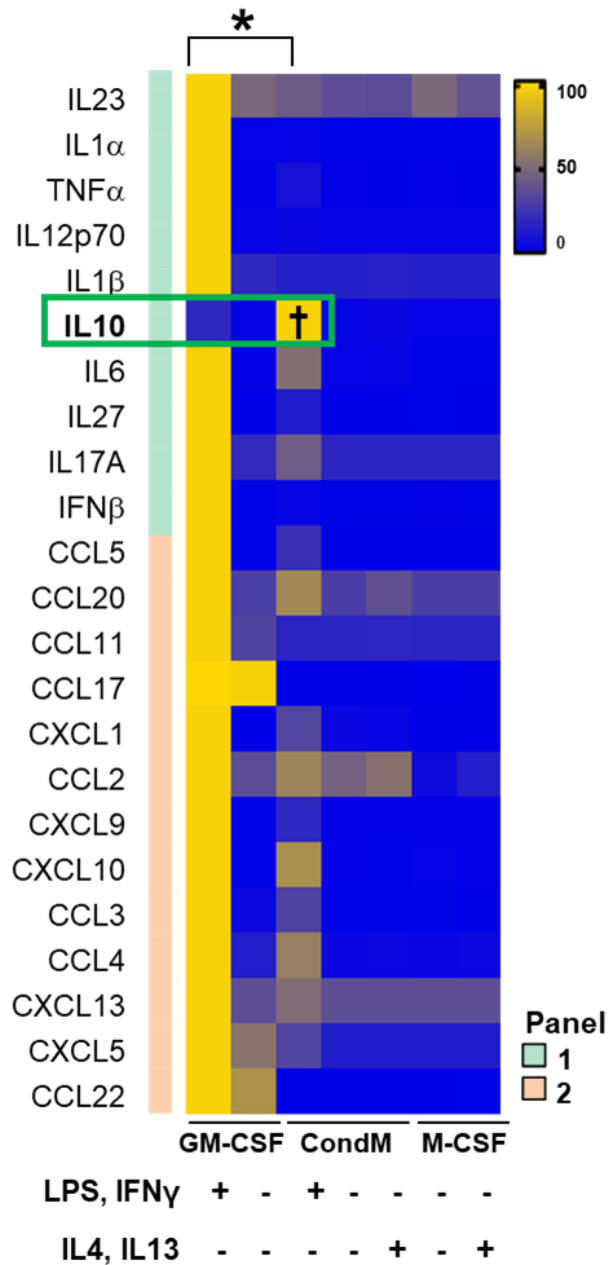


Figure 5.9 Heatmap of secretion levels of 23 cytokines and chemokines evaluated via a multi-analyte bead-based immunoassay

Each cytokine/chemokine tested secretion levels (rows) in the seven conditions (columns). Data normalised for each analyte. (\pm SEM, N=3). Two-way ANOVA test with Bonferroni's correction. Column 1 versus column 3 (*, $p < 0.0001$). IL-10 secretion levels in column 3 versus all the other conditions (†, $p < 0.0001$).

5.3 Discussion

5.3.1 The choice of using Lin⁻Sca1⁺CD31⁻PDGFR α ⁺SP⁺ CSCs

The rigorously defined population of dormant Lin⁻Sca1⁺CD31⁻PDGFR α ⁺SP⁺ CSCs showed reduced infarct size and preserved cardiac function, preventing HF. However, 12 weeks after the injections, no grafted cells were found in the heart (Nosedá et al., 2015). The fundamental concept of this PhD thesis is the paracrine hypothesis, in which long-lived cardiac improvements were due to factor(s) released by these CSCs, rather than based on the cells' ability to engraft persistently. Within the spectrum of potential cell therapies reported, there are three reasons why these CSCs were chosen.

First, addressing the controversy raised by Lee regarding cardiomyocyte creation by endogenous Sca1⁺ cells (Lee, 2018), the hypothesis of this PhD thesis is still valid because it investigated only exogenous, expanded CSCs' and their paracrine effects, not their ability to engraft and differentiate into any of the cardiac lineage populations. Therefore, even if the Lin⁻Sca1⁺CD31⁻PDGFR α ⁺SP⁺ CSCs do not engraft or differentiate, they could also benefit the recipient hearts as a therapeutic product. Furthermore, the fate-mapping studies described by Lee (2018) – failed to capture the large subset of Sca1⁺ that lacks CD31 and possesses PDGFR α (Lee, 2018), i.e., overlooking in all reported cases the precise CSCs identified by Nosedá (Nosedá et al., 2015). Presumably, this reflects technical limitations in the sensitivity of current “deleter” or “reporter” lines used for the *Cre/lox* approach.

Second, many studies rely on a single marker to define, assign, or purify cell types. The most extreme examples are the discredited c-kit (Hong et al., 2014) and the early work on SP (Sadek et al., 2009). One of the most critical lessons from the sc qRT-PCR technology is using multiple markers to obtain homogenous populations. Therefore, Lin⁻Sca1⁺CD31⁻PDGFR α ⁺SP⁺ CSCs were chosen because they are defined by a series of markers rather than a single marker.

Lastly, Lin⁻Sca1⁺CD31⁻PDGFR α ⁺SP⁺ CSCs were chosen based on functional criteria similar to two relevant studies conducted on cCFU-F by Harvey's group (Chong et al., 2011) and the work done with cardiosphere-derived cells by Marban's group (de Couto et al., 2015). Lin⁻Sca1⁺CD31⁻PDGFR α ⁺SP⁺ CSCs closely resemble the MSC-like population used by Harvey's group. Nosedá's and Harvey's cell populations have a virtually identical immunophenotype within the range of markers used by both groups. More importantly, they have a near-identical gene expression profile and share stem cell functional properties like clonogenicity or colony formation and multilineage potential (Chong et al., 2011). On the one hand, Nosedá and colleagues tested the multilineage potential of Lin⁻Sca1⁺CD31⁻PDGFR α ⁺SP⁺ CSCs as CMs, ECs, and SMCs. Using formally identical cells to Lin⁻Sca1⁺CD31⁻PDGFR α ⁺SP⁺ CSCs, Harvey's group tested the multilineage potential to form adipocytes, chondrocytes, and osteoblasts.

Marban's study of the cardiosphere-derived cells is a second comparison benchmark to be discussed (de Couto et al., 2015). The main difference between Harvey's CSCs, Lin⁻Sca1⁺CD31⁻PDGFR α ⁺SP⁺ CSCs, and Marban's cells is that CD cells are heterogeneous. Due to the lack of agreement from the scientific community on the

best cell type, Marban's group interpreted cell heterogeneity as advantageous. Marban's study had encouraging cultural and animal model results (de Couto et al., 2015). However, the clinical trial failed without efficacy (Makkar et al., 2012). This failure may be related to using heterogeneous populations rather than a well-defined homogenous population. Without purifying for a specific set of markers and enriching for a homogeneous cell population, it could be that the molecular components responsible for the observed benefits *in vitro* and animal models were then diluted in the human clinical trial.

Therefore, based on the above considerations, investigating the paracrine signals released by the strictly and rigorously defined population of dormant Lin⁻Sca1⁺CD31⁻PDGFR α ⁺SP⁺ CSCs was the most relevant and workable approach to studying post-injury cardiac benefits.

5.3.2 FACS analysis revealed an anti-inflammatory-like immunophenotype of CSC CondM-driven-M ϕ

FACS analysis showed that all seven tested conditions had equivalent F4/80⁺CD11b⁺ macrophages. CX3CR1 and CD206 helped to distinguish between pro-inflammatory-like and anti-inflammatory-like immunophenotypes. These analyses made it possible to discover that CSC CondM induced an immunophenotype similar to the M2-driven M ϕ .

5.3.3 CSC CondM+LPS+IFN γ -M ϕ and GM-CSF+LPS+IFN γ -M ϕ have different gene signatures

The critical result of the first sc qRT-PCR analysis was the discrepancy observed between the gene expression profiles of the GM-CSF+LPS+IFN γ -M ϕ and CSC CondM+LPS+IFN γ -M ϕ .

GM-CSF+LPS+IFN γ -M ϕ expressed 12 pro-inflammatory genes (cluster 1: *Cxcl1*, *Cxcl3*, *Il6*, *Inhba*, *Map4k4 Isoform 2*, *Map4k4 Isoform 3*, *F3* and *Vegfa*). Based on the literature, their expression should directly depend on the activation with LPS and IFN γ (Farber, 1997; Gordon et al., 2014; Lee et al., 2009; Martinez & Gordon, 2014; Qian et al., 2015; Tannenbaum et al., 1998). However, CSC CondM+LPS+IFN γ -M ϕ expressed for only four of these 12 genes, missing eight (cluster 2: *Cxcl9*, *Cxcl10*, *Nos2* and *Tgm2*). Two possible interpretations explain the difference between these two gene signatures. First, the expression of these eight missing genes may well depend on the combined use of GM-CSF followed by LPS and IFN γ ; alternatively, the paracrine effect of CSCs somehow prevented their expression. On the other hand, regardless of the differentiation medium used, the “core pro-inflammatory genes” (cluster 2) are expressed in both populations. Therefore, their expression depended exclusively on the activating factors (LPS and IFN γ).

5.3.4 CSC CondM+IL4+IL13-M ϕ and M-CSF+IL4+IL13-M ϕ have similar gene signatures

The critical result of the second sc qRT-PCR analysis was the similarity of the gene expression profiles of M-CSF+IL4+IL13-M ϕ and CSC Cond+IL4+IL13-M ϕ . Activation with IL-4 and IL-13 induced the upregulation of five known anti-inflammatory genes, *Arg1*, *Mrc1*, *Angptl2*, *Igf1*, and *Il1rl1*.

The paracrine effects of CSCs induced a previously undescribed subset of anti-inflammatory macrophages. The gene expression profiles of CSC CondM+IL4+IL13-M ϕ and M-CSF+IL4+IL13-M ϕ are nearly identical, showing equal levels of the critical anti-inflammatory marker gene, *Arg1*, and of the three genes that promote post-MI tissue repair and regeneration, *Igf1*, *Il1rl1* *Angptl2* (Bronte & Zanovello, 2005; Das et al., 2010; Dupasquier et al., 2006; Heinen et al., 2019; Kambara et al., 2015; Lawrence & Natoli, 2011; Lee et al., 2002). However, CSC CondM+IL4+IL13-M ϕ expressed higher levels of the M2-like markers *Mrc1* and *Gdf15* and lower levels of *Tgm2*.

Overall, differentiation of BMDMs with M-CSF or CSC CondM promoted two populations with unique gene signatures. When activated with IL-4 and IL-13, macrophages express equally high levels of the critical anti-inflammatory gene markers. These data could suggest that the paracrine effects of CSCs promote an anti-inflammatory-like macrophage phenotype based on the similar transcriptomic signature of M2-driven macrophages.

5.3.5 CSC CondM+LPS+IFN γ -M ϕ and GM-CSF+LPS+IFN γ -M ϕ have different secretomes

The secretome of the seven macrophage populations tested was then studied using a multi-analytical platform. The main advantage was the simultaneous analysis of multiple analytes and the possibility to compare the level of expressions among different macrophage populations.

The M1-driven-M ϕ induced the secretion of 22 (out of 23) pro-inflammatory molecules, opposite to the M2-driven-M ϕ , which expressed none. CSC CondM+LPS+IFN γ -M ϕ secreted 5/10-fold lower levels of the pro-inflammatory cytokines and the highest IL-10 under the conditions tested.

IL-10 plays a critical role in balancing immune and inflammatory responses and pathology. Under largely pro-inflammatory conditions and depending on the context, IL-10 expression could relate to a counter-regulatory loop or functional effects. Human monocyte-derived DCs stimulated with IL-10 alone, or LPS, express four transcriptional programs, including a unique set of genes expressed by combining these stimuli. Analysis of the genes that induce or suppress IL-10/LPS has revealed inhibition of inflammation by promoting tissue remodelling (Perrier et al., 2004).

5.4 Summary and Conclusion

This Chapter investigated the effects of paracrine signals released by dormant Lin⁻Sca1⁺CD31⁻PDGFR α ⁺SP⁺ CSCs on BMDMs, demonstrating that they promote survival and differentiation of BMDMs into a unique subtype of anti-inflammatory-like macrophage. CSC-derived macrophages sit in between the M2a and M2b macrophages described by Mantovani (Mantovani et al., 2004), based on the high expression of *Arg1* (M2a) and the high level of expression of IL-10 following LPS+IFN γ activation (M2b).

The implemented sequential gating strategy identified two distinct macrophage immunophenotypes expressing opposite surface markers. Thus, M1-driven-M ϕ were defined as F4/80⁺CD11b⁺CX3CR1⁻CD206⁻, while M2-driven-M ϕ as F4/80⁺CD11b⁺CX3CR1⁺CD206⁺. The paracrine effects of CSCs induced the production of F4/80⁺CD11b⁺CX3CR1⁺CD206⁺ macrophages. Based on this high expression of CX3CR1 and CD206, CSCs induced an anti-inflammatory-like macrophage immunophenotype comparable to M2-driven-M ϕ (p<0.0001).

Consistent with the improved immunophenotyping results, single-cell qRT-PCR showed two mutually exclusive clusters of genes enriched in GM-CSF+LPS+IFN γ -M ϕ (*Cxcl1*, *Cxcl3*, *Cxcl9*, *Cxcl10*, *Il6*, *Inhba*, *Map4k4 Isoform 2*, *Map4k4 Isoform 3*, *Nos2*, *F3*, *Tgm2* and *Vegfa*) and M-CSF+IL4+IL13-M ϕ (*Arg1*, *Angpt2*, *Igf1*, *Il1rl1* and *Mrc1*). BMDMs differentiated with CSC CondM markedly diverge from the pro-inflammatory phenotype. Specifically, CSC CondM+LPS+IFN γ -M ϕ showed a reduced induction of

the M1-associated pro-inflammatory genes: *Cxcl1*, *Cxcl3*, *Il6*, *Inhba*, *Map4k4 Isoform 2*, *Map4k4 Isoform 3*, *F3* and *Vegfa*. Conversely, CSC CondM+IL4+IL13-M ϕ were indistinguishable from the M-CSF+IL4+IL13-M ϕ , expressing similar anti-inflammatory gene levels: *Arg1*, *Agpt2*, *Igf1*, *Il1r1* and *Mrc1* ($p < 0.005$).

Finally, the multiplex bead-based flow immunoassay showed that CSC CondM inhibits the secretion of pro-inflammatory cytokines and chemokines after activation with LPS and IFN γ . CSC CondM+LPS+IFN γ -M ϕ secreted the highest levels of IL-10, indicating a potential anti-inflammatory feature of CSCs ($p < 0.0001$).

In conclusion, CSCs secrete one or more paracrine factors that promote an anti-inflammatory macrophage phenotype, disrupting the pro-inflammatory macrophage program.

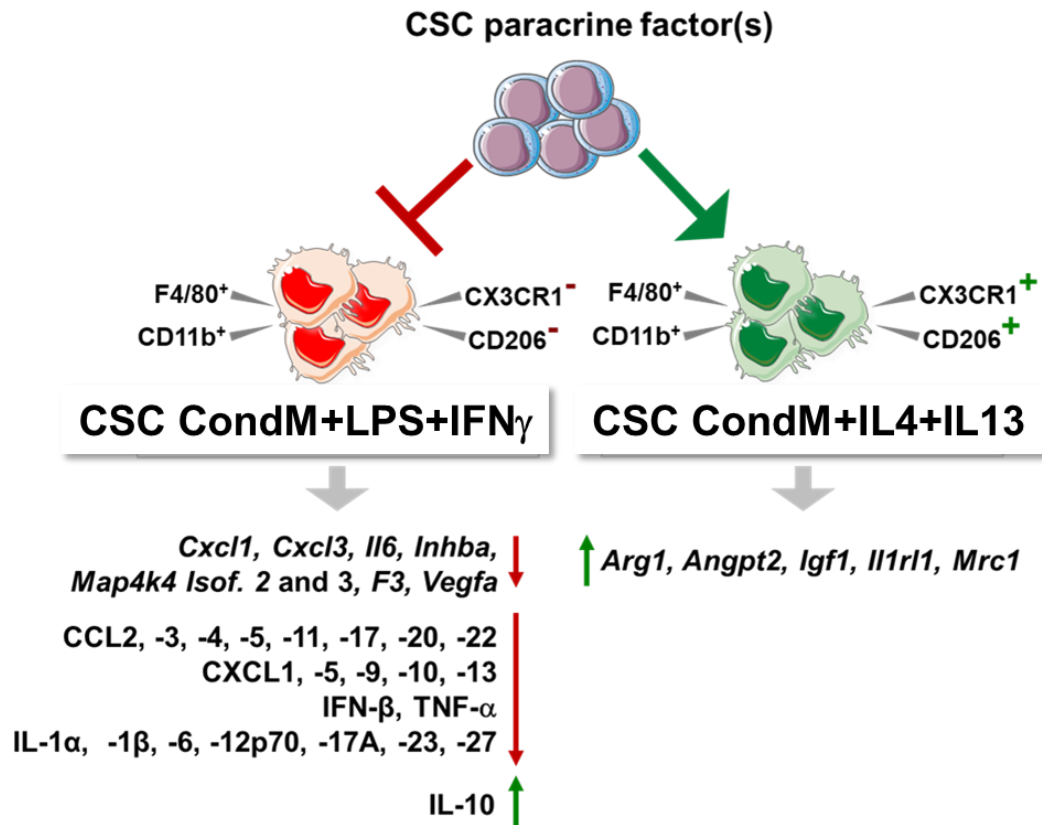


Figure 5.10 CSC CondM induces an anti-inflammatory macrophage phenotype

The paracrine effect of CSCs promotes F4/80⁺CD11b⁺CX3CR1⁺CD206⁺ macrophages. CSC CondM+LPS+IFN γ -M ϕ inhibited the M1-like pro-inflammatory signature while secreting IL-10. Conversely, CSC CondM+IL4+IL13-M ϕ express an anti-inflammatory-like phenotype.

Chapter 6 – Results III

6 Result III: Exploring whether CSC-secreted M-CSF promotes an anti-inflammatory macrophage phenotype

6.1 Introduction and rationale

The previous Chapter suggested that CSCs paracrine factors induce an anti-inflammatory-like macrophage phenotype. The final aim of this PhD thesis was to investigate what CSC-secreted signal(s) might mediate this modulation of the macrophage phenotype.

M-CSF differentiates BMDMs toward an anti-inflammatory and pro-reparative macrophage phenotype (Chitu & Stanley, 2006; Lin et al., 2008; Ma et al., 2012; Pollard, 2009; Rae et al., 2007). Data reported in this PhD thesis showed that CSC CondM induces an anti-inflammatory-like macrophage phenotype. Our group, performing a systematic complementary analysis using bulk RNA-seq and sc qRT-PCR, identified that CSCs secrete M-CSF. Therefore, CSC-secreted M-CSF could be the potential paracrine factor responsible for this macrophage phenotype (*unpublished data*), though not visualised by the multi-analyte platform used in Chapter 5.

Hence, the third objective of this PhD thesis was to determine whether CSC-secreted M-CSF is the potential factor that mediates the anti-inflammatory-like macrophage's phenotype. Therefore, this Chapter describes the experiments conducted to achieve the third aim by assessing the effects of the inhibition of the M-CSF/CSF1R pathway using two approaches:

- (i) Blocking the CSF1R activity, using the highly selective pharmacological inhibitor, BLZ945 (Pyonteck et al., 2014); and,
- (ii) Using a neutralising mAb (AFS98) (α CSF1R) that antagonises the binding between M-CSF and CSF1R (Shen et al., 2018).

6.2 Results

6.2.1 ELISA

ELISA confirmed that mouse $\text{Lin}^- \text{Sca1}^+ \text{CD31}^- \text{PDGFR}\alpha^+ \text{SP}^+$ CSCs secrete 20pg/mL of M-CSF (Fig. 6.1). Considering that circulating levels of M-CSF are ten nanograms per millilitre (Roth et al., 1997), it seemed plausible that 20pg/mL of M-CSF secreted locally by CSCs could be enough to consider it as the primary mediator of this effect.

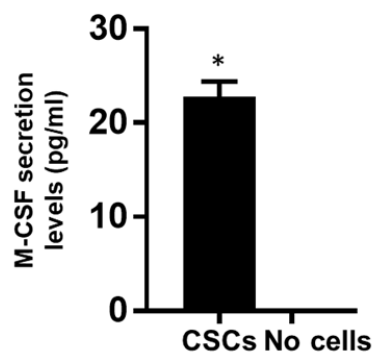


Figure 6.1 $\text{Lin}^- \text{Sca1}^+ \text{CD31}^- \text{PDGFR}\alpha^+ \text{SP}^+$ CSCs secrete M-CSF

M-CSF secreted by CSCs was tested via ELISA (N=3, \pm SEM, t-test followed by Bonferroni's correction *, $p < 0.0001$). The data were generated in collaboration with Dr McLean.

6.2.2 Pharmacological inhibition of CSF1R with BLZ945

The pharmacological inhibitor, BLZ945, was used to evaluate the role of CSC-secreted M-CSF on the macrophage immunophenotype. In a BMDMs study, BLZ945 ($EC_{50}=67\text{nM}$) inhibited the M-CSF/CSF1R activity, showing to be 1,000 times more selective against CSF1R than other tyrosine kinases receptors (Pyonteck et al., 2014). The M1-driven-M ϕ , M2-driven-M ϕ and CSC CondM-driven-M ϕ were treated with BLZ945 (67nM or 370nM) for seven days, covering differentiation and activation phases. All the populations were analysed by FACS, while due to the relevance of the activation phase on the gene expression, sc qRT-PCR was used to analyse only the activated populations.

6.2.2.1 Pharmacological inhibition of CSF1R with BLZ945 to evaluate macrophage immunophenotypes

FACS data showed that BLZ945 (370nM) reduced cell viability by 50% in CSC CondM+LPS+IFN γ -M ϕ , CSC CondM+IL4+IL13-M ϕ , and M-CSF+IL4+IL13-M ϕ (Fig. 6.2 A). The expressions of F4/80 and CD11b were analysed to evaluate whether BLZ945 affects macrophage differentiation. Interestingly, BLZ945 (370nM) decreased by 4-fold the percentage of F4/80 $^+$ CD11b $^+$ macrophages only in M-CSF-M ϕ and M-CSF+IL4+IL13-M ϕ ($p<0.05$) (Fig. 6.2 B). Finally, in none of the conditions tested, BLZ945 altered the expression of CX3CR1 and CD206 and, therefore, the anti-inflammatory macrophage immunophenotype (Fig. 6.2 C).

Overall, the FACS data showed that BLZ945 disrupted the survival of M2-driven-M ϕ and CSC CondM-driven-M ϕ , but not GM-CSF-LPS+IFN γ -M ϕ . Only in M-CSF+IL4+13-M ϕ , BLZ945 reduced F4/80⁺CD11b⁺ macrophage. As reported by others (Chitu & Stanley, 2006; Lin et al., 2008; Ma et al., 2012; Pollard, 2009; Rae et al., 2007), these data confirmed the role of the M-CSF/CSF1R signalling pathway in survival and differentiation into macrophages when used as a single factor. However, they also suggest that CSCs may secrete other factors for macrophage differentiation, responsible for compensating for the absence of M-CSF.

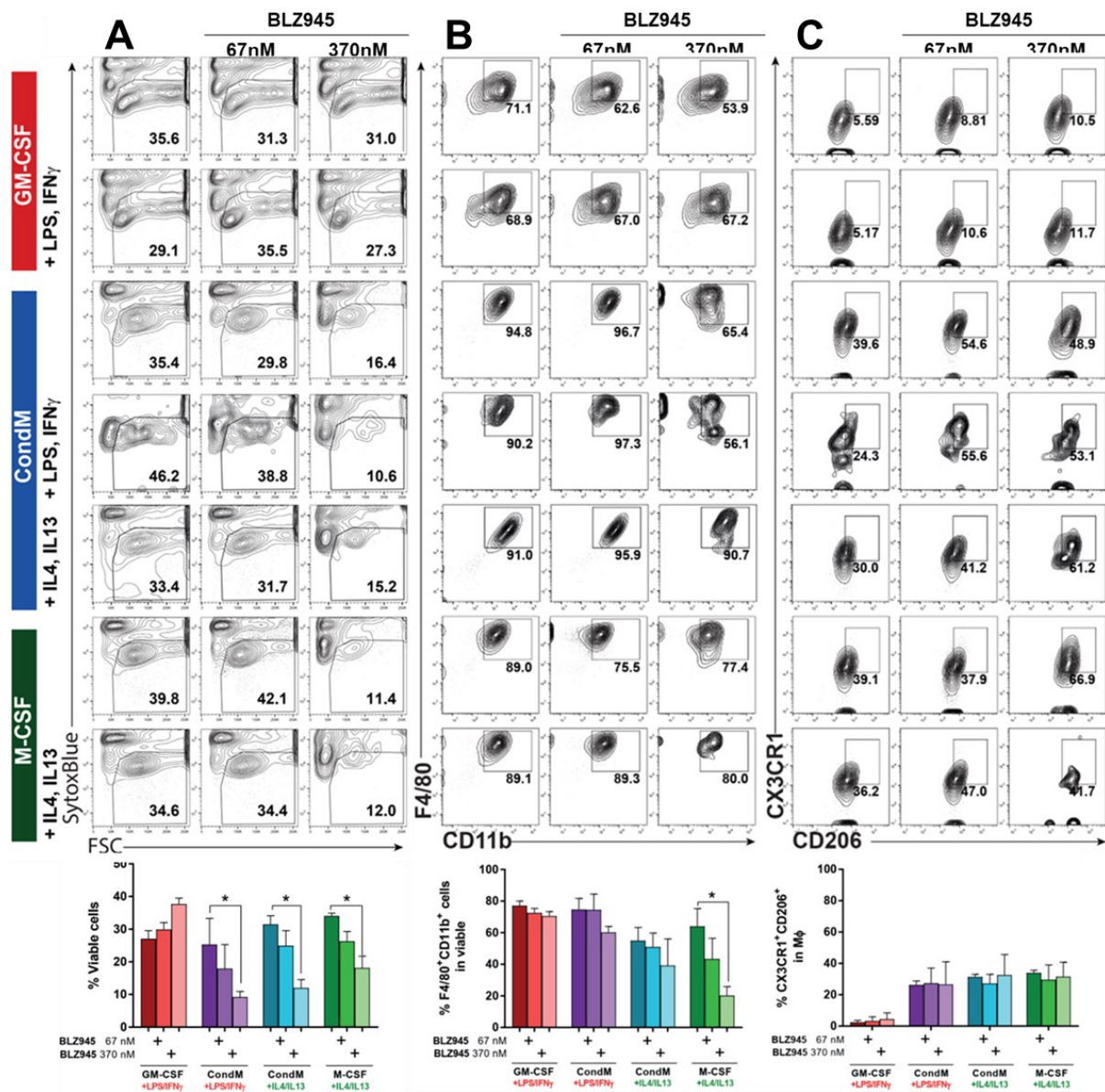


Figure 6.2 Pharmacological inhibition of CSF1R with BLZ945 to evaluate the macrophage immunophenotype.

Representative flow cytometry contour plots (TOP) and corresponding bar graphs (BOTTOM) of the seven prior culture conditions, each analysed in the absence or presence of BLZ945 (67nM and 370nM): M1-driven M ϕ (red); CSC-driven M ϕ (blue); M2-driven M ϕ (green). **A**, Live cell dye (Sytox Blue) versus FSC, measuring survival. **B**, Percentage of F4/80⁺CD11b⁺ cells in the viable cells. **C**, Percentage of CX3CR1⁺CD206⁺ cells within the F4/80⁺CD11b⁺ population. (\pm SEM, N=4). Two-way ANOVA test with Bonferroni's correction (*, p<0.05).

6.2.2.2 Single-cell qRT-PCR analysis of the effects of BLZ945 on macrophage gene signatures

After FACS analysis, the effects of BLZ945 on the gene expression profiles of activated macrophages were analysed by sc qRT-PCR. From each condition, 60 single F4/80⁺CD11b⁺ macrophages were flow-sorted. The effects of BLZ945 on the expressions of *Arg1* and *Nos2*, the key genes to distinguish pro-inflammatory and anti-inflammatory macrophages, were analysed. BLZ945 reduced levels of *Arg1* in both M-CSF+IL4+IL13-M ϕ and CSC CondM+IL4+IL13-M ϕ ($p < 0.05$ for each). On the other hand, the expressions of *Nos2* were not affected in any of the conditions tested (Fig. 6.3). Since the expression of *Nos2* was not affected, potentially consistent with the indication that BLZ945 has a specific inhibitory effect only on the M-CSF/CSF1R pathway. The following analyses focused only on the effects of BLZ945 on the gene signatures of M-CSF+IL4+IL13-M ϕ and CSC CondM+IL4+IL13-M ϕ .

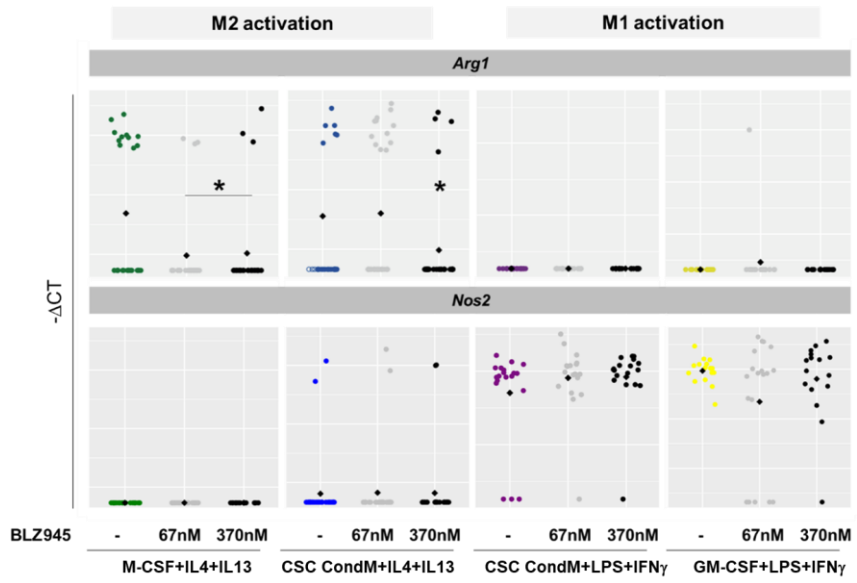


Figure 6.3 BLZ945 effects on *Arg1* and *Nos2* expression in activated macrophages
 Sc qRT-PCR expression of *Arg1* and *Nos2* in activated macrophages under BLZ945. Kruskal-Wallis/Dunn test (*, $p < 0.05$).

Focusing on M-CSF+IL4+IL13-M ϕ , the unsupervised hierarchical clustering heatmap showed one main bifurcation, reflecting the separation between M-CSF+IL4+IL13-M ϕ and BLZ945-treated macrophages (Fig. 6.4).

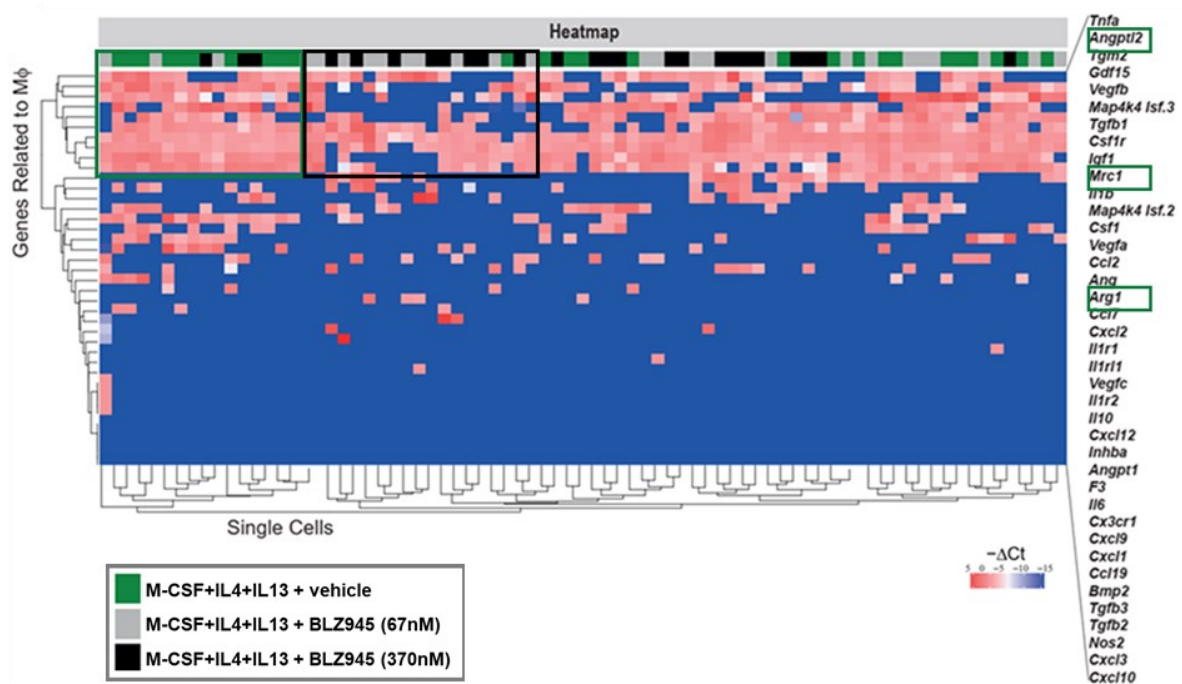


Figure 6.4 An unbiased hierarchical clustering heatmap shows the effects of BLZ945 on the gene signature of M-CSF+IL4+IL13-M ϕ

~60 single F4/80⁺CD11b⁺ cells from M-CSF+IL4+IL13-M ϕ (green), M-CSF+IL4+IL13-M ϕ +BLZ945 (67nM, grey and 370nM, black) were analysed by qRT-PCR. The unbiased hierarchical heatmap revealed three genes (green box) downregulated with BLZ945. The heatmap shows ΔCt values (blue, low or absent; red, high).

PCAs offered a better resolution for exploring this separation. Samples PC1 (16% variability) separated M-CSF+IL4+IL13-M ϕ +BLZ945 (370nM) from the M-CSF+IL4+IL13-M ϕ . Interestingly, the M-CSF+IL4+IL13-M ϕ +BLZ945 (67nM) samples were scattered across these two clusters, suggesting a dose-dependent effect of BLZ945 on the gene signature (Fig. 6.5). The PCA of the genes identified two clusters. Cluster 1 enriched for four anti-inflammatory genes (*Angpt2*, *Ang1*, *Mrc1*, *Igf1*) and

two migratory-related genes (*Ccl2* and *Ccl7*); and cluster 2 enriched for M1-like macrophage genes: *Il1 β* , *Vegf β* , *Tgf β* and *Map4k4* Isoform 2 and 3 (Fig. 6.5).

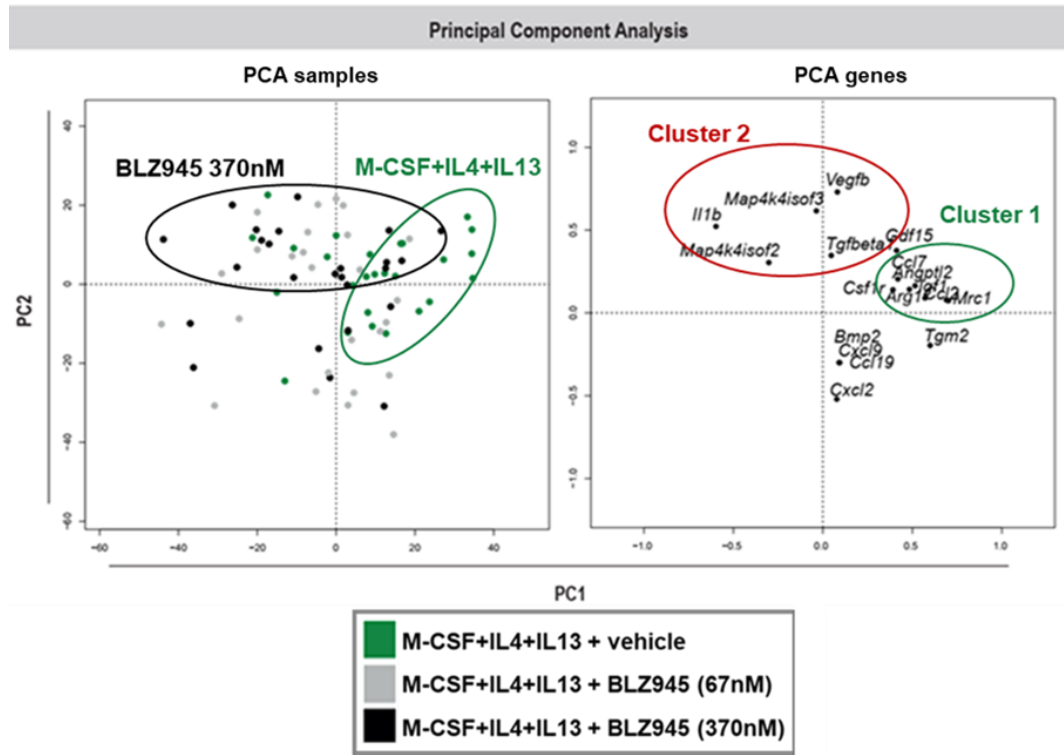


Figure 6.5 PCAs show the effects of BLZ945 on the M-CSF+IL4+IL13-M ϕ gene signature. PCA of the samples shows that PC1 separated M-CSF+IL4+IL13-M ϕ (green) and BLZ945-treated M ϕ (grey, 67nM and black, 370 nM). PCA of the score shows two clusters: cluster 1 (*Angptl2*, *Arg1*, *Mrc1*, *Igf1*, *Ccl2* and *Ccl7*); cluster 2 (*Map4k4* Isoform 2 and 3, *Il1 β* , *Vegf β* and *Tgf β*).

Dot plots show that compared to vehicle, BZL945 downregulated three of the genes in cluster 1: *Arg1* ($p=3.8 \times 10^{-2}$), *Angptl2* ($p=3.4 \times 10^{-3}$), and *Mrc1* ($p=5.4 \times 10^{-3}$). The higher the concentration of BLZ945, the greater the downregulation was observed (Fig. 6.6).

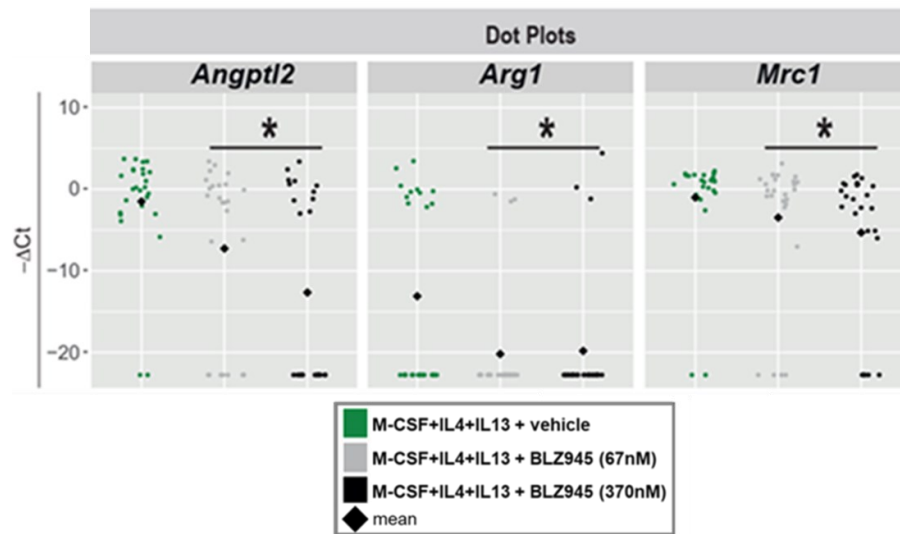


Figure 6.6 Dot plots show the effects of BLZ945 on cluster 1 expression

Dot plots show the effects of BLZ945 on the gene expression of cluster 1. *Angptl2*, *Arg1* and *Mrc1* (Kruskal-Wallis/Dunn test. *, $p < 0.05$, compared to the vehicle).

Overall, single-cell qRT-PCR analysis showed that in M-CSF+IL4+IL13-M ϕ , BLZ945 reduced the anti-inflammatory-related genes *Angptl2*, *Arg1*, and *Mrc1*, suggesting that the activity of M-CSF through CSF1R could disrupt the M2-driven gene signature of the combination use of M-CSF, IL-4 and IL-13.

The next single-cell qRT-PCR analysis investigated BLZ945 effects on CSC CondM+IL4+IL13-M ϕ . The unsupervised hierarchical clustering heatmap showed a bifurcation forming two clusters. Cluster 1 lacked seven anti-inflammatory/pro-

reparative genes, *Mrc1*, *Igf1*, *Angptl2*, *Vegfb*, *Tgm2*, *Gdf15* and *Arg1*, corresponding to the CSC CondM+IL4+IL13-M ϕ treated with BLZ945 (370nM). In contrast, cluster 2 was formed by CSC CondM+IL4+IL13-M ϕ and CSC CondM+IL4+IL13-M ϕ +BLZ945 (67nM) (Fig. 6.7).

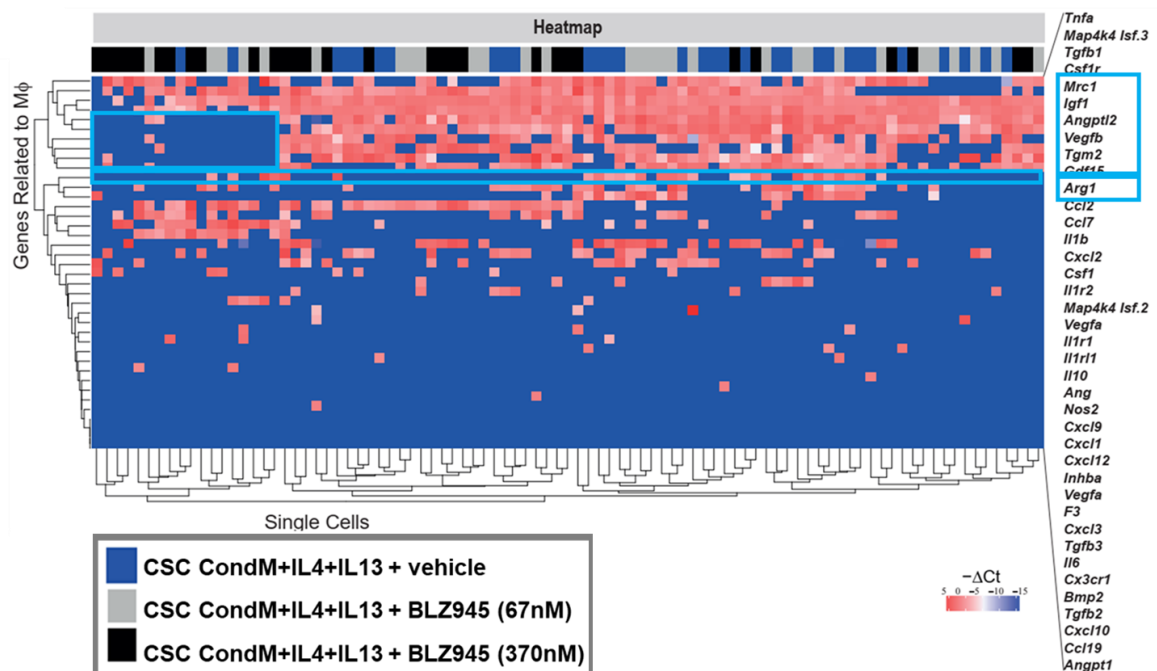


Figure 6.7 An unbiased hierarchical clustering heatmap shows the effect of BLZ945 on the CSC CondM+IL4+IL13-M ϕ gene signature.

~60 single F4/80⁺CD11b⁺ cells from CSC CondM+IL4+IL13 (blue), CSC CondM+IL4+IL13+BLZ945 (67Nm) (grey) and CSC CondM+IL4+IL13+BLZ945 (370nM) (black) were analysed by qRT-PCR. Unbiased hierarchical clustering reveals genes downregulated in cluster 1 (light blue box). The heatmap shows ΔCt values (blue, low or absent; red, high).

Dot plots showed that BLZ945 at 67nM downregulated *Arg1* ($p=4.5 \times 10^{-2}$), while at 370nM of BLZ945, the expression of four anti-inflammatory genes was downregulated:

Angptl2 ($p=2.5 \times 10^{-2}$), *Arg1* ($p=3.8 \times 10^{-2}$), *Igf1* ($p=1 \times 10^{-2}$) and *Mrc1* ($p=2.5 \times 10^{-2}$) (Fig. 6.8).

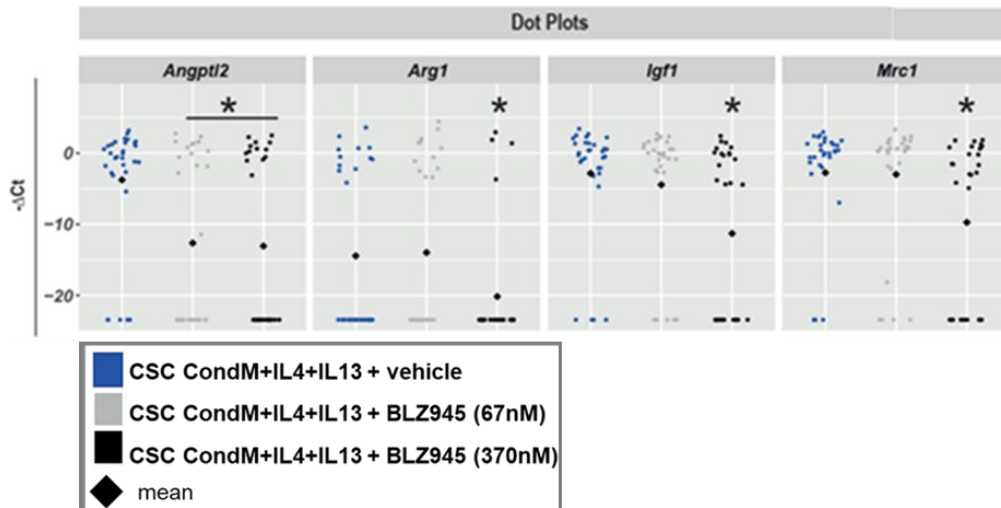


Figure 6.8 Dot plots show the effects of BLZ945 on CSC CondM+IL4+IL13-M ϕ gene expression

Dot plots show the effects of BLZ945 on the gene expression of *Angptl2*, *Arg1*, *Igf1* and *Mrc1* (Kruskal-Wallis/Dunn test. *, $p < 0.05$).

Overall, the M-CSF+IL4+IL13-M ϕ , BLZ945 disrupted the anti-inflammatory signature in CSC CondM+IL4+IL13-M ϕ . Thus, in both conditions tested, BLZ945 distributed the expression of key anti-inflammatory genes, indicating that the inhibition of the M-CSF/CSF1R pathway hampered the full activation of macrophages towards the anti-inflammatory-like phenotype.

6.2.3 Inhibition of CSF1R with neutralising mAb (AFS98): α CSF1R

As an independent, complementary approach, macrophages were cultured with a neutralising mAb (AFS98) against CSF1R (α CSF1R) that antagonises the binding between M-CSF and CSF1R (Shen et al., 2018). For the seven days of *in vitro* differentiation and activation, the M1-driven-M ϕ , M2-driven-M ϕ and CSC CondM-driven-M ϕ were treated with α CSF1R (1 μ g/100 μ l). Immunophenotypes, gene profiles, secretomes and phagocytotic activities were analysed to evaluate the effects of inhibiting the M-CSF/CSF1R pathway.

6.2.3.1 Inhibition of CSF1R with α CSF1R to evaluate macrophage immunophenotypes

Consistent with results using the CSF1R kinase inhibitor, FACS data showed that the percentage of viable cells decreased by 4-fold in M2-driven-M ϕ (M-CSF, 64% vs M-CSF+ α CSF1R, 17%; M-CSF+IL4+IL13, 66% vs M-CSF+IL4+IL13+ α CSF1R, 15%) and by 2-fold in CSC-driven-M ϕ (CSC CondM, 61% vs CSC CondM+ α CSF1R, 33%; CSC CondM+IL4+IL13, 63% vs CSC CondM+IL4+IL13+ α CSF1R, 35%) ($p < 0.05$) (Fig. 6.9 A). The differentiation into F4/80⁺CD11b⁺ macrophages was also affected by α CSF1R reduced by 20% in CSC-driven-M ϕ , while by 30% in M2-driven-M ϕ ($p < 0.05$ for each) (Fig. 6.9 B). Lastly, in CSC CondM-driven M ϕ , CX3CR1⁺CD206⁺ macrophages were reduced by 10% ($p < 0.05$) (Fig. 6.9 C).

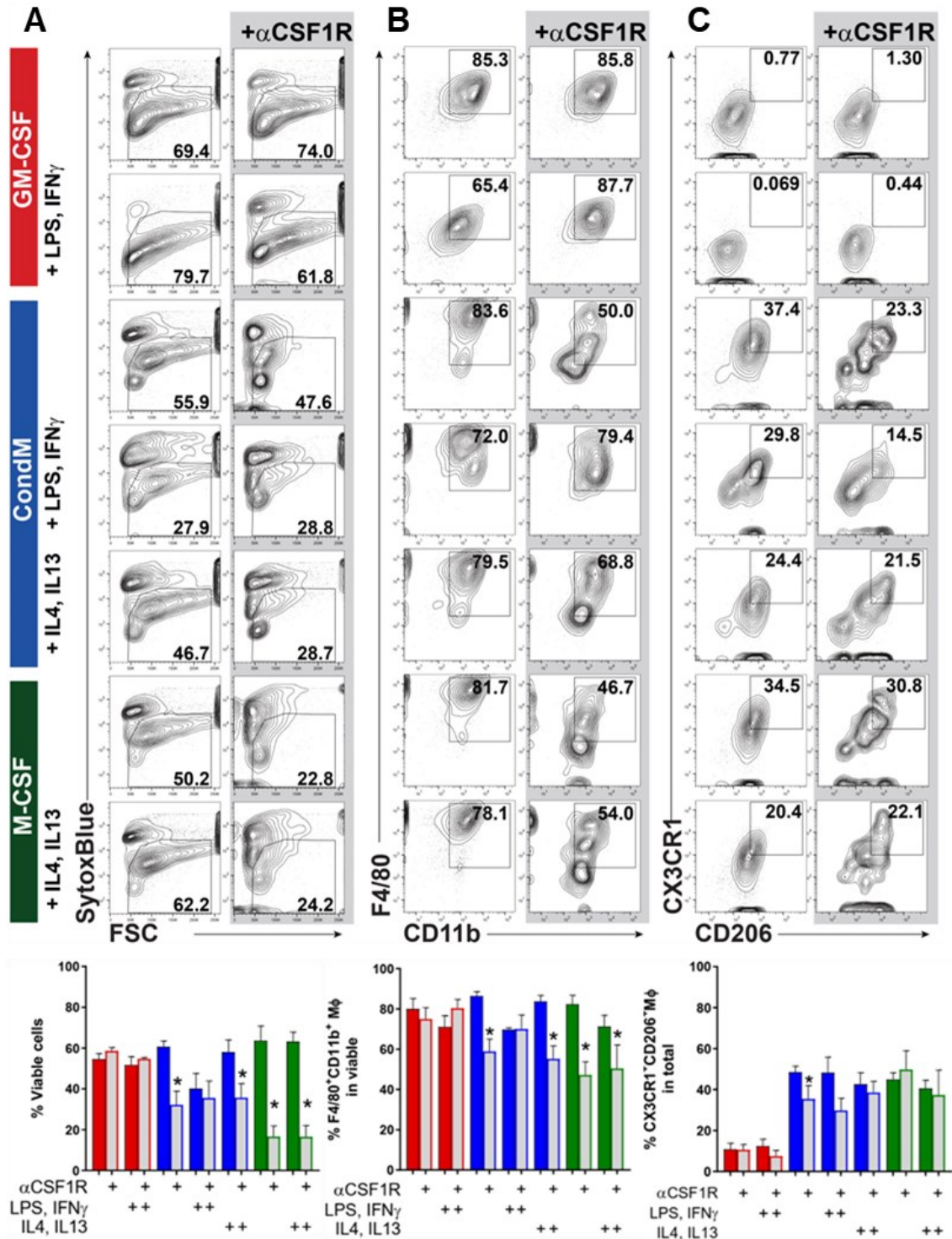


Figure 6.9 α CSF1R to evaluate macrophage immunophenotypes.

Representative flow cytometry contour plots (TOP) and corresponding bar graphs (BOTTOM) of the seven culture conditions analysed α CSF1R: M1-driven M ϕ (red); CSC-driven M ϕ (blue); M2-driven M ϕ (green). **A**, Live cells dye (Sytox Blue) versus FSC measures survivals. **B**, Percentage of F4/80⁺CD11b⁺ cells in the viable cells. **C**, Percentage of CX3CR1⁺CD206⁺ cells in F4/80⁺CD11b⁺ cells. (\pm SEM, N=5). Two-way ANOVA test with Bonferroni's correction (*, $p < 0.05$).

By contrast, the viability and percentage of F4/80⁺CD11b⁺CX3CR1⁺CD206⁺ macrophages were not affected by blocking CSF1R in CSC CondM+LPS+IFN γ -M ϕ and M1-driven-M ϕ . These results reinforced the idea that M-CSF is the critical factor secreted by CSCs, for promoting the survival and differentiation of M2-like macrophages as gauged by immunophenotype.

6.2.3.2 Single-cell qRT-PCR analysis of the effects of α CSF1R on macrophage gene signatures

Next, the effects of α CSF1R on the gene profiles of activated macrophages were analysed by flow sorting at least 60 single F4/80⁺CD11b⁺ macrophages from each condition by sc qRT-PCR. The first comparison tested α CSF1R in GM-CSF+LPS+IFN γ -M ϕ and CSC CondM+LPS+IFN γ -M ϕ , while the second tested α CSF1R in M-CSF+IL4+IL13-M ϕ and CSC CondM+IL4+IL13-M ϕ .

The unsupervised hierarchical clustering heatmap visualised the sc qRT-PCR data from the first analysis. The dendrogram of the genes showed two main bifurcations separating GM-CSF+LPS+IFN γ -M ϕ and CSC CondM+LPS+IFN γ -M ϕ (Fig. 6.10 A). α CSF1R did not interfere with the gene profiles of GM-CSF+LPS+IFN γ -M ϕ , as expected from the absence of M-CSF. In contrast, in the CSC CondM+LPS+IFN γ -M ϕ , α CSF1R led to a downregulation of *Ccl2* ($p=9.4 \times 10^{-7}$), *Ccl7* ($p=3.3 \times 10^{-3}$), *Cxcl9* ($p=1 \times 10^{-2}$), and *Vegfc* ($p=3.9 \times 10^{-2}$), and upregulation of *Inhba* ($p=2.8 \times 10^{-2}$), *Csf1* ($p=2 \times 10^{-2}$) and *Cx3cr1* ($p=2.4 \times 10^{-3}$) (Fig. 6.10 B).

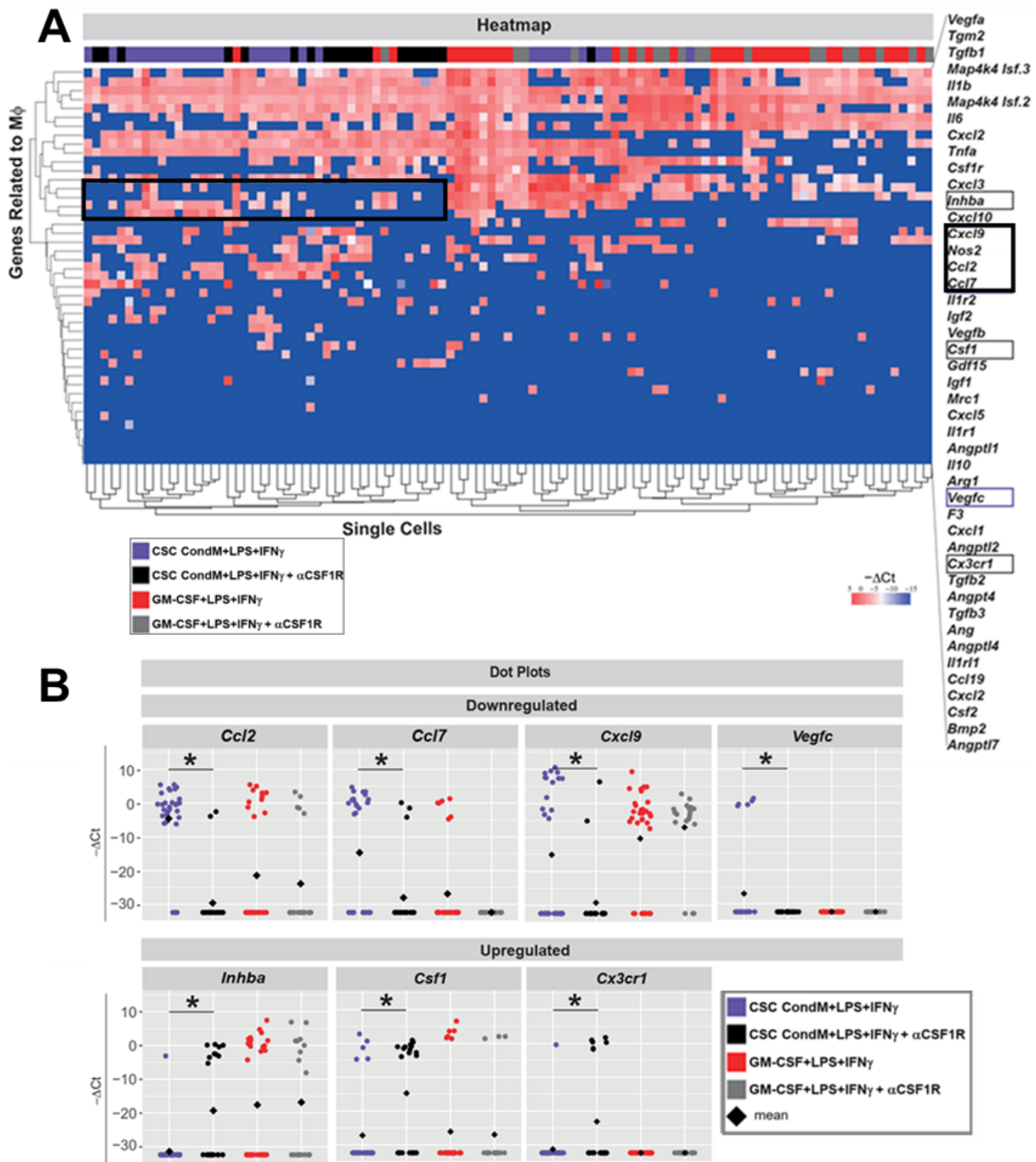


Figure 6.10 The effects of α CSF1R on the pro-inflammatory gene signature

~60 single F4/80⁺CD11b⁺ cells from each condition were analysed by qRT-PCR. **A**, the unbiased hierarchical heatmap shows that in CSC CondM+LPS+IFN γ + α CSF1R, three genes were downregulated (bold black and purple boxes), and three were upregulated (black box). The heatmap shows ΔCt values (blue, low or absent; red, high). **B**, Dot plots visualise downregulated and upregulated genes (Kruskal-Wallis/Dunn test, *, p < 0.05).

The second analysis focused on the M-CSF+IL4+IL13-M ϕ and CSC CondM+IL4+IL13-M ϕ . The unsupervised hierarchical clustering heatmap showed three main bifurcations forming three clusters. Cluster 1 includes the untreated cells (M-CSF+IL4+IL13-M ϕ and CSC CondM+IL4+IL13-M ϕ); cluster 2, M-CSF+IL4+IL13-M ϕ + α CSF1R; and cluster 3, CSC CondM+IL4+IL13-M ϕ + α CSF1R. Therefore, α CSF1R induced different downregulatory effects in M-CSF+IL4+IL13-M ϕ and CSC CondM+IL4+IL13-M ϕ (Fig. 6.11 A).

Specifically, in the M-CSF+IL4+IL13-M ϕ + α CSF1R, nine genes were downregulated: *Angptl2* ($p=1.4 \times 10^{-4}$), *Arg1* ($p=1.4 \times 10^{-4}$), *Igf1* ($p=3.8 \times 10^{-6}$) and *Mrc1* ($p=3.8 \times 10^{-5}$), *Csf1r* ($p=1 \times 10^{-3}$), *Tgm2* ($p=5.6 \times 10^{-2}$), *Tgf β 1* ($p=1.3 \times 10^{-3}$), *Ccl2* ($p=8.1 \times 10^{-2}$) and *Ccl7* ($p=9.4 \times 10^{-3}$). On the other hand, in CSC CondM+IL4+IL13-M ϕ + α CSF1R only 4 of these genes were downregulated: *Angptl2* ($p=5.3 \times 10^{-2}$), *Arg1* ($p=4.3 \times 10^{-5}$), *Igf1* ($p=5.5 \times 10^{-3}$) and *Ccl2* ($p=4.3 \times 10^{-3}$). Interestingly, dot plots allow to visualise that eight genes related to the M1-pro-inflammatory macrophage profile were upregulated in M-CSF+IL4+IL13-M ϕ + α CSF1R: *Nos2* ($p=5.8 \times 10^{-4}$), *Cxcl1* ($p=1.9 \times 10^{-2}$), *Cxcl10* ($p=1.5 \times 10^{-4}$), *Cxcl9* ($p=4.8 \times 10^{-7}$), *InhbA* ($p=3.7 \times 10^{-2}$), *Il6* ($p=4.6 \times 10^{-10}$), *Map4k4* *Isf.2* ($p=3.4 \times 10^{-2}$) and *Il1r2* ($p=1.6 \times 10^{-4}$), suggesting a possible shift of the phenotype from anti-inflammatory-like to an pro-inflammatory-like. In CSC CondM+IL4+IL13-M ϕ , only *Csf1* ($p=4.2 \times 10^{-4}$) was upregulated (Fig. 6.11 B).

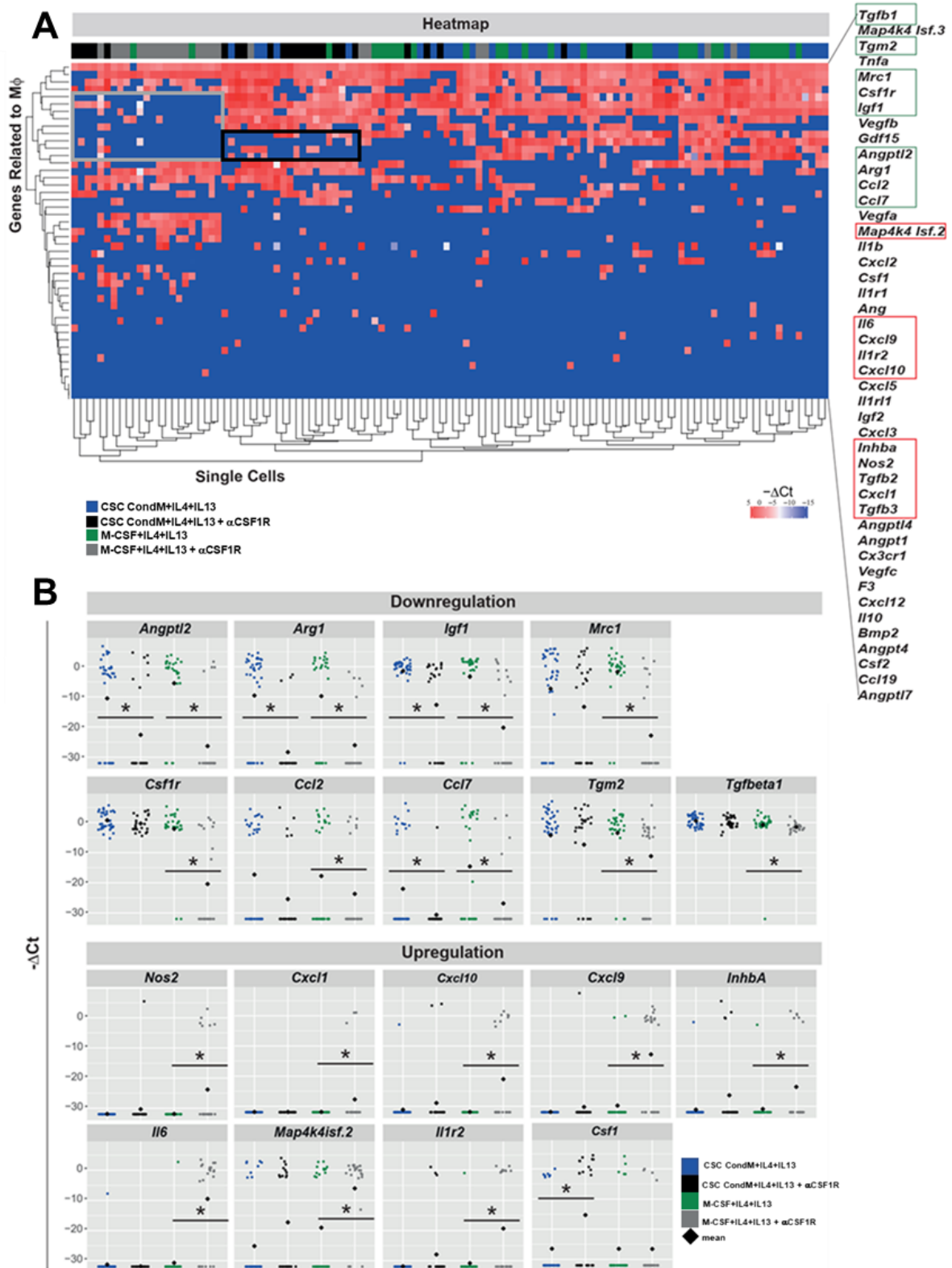


Figure 6.11 The effects of α CSF1R on the anti-inflammatory gene signature

~60 single F4/80⁺CD11b⁺ cells analysed by qRT-PCR. **A**, the unbiased hierarchical heatmap shows genes downregulated in M-CSF+IL4+IL13+ α CSF1R (grey box), in CSC CondM+IL4+IL13+ α CSF1R (black box) and upregulated in M-CSF+IL4+IL13+ α CSF1R (red box). The heatmap shows ΔCt values (blue, low or absent; red, high). **B**, Dot plots visualise downregulated and upregulated genes (Kruskal-Wallis/Dunn test, *, $p < 0.05$).

In conclusion, based on sc qRT-PCR data, α CSF1R reduced the anti-inflammatory-like gene signature in M-CSF+IL4+IL13 and CSC CondM+IL4+IL13 macrophages, altering the expression of a smaller set of genes when using CondM in lieu of M-CSF. This concurs with the inference from using BLZ945 that additional CSC-secreted factors are redundant with M-CSF for a subset of CSCs' effects.

6.2.3.3 Inhibition of CSF1R with α CSF1R to evaluate the macrophage secretome

In M-CSF+IL4+IL13-M ϕ and CSC CondM+IL4+IL13-M ϕ , α CSF1R disrupted the M2-like immunophenotype and gene signature. Therefore, the secretome of macrophages was also analysed using the multi-analytical bead-based flow immunoassay described in Chapter 5.

Unexpectedly, α CSF1R reduced the secretion of seven pro-inflammatory cytokines in GM-CSF+LPS+IFN γ -M ϕ (CCL5, CCL20, CCL11, CXCL1, CLXCL10, CCL3 and CCL4) and of CCL3 and CCL4 in CSC CondM+LPS+IFN γ .

As a possible explanation for this paradoxical result, a key finding of this experiment was the complete inhibition of IL-10 secretion by α CSF1R in CSC CondM+LPS+IFN γ -M ϕ . Therefore, a further culture condition was generated to help test whether IL-10 in M1-activated cells depends on CSC-secreted M-CSF. For this comparison, BMDMs were differentiated under M-CSF and activated with LPS and IFN γ . This new population was named M-CSF+LPS+IFN γ -M ϕ .

M-CSF+LPS+IFN γ -M ϕ secreted an amount of IL-10 similar to CSC CondM+LPS+IFN γ -M ϕ ($p < 0.0001$), indicating that IL-10 expression depends on the combination used of M-CSF (whether exogenous or CSC-secreted) and LPS and IFN γ (Fig. 6.12).

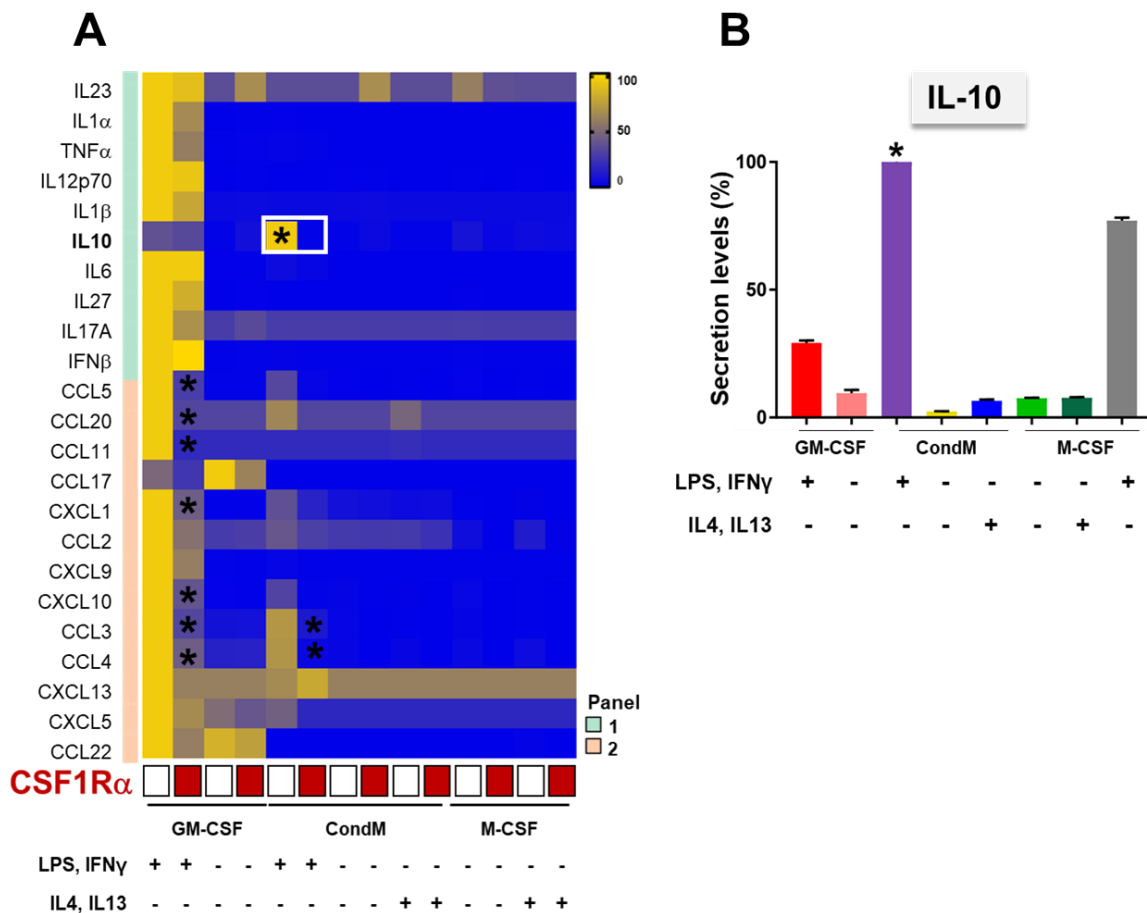


Figure 6.12 α CSF1R effects on macrophage secretome

A, A multi-analytical bead-based flow immunoassay was used to evaluate the effects of α CSF1R on macrophage secretome. Data are normalised for each analyte. **B**, Bar graph shows the secretion levels of IL-10 in the eight conditions tested in percentage. *, $p < 0.0001$ (\pm SEM, N=3) (Two-way ANOVA, multiple comparison test corrected using Bonferroni's test).

6.2.3.4 Inhibition of CSF1R with α CSF1R to evaluate macrophage phagocytosis

To test as a related functional response whether M2-like macrophages engulf dying CMs in a process that depends on the M-CSF/CSF1R pathway, a phagocyte model was then developed.. First, RAW 267.4 macrophages were fed *E.coli* bio-particles to assess phagocytic activity. RAW 264.7 macrophages treated with CSC CondM

doubled phagocytosis activity. On the other hand, α CSF1R decreased phagocytosis activity by 2-fold ($p < 0.0001$) (Fig. 6.13 A). Then, RAW 264.7 macrophages were fed dying rat CMs (H9C2) as a more relevant trigger, demonstrating that CSC CondM enhanced CM phagocytosis 2.5-fold ($p < 0.0001$). As predicted, α CSF1R inhibited this effect, so that engulfment levels returned to baseline levels ($p < 0.0001$) (Fig. 6.13 B). In conclusion, CSC CondM enhanced phagocytosis, while α CSF1R reduced its activity, indicating that it may depend on the M-CSF/CSF1R pathway.

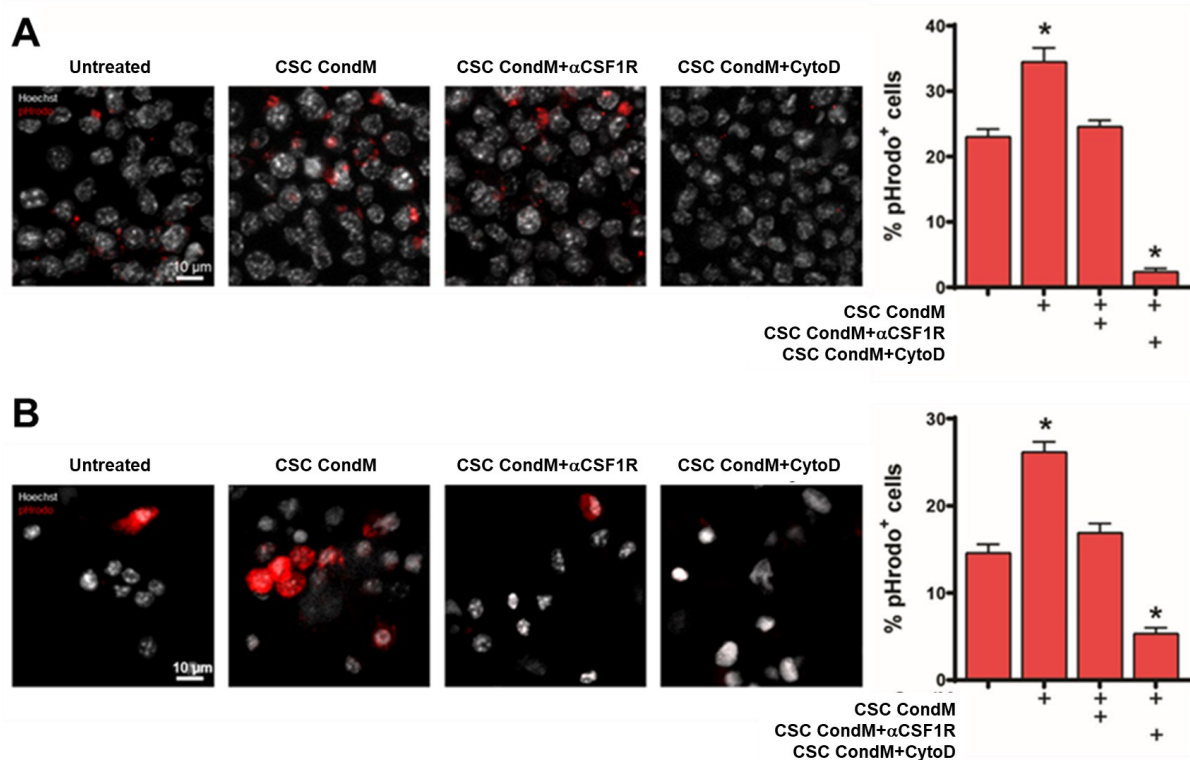


Figure 6.13 α CSF1R effects on phagocytosis

A, Phagocytosis assay on RAW 264.7 cells fed with *E.coli* bio-particles (N=20/condition). **B**, Phagocytosis assay on RAW 264.7 cells fed with apoptotic rat CMs (N=15/condition). (LEFT) Widefield fluorescence microscopy; scale bar = 100 μ m. (RIGHT) Bar graphs show the percentage of pHrodo⁺ cells. (\pm SEM). Two-way ANOVA followed by Bonferroni's test, *, $p < 0.0001$. Data were performed by Dr Miranda.

6.3 Discussion

6.3.1 CSC-secreted M-CSF promotes an anti-inflammatory-like macrophage phenotype

The entire secretome of CSCs is still unknown; however, bulk RNA-Seq, sc qRT-PCR and computational analysis revealed that human and mouse CSCs expressed M-CSF, supporting the hypothesis that Lin⁻Sca1⁺CD31⁻PDGFR α ⁺SP⁺ CSCs may induce an M2-like macrophage phenotype via this protein. ELISA confirmed that CSCs secrete 20pg/mL of M-CSF. Considering that circulating levels of M-CSF are in the range of 10ng/mL and tissue levels in the orders of tens of picograms per milligram (Roth et al., 1997), 20pg/ml is considered sufficient to modulate the macrophage phenotype.

Having shown in Chapter 5 of this PhD thesis that paracrine effects of CSCs induce an anti-inflammatory-like macrophage phenotype, the present chapter presents evidence that this is M-CSF-dependent. Therefore, two complementary interventions designed to inhibit M-CSF activity tested the role of M-CSF in promoting the M2-like macrophage phenotype induced by CSCs.

6.3.2 Pharmacological inhibition (BLZ945) of CSF1R suggested a compensatory effect CSC CondM+IL4+IL-M ϕ

Here, FACS data confirmed that BLZ945 caused 50% of cell death in M-CSF+IL4+IL13-M ϕ , CSC CondM-LPS+IFN γ -M ϕ and CSC CondM+IL4+IL13-M ϕ . When M-CSF is the only stimulus, BLZ945 reduces the percentage of F4/80⁺CD11b⁺ macrophages (M2-driven-M ϕ), while in combination with other paracrine signals from CSCs, it does not. This difference in the production of F4/80⁺CD11b⁺ macrophages suggests a redundant effector in the secretome of CSCs. Therefore, M-CSF may not be the only paracrine factor secreted by CSCs that promotes macrophage survival and differentiation. Alternatively, compensatory effects have been reported after inhibition of CSF1R in some circumstances involving CSF2R (Klemm et al., 2021).

Notwithstanding the lack of a substantial effect of the receptor tyrosine kinase inhibitor on the CSC CondM-induced immunophenotype, the investigation of the gene expression profile was informative. In both M-CSF+IL4+IL13-M ϕ and CSC CondM+IL4+IL13-M ϕ , sc qRT-PCR showed that pharmacological inhibition of CSF1R downregulated the expression of three key M2-related anti-inflammatory genes: *Arg1*, *Anptl2* and *Mrc1*. Thus, disruption of the anti-inflammatory macrophage gene signature by BLZ945 suggests that CSC-secreted M-CSF is responsible for the anti-inflammatory gene signature in CSC CondM-driven macrophages. However, confirmation by an independent criterion is always worthwhile.

6.3.3 α CSF1R confirmed that CSC-secrete M-CSF induces a unique anti-inflammatory-like macrophage phenotype

As expected from the experiments above, α CSF1R reduced BMDMs' viability and the percentage of F4/80⁺CD11b⁺CX3CR1⁺CD206⁺ macrophages in CSC CondM+IL4+IL13-M ϕ . Thus, using the blocking antibody as a complementary intervention confirms that BMDMs' survival and differentiation into macrophages with an anti-inflammatory-like immunophenotype are M-CSF-dependent.

The effects of α CSF1R on the macrophage immunophenotype provide insight into the role of M-CSF. Interestingly, those BMDMs that survive the differentiation phase expressed an anti-inflammatory-like immunophenotype. There are two interpretations for this outcome: first, as mentioned above, CSCs can secrete other factors that could induce an anti-inflammatory-like macrophage immunophenotype regardless of M-CSF; secondly, only a percentage of the BMDMs were affected by α CSF1R and died or failed to differentiate, while the rest were unaffected and had the complete anti-inflammatory-like macrophage immunophenotype: F4/80⁺CD11b⁺CX3CR1⁺CD206⁺. Proof that α CSF1R was present at saturating concentrations would help distinguish between these possibilities.

The JNK pathway regulates the development, survival and function of macrophages, including the expression of pro-inflammatory cytokines (e.g. *Tnf α* , *Ccl2*, *Tgf β 1*). In diabetic mice treated with α CSF1R, inhibition of M-CSF/CSF1R suggest a reduction of JNK pathway activity (Himes et al., 2006; Lim et al., 2009). Here, a similar impact

on the gene expression profile of CSC CondM+LPS+IFN γ -M ϕ has been observed. α CSF1R reduced the expression of pro-inflammatory genes (*Cxcl9*, *Vegfc*, *Inhba*).

Interestingly, there is a slight difference in the gene panel affected by α CSF1R in M-CSF+IL4+IL13-M ϕ and CSC CondM+IL4+IL13-M ϕ , indicating their unique gene signatures. In M-CSF+IL4+IL13-M ϕ , α CSF1R downregulated nine anti-inflammatory genes and upregulated eight pro-inflammatory genes. On the other hand, in CSC CondM+IL4+IL13-M ϕ , α CSF1R downregulated four of these nine anti-inflammatory genes. The anti-inflammatory genes downregulated by α CSF1R in both macrophage populations were *Arg1*, *Angptl2*, *Igf1* and *Ccl2*, indicating that the expression of these genes was explicitly contingent on the M-CSF/CSF1R pathway, with no other factor(s) in CSC CondM able to compensate for the disruption of the signal.

Furthermore, the evaluation of macrophage secretomes showed that inhibition of M-CSF suppressed IL-10 secretion in CSC CondM+LPS+IFN γ -M ϕ . A new culture condition was designed to test whether IL-10 secretion depends on the M-CSF/CSF1R pathway following LPS+IFN γ activation. Thus, α CSF1R, inhibiting CSC-secreted M-CSF, disrupted IL-10 secretion. In this tested condition, and for the secretion of this interleukin, the paracrine factors of CSCs could not generate any compensatory effect.

Macrophages promote tissue repair also via clearance of the damaged heart by engulfing dying CMs (Cook et al., 2014; Fildes et al., 2009; Frangogiannis, 2012; Frangogiannis, 2015, 2014; Moran et al., 2014; Mozaffarian, 2016; Prabhu, 2005; Stone et al., 2016; Sutton & Sharpe, 2000). The phagocytosis of debris and dead cells

helps resolve the inflammation. Thus, promoting the anti-inflammatory-like macrophage phenotype enhances heart repair and regeneration (Prabhu & Frangogiannis, 2016). Therefore, the final experiment investigated the functional role of the M-CSF/CSF1R pathway in regulating phagocytosis.

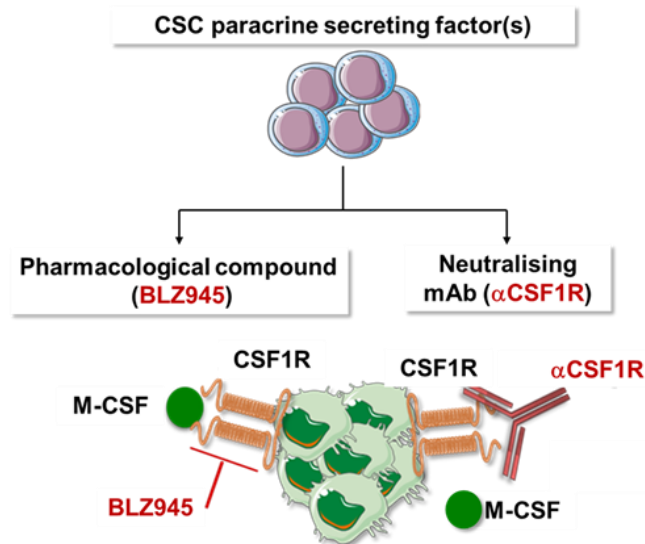
Mouse-derived RAW 264.7 macrophages have been used extensively *in vitro* studies because they are mature macrophages with an M2-like phenotype without stimulation (Zhang et al., 2012). The benefits of using RAW 264.7 macrophages include (i) easy-to-maintain cell line, (ii) highly reproducible results, and (iii) cost-effectiveness compared to the BMDMs, especially for initial screenings.

Here, the phagocytic activity of RAW 264.7 macrophages was enhanced by the co-culture with CSC CondM. CSC-secreted M-CSF improved the capacity of RAW 267.4 macrophages to engulf *E.coli* bio-particles and dying rat CMs. Conversely, inhibition of the M-CSF/CSF1R pathway using α CSF1R suppressed the positive effect obtained by CSCs, returning phagocytosis activity to baseline. Therefore, the enhanced phagocytosis activity may depend on M-CSF secreted by CSCs. This provisional conclusion would be strengthened by using at least one complementary inhibitor, such as BLZ945, for the cells' immunophenotype and gene expression profile.

6.4 Summary and Conclusion

The CSCs secretome is not yet fully known. Here, bulk RNA-Seq combined with single-cell and computational analysis identified at least one factor released by CSCs whose function is associated with macrophages: M-CSF. M-CSF is a known growth factor for macrophage differentiation towards the M2-like anti-inflammatory side of the macrophage phenotypes spectrum (Lin et al., 2008; Ma et al., 2012; Pollard, 2009; Rae et al., 2007). Therefore, two loss-of-function experiments tested whether CSC-secreted M-CSF is responsible for the anti-inflammatory-like subtype of CSC CondM-induced macrophage phenotypes. The main results of the effects of the pharmacological inhibitor BLZ945 and the neutralising antibody against CSF1R (α CSF1R) are summarised in Figure 6.14.

In conclusion, these results confirmed the original hypothesis of this PhD thesis. CSCs secreted at least one paracrine factor, M-CSF, which induces a unique subtype of M2-like macrophage phenotype. These results do not rule out the possibility that one or more additional paracrine factors may also be needed to induce the anti-inflammatory-like phenotype if the M-CSF pathway is inhibited.



BLZ945		αCSFR1
Immunophenotype		
50%	Viability	40%
n/a	% Mϕ (F4/80⁺CD11b⁺)	20%
n/a	% M2-like Mϕ (CX3CR1⁺CD206⁺)	10%
Gene expression		
50%	<i>Arg1, Angptl2, Igf1, Mrc1</i>	50%
Secretome		
n/a	+LPS+IFNγ IL-10	100%
Functional activity		
n/a	Phagocytosis of dead CMs	30%

Figure 6.14 CSF1R inhibition disrupts the anti-inflammatory CSC-driven macrophage phenotype

The CSC-secrete M-CSF activity was inhibited using pharmacological inhibition of CSF1R, BLZ945 (LEFT) and neutralising monoclonal antibodies against CSF1R, αCSF1R (RIGHT). The results of each inhibitory system were summarised in the table, indicating the different parameters measured (immunophenotype, gene expression, secretome profile, and functional activity) (n/a, non-evaluated).

Chapter 7 - General Discussion

7.1 General Discussion

7.1.1 CSC-secreted M-CSF induces a unique anti-inflammatory-like macrophage phenotype that may provide a therapeutic strategy to support post-MI heart repair and regeneration

Despite considerable advances in cardiac regenerative medicine and age-adjusted reduction in mortality rate, the overall progression of ischemic heart disease reduction is still weak. Instead, the prevalence is forecasted to increase over the next ten years (Roth et al., 2018). Hence, the unmet need is to find new strategies to reduce or prevent heart damage. Lin⁻Sca1⁺CD31⁻PDGFR α ⁺SP⁺ CSCs have been shown to reduce infarct size and improve cardiac pump function, despite the lack of durable engraftment (Nosedá et al., 2015). As a postulated explanation for this paradox, Lin⁻Sca1⁺CD31⁻PDGFR α ⁺SP⁺ CSCs might secrete factors that affect multiple cell types in the heart, including macrophages, during post-injury inflammation. Hence, this PhD thesis hypothesised that the paracrine signals released by Lin⁻Sca1⁺CD31⁻PDGFR α ⁺SP⁺ CSCs could modulate BMDMs toward an anti-inflammatory/reparative macrophage phenotype.

This PhD thesis investigated the complexity of CSC-driven-M ϕ phenotypes by designing an *in vitro* experimental system to produce pro- and anti-inflammatory macrophages as the extreme benchmarks and then gauged the CSC-driven-M ϕ against these. Complementary approaches were used to investigate the generated

populations' immunophenotype, single-cell gene signatures, secretome and functional activity.

CSC CondM disrupts the full activation of the pro-inflammatory macrophage phenotype by promoting a unique and distinctive anti-inflammatory macrophage phenotype which, while sharing some characteristics with M2a and M2b, was also distinguishable from them, indicating the unique stimulation pattern of CSCs (Gordon, 2002; Mantovani et al., 2004; Martinez et al., 2008; Scotton et al., 2005; Stein et al., 1992). These CSC-driven-M ϕ expressed high levels of the M2 surface markers, CX3CR1 and CD206, and the anti-inflammatory genes *Arg1*, *Angptl2*, *Mrc1*, *Igf1* and *Il1rl1*. Demonstrating that CSC CondM promotes an anti-inflammatory signal even in pro-inflammatory stimulation, CSC CondM+LPS+IFN γ -M ϕ exhibits a distinct secretome characterised by a high level of IL-10 expression.

Two independent perturbations designed to inhibit the M-CSF/CSF1R pathway demonstrated that M-CSF is an essential paracrine factor secreted by CSCs that regulates BMDMs' differentiation into macrophages with an anti-inflammatory-like phenotype. However, only a subset of the anti-inflammatory-related genes induced by CSC CondM was blocked, suggesting the importance of one or more additional paracrine factors. Additionally, inhibition of M-CSF led to the conclusion that it induces the expression of IL-10 in CSC CondM+LPS+IFN γ -M ϕ . Finally, the phagocytosis assay showed that CSC CondM improved this *in vitro* surrogate of heart repair, the engulfment of dying CMs via the M-CSF/CSF1R pathway.

In conclusion, CSC-secreted M-CSF induces an anti-inflammatory-like macrophage phenotype. This shift may provide a therapeutic strategy to support post-MI heart repair and regeneration (Frangogiannis, 2008; Lavine et al., 2014). However, more analysis must be conducted by moving to *in vivo* experiments and identifying the additional factors contributing to the full range of CSC CondM's effects on the macrophage transcriptome.

7.1.2 Insight into CSC-driven phenotype

CSC CondM+IL4+IL13-M ϕ upregulate the expression of *Gdf15* and *Mrc1*, encoding CD206. Interestingly, *Mrc1* expression is known to be mediated by GDF15 protein (Bosisio et al., 2002; Dinarello, 1991; Jablonski et al., 2015; Mantovani et al., 2002; Shintani et al., 2016). MRC1/CD206⁺ macrophages regulate inflammation, clearing the blood from inflammatory cytokines while assuming a pro-fibrotic role, characterised by the expression of members of the TGF β superfamily (e.g. TGF β 1) (Bellón et al., 2011). In some settings, such as atherosclerosis, collagen production prompted by MRC1/CD206⁺ macrophages positively impacts the stability of the plaque (Medbury et al., 2013). Despite the scientific case for M-CSF to be essential for the M2-like phenotype, other factors, such as IL-4, IL-13, IL-10, and glucocorticoids, induce subtypes of anti-inflammatory-like macrophages (e.g. M2a, M2b, M2c) (Mantovani et al., 2004). More newly reported factors like IL-38 can mediate this transition and have proven therapeutic potential in myocardial injury (Li et al., 2022). CSC-driven-M ϕ showed both anti-inflammatory and fibrotic features. Due to lack of time, it was

impossible to do more experiments to draw a functional conclusion on the role of CSC-driven-M ϕ in cardiac fibrosis.

7.2 Study limitations and future implications

7.2.1 Model system and assay limitations

This study was carried out using an *in vitro* system, combined with flow cytometry and single-cell qRT-PCR analysis as the main approaches to investigate the macrophage phenotypes induced by the paracrine effects of CSC. There are many advantages to using flow sorting and sc qRT-PCR. Flow cytometry allows for characterising, capturing, selecting, and sorting single cells based on their surface markers. These cells can then be analysed by sc qRT-PCR to identify better co-expression and variation of the gene expression profile in each cell at a relatively fast speed (~ 24 hrs). However, these technologies have limitations (Massaia et al., 2018).

In this study, the main limitation was the selection of which surface and gene markers to use based on the literature as indicators of the pro- and anti-inflammatory-related phenotypes. As extensively reviewed by Massaia and colleagues, several alternative single-cell technologies do not require choosing what to test in advance (Massaia et al., 2018). Hence, using these other single-cell-based technologies would have been an advantage in conducting an unbiased investigation of macrophage phenotypes that is fully transcriptome-wide.

Single-cell INDEX sorting is a technology based on single-cell flow cytometry that does not require prior knowledge of the surface markers to be used. INDEX sorting allows depositing single cells without reference to their surface markers and analysing them retrospectively. Therefore, INDEX sorting could be used to understand the functions

of macrophages at a deeper level and even identify new surface markers (Busse et al., 2014; Hayashi et al., 2010; Osborne et al., 2015; Penter et al., 2018; Schulte et al., 2015). Introducing INDEX sorting technology into this set of experiments, followed by sc qRT-PCR or the deeper methods below, could be an impartial bridge between the immunophenotype and the gene signature (Penter et al., 2018).

A different approach to studying macrophage gene expression profiles uses scRNA-seq, which sequences the whole transcriptome at the single-cell level. The use of scRNA-seq can be considered an explorative resource to highlight new genes related to macrophage phenotypes (Herring et al., 2018; Jaitin et al., 2014; Treutlein et al., 2014; Wilson et al., 2015). Several scRNA-seq experimental pipelines can be used, from SMART-seq2, 10X Genomics to Drop-seq (Massaia et al., 2018). ScRNA-Seq can also be associated with other single-cell technologies, such as ATAC-Seq (Xie et al., 2022; Zhang et al., 2021) or single-cell proteomics (scProteomics) (Woo et al., 2022). ScProteomics, for instance, can identify and quantify low-expressed proteins using cutting-edge technologies, such as ion-mobility-enhanced mass spectrometry acquisition and peptide identification method. However, improving scProteomics sensitivity via enhancing protein/peptide recovery and the resolution of peptide separation will be needed to reach the same depth of the sc RNA-Seq technologies (Woo et al., 2022).

Overall, single-cell technologies are expanding, opening unprecedented opportunities to study deeper biological systems and reveal crucial mechanisms almost invisible in a bulk approach. Therefore, single-cell analysis is currently applied to genomes and

transcriptomes and other 'omics, from proteomics to metabolomics and epigenomics, to study characteristics of macrophage states.

Due to time constraints, future work on using scRNA-seq to analyse macrophage transcripts is not reported in this PhD thesis. Still, it is a current platform in the supervisor's research and grant applications.

7.2.2 Identification of paracrine factors secreted by CSC that work in synergy with M-CSF

This work is based on the paracrine hypothesis that CSCs, rigorously characterised by Nosedá and colleagues, improved cardiac function without cell engraftment (Nosedá et al., 2015). As detailed above, using Nosedá's CSCs was supported by a close match to the reported c-CFU-F as a cardiac MSC equivalent (Chong et al., 2011). These two cell types shared the co-expression of PDGFR α with Sca1, enrichment for many heart-forming transcription factors, and clonogenic and multilineage potential (Chong et al., 2011; Nosedá et al., 2015).

This PhD thesis confirmed that CSCs secreted M-CSF is indispensable for generating a distinct subtype of anti-inflammatory-like macrophage phenotype. M-CSF was essential for many of the effects studied, including phagocytosis of dying CM as the functional readout. However, there is a limitation to consider. CSCs secrete other, partially redundant factors, contributing to this CSC-induced-anti-inflammatory-driven macrophage phenotype. This was most evident in the CSC-induced anti-inflammatory-

related transcriptome in the present study. Thus, it would be interesting to investigate what other factors work alongside M-CSF, including whether their effects are additive, synergistic, or complementary.

Future experiments could identify which other potential paracrine factors could interact with M-CSF in the macrophage phenotype. Bulk and single-cell RNA-seq could predict candidate paracrine factors and potential ligand-receptor interactions with macrophages. At the same time, cytokine array screening and mass spectrometry, including single-cell methods, can be used to identify the enrichment of a mix of cytokines, chemokines, and antagonists in the secretome of CSC.

7.2.3 Therapeutic benefits of translation

The data provide a framework for developing a CSC-secreted M-CSF protocol to induce therapeutic anti-inflammatory macrophages for clinical use to enhance cardiac regeneration and tissue repair. The present results suggest that the anti-inflammatory-like macrophage phenotype generated by CSCs could potentially contribute to heart repair and regeneration. However, due to the lack of time, it was impossible to explore whether the CSC-secreted M-CSF could induce an anti-inflammatory-like macrophage phenotype *in vivo* and, if so, what is the net effect of disrupting this circuit on cardiac structure and function.

Scientifically, accessible and better-characterised BMDMs were used as a first step towards understanding the phenotypic modulation of cardiac-resident macrophages.

It would be necessary to rigorously verify the conclusion of this study with macrophages taken from the heart itself. Furthermore, an exciting approach to creating the basis for a pre-clinical animal model would be generating a lineage-restricted and drug-inducible KO mouse line, where *Csf1r* is ablated in monocytes and macrophages. After MI induction, using I/R injury in genetically modified mice, it would be possible to measure the damage in an environment where other aspects of the inflammatory response are still present. This would avoid less accurate and cruder macrophage-depletion experiments, such as clodronate, and the inherent limitations of pharmacological inhibition of CSF1R (Leblond et al., 2015). Examples of a genetic dissection to probe the role of cytokines and chemokines in myocardial infarction include Feng and colleagues' work allowed to identify an alternative way to suppress inflammation post-MI via promoting recruitment of Treg following inhibition of CCL17 in CCR2⁺ macrophages and DCs (Feng et al., 2022). Cardiac inflammation and consequent HF were also attenuated by deleting the IL-17A signalling pathway in cardiac Sca1⁺ fibroblast (Chen et al., 2018). In parallel, and of more immediate translational relevance, another interesting experiment would include in this experimental setting the administration of M-CSF within the first 24 hours to see whether this factor could rescue the adverse effects caused by MI (Okazaki et al., 2007).

Future studies need to be conducted to find a better translation path. M-CSF alone, or in combination with other factors secreted by CSCs, could be administrated to the heart systemically. A potential niche application is the administration of M-CSF using tissue engineering strategies via patches, scaffolds (Peña et al., 2018) or injectable hydrogels, which are adaptable to a minimally invasive approach (Fomby et al., 2010;

Hasan et al., 2015; Tous et al., 2011). The use of tissue engineering strategies has recently become very important because they offer the possibility of delivering the beneficial factor in an immediate, slow and constant release during MI. Considering that the M-CSF modulates the post-MI immune response, it is also essential to optimise the time of the application to enhance its beneficial effect. Interestingly, G-CSF (Achilli et al., 2019) and other cytokines, like the IL-6 receptor antagonist, tocilizumab (Kleveland et al., 2016), have been used in clinical trials; however, M-CSF and any other anti-inflammatory stimuli have been tested yet.

7.3 Conclusive summary

In conclusion, this PhD thesis demonstrated that CSC-secreted M-CSF is essential as a paracrine factor that induces an anti-inflammatory-like macrophage phenotype. First, CSC CondM-driven macrophages have a distinct anti-inflammatory like immunophenotype, defined as F4/80⁺CD11b⁺CX3CR1⁺CD206⁺. Secondly, they also have an anti-inflammatory and pro-fibrotic gene signature based on the induction of *Arg1*, *Angpt2*, *Igf1*, *Il1rl1*, *Mrc1* and *Gdf15*. Finally, they exhibit improved phagocytosis of dying CM, dependent on the M-CSF/CSF1R pathway (Fig. 7.1).

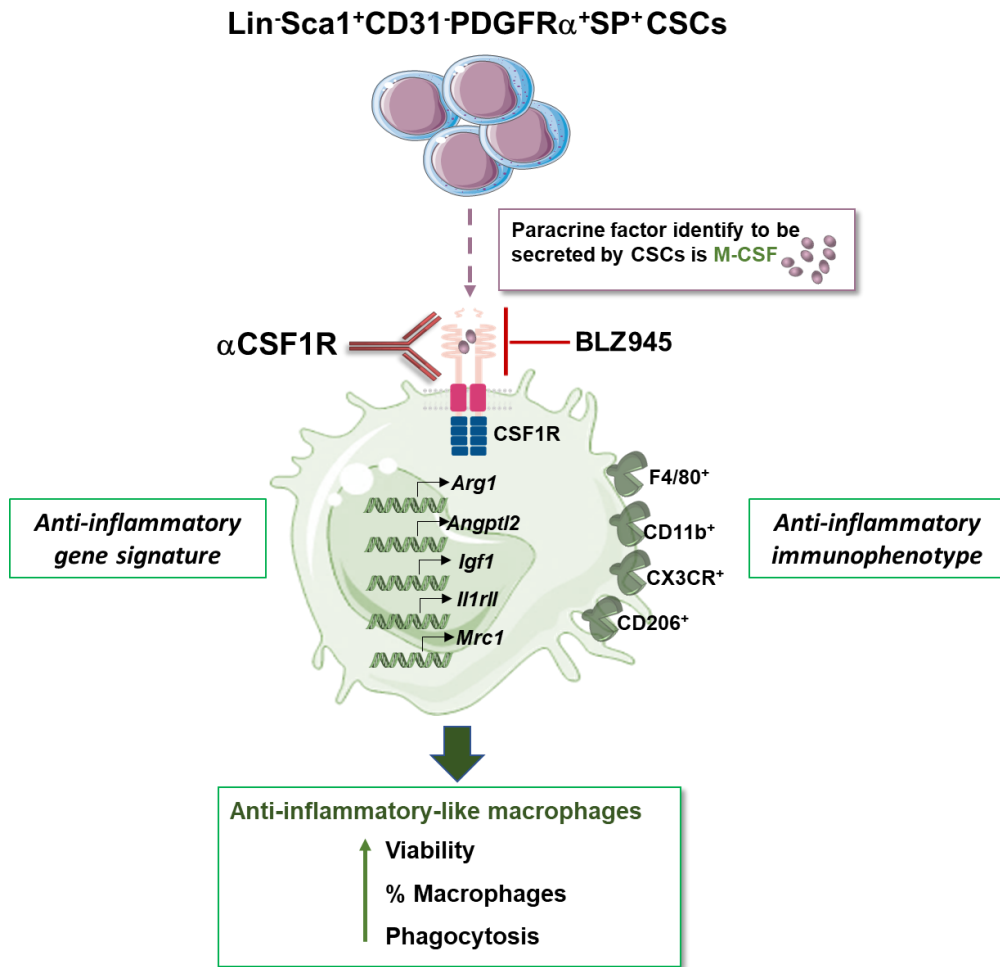


Figure 7.1 Conclusive summary

CSC-secreted M-CSF improved BMDMs' viability, differentiation into an anti-inflammatory like macrophage phenotype based on high levels of expression of surface markers F4/80, CD11b, CX3CR1, and CD206, and the gene signature (*Arg1*, *Angpt2*, *Igf1*, *Il1r1l*, *Mrc1*), and enhanced phagocytosis capacity.

References

- Abdolmaleki, F., Farahani, N., Hayat, S. M. G., Pirro, M., Bianconi, V., Barreto, G. E., & Sahebkar, A. (2018). The role of efferocytosis in autoimmune diseases. *Front. Immunol*, *9*, 1–13.
- Abe, M., Shintani, Y., Eto, Y., Harada, K., Kosaka, M., & Matsumoto, T. (2002). Potent induction of activin A secretion from monocytes and bone marrow stromal fibroblasts by cognate interaction with activated T cells. *J. Leukoc. Biol.*, *72*, 347–352.
- Achilli, F., Pontone, G., Bassetti, B., Squadroni, L., Campodonico, J., Corrada, E., Facchini, C., Mircoli, L., Esposito, G., Scarpa, D., Pidello, S., Righetti, S., Di Gennaro, F., Guglielmo, M., Muscogiuri, G., Baggiano, A., Limido, A., Lenatti, L., Di Tano, G., Pompilio, G. (2019). G-CSF for extensive STEMI: results from the STEM-AMI OUTCOME CMR Substudy. *Circ. Res.*, *125*, 295–306.
- Adams, J. L., & Czuprynski, C. J. (1994). Mycobacterial cell wall components induce the production of TNF-alpha, IL-1, and IL-6 by bovine monocytes and the murine macrophage cell line RAW 264.7. *Microb.Pathog.*, *16*, 401–411.
- Aguirre, A., Sancho-Martinez, I., & Izpisua Belmonte, J. C. (2013). Reprogramming toward heart regeneration: Stem cells and beyond. *Cell Stem Cell*, *12*, 275–284.
- Akimov, S. S., & Belkin, A. M. (2001). Cell surface tissue transglutaminase is involved in adhesion and migration of monocytic cells on fibronectin. *Blood*, *98*, 1567–1576.
- Akimov, S. S., Krylov, D., Fleischmana, L. F., & Belkin, A. M. (2000). Tissue transglutaminase is an integrin-binding adhesion coreceptor for fibronectin. *JCB*, *148*, 825–838.
- Akira, S (2003). Toll-Like receptor signaling. *J. Biol. Chem.*, *5*(1), 38105–38109.
- Akira, S., Isshiki, H., Sugita, T., Tanabe Kinoshita, O. S., Nishio, Y., Nakajima, T., Hirano, T., & Kishimoto, T. (1990). A nuclear factor for IL-6 expression (NF-IL6) is a member of a C/EBP family. *EMBO J.*, *9*, 1897–1906.
- Ali, H., Braga, L., & Giacca, M. (2020). Cardiac regeneration and remodelling of the cardiomyocyte cytoarchitecture. *FEBS J*, *287*, 417–438.
- Altara, R., Manca, M., Hessel, M. H., Gu, Y., van Vark, L. C., Akkerhuis, K. M., Staessen, J. A., Struijker-Boudier, H. A. J., Booz, G. W., & Blankesteyjn, W. M. (2016). CXCL10 is a circulating inflammatory marker in patients with advanced heart failure: a pilot study. *J Cardiovasc Transl Res*, *9*, 302–314.
- Ambrosy, A. P., Fonarow, G. C., Butler, J., & Al., E. (2014). The global health and economic burden of hospitalizations for heart failure: Lessons learned from hospitalized heart failure registries. *J Am Coll Cardiol.*, *63*, 1123–1133.
- Anderson, C. F., & Mosser, D. M. (2002). A novel phenotype for an activated macrophage: the type 2 activated macrophage. *J. Leukoc. Biol.*, *72*, 101–106.
- Anderson, J. L., & Morrow, D. A. (2017). Acute Myocardial Infarction. *N Engl J Med*, *376*, 2053–2064.
- Anker, S. D., Volterrani, M., Pflaum, C. D., Strasburger, C. J., Osterziel, K. J., Doehner, W., Ranke, M. B., Poole-Wilson, P. A., Giustina, A., Dietz, R., & Coats, A. J. S. (2001). Acquired growth hormone resistance in patients with chronic heart failure: Implications for therapy with growth hormone. *J Am Coll Cardiol*, *38*, 443–452.
- Aouadi, M., Tesz, G. J., Nicoloro, S. M., Wang, M., Chouinard, M., Soto, E., Ostroff, G. R., & Czech, M. P. (2010). Orally delivered siRNA targeting macrophage Map4k4 suppresses systemic inflammation. *Nature*, *458*, 1180–1184.
- Arnold, L., Henry, A., Poron, F., Baba-amer, Y., Rooijen, N. Van, Plonquet, A., Gherardi, R. K., & Chazaud, B. (2007). Inflammatory monocytes recruited after skeletal muscle injury switch into antiinflammatory macrophages to support myogenesis. *J Exp Med*. *204*, 1057–1069.

- Arslan, F., de Kleijn, D. P., & Pasterkamp, G. (2011). Innate immune signaling in cardiac ischemia. *Nat. Rev. Cardiol.*, *8*, 292–300.
- Arslan, F., Smeets, M. B., O'Neill, L. a J., Keogh, B., McGuirk, P., Timmers, L., Tersteeg, C., Hoefler, I. E., Doevendans, P. a., Pasterkamp, G., & De Kleijn, D. P. V. (2010). Myocardial ischemia/reperfusion injury is mediated by leukocytic toll-like receptor-2 and reduced by systemic administration of a novel anti-toll-like receptor-2 antibody. *Circulation* *121*, 80–90.
- Asakura, A., & Rudnicki, M. A. (2002). Side population cells from diverse adult tissues are capable of in vitro hematopoietic differentiation. *Exp. Hematol.*, *30*, 1339–1345.
- Asare, P. F., Roscioli, E., Hurtado, P. R., Tran, H. B., Mah, C. Y., & Hodge, S. (2020). LC3-Associated Phagocytosis (LAP): A potentially influential mediator of efferocytosis-related tumor progression and aggressiveness. *Front. Oncol.*, *10*, 1–14.
- Augustin, H. G., & Koh, G. Y. (2017). Organotypic vasculature: From descriptive heterogeneity to functional pathophysiology. *Science*, *357*, 771.
- Aurora, A. B., & Olson, E. N. (2014). Immune modulation of stem cells and regeneration. *Cell Stem Cell*, *15*, 14–25.
- Aurora, A. B., Porrello, E. R., Tan, W., Mahmoud, A. I., Hill, J. A., Bassel-Duby, R., Sadek, H. A., & Olson, E. N. (2014). Macrophages are required for neonatal heart regeneration. *J. Clin. Investig.*, *124*, 1382–1392.
- Bailey, B., Fransioli, J., Gude, N. A., Alvarez, R., Zhan, X., Gustafsson, Å. B., & Sussman, M. A. (2012). Sca-1 knockout impairs myocardial and cardiac progenitor cell function. *Circ. Res.*, *111*, 750–760.
- Balsam, L. B., Wagers, A. J., Christensen, J. L., Kofidis, T., Weissmann, I. L., & Robbins, R. C. (2004). Haematopoietic stem cells adopt mature haematopoietic fates in ischaemic myocardium. *Nature*, *428*, 668–673.
- Banerjee, M. N., Bolli, R., & Hare, J. M. (2018). Clinical studies of cell therapy in cardiovascular medicine recent developments and future directions. *Circ. Res.*, *123*, 266–287.
- Barile, L., Lionetti, V., Cervio, E., Matteucci, M., Gherghiceanu, M., Popescu, L. M., Torre, T., Siclari, F., Moccetti, T., & Vassalli, G. (2014). Extracellular vesicles from human cardiac progenitor cells inhibit cardiomyocyte apoptosis and improve cardiac function after myocardial infarction. *Cardiovasc. Res.*, *103*, 530–541.
- Bartocci, A., Mastrogiannis, D. S., Migliorati, G., Stockert, R. J., Wolkoff, A. W., & Stanley, E. R. (1987). Macrophages specifically regulate the concentration of their own growth factor in the circulation. *PNAS*, *84*, 6179–6183.
- Bashir, S., Sharma, Y., Elahi, A., & Khan, F. (2016). Macrophage polarization: the link between inflammation and related diseases. *Inflamm. Res.*, *65*, 1–11.
- Bauer, R. J., Gibbons, J. A., Bell, D. P., Luo, Z. P., & Young, J. D. (1994). Nonlinear pharmacokinetics of recombinant human macrophage colony-stimulating factor (M-CSF) in rats. *J. Pharmacol. Exp. Ther.*, *268*, 152–158.
- Becker, L., Liu, N. C., Averill, M. M., Yuan, W., Pamir, N., Peng, Y., Irwin, A. D., Fu, X., Bornfeldt, K. E., & Heinecke, J. W. (2012). Unique proteomic signatures distinguish macrophages and dendritic cells. *PLoS ONE*, *7*, 1–12.
- Becker, T., Ebsen, M., & Christoph, R. (2014). Tumor-associated macrophages exhibit pro- and anti-inflammatory properties by which they impact on pancreatic tumorigenesis. *Int. J. Cancer.*, *135*, 843–861.
- Beckmann, N., Giorgetti, E., Neuhaus, A., Zurbrugg, S., Accart, N., Smith, P., Perdoux, J., Perrot, L., Nash, M., Desrayaud, S., Wipfli, P., Friauff, W., & Shimshek, D. R. (2018). Brain region-specific

- enhancement of remyelination and prevention of demyelination by the CSF1R kinase inhibitor BLZ945. *Acta Neuropathol. Commun.*, 6, 9.
- Behfar, A., Crespo-Diaz, R., Terzic, A., & Gersh, B. J. (2014). Cell therapy for cardiac repair-lessons from clinical trials. *Nat. Rev. Cardiol.*, 11, 232–246.
- Bellón, T., Martínez, V., Lucendo, B., Del Peso, G., Castro, M. J., Aroeira, L. S., Rodríguez-Sanz, A., Ossorio, M., Sánchez-Villanueva, R., Selgas, R., & Bajo, M. A. (2011). Alternative activation of macrophages in human peritoneum: Implications for peritoneal fibrosis. *Nephrol. Dial. Transplant.* 26, 2995–3005.
- Beltrami, A., Urbanek, K., Kajstura, J., Yan, S., Finato, N., Bussani, R., Nadal-Ginard, B., Silvestri, F., Leri, A., Beltrami, C., & Anversa, P. (2001). Evidence that human cardiac myocytes divide after myocardial infarction. *NEJM*, 344, 1750-1757.
- Beltrami, Barlucchi, L., Torella, D., Baker, M., Limana, F., Chimenti, S., Kasahara, H., Rota, M., Musso, E., Urbanek, K., Leri, A., Kajstura, J., & Nadal-Ginard, B. (2003). Adult cardiac stem cells are multipotent and support myocardial regeneration. *Cell*, 114, 763–776.
- Ben-Mordechai, T., Palevski, D., Glucksam-Galnoy, Y., Elron-Gross, I., Margalit, R., & Leor, J. (2015). Targeting macrophage subsets for infarct repair. *JCPT*, 20, 36–51
- Bendall, S. C., Davis, K. L., Amir, E. A. D., Tadmor, M. D., Simonds, E. F., Chen, T. J., Shenfeld, D. K., Nolan, G. P., & Pe'Er, D. (2014). Single-cell trajectory detection uncovers progression and regulatory coordination in human b cell development. *Cell*, 157, 714–725.
- Bengtsson, M., Ståhlberg, A., Rorsman, P., & Kubista, M. (2005). Gene expression profiling in single cells from the pancreatic islets of Langerhans reveals lognormal distribution of mRNA levels. *Genome Res.* 15, 1388–1392.
- Benjamin, E. J., Muntner, P., Alonso, A., Bittencourt, M. S., Callaway, C. W., Carson, A. P., Chamberlain, A. M., Chang, A. R., Cheng, S., Das, S. R., Delling, F. N., Djousse, L., Elkind, M. S. V., Ferguson, J. F., Fornage, M., Jordan, L. C., Khan, S. S., Kissela, B. M., Knutson, K. L., Virani, S. S. (2019). Heart disease and stroke statistics-2019 update: a report from the american heart association. *Circulation*, 139, e56-e528.
- Bergmann, O., Bhardwaj, R. D., Bernard, S., Zdunek, S., Walsh, S., Zupicich, J., Alkass, K., Buchholz, B. a, Jovinge, S., Frisé, J., Bergmann, O., Bhardwaj, R. D., Bernard, S., Zdunek, S., Barnabi-heider, F., Walsh, S., Zupicich, J., Alkass, K., Buchholz, B. a, ... Frisnt, J. (2009). Evidence for cardiomyocyte renewal in humans. *Science*, 324, 98–102.
- Bergmann, O., Zdunek, S., Alkass, K., Druid, H., Bernard, S., & Frisé, J. (2011). Identification of cardiomyocyte nuclei and assessment of ploidy for the analysis of cell turnover. *Exp. Cell Res.* 317(2), 188–194.
- Bergmann, O., Zdunek, S., Felker, A., Salehpour, M., Alkass, K., Bernard, S., Sjöström, S. L., Szewczykowska, M., Jackowska, T., Dos Remedios, C., Malm, T., Andrä, M., Jashari, R., Nyengaard, J. R., Possnert, G., Jovinge, S., Druid, H., & Frisé, J. (2015). Dynamics of cell generation and turnover in the human heart. *Cell*, 161, 1566–1575.
- Biagioli, M., Carino, A., Cipriani, S., Francisci, D., Marchianò, S., Scarpelli, P., Sorcini, D., Zampella, A., & Fiorucci, S. (2017). The bile acid receptor gpbar1 regulates the m1/m2 phenotype of intestinal macrophages and activation of gpbar1 rescues mice from murine colitis. *J. Immunol.*, 199, 718–733.
- Bianchi, M. E. (2007). DAMPs, PAMPs and alarmins: all we need to know about danger. *J. Leukoc. Biol.* 81, 1–5.
- Biswas, S. K., Chittechath, M., Shalova, I. N., & Lim, J. Y. (2012). Macrophage polarization and plasticity in health and disease. *Immunol. Res.*, 53, 11–24.
- Biswas, S. K., & Mantovani, A. (2012). Orchestration of metabolism by macrophages. *Cell Metab.*, 15, 432–437.

- Björndahl, M., Cao, R., Nissen, L. J., Clasper, S., Johnson, L. A., Xue, Y., Zhou, Z., Jackson, D., Hansen, A. J., & Cao, Y. (2005). Insulin-like growth factors 1 and 2 induce lymphangiogenesis in vivo. *Proc. Natl. Acad. Sci. U.S.A.* *102*, 15593–15598.
- Blankenberg, S., & Zeller, T. (2017). Chronic coronary artery disease: a companion to braunwald's heart disease. *Elsevier Sc.*
- Bock-Marquette, I., Saxena, A., White, M. D., Michael DiMaio, J., & Srivastava, D. (2004). Thymosin β 4 activates integrin-linked kinase and promotes cardiac cell migration, survival and cardiac repair. *Nature*, *432*.
- Boehme, S. A., Lio, F. M., Maciejewski-Lenoir, D., Bacon, K. B., & Conlon, P. J. (2000). The chemokine fractalkine inhibits fas-mediated cell death of brain microglia. *J Immunol.* *165*, 397–403.
- Bolli, R., Chugh, A., D'Amario, D., Loughran, J. H., Stoddard, M. F., Ikram, S., Beache, G. M., Wagner, S. G., Leri, A., Hosoda, T., Elmore, J. B., Goihberg, P., Cappetta, D., Solankhi, N. K., Fahsah, I., Rokosh, D. G., Slaughter, M. S., Kajstura, J., & Anversa, P. (2011). Effect of cardiac stem cells in patients with ischemic cardiomyopathy: initial results of the SCIPIO Trial. *Lancet.* *2011*, 1847–1857.
- Bonecchi, R., Facchetti, F., Dusi, S., Luini, W., Lissandrini, D., Simmelink, M., Locati, M., Bernasconi, S., Allavena, P., Brandt, E., Rossi, F., Mantovani, A., & Sozzani, S. (2000). Induction of functional IL-8 receptors by IL-4 and IL-13 in human monocytes. *J Immunol*, *164*, 3862–3869.
- Bonecchi, R., Sozzani, S., Stine, J. T., Luini, W., Amico, G. D., Allavena, P., Chantry, D., Mantovani, A., & Bonecchi, B. R. (1998). Divergent effects of interleukin-4 and interferon- γ on macrophage-derived chemokine production: an amplification circuit of polarized T helper 2 responses. *Blood*, *92*, 2668–2671.
- Bosco, M. C., Puppo, M., Pastorino, S., Mi, Z., Melillo, G., Massazza, S., Rapisarda, A., & Varesio, L. (2004). Hypoxia selectively inhibits monocyte chemoattractant protein-1 production by macrophages. *J Immunol.* *172*, 1681–1690.
- Bosisio, D., Polentarutti, N., Sironi, M., Bernasconi, S., Miyake, K., Webb, G. R., Martin, M. U., Mantovani, A., & Muzio, M. (2002). Stimulation of toll-like receptor 4 expression in human mononuclear phagocytes by interferon- γ : A molecular basis for priming and synergism with bacterial lipopolysaccharide. *Blood*, *99*, 3427–3431.
- Boyer, S. W., Schroeder, A. V., Smith-Berdan, S., & Forsberg, E. C. (2011). All hematopoietic cells develop from hematopoietic stem cells through Flk2/Flt3-positive progenitor cells. *Cell Stem Cell*, *9*, 64–73.
- Bradfute, S. B., Graubert, T. A., & Goodell, M. A. (2005). Roles of Sca-1 in hematopoietic stem/progenitor cell function. *Exp Hematol*, *33*, 836–843.
- Brand, K., Fowler, B. J., Edgington, T. S., & Mackman, N. (1991). Tissue factor mRNA in THP-1 monocytic cells is regulated at both transcriptional and posttranscriptional levels in response to lipopolysaccharide. *Mol. Cell. Bio.*, *11*, 4732–4738.
- Braunwald, E. (2015). The war against heart failure: The Lancet lecture. *The Lancet*, *385*, 812–824.
- Bronte, V., & Zanovello, P. (2005). Regulation of immune responses by L-arginine metabolism. *Nat Rev Immunol*, *5*, 641–654.
- Bruce, A. C., Kelly-Goss, M. R., Heuslein, J. L., Meisner, J. K., Price, R. J., & Peirce, S. M. (2014). Monocytes are recruited from venules during arteriogenesis in the murine spinotrapezius ligation model. *ATVB*, *34*, 2012–2022.
- Bryant-Hudson, K. M., Gurung, H. R., Zheng, M., & Carr, D. J. J. (2014). Tumor necrosis factor alpha and interleukin-6 facilitate corneal lymphangiogenesis in response to herpes simplex virus 1 infection. *J. Virol.*, *88*, 14451–14457.

- Buenrostro, J. D., Corces, M. R., Lareau, C. A., Wu, B., Schep, A. N., Aryee, M. J., Majeti, R., Chang, H. Y., & Greenleaf, W. J. (2018). Integrated single-cell analysis maps the continuous regulatory landscape of human hematopoietic differentiation. *Cell*, *173*, 1535-1548.
- Buerke, M., Murohara, T., Skurk, C., Nuss, C., Tomaselli, K., & Lefer, A. M. (1995). Cardioprotective effect of insulin-like growth factor I in myocardial ischemia followed by reperfusion. *PNAS*, *92*, 8031–8035.
- Bui, A. L., Horwich, T. B., & Fonarow, G. C. (2011). Epidemiology and risk profile of heart failure. *Nat. Rev. Cardiol.*, *8*, 1–20.
- Bukowski, R. M., Budd, G. T., Gibbons, J. A., Bauer, R. J., Childs, A., Finke, J., Antal, J., Tuason, L., Lorenzi, V., & McLain, D. (1994). Phase I trial of subcutaneous recombinant macrophage colony-stimulating factor: clinical and immunomodulatory effects. *J Clin Oncol*, *12*, 97–106.
- Burchfield, J. S., Xie, M., & Hill, J. A. (2013). Pathological ventricular remodeling: mechanisms: Part 1 of 2. *Circulation*, *128*, 388–400.
- Burgess, M., Wicks, K., Gardasevic, M., & Mace, K. A. (2019). CX3CR1 expression identifies distinct macrophage populations that contribute differentially to inflammation and repair. *ImmunoHorizons*, *3*, 262–273.
- Burns, C. J., & Wilks, A. F. (2011). c-FMS inhibitors: a patent review. *Expert Opin Ther Pat*, *21*, 147-165.
- Busse, C. E., Czogiel, I., Braun, P., Arndt, P. F., & Wardemann, H. (2014). Single-cell based high-throughput sequencing of full-length immunoglobulin heavy and light chain genes. *EJI*, *44*, 597–603.
- Caescu, C. I., Guo, X., Tesfa, L., Bhagat, T. D., Verma, A., Zheng, D., & Stanley, E. R. (2015). Colony stimulating factor-1 receptor signaling networks inhibit mouse macrophage inflammatory responses by induction of microRNA-21. *Blood*, *125*, e1–e13.
- Cahill, T. J., Choudhury, R. P., & Riley, P. R. (2017). Heart regeneration and repair after myocardial infarction: Translational opportunities for novel therapeutics. *Nat. Rev. Drug Discov.*, *16*, 699–717.
- Cai, C.-L., Liang, X., Shi, Y., Chu, P.-H., Pfaff, S. L., Chen, J., & Sylvania, E. (2003). *Isl1* identifies a cardiac progenitor population that proliferates prior to differentiation and contributes a majority of cells to the heart. *Dev. Cell.*, *5*, 877–889.
- Campbell, I. K., Rich, M. J., Bischof, R. J., & Hamilton, J. A. (2000). The colony-stimulating factors and collagen-induced arthritis: exacerbation of disease by M-CSF and G-CSF and requirement for endogenous M-CSF. *J Leu Biol*, *68*, 144–150.
- Campderrós, L., Moure, R., Cairó, M., Gavalda-Navarro, A., Quesada-López, T., Cereijo, R., Giralt, M., Villarroya, J., & Villarroya, F. (2019). Brown adipocytes secrete GDF15 in response to thermogenic activation. *Obesity*, *27*, 1606–1616.
- Cannarile, M. A., Weisser, M., Jacob, W., Jegg, A. M., Ries, C. H., & Rüttinger, D. (2017). Colony-stimulating factor 1 receptor (CSF1R) inhibitors in cancer therapy. *JITC*, *5*, 1–13.
- Cano-Martínez, A., Vargas-González, A., Guarnier-Lans, V., Prado-Zayago, E., León-Olea, M., & Nieto-Lima, B. (2010). Functional and structural regeneration in the axolotl heart (*Ambystoma mexicanum*) after partial ventricular amputation. *Arch Cardiol Mex*, *80*, 79–86.
- Cao, S., Liu, J., Chesi, M., Bergsagel, P. L., Ho, I.-C., Donnelly, R. P., & Ma, X. (2002). Differential regulation of IL-12 and IL-10 gene expression in macrophages by the basic leucine zipper transcription factor c-maf fibrosarcoma. *J. Immunol.*, *169*, 5715–5725.
- Caplice, N. M., DeVoe, M. C., Choi, J., Dahly, D., Murphy, T., Spitzer, E., Van Geuns, R., Maher, M. M., Tuite, D., Kerins, D. M., Ali, M. T., Kalyar, I., Fahy, E. F., Khider, W., Kelly, P., Kearney, P. P., Curtin, R. J., O’Shea, C., Vaughan, C. J., McFadden, E. P. (2018). Randomized placebo controlled trial evaluating the safety and efficacy of single low-dose intracoronary insulin-like growth factor

- following percutaneous coronary intervention in acute myocardial infarction (RESUS-AMI). *Am. Heart J.* 200, 110–117.
- Cebon, J., Layton, J. E., Maher, D., & Morstyn, G. (1994). Endogenous haemopoietic growth factors in neutropenia and infection. *Br. J. Haematol.*, 86(2), 265–274.
- Cekic, C., & Linden, J. (2016). Purinergic regulation of the immune system. *Nat. Rev. Immunol.* 16(3), 177–192.
- Cenci, S., Weitzmann, M. N., Gentile, M. A., Aisa, M. C., & Pacifici, R. (2000). M-CSF neutralization and Egr-1 deficiency prevent ovariectomy-induced bone loss. *J. Clin. Investig.*, 105(9), 1279–1287.
- Chao, W., Matsui, T., Novikov, M. S., Tao, J., Li, L., Liu, H., Ahn, Y., & Rosenzweig, A. (2003). Strategic advantages of insulin-like growth factor-I expression for cardioprotection. *J. Gene Med.*, 5(4), 277–286.
- Cheers, C., Haigh, A. M., Kelso, A., Metcalf, D., Stanley, E. R., & Young, A. M. (1988). Production of colony-stimulating factors (CSFs) during infection: Separate determinations of macrophage-, granulocyte-, granulocyte-macrophage-, and multi-CSFs. *Infect Immun.* 56(1), 247–251.
- Chen, G., Bracamonte-Baran, W., Diny, N. L., Hou, X., Talor, M. V., Fu, K., Liu, Y., Davogustto, G., Vasquez, H., Taegtmeier, H., Frazier, O. H., Waisman, A., Conway, S. J., Wan, F., & Čiháková, D. (2018). Sca-1 + cardiac fibroblasts promote development of heart failure. *Eur. J. Immunol.* 8, 1522–1538.
- Chen, H. J., Li Yim, A. Y. F., Griffith, G. R., de Jonge, W. J., Mannens, M. M. A. M., Ferrero, E., Henneman, P., & de Winther, M. P. J. (2019). Meta-analysis of in vitro-differentiated macrophages identifies transcriptomic signatures that classify disease macrophages in vivo. *Front. Immunol.* 10, 1–15.
- Chen, S., Yang, J., Wei, Y., & Wei, X. (2020). Epigenetic regulation of macrophages: from homeostasis maintenance to host defense. *Cell. Mol. Immunol.* 17, 36–49.
- Chien, K. R., Frisén, J., Fritsche-Danielson, R., Melton, D. A., Murry, C. E., & Weissman, I. L. (2019). Regenerating the field of cardiovascular cell therapy. *Nat. Biotechnol.*, 37, 232–237.
- Chihara, T., Suzu, S., Hassan, R., Chutiwitoonchai, N., Hiyoshi, M., Motoyoshi, K., Kimura, F., & Okada, S. (2010). IL-34 and M-CSF share the receptor Fms but are not identical in biological activity and signal activation. *Cell Death Differ.* 17, 1917–1927.
- Chimenti, I., Smith, R. R., Li, T.-S. S., Gerstenblith, G., Messina, E., Giacomello, A., & Marbán, E. (2010). Relative roles of direct regeneration versus paracrine effects of human cardiosphere-derived cells transplanted into infarcted mice. *Circ. Res.*, 5, 971–980.
- Chitu, V., & Stanley, E. R. (2006). Colony-stimulating factor-1 in immunity and inflammation. *Curr. Opin. Immunol.* 18, 39–48.
- Chometon, T. Q., Da Silva Siqueira, M., Sant'anna, J. C., Almeida, M. R., Gandini, M., De Almeida Nogueira, A. C. M., & Antas, P. R. Z. (2020). A protocol for rapid monocyte isolation and generation of singular human monocytederived dendritic cells. *PLoS ONE*, 15, 1–16.
- Chong, J. J. H., Chandrakanthan, V., Xaymardan, M., Asli, N. S., Li, J., Ahmed, I., Heffernan, C., Menon, M. K., Scarlett, C. J., Rashidianfar, A., Biben, C., Zoellner, H., Colvin, E. K., Pimanda, J. E., Biankin, A. V., Zhou, B., Pu, W. T., Prall, O. W. J., & Harvey, R. P. (2011). Adult cardiac-resident MSC-like stem cells with a proepicardial origin. *Cell Stem Cell*, 9, 527–540.
- Chong, J. J. H., Forte, E., & Harvey, R. P. (2014). Developmental origins and lineage descendants of endogenous adult cardiac progenitor cells. *Stem Cell Res.*, 13, 592–614.
- Chong, S. Z., & Angeli, V. (2019). Cavity macrophages get to the heart of the issue. *Immunity*, 51, 7–9.

- Chuang, H.-C., Sheu, W. H.-H., Lin, Y.-T., Tsai, C.-Y., Yang, C.-Y., Cheng, Y.-J., Huang, P.-Y., Li, J.-P., Chiu, L.-L., Wang, X., Xie, M., Schneider, M. D., & Tan, T.-H. (2014). HGK/MAP4K4 deficiency induces TRAF2 stabilization and Th17 differentiation leading to insulin resistance. *Nat. Commun.*, *5*, 4602.
- Chung, J., Koyama, T., Ohsawa, M., Shibamiya, A., Hoshi, A., & Hirosawa, S. (2007). 1,25(OH)(2)D(3) blocks TNF-induced monocytic tissue factor expression by inhibition of transcription factors AP-1 and NF-kappaB. *Lab. Invest.*, *87*, 540–547.
- Citro, R., Rigo, F., D'Andrea, A., Ciampi, Q., Parodi, G., Provenza, G., Piccolo, R., Mirra, M., Zito, C., Giudice, R., Patella, M. M., Antonini-Canterin, F., Bossone, E., Piscione, F., & Salerno-Uriarte, J. (2014). Echocardiographic correlates of acute heart failure, cardiogenic shock, and in-hospital mortality in tako-tsubo cardiomyopathy. *JACC: Cardiovas Imaging* *7*, 119–129.
- Claycomb, W. C. (1992). Control of cardiac muscle cell division. *Trends Cardiovasc. Med.* *2*, 231–236.
- Cole, D. J., Sanda, M. G., Yang, J. C., Schwartzentruber, D. J., Weber, J., Ettinghausen, S. E., Pockaj, B. A., Kim, H. I., Levin, R. D., Pogrebniak, H. W., Balkissoon, J., Fenton, R. M., DeBarge, L. R., Kaye, J., Rosenberg, S. A., & Parkinson, D. R. (1994). Phase I trial of recombinant human macrophage colony-stimulating factor administered by continuous intravenous infusion in patients with metastatic cancer. *JNCI*, *86*, 39–45.
- Constantinou, C., Miranda, A. M. A., Chaves, P., Bellahcene, M., Massaia, A., Cheng, K., Samari, S., Rothery, S. M., Chandler, A. M., Schwarz, R. P., Harding, S. E., Punjabi, P., Schneider, M., & Nosedà, M. (2020). Human pluripotent stem cell-derived cardiomyocytes as a target platform for paracrine protection by cardiac mesenchymal stromal cells. *Sci. Rep.*, 1–18.
- Conway, J. G., McDonald, B., Parham, J., Keith, B., Rusnak, D. W., Shaw, E., Jansen, M., Lin, P., Payne, A., Crosby, R. M., Johnson, J. H., Frick, L., Lin, M. H. J., Depee, S., Tadepalli, S., Votta, B., James, I., Fuller, K., Chambers, T. J., ... Hutchins, J. T. (2005). Inhibition of colony-stimulating-factor-1 signaling in vivo with the orally bioavailable cFMS kinase inhibitor GW2580. *PNAS*, *102*, 16078–16083.
- Conway, J. G., Pink, H., Bergquist, M. L., Han, B., Depee, S., Tadepalli, S., Lin, P., Crumrine, R. C., Binz, J., Clark, R. L., Selph, J. L., Stimpson, S. A., Hutchins, J. T., Chamberlain, S. D., & Brodie, T. A. (2008). Effects of the cFMS kinase inhibitor 5-(3-methoxy-4-((4-methoxybenzyl)oxy)benzyl)pyrimidine-2,4-diamine (GW2580) in normal and arthritic rats? *J. Pharmacol. Exp. Ther.*, *326*, 41–50.
- Cook, C., Cole, G., Asaria, P., Jabbour, R., & Francis, D. P. (2014). The annual global economic burden of heart failure. *Int. J. Cardiol.*, *171*, 368–376.
- Corbera-Bellalta, M., Planas-Rigol, E., Lozano, E., Terrades-García, N., Alba, M. A., Prieto-González, S., García-Martínez, A., Albero, R., Enjuanes, A., Espígol-Frigolé, G., Hernández-Rodríguez, J., Roux-Lombard, P., Ferlin, W. G., Dayer, J. M., Kosco-Vilbois, M. H., & Cid, M. C. (2016). Blocking interferon γ reduces expression of chemokines CXCL9, CXCL10 and CXCL11 and decreases macrophage infiltration in ex vivo cultured arteries from patients with giant cell arteritis. *ARD*, *75*, 1177–1186.
- Crossman, D. C., Carr, D. P., Tuddenham, E. G., Pearson, J. D., & McVey, J. H. (1990). The regulation of tissue factor mRNA in human endothelial cells in response to endotoxin or phorbol ester. *JBC*, *265*, 9782–9787.
- Crowther, M., Brown, N. J., Bishop, E. T., & Lewis, C. E. (2001). Microenvironmental influence on macrophage regulation of angiogenesis in wounds and malignant tumors. *J. Leukoc. Biol.*, *70*, 478–490.
- Crozat, K., Guiton, R., Guilliams, M., Henri, S., Baranek, T., Schwartz-Cornil, I., Malissen, B., & Dalod, M. (2010). Comparative genomics as a tool to reveal functional equivalences between human and mouse dendritic cell subsets. *Immunol. Rev.*, *234*, 177–198.

- Curado, S., Anderson, R. M., Jungblut, B., Mumm, J., Schroeter, E., & Stainier, D. Y. R. (2007). Conditional targeted cell ablation in zebrafish: A new tool for regeneration studies. *Dev. Dyn.*, *236*, 1025–1035.
- Cursiefen, C., Maruyama, K., Bock, F., Saban, D., Sadrai, Z., Lawler, J., Dana, R., & Masli, S. (2011). Thrombospondin 1 inhibits inflammatory lymphangiogenesis by CD36 ligation on monocytes. *J Exp Med*, *208*, 1083–1092.
- Dai, X. M., Ryan, G. R., Hapel, A. J., Dominguez, M. G., Russell, R. G., Kapp, S., Sylvestre, V., & Stanley, E. R. (2002). Targeted disruption of the mouse colony-stimulating factor 1 receptor gene results in osteopetrosis, mononuclear phagocyte deficiency, increased primitive progenitor cell frequencies, and reproductive defects. *Blood*, *99*, 111–120.
- Dalerba, P., Kalisky, T., Sahoo, D., Rajendran, P. S., Rothenberg, M. E., Leyrat, A. A., Sim, S., Okamoto, J., Johnston, D. M., Qian, D., Zabala, M., Bueno, J., Neff, N. F., Wang, J., Shelton, A. A., Visser, B., Hisamori, S., Shimono, Y., Van De Wetering, M., Quake, S. R. (2011). Single-cell dissection of transcriptional heterogeneity in human colon tumors. *Nat. Biotechnol.*, *29*, 1120–1127.
- Danenberg, H. D., Fishbein, I., Gao, J., Mönkkönen, J., Reich, R., Gati, I., Moerman, E., & Golomb, G. (2002). Macrophage depletion by clodronate-containing liposomes reduces neointimal formation after balloon injury in rats and rabbits. *Circulation*, *106*, 599–605.
- Dark, J. H. (2009). More and better donors for cardiac transplantation. *Eur Heart J*, *30*, 1690–1691.
- Das, P., Lahiri, A., Lahiri, A., & Chakravorty, D. (2010). Modulation of the arginase pathway in the context of microbial pathogenesis: A metabolic enzyme moonlighting as an immune modulator. *PLoS Pathogens*, *6*, e1000899.
- Davies, L. C., Rosas, M., Jenkins, S. J., Liao, C.-T., Scurr, M. J., Brombacher, F., Fraser, D. J., Allen, J. E., Jones, S. a, & Taylor, P. R. (2013). Distinct bone marrow-derived and tissue-resident macrophage lineages proliferate at key stages during inflammation. *Nat Commun*, *4*, 1886.
- de Couto, G. (2019). Macrophages in cardiac repair: Environmental cues and therapeutic strategies. *Exp. Mol. Med.*, *51*, 159.
- de Couto, G., Liu, W., Tseliou, E., Sun, B., Makkar, N., Kanazawa, H., Arditì, M., & Marbn, E. (2015). Macrophages mediate cardioprotective cellular postconditioning in acute myocardial infarction. *J. Clin. Investig.*, *125*, 3147–3162.
- De Filippo, K., Henderson, R. B., Laschinger, M., & Hogg, N. (2008). Neutrophil chemokines KC and Macrophage-inflammatory protein-2 are newly synthesized by tissue macrophages using distinct TLR signaling pathways. *J. Immunol. Res.*, *180*, 4308–4315.
- DeBerge, M., Yeap, X. Y., Dehn, S., Zhang, S., Grigoryeva, L., Misener, S., Procissi, D., Zhou, X., Lee, D. C., Muller, W. A., Luo, X., Rothlin, C., Tabas, I., & Thorp, E. B. (2017). MerTK cleavage on resident cardiac macrophages compromises repair after myocardial ischemia reperfusion injury. *Circ. Res.*, *121*, 930–940.
- DeLaughter, D. M., Bick, A. G., Wakimoto, H., McKean, D., Gorham, J. M., Kathiriya, I. S., Hinson, J. T., Homsy, J., Gray, J., Pu, W., Bruneau, B. G., Seidman, J. G., & Seidman, C. E. (2016). Single-cell resolution of temporal gene expression during heart development. *Dev. Cell*, *39*, 480–490.
- Delneste, Y., Charbonnier, P., Herbault, N., Magistrelli, G., Caron, G., Bonnefoy, J. Y., & Jeannin, P. (2003). Interferon- γ switches monocyte differentiation from dendritic cells to macrophages. *Blood*, *101*, 143–150.
- den Haan, M. C., Grauss, R. W., Smits, A. M., Winter, E. M., Van Tuyn, J., Pijnappels, D. A., Steendijk, P., Gittenberger-De Groot, A. C., van der Laarse, A., Fibbe, W. E., De Vries, A. A. F., Schalij, M. J., Doevendans, P. A., Goumans, M. J., & Atsma, D. E. (2012). Cardiomyogenic differentiation-independent improvement of cardiac function by human cardiomyocyte progenitor cell injection in ischaemic mouse hearts. *J Cell Mol Med*, *16*, 1508–1521.

- Deng, Q., Ramskold, D., Reinius, B., & Sandberg, R. (2014). Single-cell RNA-seq reveals dynamic, random monoallelic gene expression in mammalian cells. *Science*, *343*.
- Deshmane, S. L., Kremlev, S., Amini, S., & Sawaya, B. E. (2009). Monocyte chemoattractant protein-1 (MCP-1): An overview. *J. Interferon Cytokine Res.*, *29*, 313–325.
- Dewald, O., Frangogiannis, N. G., Zoerlein, M., Duerr, G. D., Klemm, C., Knuefermann, P., Taffet, G., Michael, L. H., Crapo, J. D., Welz, A., & Entman, M. L. (2003). Development of murine ischemic cardiomyopathy is associated with a transient inflammatory reaction and depends on reactive oxygen species. *PNAS*, *100*, 2700–2705
- Dewald, O., Zymek, P., Winkelmann, K., Koerting, A., Ren, G., Abou-Khamis, T., Michael, L. H., Rollins, B. J., Entman, M. L., & Frangogiannis, N. G. (2005). CCL2/monocyte chemoattractant protein-1 regulates inflammatory responses critical to healing myocardial infarcts. *Circ. Res.*, *96*, 881–889.
- Dewar, A. L., Cambareli, A. C., Zannettino, A. C. W., Miller, B. L., Doherty, K. V., Hughes, T. P., & Bruce Lyons, A. (2005). Macrophage colony-stimulating factor receptor c-fms is a novel target of imatinib. *Blood*, *105*, 3127–3132.
- Dey, A., She, H., Kim, L., Boruch, A., Guris, D. L., Carlberg, K., Sebt, S. M., Woodley, D. T., Imamoto, A., & Li, W. (2000). Colony-stimulating factor-1 receptor utilizes multiple signaling pathways to induce cyclin D2 expression. *Mol. Biol. Cell*, *11*, 3835–3848.
- Di Cesare, M., Bentham, J., Stevens, G. A., Zhou, B., Danaei, G., Lu, Y., Bixby, H., Cowan, M. J., Riley, L. M., Hajifathalian, K., Fortunato, L., Taddei, C., Bennett, J. E., Ikeda, N., Khang, Y. H., Kyobutungi, C., Laxmaiah, A., Li, Y., Lin, H. H., ... Cisneros, J. Z. (2016). Trends in adult body-mass index in 200 countries from 1975 to 2014: A pooled analysis of 1698 population-based measurement studies with 19.2 million participants. *The Lancet*, *387*, 1377–1396.
- Dick, S. A., Macklin, J. A., Nejat, S., Momen, A., Clemente-Casares, X., Althagafi, M. G., Chen, J., Kantores, C., Hosseinzadeh, S., Aronoff, L., Wong, A., Zaman, R., Barbu, I., Besla, R., Lavine, K. J., Razani, B., Ginhoux, F., Husain, M., Cybulsky, M. I., Epelman, S. (2019). Self-renewing resident cardiac macrophages limit adverse remodeling following myocardial infarction. *Nat. Immunol.*, *20*, 29–39.
- Diercks, A., Kostner, H., & Ozinsky, A. (2009). Resolving cell population heterogeneity: Real-time PCR for simultaneous multiplexed gene detection in multiple single-cell samples. *PLoS ONE*, *4*, e6326.
- Dimmeler, S., & Leri, A. (2008). Aging and disease as modifiers of efficacy of cell therapy. *Circ. Res.*, *102*, 1319–1330.
- Dinarelli, C. (1991). Interleukin-1 and Interleukin-1 antagonism. *Blood*, *1*, 1627–1653.
- Ding, J., Adiconis, X., Simmons, S. K., Kowalczyk, M. S., Hession, C. C., Marjanovic, N. D., Hughes, T. K., Wadsworth, M. H., Burks, T., Nguyen, L. T., Kwon, J. Y. H., Barak, B., Ge, W., Kedaigle, A. J., Carroll, S., Li, S., Hacohen, N., Rozenblatt-Rosen, O., Shalek, A. K., Levin, J. Z. (2020). Systematic comparison of single-cell and single-nucleus RNA-sequencing methods. *Nat. Biotechnol.* *38*, 737–746.
- Dobaczewski, M., Gonzalez-Quesada, C., & Frangogiannis, N. G. (2010). The extracellular matrix as a modulator of the inflammatory and reparative response following myocardial infarction. *J. Mol. Cell. Cardiol.*, *48*, 504–511.
- Dong, Y., Arif, A. A., Poon, G. F. T., Hardman, B., Dosanjh, M., & Johnson, P. (2016). Generation and identification of GM-CSF derived alveolar-like macrophages and dendritic cells from mouse bone marrow. *J. Vis. Exp.*, *25*, 1–7.
- Dorn, G. W. (2009). Novel pharmacotherapies to abrogate postinfarction ventricular remodeling. *Nat. Rev. Cardiol.*, *6*, 283–291.

- Duerr, R. L., Huang, S., Miraliakbar, H. R., Clark, R., Chien, K. R., & Ross, J. (1995). Insulin-like growth factor-1 enhances ventricular hypertrophy and function during the onset of experimental cardiac failure. *J. Clin. Investig.*, *95*, 619–627.
- Dupasquier, M., Stoitzner, P., Wan, H., Cerqueira, D., Van Oudenaren, A., Voerman, J. S. A., Denda-Nagai, K., Irimura, T., Raes, G., Romani, N., & Leenen, P. J. M. (2006). The dermal microenvironment induces the expression of the alternative activation marker CD301/mMGL in mononuclear phagocytes, independent of IL-4/IL-13 signaling. *J. Leukoc. Biol.*, *80*, 838–849.
- Durruthy-Durruthy, R., & Heller, S. (2015). Applications for single cell trajectory analysis in inner ear development and regeneration. *Cell Tissue Res.*, *361*, 49–57.
- Dutta, P., & Nahrendorf, M. (2015). Monocytes in myocardial infarction. *ATVB*, *35*, 1066–1070.
- Eberwine, J., Yeh, H., Miyashiro, K., Cao, Y., Nair, S., Finnell, R., Zettel, M., & Coleman, P. (1992). Analysis of gene expression in single live neurons. *PNAS*, *89*, 3010–3014.
- El-Gamal, M. I., Al-Ameen, S. K., Al-Koumi, D. M., Hamad, M. G., Jalal, N. A., & Oh, C. H. (2018). Recent advances of colony-stimulating factor-1 receptor (CSF-1R) kinase and its inhibitors. *J. Med. Chem.*, *61*, 5450–5466.
- Eligini, S., Fiorelli, S., Tremoli, S., & Colli, S. (2020). Inhibition of transglutaminase 2 reduces efferocytosis in human macrophages: Role of CD14 and SR-AI receptors. *Nutr Metab Cardiovasc Dis*, *26*, 992–930.
- Ellison, G. M., Torella, D., Dellegrottaglie, S., Perez-Martinez, C., Perez De Prado, A., Vicinanza, C., Purushothaman, S., Galuppo, V., Iaconetti, C., Waring, C. D., Smith, A., Torella, M., Cuellas Ramon, C., Gonzalo-Orden, J. M., Agosti, V., Indolfi, C., Galianes, M., Fernandez-Vazquez, F., & Nadal-Ginard, B. (2011). Endogenous cardiac stem cell activation by insulin-like growth factor-1/hepatocyte growth factor intracoronary injection fosters survival and regeneration of the infarcted pig heart. *J. Am. Coll. Cardiol.*, *58*, 977–986.
- Ellison, G. M., Vicinanza, C., Smith, A. J., Aquila, I., Leone, A., Waring, C. D., Henning, B. J., Stirparo, G. G., Papait, R., Scarfò, M., Agosti, V., Viglietto, G., Condorelli, G., Indolfi, C., Ottolenghi, S., Torella, D., & Nadal-Ginard, B. (2013). Adult c-kit⁺ cardiac stem cells are necessary and sufficient for functional cardiac regeneration and repair. *Cell*, *154*, 827–842.
- Ensan, S., Li, A., Besla, R., Degousee, N., Cosme, J., Roufaiel, M., Shikatani, E. A., El-Maklizi, M., Williams, J. W., Robins, L., Li, C., Lewis, B., Yun, T. J., Lee, J. S., Wieghofer, P., Khattar, R., Farrokhi, K., Byrne, J., Ouzounian, M., Robbins, C. S. (2016). Self-renewing resident arterial macrophages arise from embryonic CX3CR1⁺ precursors and circulating monocytes immediately after birth. *Nat. Immunol.*, *17*, 159–168.
- Epelman, S., Lavine, K. J., & Randolph, G. J. (2014). Origin and functions of tissue macrophages. *Immunity*, *41*, 21–35.
- Epelman, S., Mann, D. L., Lavine, K. J., Beaudin, A. E., Sojka, D. K., Carrero, J. A., Calderon, B., Brija, T., Gautier, E. L., Ivanov, S., Satpathy, A. T., Schilling, J. D., Schwendener, R., Sergin, I., Razani, B., Forsberg, E. C., Yokoyama, W. M., Unanue, E. R., Colonna, M., ... Mann, D. L. (2014). Embryonic and adult-derived resident cardiac macrophages are maintained through distinct mechanisms at the steady state and during inflammation. *Immunity*, *40*, 91–104.
- Ernoffsson, M., & Siegbahn, A. (1996). Platelet-derived growth factor-BB and monocyte chemotactic protein-1 induce human peripheral blood monocytes to express tissue factor. *Thromb. Res.*, *83*, 307–320.
- Eschenhagen, T., Bolli, R., Braun, T., Field, L. J., Fleischmann, B. K., Frisén, J., Giacca, M., Hare, J. M., Houser, S., Lee, R. T., Marbán, E., Martin, J. F., Molkentin, J. D., Murry, C. E., Riley, P. R., Ruiz-Lozano, P., Sadek, H. A., Sussman, M. A., & Joseph A. Hill, M. (2017). Cardiomyocyte regeneration: a consensus statement. *Circulation*, 680–686.

- Espinosa-Heidmann, D. G., Suner, I. J., Hernandez, E. P., Monroy, D., Csaky, K. G., & Cousins, S. W. (2003). Macrophage depletion diminishes lesion size and severity in experimental choroidal neovascularization. *IOVS*, *44*, 3586–3592.
- Eulalio, A., Mano, M., Ferro, M. D., Zentilin, L., Sinagra, G., Zacchigna, S., & Giacca, M. (2012). Functional screening identifies miRNAs inducing cardiac regeneration. *Nature*, *492*, 376–381.
- Evans, R., Shultz, L. D., Dranoff, G., Fuller, J. A., & Kamdar, S. J. (1998). CSF-1 regulation of Il6 gene expression by murine macrophages: A pivotal role for GM-CSF. *J. Leukoc. Biol.*, *64*, 810–816.
- Fabbi, P., Spallarossa, P., Garibaldi, S., Barisione, C., Mura, M., Altieri, P., Rebesco, B., Monti, M. G., Canepa, M., Ghigliotti, G., Brunelli, C., & Ameri, P. (2015). Doxorubicin impairs the insulin-like growth factor-1 system and causes insulin-like growth factor-1 resistance in cardiomyocytes. *PLoS ONE*, *10*, 1–14.
- Falcone, D. J., Khan, K. M. F., Layne, T., & Fernandes, L. (1998). Macrophage formation of angiostatin during inflammation: a byproduct of the activation of plasminogen. *JBC*, *273*, 31480–31485.
- Fan, Y., Ye, J., Shen, F., Zhu, Y., Yeghiazarians, Y., Zhu, W., Chen, Y., Lawton, M. T., Young, W. L., & Yang, G. Y. (2008). Interleukin-6 stimulates circulating blood-derived endothelial progenitor cell angiogenesis in vitro. *JCBFM*, *28*, 90–98.
- Farbehi, N., Patrick, R., Dorison, A., Xaymardan, M., Janbandhu, V., Ho, J. W. K., Wystub-Lis, K., Nordon, R. E., & Harvey, R. P. (2019). Single-cell expression profiling reveals dynamic flux of cardiac stromal, vascular and immune cells in health and injury. *ELife*, 1–39.
- Farber, J. M. (1997). Mig and IP-10: CXC chemokines that target lymphocytes. *J. Leukoc. Biol.*, *61*, 246–257.
- Felcht, M., Luck, R., Schering, A., Seidel, P., Srivastava, K., Hu, J., Bartol, A., Kienast, Y., Vettel, C., Loos, E. K., Kutschera, S., Bartels, S., Appak, S., Besemfelder, E., Terhardt, D., Chavakis, E., Wieland, T., Klein, C., Thomas, M., Augustin, H. G. (2012). Angiopoietin-2 differentially regulates angiogenesis through TIE2 and integrin signaling. *J. Clin. Investig.*, *122*(6), 1991–2005.
- Feng, G., Bjpai, G., Ma, P., Koenig, A., Bredemeyer, A., Lokshina, I., Lai, L., Forster, I., Leuschner, F., Kreisler, D., & K., L. (2022). CCL17 Aggravates myocardial injury by suppressing recruitment of regulatory T cells. *Circulation*, *145*, 765–782.
- Ferrari, G., Cook, B., Terushkin, V., Pintucci, G., & Mignatti, P. (2009). Transforming growth factor-beta 1 (tgf-β1) induces angiogenesis through vascular endothelial growth factor (vegf)-mediated apoptosis. *J Cell Physiol*, *219*, 449–458.
- Ferraro, B., Leoni, G., Hinkel, R., Ormanns, S., Paulin, N., Ortega-Gomez, A., Viola, J. R., de Jong, R., Bongiovanni, D., Bozoglu, T., Maas, S. L., D'Amico, M., Kessler, T., Zeller, T., Hristov, M., Reutelingsperger, C., Sager, H. B., Döring, Y., Nahrendorf, M., Soehnlein, O. (2019). Pro-angiogenic macrophage phenotype to promote myocardial repair. *J. Am. Coll. Cardiol.*, *73*, 2990–3002.
- Fiedler, L., Maifoshie, E., & Schneider, M. (2014). Mouse Models of the Nuclear Envelopathies and Related Diseases. Book chapter. 109.
- Fiedler, L. R., Chapman, K., Xie, M., Maifoshie, E., Jenkins, M., Golfroush, P. A., Bellahcene, M., Nosedà, M., Faust, D., Jarvis, A., Newton, G., Paiva, M. A., Harada, M., Stuckey, D. J., Song, W., Habib, J., Narasimham, P., Aqil, R., Sanmugalingam, D., Schneider, M. D. (2019). MAP4K4 inhibition promotes survival of human stem cell-derived cardiomyocytes and reduces infarct size in vivo. *Cell Stem Cell*, 1–13.
- Fiedler, U., Reiss, Y., Scharpfenecker, M., Grunow, V., Koidl, S., Thurston, G., Gale, N. W., Witzenrath, M., Rosseau, S., Suttorp, N., Sobke, A., Herrmann, M., Preissner, K. T., Vajkoczy, P., & Augustin, H. G. (2006). Angiopoietin-2 sensitizes endothelial cells to TNF- α and has a crucial role in the induction of inflammation. *Nat. Med.* *12*, 235–239.

- Fildes, J. E., Shaw, S. M., Yonan, N., & Williams, S. G. (2009). The Immune system and chronic heart failure. is the heart in control? *J. Am. Coll. Cardiol.*, *53*, 1013–1020.
- Fleetwood, A. J., Dinh, H., Cook, A. D., Hertzog, P. J., & Hamilton, J. A. (2009). GM-CSF- and M-CSF-dependent macrophage phenotypes display differential dependence on Type I interferon signaling. In *J. Leukoc. Biol.*, *86*, 411–421.
- Fleetwood, A. J., Lawrence, T., Hamilton, J. A., & Cook, A. D. (2007). Granulocyte-Macrophage colony-stimulating factor (CSF) and macrophage csf-dependent macrophage phenotypes display differences in cytokine profiles and transcription factor activities: implications for CSF blockade in inflammation. *J. Immunol. Res.*, *178*, 5245–5252.
- Fomby, P., Cherlin, A. J., Hadjizadeh, A., Doillon, C. J., Sueblinvong, V., Weiss, D. J., Bates, J. H. T., Gilbert, T., Liles, W. C., Lutzko, C., Rajagopal, J., Prockop, D. J., Chambers, D., Giangreco, A., Keating, A., Kotton, D., Lelkes, P. I., Wagner, D. E., & Prockop, D. J. (2010). Stem cells and cell therapies in lung biology and diseases: Conference report. *Ann. Am. Thorac. Soc.*, *12*, 181–204.
- Fontes, J. A., Rose, N. R., & Čiháková, D. (2015). The varying faces of IL-6: From cardiac protection to cardiac failure. *Cytokine*, *74*, 62–68.
- Forbes, S. J., & Rosenthal, N. (2014). Preparing the ground for tissue regeneration: from mechanism to therapy. *Nat. Med.*, *20*, 857–869.
- Fordham, J. B., Hua, J., Morwood, S. R., Schewitz-Bowers, L. P., Copland, D. A., Dick, A. D., & Nicholson, L. B. (2012). Environmental conditioning in the control of macrophage thrombospondin-1 production. *Sci. Rep.*, *2*, 512.
- Forouzanfar, M. H., Afshin, A., Alexander, L. T., Biryukov, S., Brauer, M., Cercy, K., Charlson, F. J., Cohen, A. J., Dandona, L., Estep, K., Ferrari, A. J., Frostad, J. J., Fullman, N., Godwin, W. W., Griswold, M., Hay, S. I., Kyu, H. H., Larson, H. J., Lim, S. S., Zhu, J. (2016). Global, regional, and national comparative risk assessment of 79 behavioural, environmental and occupational, and metabolic risks or clusters of risks, 1990–2015: a systematic analysis for the Global Burden of Disease Study 2015. *The Lancet*, *388*, 1659–1724.
- Forte, E., Furtado, M. B., & Rosenthal, N. (2018). The interstitium in cardiac repair: role of the immune–stromal cell interplay. *Nat. Rev. Cardiol.*, *15*, 601–616.
- Fowles, L. F., Martin, M. L., Nelsen, L., Stacey, K. J., Redd, D., Clark, Y. M., Nagamine, Y., McMahon, M., Hume, D. A., & Ostrowski, M. C. (1998). Persistent activation of mitogen-activated protein kinases p42 and p44 and ets-2 phosphorylation in response to colony-stimulating factor 1/c-fms signaling. *Mol. Cell. Biol.*, *18*, 5148–5156.
- Faccarollo, D., Galuppo, P., & Bauersachs, J. (2012). Novel therapeutic approaches to post-infarction remodelling. *Cardiovasc. Res.*, *94*, 293–303.
- Frame, J. M., McGrath, K. E., & Palis, J. (2013). Erythro-myeloid progenitors: “Definitive” hematopoiesis in the conceptus prior to the emergence of hematopoietic stem cells. *Blood Cells Mol. Dis.*, *51*, 220–225.
- Francke, A., Herold, J., Weinert, S., Strasser, R. H., & Braun-Dullaeus, R. C. (2011). Generation of mature murine monocytes from heterogeneous bone marrow and description of their properties. *J. Histochem. Cytochem.*, *59*, 813–825.
- François, B., Trimoreau, F., Vignon, P., Fixe, P., Praloran, V., & Gastinne, H. (1997). Thrombocytopenia in the sepsis syndrome: role of hemophagocytosis and macrophage colony-stimulating factor. *Am. J. Med.*, *103*, 114–120.
- Frangogiannis. (2015). Emerging roles for macrophages in cardiac injury: cytoprotection, repair, and regeneration. *The J. Clin. Investig.*, *125*, 1–4.

- Frangogiannis, N. G., Mendoza, L. H., Lewallen, M., Michael, L. H., Smith, C. W., & Entman, M. L. (2001). Induction and suppression of interferon-inducible protein 10 in reperfused myocardial infarcts may regulate angiogenesis. *FASEB J.*, *15*, 1428–1430.
- Frangogiannis, N., Wayne Smith, G., & Entman, M. L. (2002). The inflammatory response in myocardial infarction. *Cardiovasc. Res.*, *53*, 31–47.
- Frangogiannis, N. G. (2006). Comprehensive invited review - the mechanistic basis of infarct healing. *Ars*, *8*, 691.
- Frangogiannis, N. G. (2008). The immune system and cardiac repair. *Pharmacol. Res. Commun.*, *58*, 88–111.
- Frangogiannis, Nikolaos G. (2012). Regulation of the inflammatory response in cardiac repair. *Circ. Res.*, *110*, 159–173.
- Frangogiannis, Nikolaos G., Lindsey, M. L., Michael, L. H., Youker, K. A., Bressler, R. B., Mendoza, L. H., Spengler, R. N., Smith, C. W., & Entman, M. L. (1998). Resident cardiac mast cells degranulate and release preformed TNF- α , initiating the cytokine cascade in experimental canine myocardial ischemia/reperfusion. *Circulation*, *98*, 699–710.
- Frangogiannis, Nikolaos G. (2007). Chemokines in ischemia and reperfusion. *RPTH*, *97*, 747.
- Frangogiannis, Nikolaos G. (2015). Inflammation in cardiac injury, repair and regeneration. *Curr. Opin. Cardiol.*, *30*, 240–245.
- Frangogiannis, Nikolaos, Mendoza, L. H., Ren, G., Akrivakis, S., Jackson, P. L., Michael, L. H., Smith, C. W., Entman, M. L., Cokkinos, V., Nihoyannopoulos, P., Frangogiannis, N. G., Mendoza, L. H., Ren, G., Akrivakis, S., Jackson, P. L., Michael, L. H., Smith, C. W., Entman, M. L., Nikolaos, G., Entman, M. L. (2003). MCSF expression is induced in healing myocardial infarcts and may regulate monocyte and endothelial cell phenotype MCSF expression is induced in healing myocardial infarcts and may regulate monocyte and endothelial cell phenotype. *Am J Physiol Heart Circ Physiol*, *285*, 483–492.
- Frantz, S., Hofmann, U., Fraccarollo, D., Sch??fer, A., Kranepuhl, S., Hagedorn, I., Nieswandt, B., Nahrendorf, M., Wagner, H., Bayer, B., Pachel, C., Sch??n, M. P., Kneitz, S., Bobinger, T., Weidemann, F., Ertl, G., & Bauersachs, J. (2013). Monocytes/macrophages prevent healing defects and left ventricular thrombus formation after myocardial infarction. *FASEB J.*, *27*, 871–881.
- Frantz, S., Kobzik, L., Kim, Y. D., Fukazawa, R., Medzhitov, R., Lee, R. T., & Kelly, R. A. (1999). Toll4 (TLR4) expression in cardiac myocytes in normal and failing myocardium. *J. Clin. Investig.*, *104*, 271–280.
- Frasca, D., Landin, A. M., Riley, R. L., & Blomberg, B. B. (2008). Mechanisms for decreased function of B cells in aged mice and humans. *J. Immunol. Res.*, *180*, 2741–2746.
- Fuchs, M., Hilfiker, A., Kaminski, K., Hilfiker-Kleiner, D., Guener, Z., Klein, G., Podewski, E., Schieffer, B., Rose-John, S., & Drexler, H. (2003). Role of interleukin-6 for LV remodeling and survival after experimental myocardial infarction. *FASEB J.*, *17*, 2118–2120.
- Fukada, T., Hibi, M., Yamanaka, Y., Takahashi-Tezuka, M., Fujitani, Y., Yamaguchi, T., Nakajima, K., & Hirano, T. (1996). Two signals are necessary for cell proliferation induced by a cytokine receptor gp130: Involvement of STAT3 in anti-apoptosis. *Immunity*, *5*, 449–460.
- Funaba, M., Ikeda, T., Ogawa, K., Murakami, M., & Abe, M. (2003). Role of activin A in murine mast cells: modulation of cell growth, differentiation, and migration. *J. Leukoc. Biol.*, *73*, 793–801.
- Furth, R. van, & Cohn, Z. A. (1968). The origin and kinetics of mononuclear phagocytes. *J Exp Med*, *128*, 415–435.
- Gallego-Colon, E., Sampson, R. D., Sattler, S., Schneider, M. D., Rosenthal, N., & Tonkin, J. (2015). Cardiac-restricted IGF-1Ea overexpression reduces the early accumulation of inflammatory myeloid

- cells and mediates expression of extracellular matrix remodelling genes after myocardial infarction. *Mediat. Inflamm.*, 2015, 484357.
- Gallet, R., Dawkins, J., Valle, J., Simsolo, E., De Couto, G., Middleton, R., Tseliou, E., Luthringer, D., Kreke, M., Smith, R. R., Marbán, L., Ghaleh, B., & Marbán, E. (2017). Exosomes secreted by cardiosphere-derived cells reduce scarring, attenuate adverse remodelling, and improve function in acute and chronic porcine myocardial infarction. *Eur Heart J*, 38, 201–211.
- Galvez, B. G., Sampaolesi, M., Barbuti, A., Crespi, A., Covarello, D., Brunelli, S., Dellavalle, A., Crippa, S., Balconi, G., Cuccovillo, I., Molla, F., Staszewsky, L., Latini, R., DiFrancesco, D., & Cossu, G. (2008). Cardiac mesoangioblasts are committed, self-renewable progenitors, associated with small vessels of juvenile mouse ventricle. *Cell Death Differ.*, 15, 1417–1428.
- Garcia, S., Hartkamp, L. M., Malvar-Fernandez, B., van Es, I. E., Lin, H., Wong, J., Long, L., Zanghi, J. A., Rankin, A. L., Masteller, E. L., Wong, B. R., Radstake, T. R. D. J., Tak, P. P., & Reedquist, K. A. (2016). Colony-stimulating factor (CSF) 1 receptor blockade reduces inflammation in human and murine models of rheumatoid arthritis. *Arthritis Research and Therapy*, 18, 1–14.
- Gautiar, E. L., Shay, T., Miller, J., Greter, M., Jakubzick, C., Ivanov, S., Helft, J., Chow, A., Elpek, K. G., Gordonov, S., Mazloom, A. R., Ma'Ayan, A., Chua, W. J., Hansen, T. H., Turley, S. J., Merad, M., Randolph, G. J., Best, A. J., Knell, J., ... Benoist, C. (2012). Gene-expression profiles and transcriptional regulatory pathways that underlie the identity and diversity of mouse tissue macrophages. *Nat. Immunol.*, 13, 1118–1128.
- Geissmann, F., Jung, S., & Littman, D. R. (2003). Blood monocytes consist of two principal subsets with distinct migratory properties. *Immunity*, 19, 71–82.
- Gessani, S., Belardelli, F., Pecorelli, A., & Puddu, P. (1989). Bacterial lipopolysaccharide and gamma interferon induce transcription of beta interferon mRNA and interferon secretion in murine macrophages. *J. Virol.*, 63, 2785–2789.
- Ginhoux, F., Greter, M., Leboeuf, M., Nandi, S., See, P., Gokhan, S., Mehler, M. F., Conway, S. J., Ng, L. G., Stanley, E. R., Samokhvalov, I. M., & Merad, M. (2010). Fate Mapping analysis reveals that adult microglia derive from primitive macrophages. *Science*, 701, 841–845.
- Gladka, M. M., Molenaar, B., De Ruiter, H., Van Der Elst, S., Tsui, H., Versteeg, D., Lacraz, G. P. A., Huibers, M. M. H., Van Oudenaarden, A., & Van Rooij, E. (2018). Single-cell sequencing of the healthy and diseased heart reveals cytoskeleton-associated protein 4 as a new modulator of fibroblasts activation. *Circulation*, 138, 166–180.
- Gleissner, C. A., Shaked, I., Little, K. M., & Ley, K. (2010). CXC chemokine ligand 4 induces a unique transcriptome in monocyte-derived macrophages. *J. Immunol. Res.*, 184, 4810–4818.
- Gnecchi, M., He, H., Liang, O., Melo, L., Morello, F., Mu, H., Noiseux, N., Zhang, L., Pratt, R., Ingwall, J., & Dzau, V. (2005). Paracrine action accounts for marked protection of ischemic heart by Akt-modified mesenchymal stem cells. *Nat. Med.*, 11, 367–368.
- Godwin, J. W., Debuque, R., Salimova, E., & Rosenthal, N. A. (2017). Heart regeneration in the salamander relies on macrophage-mediated control of fibroblast activation and the extracellular landscape. *NPJ Regen. Med.*, 2, 1–11.
- Gomez Perdiguero, E., Klapproth, K., Schulz, C., Busch, K., Azzoni, E., Crozet, L., Garner, H., Trouillet, C., de Bruijn, M. F., Geissmann, F., & Rodewald, H.-R. (2015). Tissue-resident macrophages originate from yolk-sac-derived erythro-myeloid progenitors. *Nature*, 518, 547–551.
- González-Rosa, J. M., Burns, C. E., & Burns, C. G. (2017). Zebrafish heart regeneration: 15 years of discoveries. *Regen.*, 4, 105–123.
- González-Rosa, J. M., Martín, V., Peralta, M., Torres, M., & Mercader, N. (2011). Extensive scar formation and regression during heart regeneration after cryoinjury in zebrafish. *Dev.*, 138(9), 1663–1674.

- Gordon, S. (2003). Alternative activation of macrophages. *Nature Rev. Immunol.*, 3, 23–35.
- Gordon, Siamon, & Martinez, F. O. (2010). Alternative activation of macrophages: mechanism and functions. *Immunity*, 32, 593–604.
- Gordon, Siamon, & Plüddemann, A. (2017). Tissue macrophages: heterogeneity and functions. *BMC Biology*, 15, 1–18.
- Gordon, S., Plüddemann, A., & M. Estrada, F. (2014). Macrophage heterogeneity in tissues: Phenotypic diversity and functions. *Immunol. Rev.*, 262, 36–55.
- Gordon, S., & Taylor, P. R. (2005). Monocyte and macrophage heterogeneity. *Nat. Rev. Immunol.*, 5, 953–964.
- Gordon, S. (2002). Alternative activation of macrophage. *Nat. Rev. Immunol.*, 67, 245–248.
- Gorman, M. J., Caine, E. A., Zaitsev, K., Begley, M. C., Weger-Lucarelli, J., Uccellini, M. B., Tripathi, S., Morrison, J., Yount, B. L., Dinnon, K. H., Rückert, C., Young, M. C., Zhu, Z., Robertson, S. J., McNally, K. L., Ye, J., Cao, B., Mysorekar, I. U., Ebel, G. D., Diamond, M. S. (2018). An immunocompetent mouse model of zika virus infection. *Cell Host Microbe*, 23, 672-685.e6.
- Gosselin, D., Skola, D., Coufal, N. G., Holtman, I. R., Schlachetzki, J. C. M., Sajti, E., Jaeger, B. N., O'Connor, C., Fitzpatrick, C., Pasillas, M. P., Pena, M., Adair, A., Gonda, D. D., Levy, M. L., Ransohoff, R. M., Gage, F. H., & Glass, C. K. (2017). An environment-dependent transcriptional network specifies human microglia identity. *Science*, 356, 1248–1259.
- Gow, D. J., Sester, D. P., & Hume, D. A. (2010). CSF-1, IGF-1, and the control of postnatal growth and development. *J. Leukoc. Biol.*, 88, 475–481.
- Gray, W. D., French, K. M., Ghosh-Choudhary, S., Maxwell, J. T., Brown, M. E., Platt, M. O., Searles, C. D., & Davis, M. E. (2015). Identification of therapeutic covariant microRNA clusters in hypoxia-treated cardiac progenitor cell exosomes using systems biology. *Circ. Res.*, 116, 255–263.
- Gregory, C. D., & Devitt, A. (2004). The macrophage and the apoptotic cell: An innate immune interaction viewed simplistically? *Immunology*, 113, 1–14.
- Grimshaw, M. J., & Balkwill, F. R. (2001). Inhibition of monocyte and macrophage chemotaxis by hypoxia and inflammation - A potential mechanism. *Eur. J Immunol.* 31, 480–489.
- Grimsley, C., & Ravichandran, K. S. (2003). Cues for apoptotic cell engulfment: eat-me, don't eat-me and come-get-me signals. *Trends Cell Biol.*, 13, 648–656.
- Grün, D., Muraro, M. J., Boisset, J. C., Wiebrands, K., Lyubimova, A., Dharmadhikari, G., van den Born, M., van Es, J., Jansen, E., Clevers, H., de Koning, E. J. P., & van Oudenaarden, A. (2016). De novo prediction of stem cell identity using single-cell transcriptome data. *Cell Stem Cell*, 19, 266–277.
- Grün, D., & Van Oudenaarden, A. (2015). Design and analysis of single-cell sequencing experiments. *Cell*, 163, 799–810.
- Guha, M., & Mackman, N. (2002). The phosphatidylinositol 3-kinase-Akt pathway limits lipopolysaccharide activation of signaling pathways and expression of inflammatory mediators in human monocytic cells. *JBC*, 277, 32124–32132.
- Guilliams, M., De Kleer, I., Henri, S., Post, S., Vanhoutte, L., De Prijck, S., Deswarte, K., Malissen, B., Hammad, H., & Lambrecht, B. N. (2013). Alveolar macrophages develop from fetal monocytes that differentiate into long-lived cells in the first week of life via GM-CSF. *The J Exp Med*, 210, 1977–1992.
- Gupta, V., & Poss, K. D. (2012). Clonally dominant cardiomyocytes direct heart morphogenesis. *Nature*, 484, 479–484.

- Gwechenberger, M., Mendoza, L. H., Youker, K. A., Frangogiannis, N. G., Wayne Smith, C., Michael, L. H., & Entman, M. L. (1999). Cardiac myocytes produce interleukin-6 in culture and in viable border zone of reperfused infarctions. *Circulation*, *99*, 546–551.
- Gyöngyösi, M., Wojakowski, W., Navarese, E. P., & Moya, L. (2016). Meta-analyses of human cell-based cardiac regeneration therapies: Controversies in meta-analyses results on cardiac cell-based regenerative studies. *Circ. Res.*, *118*, 1254–1263.
- Hagar, J. A., Powell, D. A., Aachoui, Y., Ernst, R. K., & Miao, E. A. (2013). Cytoplasmic LPS activates caspase-11: implications in TLR4-independent endotoxic shock. *Science*, *341*, 1250–1253.
- Hamilton, J. A. (2008). Colony-stimulating factors in inflammation and autoimmunity. *Nat Immunol.*, *23*, 533–544.
- Han, X., Zhang, Y., Yin, L., Zhang, L., Wang, Y., Zhang, H., & Li, B. (2018). Statin in the treatment of patients with myocardial infarction. *Medicine* *12*, 10–13.
- Hansen, G., Hercus, T. R., McClure, B. J., Stomski, F. C., Dottore, M., Powell, J., Ramshaw, H., Woodcock, J. M., Xu, Y., Guthridge, M., McKinstry, W. J., Lopez, A. F., & Parker, M. W. (2008). The structure of the GM-CSF receptor complex reveals a distinct mode of cytokine receptor activation. *Cell*, *134*, 496–507.
- Hare, J. M., Fishman, J. E., Gerstenblith, G., DiFede Velazquez, D. L., Zambrano, J. P., Suncion, V. Y., Tracy, M., Ghersin, E., Johnston, P. V., Brinker, J. A., Breton, E., Davis-Sproul, J., Schulman, I. H., Byrnes, J., Mendizabal, A. M., Lowery, M. H., Rouy, D., Altman, P., Wong Po Foo, C., Heldman, A. W. (2012). Comparison of allogeneic vs autologous bone marrow-derived mesenchymal stem cells delivered by transendocardial injection in patients with ischemic cardiomyopathy: The POSEIDON randomized trial. *JAMA*, *308*, 2369–2379.
- Harel-Adar, T., Mordechai, T. Ben, Amsalem, Y., Feinberg, M. S., Leor, J., & Cohen, S. (2011). Modulation of cardiac macrophages by phosphatidylserine-presenting liposomes improves infarct repair. *PNAS*, *108*, 1827–1832.
- Hart, P. H., Vitti, G. F., Burgess, D. R., Whitty, G. A., Piccoli, D. S., & Hamilton, J. A. (1989). Potential antiinflammatory effects of interleukin 4: suppression of human monocyte tumor necrosis factor alpha, interleukin 1, and prostaglandin E2. *PNAS*, *86*, 3803–3807.
- Hasan, A., Khattab, A., Islam, M. A., Hweij, K. A., Zeitouny, J., Waters, R., Sayegh, M., Hossain, M. M., & Paul, A. (2015). Injectable hydrogels for cardiac tissue repair after myocardial infarction. *Adv. Sci. Lett.*, *2*, 1–18.
- Hashimoto, D., Chow, A., Greter, M., Saenger, Y., Kwan, W. H., Leboeuf, M., Ginhoux, F., Ochando, J. C., Kunisaki, Y., van Rooijen, N., Liu, C., Teshima, T., Heeger, P. S., Stanley, E. R., Frenette, P. S., & Merad, M. (2011). Pretransplant CSF-1 therapy expands recipient macrophages and ameliorates GVHD after allogeneic hematopoietic cell transplantation. *J Exp Med*, *208*, 1069–1082.
- Hashimoto, D., Chow, A., Noizat, C., Teo, P., Beasley, M. B., Leboeuf, M., Becker, C. D., See, P., Price, J., Lucas, D., Greter, M., Mortha, A., Boyer, S. W., Forsberg, E. C., Tanaka, M., van Rooijen, N., García-Sastre, A., Stanley, E. R., Ginhoux, F., Camilla, E. (2013). Tissue-resident macrophages self-maintain locally throughout adult life with minimal contribution from circulating monocytes. *Immunity*, *38*, 792–804.
- Hashimoto, H., Wang, Z., Garry, G. A., Malladi, V. S., Botten, G. A., Ye, W., Zhou, H., Osterwalder, M., Dickel, D. E., Visel, A., Liu, N., Bassel-Duby, R., & Olson, E. N. (2019). Cardiac reprogramming factors synergistically activate genome-wide cardiogenic stage-specific enhancers. *Cell Stem Cell*, *25*, 69-86.e5.
- Hashimshony, T., Senderovich, N., Avital, G., Klochendler, A., de Leeuw, Y., Anavy, L., Gennert, D., Li, S., Livak, K. J., Rozenblatt-Rosen, O., Dor, Y., Regev, A., & Yanai, I. (2016). CEL-Seq2: sensitive highly-multiplexed single-cell RNA-Seq. *Genome Biol.*, *17*, 1–7.

- Hashimshony, T., Wagner, F., Sher, N., & Yanai, I. (2012). CEL-Seq: single-cell RNA-Seq by multiplexed linear amplification. *Cell Rep.*, 2, 666–673.
- Hass, R., Kasper, C., Böhm, S., & Jacobs, R. (2011). Different populations and sources of human mesenchymal stem cells (MSC): A comparison of adult and neonatal tissue-derived MSC. *Cell Commun. Signal*, 9, 12.
- Haubner, B. J., Adamowicz-Brice, M., Khadayate, S., Tiefenthaler, V., Metzler, B., Aitman, T., & Penninger, J. M. (2012). Complete cardiac regeneration in a mouse model of myocardial infarction. *Aging*, 4, 966–977.
- Hausenloy, D. J., & Yellon, D. M. (2009). Cardioprotective growth factors. *Cardiovasc. Res.*, 83, 179–194.
- Hayashi, T., Shibata, N., Okumura, R., Kudome, T., Nishimura, O., Tarui, H., & Agata, K. (2010). Single-cell gene profiling of planarian stem cells using fluorescent activated cell sorting and its “index sorting” function for stem cell research. *Dev. Growth Differ.*, 52, 131–144.
- He, M., He, X., Xie, Q., Chen, F., & He, S. (2006). Angiotensin II induces the expression of tissue factor and its mechanism in human monocytes. *Thromb. Res.*, 117, 579–590.
- Heger, J., Schiegnitz, E., Von Waldthausen, D., Anwar, M. M., Piper, H. M., & Euler, G. (2010). Growth differentiation factor 15 acts anti-apoptotic and pro-hypertrophic in adult cardiomyocytes. *J. Cell. Physiol.*, 224, 120–126.
- Heidenreich, P. A., Albert, N. M., Allen, L. A., Bluemke, D. A., Butler, J., Fonarow, C., Ikonomidis, J. S., Khavjou, O., Konstam, M. A., Maddox, T. M., Nichol, G., Pham, M., Piña, I. L., & Trogon, J. G. (2013). Forecasting the impact of heart failure in the United States. *Circ Heart Fail*, 6, 606–619.
- Heidt, T., Courties, G., Dutta, P., Sager, H. B., Sebas, M., Iwamoto, Y., Sun, Y., Da Silva, N., Panizzi, P., Van Der Lahn, A. M., Swirski, F. K., Weissleder, R., & Nahrendorf, M. (2014). Differential contribution of monocytes to heart macrophages in steady-state and after myocardial infarction. *Circ. Res.*, 115, 284–295.
- Heinen, A., Nederlof, R., Panjwani, P., Szychala, A., Tschaidse, T., Reffelt, H., Boy, J., Raupach, A., Gödecke, S., Petzsch, P., Köhrer, K., Grandoch, M., Petz, A., Fischer, J. W., Alter, C., Vasilevska, J., Lang, P., & Gödecke, A. (2019). IGF1 Treatment improves cardiac remodeling after infarction by targeting myeloid cells. *Mol. Ther.*, 27, 46–58.
- Heinrichs, D., Brandt, E. F., Fischer, P., Köhncke, J., Wirtz, T. H., Guldiken, N., Djudjaj, S., Boor, P., Kroy, D., Weiskirchen, R., Bucala, R., Wasmuth, H. E., Strnad, P., Trautwein, C., Bernhagen, J., & Berres, M. (2021). Unexpected pro-fibrotic effect of MIF in non-alcoholic steatohepatitis is linked to a shift in NKT cell populations. *Cells* 10, 252.
- Hercus, T. R., Thomas, D., Guthridge, M. A., Ekert, P. G., King-Scott, J., Parker, M. W., & Lopez, A. F. (2009). The granulocyte-macrophage colony-stimulating factor receptor: Linking its structure to cell signaling and its role in disease. *Blood*, 114, 1289–1298.
- Herring, C. A., Banerjee, A., McKinley, E. T., Simmons, A. J., Ping, J., Roland, J. T., Franklin, J. L., Liu, Q., Gerdes, M. J., Coffey, R. J., & Lau, K. S. (2018). Unsupervised trajectory analysis of single-cell RNA-Seq and imaging data reveals alternative tuft cell origins in the gut. *Cell Systems*, 6, 37-51.e9.
- Hesse, M., Raulf, A., Pilz, G. A., Haberlandt, C., Klein, A. M., Jabs, R., Zaehres, H., Fügemann, C. J., Zimmermann, K., Trebicka, J., Welz, A., Pfeifer, A., Röhl, W., Kotlikoff, M. I., Steinhäuser, C., Götz, M., Schöler, H. R., & Fleischmann, B. K. (2012). Direct visualization of cell division using high-resolution imaging of M-phase of the cell cycle. *Nat Commun*, 3.
- Hidaka, T., Akada, S., Teranishi, A., Morikawa, H., Sato, S., Yoshida, Y., Yajima, A., Yaegashi, N., Okamura, K., & Saito, S. (2003). Mirimostim (macrophage colony-stimulating factor; M-CSF) improves chemotherapy-induced impaired natural killer cell activity, The1 Th2 balance and granulocyte function. *Cancer Sci.*, 94, 814–820.

- Hierlihy, A. M., Seale, P., Lobe, C. G., Rudnicki, M. A., & Megeney, L. A. (2002). The post-natal heart contains a myocardial stem cell population. *FEBS Letters*, *530*, 239–243.
- Hilgendorf, I., Gerhardt, L. M. S., Tan, T. C., Winter, C., Holderried, T. A. W., Chousterman, B. G., Iwamoto, Y., Liao, R., Zirlik, A., Scherer-Crosbie, M., Hedrick, C. C., Libby, P., Nahrendorf, M., Weissleder, R., & Swirski, F. K. (2014). Ly-6Chigh monocytes depend on nr4a1 to balance both inflammatory and reparative phases in the infarcted myocardium. *Circ. Res.*, *114*, 1611–1622.
- Himes, S. R., Sester, D. P., Ravasi, T., Cronau, S. L., Sasmono, T., & Hume, D. A. (2006). The JNK are important for development and survival of macrophages. *J. Immunol. Res.*, *176*, 2219–2228.
- Hochreiter-Hufford, A., & Ravichandran, K. S. (2013). Clearing the dead: apoptotic cell sensing, recognition, engulfment, and digestion. *Cold Spring Harb. perspect. biol.*, *5*, 1–20.
- Hockel, M., Jung, W., Vaupel, P., Rabes, H., Khaledpour, C., & Wissler, J. H. (1988). Purified monocyte-derived angiogenic substance (angiotropin) induces controlled angiogenesis associated with regulated tissue proliferation in rabbit skin. *J. Clin. Investig.*, *82*, 1075–1090.
- Hockel, M., Sasse, J., & JH, W. (1987). Purified monocyte-derived angiogenic substance (angiotropin) stimulates migration, phenotypic changes, and “tube formation” but not proliferation of capillary endothelial cells in vitro. *J. Cell. Physiol.*, *133*, 1–13.
- Hoeffel, G., Chen, J., Lavin, Y., Low, D., Almeida, F. F., See, P., Beaudin, A. E., Lum, J., Low, I., Forsberg, E. C., Poidinger, M., Zolezzi, F., Larbi, A., Ng, L. G., Chan, J. K. Y., Greter, M., Becher, B., Samokhvalov, I. M., Merad, M., & Ginhoux, F. (2015). C-Myb+ erythro-myeloid progenitor-derived fetal monocytes give rise to adult tissue-resident macrophages. *Immunity*, *42*, 665–678.
- Hoffman, F. M. (2005). Outcomes and complications after heart transplantation. *J Cardiovasc Nurs*, *20*, 31–42.
- Holmes, C., & Stanford, W. L. (2007). Concise review: stem cell antigen-1: expression, function, and enigma. *Stem Cells*, *25*, 1339–1347.
- Hong, K. U., Guo, Y., Li, Q. H., Cao, P., Al-Maqtari, T., Vajravelu, B. N., Du, J., Book, M. J., Zhu, X., Nong, Y., Bhatnagar, A., & Bolli, R. (2014). C-Kit+ cardiac stem cells alleviate post-myocardial infarction left ventricular dysfunction despite poor engraftment and negligible retention in the recipient heart. *PLoS ONE*, *9*, 1–7.
- Horner, Â. M., Tam, C., Loda, M., Gu, L., Tseng, S., & Rollins, B. J. (2000). Control of Th2 polarization by the chemokine monocyte chemoattractant protein-1. *Nature*, *404*, 407–411.
- Houser, S. R., Margulies, K. B., Murphy, A. M., Spinale, F. G., Francis, G. S., Prabhu, S. D., Rockman, H. A., Kass, D. A., Molkentin, J. D., Sussman, M. A., & Koch, W. J. (2012). Animal models of heart failure a scientific statement from the american heart association. *Circ. Res.*, 131–150.
- Howangyin, K. Y., Zlatanova, I., Pinto, C., Ngkelo, A., Cochain, C., Rouanet, M., Vilar, J., Lemitre, M., Stockmann, C., Fleischmann, B. K., Mallat, Z., & Silvestre, J. S. (2016). Myeloid-epithelial-reproductive receptor tyrosine kinase and milk fat globule epidermal growth factor 8 coordinately improve remodeling after myocardial infarction via local delivery of vascular endothelial growth factor. *Circulation*, *133*, 826–839.
- Hsieh, P. C. H., Segers, V. F. M., Davis, M. E., MacGillivray, C., Gannon, J., Molkentin, J. D., Robbins, J., & Lee, R. T. (2007). Evidence from a genetic fate-mapping study that stem cells refresh adult mammalian cardiomyocytes after injury. *Nat. Med.*, *13*, 970–974.
- Hsu, C. W., Poché, R. A., Saik, J. E., Ali, S., Wang, S., Yosef, N., Calderon, G. A., Scott, L., Vadakkan, T. J., Larina, I. V., West, J. L., & Dickinson, M. E. (2015). Improved angiogenesis in response to localized delivery of macrophage-recruiting molecules. *PLoS ONE*, *10*, 1–27.
- Hsueh, Y. C., Wu, J. M. F., Yu, C. K., Wu, K. K., & Hsieh, P. C. H. (2014). Prostaglandin E2 promotes post-infarction cardiomyocyte replenishment by endogenous stem cells. *EMBO Mol. Med.*, *6*, 496–503.

- Hu, N., Joseph Yost, H., & Clark, E. B. (2001). Cardiac morphology and blood pressure in the adult zebrafish. *Anat. Rec.*, *264*, 1–12.
- Huang, X. P., Sun, Z., Miyagi, Y., Kinkaid, H. M. D., Zhang, L., Weisel, R. D., & Li, R. K. (2010). Differentiation of allogeneic mesenchymal stem cells induces immunogenicity and limits their long-term benefits for myocardial repair. *Circulation*, *122*, 2419–2429. 1
- Hubbard, N. E., Lim, D., Mukutmoni, M., Cai, A., & Erickson, K. L. (2005). Expression and regulation of murine macrophage angiopoietin-2. *Cell. Immunol.*, *234*, 102–109.
- Huebener, P., Abou-Khamis, T., Zymek, P., Bujak, M., Ying, X., Chatila, K., Haudek, S., Thakker, G., & Frangogiannis, N. G. (2008). CD44 is critically involved in infarct healing by regulating the inflammatory and fibrotic response. *J. Immunol. Res.*, *180*, 2625–2633.
- Hulsmans, M., Clauss, S., Xiao, L., Aguirre, A. D., King, K. R., Alan, H., William J., H., Eike M., W., Gunnar, S., Gabriel, C., Yoshiko, I., Yuan, S., Andrej J., S., Hendrik B., S., Kory J., L., Gregory A., F., Diane E., C., Nicolas, D. S., Lucile, M., Nahrendorf, M. (2017). Macrophages facilitate electrical conduction in the heart maarten. *Cell*, *169*, 510–522.
- Hume, D A, Pavli, P., Donahue, R. E., & Fidler, I. J. (1988). The effect of human recombinant macrophage colony-stimulating factor (CSF-1) on the murine mononuclear phagocyte system in vivo. *J Immunol* *141*, 3405–3409.
- Hume, David A., & MacDonald, K. P. A. (2012). Therapeutic applications of macrophage colony-stimulating factor-1 (CSF-1) and antagonists of CSF-1 receptor (CSF-1R) signaling. *Blood*, *119*, 1810–1820.
- Huynh, M. L. N., Fadok, V. A., & Henson, P. M. (2002). Phosphatidylserine-dependent ingestion of apoptotic cells promotes TGF- β 1 secretion and the resolution of inflammation. *J. Clin. Investig.*, *109*, 41–50.
- Ibrahim, A. G. E., Cheng, K., & Marbán, E. (2014). Exosomes as critical agents of cardiac regeneration triggered by cell therapy. *Stem Cell Rep.*, *2*, 606–619.
- Iqbal, M. B., Johns, M., Cao, J., Liu, Y., Yu, S., Hyde, G. D., Laffan, M. a, Marchese, F. P., Cho, S. H., Clark, A. R., Gavins, F. N., Woollard, K. J., Blackshear, P. J., Mackman, N., Dean, J. L., Boothby, M., & Haskard, D. O. (2014). PARP-14 combines with tristetraprolin in the selective posttranscriptional control of macrophage tissue factor expression. *RPTH*, *124*, 3646–3656.
- Iqbal, M. B., & Uk, M. M. (2013). *Novel mechanisms for the post-transcriptional regulation of monocyte-macrophage tissue factor expression by.*
- Irvine, K. M., Burns, C. J., Wilks, A. F., Su, S., Hume, D. A., Sweet, M. J., Irvine, K. M., Burns, C. J., Wilks, A. F., Su, S., Hume, D. A., & Sweet, M. J. (2006). A CSF-1 receptor kinase inhibitor targets effector functions and inhibits pro-inflammatory cytokine production from murine macrophage populations. *FASEB J.*, *20*, 1921–1923.
- Ishigami, S., Ohtsuki, S., Tarui, S., Ousaka, D., Eitoku, T., Kondo, M., Okuyama, M., Kobayashi, J., Baba, K., Arai, S., Kawabata, T., Yoshizumi, K., Tateishi, A., Kuroko, Y., Iwasaki, T., Sato, S., Kasahara, S., Sano, S., & Oh, H. (2015). Intracoronary autologous cardiac progenitor cell transfer in patients with hypoplastic left heart syndrome: The TICAP Prospective Phase 1 Controlled Trial. *Circ. Res.*, *116*, 653–664.
- Islam, S., Zeisel, A., Joost, S., La Manno, G., Zajac, P., Kasper, M., Lönnerberg, P., & Linnarsson, S. (2014). Quantitative single-cell RNA-seq with unique molecular identifiers. *Nat. Methods*, *11*, 163–166.
- Italiani, P., & Boraschi, D. (2014). From monocytes to M1/M2 macrophages: Phenotypical vs. functional differentiation. *Front. Immunol.*, 1–22.
- Ito, C. Y., Li, C. Y. J., Bernstein, A., Dick, J. E., & Stanford, W. L. (2003). Hematopoietic stem cell and progenitor defects in Sca-1/Ly-6A–null mice. *Blood*, *101*, 517–523.

- Ito, S., Ansari, P., Sakatsume, M., Dickensheets, H., Vazquez, N., Donnelly, R. P., Larner, A. C., & Finbloom, D. S. (1999). Interleukin-10 inhibits expression of both interferon alpha- and interferon gamma-induced genes by suppressing tyrosine phosphorylation of STAT1. *Blood*, *93*, 1456–1463.
- Ivashkiv, L. B. (2013). Epigenetic regulation of macrophage polarization and function. *Trends Immunol*, *34*, 216–223.
- Jablonski, K., Amici, S., Webb, L., Ruiz-Rosado, J. D., Popovich, P., Partida-Sanchez, S., & Guerau-de-Arellano, M. (2015). Novel markers to delineate murine M1 and M2 macrophages. *Plos One*, *10*, e0145342.
- Jackson, K. A., & Bleunvenn, L. E. B. H. (2001). Regeneration of ischemic cardiac muscle and vascular endothelium by adult stem cells. *JCI*, *107*, 1395–1402.
- Jaitin, D. A., Kenigsberg, E., Keren-Shaul, H., Elefant, N., Paul, F., Zaretsky, I., Mildner, A., Cohen, N., Jung, S., Tanay, A., & Amit, I. (2014). Massively parallel single cell RNA-Seq for marker-free decomposition of tissues into cell types. *Science*, *343*, 776–779.
- Jakubowski, A. A., Bajorin, D. F., Templeton, M. A., Chapman, P. B., Cody, B. V., Thaler, H., Tao, Y., Filippa, D. A., Williams, L., Sherman, M. L., Garnick, M. B., & Houghton, A. N. (1996). Phase I study of continuous-infusion recombinant macrophage colony-stimulating factor in patients with metastatic melanoma. *Clin. Cancer Res.*, *2*, 295–302.
- Jakubzick, C., Gautier, E. L., Gibbins, S. L., Sojka, D. K., Schlitzer, A., Johnson, T. E., Ivanov, S., Duan, Q., Bala, S., Condon, T., VanRooijen, N., Grainger, J. R., Belkaid, Y., Ma'ayan, A., Riches, D. W. H., Yokoyama, W. M., Ginhoux, F., Henson, P. M., & Randolph, G. J. (2013). Minimal differentiation of classical monocytes as they survey steady-state tissues and transport antigen to lymph nodes. *Immunity*, *39*, 599–610.
- Jenkins, S. J., Ruckerl, D., Cook, P. C., Jones, L. H., Finkelman, F. D., van Rooijen, N., MacDonald, A. S., & Allen, J. E. (2011). Local macrophage proliferation, rather than recruitment from the blood, is a signature of TH2 inflammation. *Science*, *332*, 1284–1288.
- Jetten, N., Verbruggen, S., Gijbels, M. J., Post, M. J., De Winther, M. P. J., & Donners, M. M. P. C. (2014). Anti-inflammatory M2, but not pro-inflammatory M1 macrophages promote angiogenesis in vivo. *Angiogenesis*, *17*, 109–118.
- Jing, H., Vassiliou, E., & Ganea, D. (2003). Prostaglandin E2 inhibits production of the inflammatory chemokines CCL3 and CCL4 in dendritic cells. *J. Leukoc. Biol.*, *74*, 868–879.
- Johnston, P. V., T. Sasano, P., K. Mills, ST. Lee, R. Ruckdeschel Smith, A. C. Lardo, P., S. Lai, C. Steenbergen, G. Gerstenblith, & E. Marbán, (2009). Engraftment, differentiation and functional benefits of autologous cardiosphere-derived cells in porcine ischemic cardiomyopathy. *Circulation*, *60*, 79–87.
- Jones, K. L., Mansell, A., Patella, S., Scott, B. J., Hedger, M. P., De Kretser, D. M., & Phillips, D. J. (2007). Activin A is a critical component of the inflammatory response, and its binding protein, follistatin, reduces mortality in endotoxemia. *PNAS*, *104*, 16239–16244.
- Jopling, C., Sleep, E., Raya, M., Martí, M., Raya, A., & Belmonte, J. C. I. (2010). Zebrafish heart regeneration occurs by cardiomyocyte dedifferentiation and proliferation. *Nature*, *464*, 606–609.
- Jose, M. D., Le Meur, Y., Atkins, R. C., & Chadban, S. J. (2003). Blockade of macrophage colony-stimulating factor reduces macrophage proliferation and accumulation in renal allograft rejection. *Am. J. Transplant.*, *3*, 294–300.
- Jung, J. I., Cho, H. J., Jung, Y. J., Kwon, S. H., Her, S., Choi, S. S., Shin, S. H., Lee, K. W., & Park, J. H. Y. (2015). High-fat diet-induced obesity increases lymphangiogenesis and lymph node metastasis in the B16F10 melanoma allograft model: roles of adipocytes and M2-macrophages. *IJC*, *136*, 258–270.

- Jung, S. B., Choi, M. J., Ryu, D., Yi, H. S., Lee, S. E., Chang, J. Y., Chung, H. K., Kim, Y. K., Kang, S. G., Lee, J. H., Kim, K. S., Kim, H. J., Kim, C. S., Lee, C. H., Williams, R. W., Kim, H., Lee, H. K., Auwerx, J., & Shong, M. (2018). Reduced oxidative capacity in macrophages results in systemic insulin resistance. *Nat Commun*, *9*.
- Kadl, A., Meher, A. K., Sharma, P. R., Lee, M. Y., Doran, A. C., Johnstone, S. R., Elliott, M. R., Gruber, F., Han, J., Chen, W., Kensler, T., Ravichandran, K. S., Isakson, B. E., Wamhoff, B. R., & Leitinger, N. (2010). Identification of a novel macrophage phenotype that develops in response to atherogenic phospholipids via Nrf2. *Circ. Res.*, *107*, 737–746.
- Kagan, J. C., Su, T., Horng, T., Chow, A., Akira, S., & Medzhitov, R. (2008). TRAM couples endocytosis of Toll-like receptor 4 to the induction of interferon- β . *Nat Immunol.*, *9*, 361–368.
- Kambara, K., Ohashi, W., Tomita, K., Takashina, M., Fujisaka, S., Hayashi, R., Mori, H., Tobe, K., & Hattori, Y. (2015). In vivo depletion of CD206+ M2 macrophages exaggerates lung injury in endotoxemic mice. *Am. J. Pathol.*, *185*, 162–171.
- Kawaguchi, N., Smith, A. J., Waring, C. D., Hasan, M. K., Miyamoto, S., Matsuoka, R., & Ellison, G. M. (2010). c-kitpos GATA-4 high rat cardiac stem cells foster adult cardiomyocyte survival through IGF-1 paracrine signalling. *PLoS ONE*, *5*.
- Kayagaki, N., Wong, M. T., Stowe, I. B., Ramani, S. R., Gonzalez, L. C., Akashi-takamura, S., Miyake, K., Zhang, J., Lee, W. P., Forsberg, L. S., Carlson, R. W., & Dixit, V. M. (2013). Noncanonical inflammasome activation by intracellular LPS activation by intracellular LPS independent of TLR4. *Science*, *130*, 1246–1249.
- Kempf, T., Eden, M., Strelau, J., Naguib, M., Willenbockel, C., Tongers, J., Heineke, J., Kotlarz, D., Xu, J., Molckentin, J. D., Niessen, H. W., Drexler, H., & Wollert, K. C. (2006). The transforming growth factor- β superfamily member growth-differentiation factor-15 protects the heart from ischemia/reperfusion injury. *Circ. Res.*, *98*, 351–360.
- Keshet, Y., & Seger, R. (2010). The MAP kinase signaling cascades: a system of hundreds of components regulates a diverse array of physiological functions. *Methods Mol. Biol.*, *661*, 3-38.
- Kikuchi, K., Holdway, J. E., Werdich, A. A., Anderson, R. M., Fang, Y., Egnaczyk, G. F., Evans, T., MacRae, C. A., Stainier, D. Y. R., & Poss, K. D. (2010). Primary contribution to zebrafish heart regeneration by gata4+ cardiomyocytes. *Nature*, *464*, 601–605.
- Kim, K. E., Cho, C. H., Kim, H. Z., Baluk, P., McDonald, D. M., & Koh, G. Y. (2007). In vivo actions of angiopoietins on quiescent and remodeling blood and lymphatic vessels in mouse airways and skin. *ATVB*, *27*, 564–570.
- Kim, M., & Morshead, C. M. (2003). Distinct populations of forebrain neural stem and progenitor cells can be isolated using side-population analysis. *J. Neurosci. Res.*, *23*, 10703–10709.
- Kinnaird, T., Stabile, E., Burnett, M. S., Shou, M., Lee, C. W., Barr, S., Fuchs, S., & Epstein, S. E. (2004). Local delivery of marrow-derived stromal cells augments collateral perfusion through paracrine mechanisms. *Circulation*, *109*, 1543–1549.
- Klemm, F., Möckl, A., Salamero-Boix, A., Alekseeva, T., Schäffer, A., Schulz, M., Niesel, K., Maas, R. R., Groth, M., Elie, B. T., Bowman, R. L., Hegi, M. E., Daniel, R. T., Zeiner, P. S., Zinke, J., Harter, P. N., Plate, K. H., Joyce, J. A., & Sevenich, L. (2021). Compensatory CSF2-driven macrophage activation promotes adaptive resistance to CSF1R inhibition in breast-to-brain metastasis. *Nat. Rev. Cancer.*, *2*, 1086–1101
- Kleveland, O., Kunszt, G., Bratlie, M., Ueland, T., Broch, K., Holte, E., Michelsen, A. E., Bendz, B., Amundsen, B. H., Espevik, T., Aakhus, S., Damås, J. K., Aukrust, P., Wiseth, R., & Gullestad, L. (2016). Effect of a single dose of the interleukin-6 receptor antagonist tocilizumab on inflammation and troponin T release in patients with non-ST-elevation myocardial infarction: A double-blind, randomized, placebo-controlled phase 2 trial. *Eur. J. Cardiol.*, *37*, 2406–2413.

- Kolodziejczyk, A. A., Kim, J. K., Svensson, V., Marioni, J. C., & Teichmann, S. A. (2015). The technology and biology of single-cell RNA sequencing. *Mol Cell*, *54*, 610–620.
- Kovacic, J. C., & Fuster, V. (2001). Cell therapy for patients with acute myocardial infarction ACCRUED evidence to date. *Circ. Res.*, 1287–1290.
- Kratochvill, F., Neale, G., Haverkamp, M., Dyer, M. A., Qualls, J. E., Murray, P. J., Kratochvill, F., Neale, G., Haverkamp, J. M., Velde, L. Van De, & Smith, A. M. (2015). Article TNF counterbalances the emergence of M2 tumor article TNF counterbalances the emergence of M2 Tumor macrophages. *Cell Rep.*, *12*, 1902–1914.
- Krausgruber, T., Blazek, K., Smallie, T., Alzabin, S., Lockstone, H., Sahgal, N., Hussell, T., Feldmann, M., & Udalova, I. A. (2011). IRF5 promotes inflammatory macrophage polarization and T H1-TH17 responses. *Nat. Immunol.*, *12*, 231–238.
- Kroehne, V., Freudenreich, D., Hans, S., Kaslin, J., & Brand, M. (2011). Regeneration of the adult zebrafish brain from neurogenic radial glia-type progenitors. *Dev*, *138*, 4831–4841.
- Kubota, Y., Takubo, K., Shimizu, T., Ohno, H., Kishi, K., Shibuya, M., Saya, H., & Suda, T. (2009). M-CSF inhibition selectively targets pathological angiogenesis and lymphangiogenesis. *J Exp Med*, *206*, 1089–1102.
- Kurowska-Stolarska, M., Stolarski, B., Kewin, P., Murphy, G., Corrigan, C. J., Ying, S., Pitman, N., Mirchandani, A., Rana, B., van Rooijen, N., Shepherd, M., McSharry, C., McInnes, I. B., Xu, D., & Liew, F. Y. (2009). IL-33 amplifies the polarization of alternatively activated macrophages that contribute to airway inflammation. *J. Immunol. Res.*, *183*, 6469–6477.
- Kuwahara, G., Nishinakamura, H., Kojima, D., Tashiro, T., & Kodama, S. (2014). GM-CSF treated F4/80+ BMCs improve murine hind limb ischemia similar to M-CSF differentiated macrophages. *PLoS ONE*, *9*.
- Kuznetsova, T., Prange, K. H. M., Glass, C. K., & de Winther, M. P. J. (2020). Transcriptional and epigenetic regulation of macrophages in atherosclerosis. *Nature Rev. Cardiol.*, *17*, 216–228.
- Lambert, J. M., Lopez, E. F., & Lindsey, M. L. (2008). Macrophages role following myocardial infarction. *Int. J. Cardiol.*, *130*, 147–158.
- Lancet, T. (2015). Expression of concern: The SCIPPIO trial. *The Lancet*, *383*, 1279.
- Landsman, L., Liat, B. O., Zernecke, A., Kim, K. W., Krauthgamer, R., Shagdarsuren, E., Lira, S. A., Weissman, I. L., Weber, C., & Jung, S. (2009). CX3CR1 is required for monocyte homeostasis and atherogenesis by promoting cell survival. *Blood*, *113*, 963–972.
- Lang, R., Patel, D., Morris, J. J., Rutschman, R. L., & Murray, P. J. (2002). Shaping Gene expression in activated and resting primary macrophages by IL-10. *J. Immunol. Res.*, *169*, 2253–2263.
- Laugwitz, K.-L., Moretti, A., Caron, L., Nakano, A., & Chien, K. R. (2008). Islet1 cardiovascular progenitors: a single source for heart lineages? *Dev.*, *135*, 193–205.
- Laugwitz, Karl-Ludwig, Moretti, A., Lam, A., Gruber, P., Chen, Y., Woodard, S., Lin, L.-Z., Cai, C.-L., Lu, M. M., Reth, M., Platoshyn, O., Yuan, J. X.-J., Evans, S., & Chien, K. R. (2005). Postnatal isl1+ cardioblasts enter fully differentiated cardiomyocyte lineages. *Nature*, *10*, 647–653.
- Lavin, Y., Kobayashi, S., Leader, A., Amir, E. ad D., Elefant, N., Bigenwald, C., Remark, R., Sweeney, R., Becker, C. D., Levine, J. H., Meinhof, K., Chow, A., Kim-Shulze, S., Wolf, A., Medaglia, C., Li, H., Rytlewski, J. A., Emerson, R. O., Solovyov, A., Merad, M. (2017). Innate immune landscape in early lung adenocarcinoma by paired single-cell analyses. *Cell*, *169*, 750-765.e17.
- Lavine, K. J., Epelman, S., Uchida, K., Weber, K. J., Nichols, C. G., Schilling, J. D., Ornitz, D. M., Randolph, G. J., & Mann, D. L. (2014). Distinct macrophage lineages contribute to disparate patterns of cardiac recovery and remodeling in the neonatal and adult heart. *PNAS*, *111*, 16029–16034.

- Lavine, K. J., Pinto, A. R., Epelman, S., Kopecky, B. J., Clemente-casares, X., Godwin, J., Rosenthal, N., & Kovacic, J. C. (2018). The macrophage in cardiac homeostasis and disease jacc macrophage in CVD series (Part 4). *J. Am. Coll. Cardiol.*, 72(18).
- Lawrence, T., & Natoli, G. (2011). Transcriptional regulation of macrophage polarization: enabling diversity with identity. *Nat. Rev. Immunol.*, 11(1), 750–761.
- Lázár, E., Sadek, H. A., & Bergmann, O. (2017). Cardiomyocyte renewal in the human heart: Insights from the fall-out. *Eur* 38, 2333–2339.
- Lê, S., Josse, J., & Husson, F. (2008). FactoMineR: An R Package for Multivariate Analysis. *J. Stat. Softw.*, 25(1).
- Le, T. Y. L., Thavapalachandran, S., Kizana, E., & Chong, J. J. (2017). New developments in cardiac regeneration. *Heart Lung Circ.*, 26, 316–322.
- Leblond, A. L., Klinkert, K., Martin, K., Turner, E. C., Kumar, A. H., Browne, T., & Caplice, N. M. (2015). Systemic and cardiac depletion of M2 macrophage through CSF-1R signaling inhibition alters cardiac function post myocardial infarction. *PLoS ONE*, 10, 1–13.
- Lee, C. M., & Hu, J. (2013). Cell density during differentiation can alter the phenotype of bone marrow-derived macrophages. *Cell Biosci*, 3, 3–7.
- Lee, E. Y., Lee, Z. H., & Song, Y. W. (2009). CXCL10 and autoimmune diseases. *Autoimmun. Rev.*, 8, 379–383.
- Lee, Mejeong, Aoki, M., Kondo, T., Kobayashi, K., Okumura, K., Komori, K., & Murohara, T. (2005). Therapeutic angiogenesis with intramuscular injection of low-dose recombinant granulocyte-colony stimulating factor. *ATVB*, 25, 2535–2541.
- Lee, Myoungsoo, Lee, Y., Song, J., Lee, J., & Chang, S. (2018). Tissue-specific role of CX3 CR1 expressing immune cells and their relationships with human disease. *Immune Netw.*, 18, 1–19.
- Lee, R. T. (2018). Adult cardiac stem cell concept and the process of science. *Circulation*, 2940–2942.
- Lee, S., Wolf, P., Escudero, R., Deutsch, R., & Jamieson, SW Thistlethwaite, P. (2000). Early expression of angiogenesis in acute myocardial ischemia and infarction. *N Engl J Med*, 342, 626–633.
- Lee, Sena J., Evers, S., Roeder, D., Parlow, A. F., Risteli, J., Risteli, L., Lee, Y. C., Feizi, T., Langen, H., & Nussenzweig, M. C. (2002). Mannose receptor-mediated regulation of serum glycoprotein homeostasis. *Science*, 295, 1898–1901. 40
- Lee, Seung Jun, Lee, C. K., Kang, S., Park, I., Kim, Y. H., Kim, S. K., Hong, S. P., Bae, H., He, Y., Kubota, Y., & Koh, G. Y. (2018). Angiopoietin-2 exacerbates cardiac hypoxia and inflammation after myocardial infarction. *J. Clin. Investig.*, 128, 5018–5033.
- Leibovich, S. J., Polverini, P. J., Shepard, H. M., Wiseman, D. M., Shively, V., & Nuseir, N. (1987). Macrophage-induced angiogenesis is mediated by tumour necrosis factor- α . *Nature*, 329, 630–632.
- Leid, J., Carrelha, J., Boukarabila, H., Epelman, S., Jacobsen, S. E. W., & Lavine, K. J. (2016). Primitive embryonic macrophages are required for coronary development and maturation. *Circ. Res.*, 118, 1498–1511.
- Lenzo, J. C., Turner, A. L., Cook, A. D., Vlahos, R., Anderson, G. P., Reynolds, E. C., & Hamilton, J. A. (2012). Control of macrophage lineage populations by CSF-1 receptor and GM-CSF in homeostasis and inflammation. *Immunol. Cell Biol.*, 90, 429–440.
- Leor, J., Rozen, L., Zulloff-Shani, A., Feinberg, M. S., Amsalem, Y., Barbash, I. M., Kachel, E., Holbova, R., Mardor, Y., Daniels, D., Ocherashvilli, A., Orenstein, A., & Danon, D. (2006). Ex vivo activated human macrophages improve healing, remodeling, and function of the infarcted heart. *Circulation*, 114, 94–100.

- Lestuzzi, C. (2016). Primary tumors of the heart. *Curr. Opin. Cardiol.*, *31*, 593–598.
- Letterio, J., & Roberts, A. (1998). Regulation of immune responses by TGF- β . *Annu. Rev. Immunol.*, *16*, 137–161.
- Leuschner, F., Dutta, P., Gorbatov, R., Novobrantseva, T. I., Donahoe, J. S., Courties, G., Lee, K. M., Kim, J. I., Markmann, J. F., Marinelli, B., Panizzi, P., Lee, W. W., Iwamoto, Y., Milstein, S., Epstein-Barash, H., Cantley, W., Wong, J., Cortez-Retamozo, V., Newton, A., ... Nahrendorf, M. (2011). Therapeutic siRNA silencing in inflammatory monocytes in mice. *Nat. Biotechnol.*, *29*, 1005–1010.
- Levy, D., Kenchaiah, S., Larson, M. G., Benjamin, E. J., Kupka, M. J., Ho, K. K. L., Murabito, J. M., & Vasan, R. S. (2002). Long-term trends in the incidence of and survival with heart failure. *NEJM*, *347*, 1397–1402.
- Lewis, C. E., & Pollard, J. W. (2006). Distinct role of macrophages in different tumor microenvironments. *Cancer Res.*, *66*, 605–612.
- Lewis, J. C., Bennett-Cain, a L., DeMars, C. S., Doellgast, G. J., Grant, K. W., Jones, N. L., & Gupta, M. (1995). Procoagulant activity after exposure of monocyte-derived macrophages to minimally oxidized low density lipoprotein. Co-localization of tissue factor antigen and nascent fibrin fibers at the cell surface. *The Am. J. Pathol.*, *147*, 1029–1040.
- Li, G., Plonowska, K., Kuppusamy, R., Sturzu, A., & Wu, S. M. (2015). Identification of cardiovascular lineage descendants at single-cell resolution. *Dev.*, *142*, 846–857.
- Li, Qiong, Li, B., Wang, X., Leri, A., Jana, K. P., Liu, Y., Kajstura, J., Baserga, R., & Anversa, P. (1997). Overexpression of insulin-like growth factor-1 in mice protects from myocyte death after infarction, attenuating ventricular dilation, wall stress, and cardiac hypertrophy. *J. Clin. Investig.*, *100*, 1991–1999.
- Li, Qiutang, & Verma, I. M. (2002). NF- κ B regulation in the immune system. *Nat. Rev. Immunol.*, *2*, 725–734.
- Li, T.-S. S., Cheng, K., Malliaras, K., Smith, R. R., Zhang, Y., Sun, B., Matsushita, N., Blusztajn, A., Terrovitis, J., Kusuoka, H., Marbán, L., & Marbán, E. (2012). Direct comparison of different stem cell types and subpopulations reveals superior paracrine potency and myocardial repair efficacy with cardiosphere-derived cells. *JACC*, *59*, 942–953.
- Li, W., Hsiao, H.-M., Higashikubo, R., Saunders, B. T., Bharat, A., Goldstein, D. R., Krupnick, A. S., Gelman, A. E., Lavine, K. J., & Kreisel, D. (2016). Heart-resident CCR2⁺ macrophages promote neutrophil extravasation through TLR9/MyD88/CXCL5 signaling. *JCI Insight*, *1*, 1–14.
- Lim, A. K. H., Ma, F. Y., Nikolic-Paterson, D. J., Thomas, M. C., Hurst, L. A., & Tesch, G. H. (2009). Antibody blockade of c-fms suppresses the progression of inflammation and injury in early diabetic nephropathy in obese db/db mice. *Diabetologia*, *52*, 1669–1679.
- Lim, H. Y., Lim, S. Y., Tan, C. K., Thiam, C. H., Goh, C. C. C., Carbajo, D., Chew, S. H. S., See, P., Chakarov, S., Wang, X. N., Lim, L. H., Johnson, L. A., Lum, J., Fong, C. Y., Bongso, A., Biswas, A., Goh, C. C. C., Evrard, M., Yeo, K. P., Angeli, V. (2018). Hyaluronan receptor LYVE-1-expressing macrophages maintain arterial tone through hyaluronan-mediated regulation of smooth muscle cell collagen. *Immunity*, *49*, 326-341.e7.
- Limana, F., Zacheo, A., Mocini, D., Mangoni, A., Borsellino, G., Diamantini, A., De Mori, R., Battistini, L., Vigna, E., Santini, M., Loiaconi, V., Pompilio, G., Germani, A., & Capogrossi, M. C. (2007). Identification of myocardial and vascular precursor cells in human and mouse epicardium. *Circ. Res.*, *101*, 1255–1265.
- Lin, H., Lee, E., Hestir, K., Leo, C., Huang, M., Bosch, E., Halenbeck, R., Wu, G., Zhou, A., Behrens, D., Hollenbaugh, D., Linnemann, T., Qin, M., Wong, J., Chu, K., Doberstein, S. K., & Williams, L. T. (2008). Discovery of a cytokine and its receptor by functional screening of the extracellular proteome. *Science*, *707*, 807–811.

- Lin, Y., Roberts, T. J., Sriram, V., Cho, S., & Brutkiewicz, R. R. (2003). Myeloid marker expression on antiviral CD8+T cells following an acute virus infection. *Eur. J Immunol.* *33*, 2736–2743.
- Lind, L., Siegbahn, A., Lindahl, B., Stenemo, M., Sundström, J., & Ärnlov, J. (2015). Discovery of new risk markers for ischemic stroke using a novel targeted proteomics chip. *Stroke*, *46*, 3340–3347.
- Lionakis, M. S., Swamydas, M., Fischer, B. G., Plantinga, T. S., Johnson, M. D., Jaeger, M., Green, N. M., Masedunskas, A., Weigert, R., Mikelis, C., Wan, W., Lee, C. R., Lim, J. K., Rivollier, A., Yang, J. C., Laird, G. M., Wheeler, R. T., Alexander, B. D., Perfect, J. R., Murphy, P. M. (2013). CX3CR1-dependent renal macrophage survival promotes. *J Clin Invest.*, *123*, 5035–5051.
- Litviňuková, M., Talavera-López, C., Maatz, H., Reichart, D., Worth, C. L., Lindberg, E. L., Kanda, M., Polanski, K., Heinig, M., Lee, M., Nadelmann, E. R., Roberts, K., Tuck, L., Fasouli, E. S., DeLaughter, D. M., McDonough, B., Wakimoto, H., Gorham, J. M., Samari, S., Teichmann, S. A. (2020). Cells of the adult human heart. *Nature*, *588*, 466–472.
- Liu, M. L., Nagai, T., Tokunaga, M., Iwanaga, K., Matsuura, K., Takahashi, T., Kanda, M., Kondo, N., Naito, A. T., Komuro, I., & Kobayashi, Y. (2014). Anti-inflammatory peptides from cardiac progenitors ameliorate dysfunction after myocardial infarction. *JAHA*, *3*, 1–25.
- Liu, N., Liu, L., & Pan, X. (2014). Single-cell analysis of the transcriptome and its application in the characterization of stem cells and early embryos. *Cell. Mol. Life Sci.*, *71*, 2707–2715.
- Llorens-Bobadilla, E., Zhao, S., Baser, A., Saiz-Castro, G., Zwadlo, K., & Martin-Villalba, A. (2015). Single-cell transcriptomics reveals a population of dormant neural stem cells that become activated upon brain injury. *Cell Stem Cell*, *17*, 329–340.
- Locati, M., Mantovani, A., & Sica, A. (2013). Macrophage activation and polarization as an adaptive component of innate immunity. *Adv. Immunol.*, *120*, 163–184.
- Lokeshwar, B. L., & Lin, H. S. (1988). Development and characterization of monoclonal antibodies to murine macrophage colony-stimulating factor. *J. Immunol*, *141*, 483–488.
- López-Peláez, M., Soria-Castro, I., Boscá, L., Fernández, M., & Alemany, S. (2011). Cot/tpl2 activity is required for TLR-induced activation of the Akt p70 S6k pathway in macrophages: Implications for NO synthase 2 expression. *Eur. J Immunol.* *41*, 1733–1741.
- Losordo, D. W., Henry, T. D., Davidson, C., Sup Lee, J., Costa, M. A., Bass, T., Mendelsohn, F., Fortuin, F. D., Pepine, C. J., Traverse, J. H., Amrani, D., Ewenstein, B. M., Riedel, N., Story, K., Barker, K., Povsic, T. J., Harrington, R. A., & Schatz, R. A. (2011). Intramyocardial, autologous CD34+ cell therapy for refractory angina. *Circ. Res.*, *109*, 428–436.
- Losordo, D. W., Schatz, R. A., White, C. J., Udelson, J. E., Veereshwarayya, V., Durgin, M., Poh, K. K., Weinstein, R., Kearney, M., Chaudhry, M., Burg, A., Eaton, L., Heyd, L., Thorne, T., Shturman, L., Hoffmeister, P., Story, K., Zak, V., Dowling, D., ... Henry, T. D. (2007). Intramyocardial transplantation of autologous CD34+ stem cells for intractable angina: A phase I/IIa double-blind, randomized controlled trial. *Circulation*, *115*(25), 3165–3172.
- Loughner, C. L., Bruford, E. A., Mcandrews, M. S., Delp, E. E., & Swamynathan, S. (2016). Organization, evolution and functions of the human and mouse Ly6 / uPAR family genes. *Hum. Genomics.*, *21*, 10.
- Lumeng, C. N., Bodzin, J. L., & Saltiel, A. R. (2007). Obesity induces a phenotypic switch in adipose tissue macrophage polarization. *J Clin Invest*, *117*, 175–184.
- Lundy, S. D., Gantz, J. A., Pagan, C. M., Filice, D., & Laflamme, M. A. (2014). Pluripotent stem cell derived cardiomyocytes for cardiac repair. *Curr. Treat. Options Cardiovasc. Med.*, *16*.
- Ma, Q., Zhou, B., & Pu, W. T. (2008). Reassessment of Isl1 and Nkx2-5 cardiac fate maps using a Gata4-based reporter of Cre activity. *Dev. Biol.*, *323*(1), 98–104.

- Ma, Xiaojing, Gri, G., & Trinchieri, G. (1997). A Novel ets-2-Related Nuclear Factor Is Involved in Transcriptional Activation and LPS Stimulation of Monocytic Cells. *J. Biol. Chem.*, 272, 10389–10395.
- Ma, Xiaolei, Lin, W. Y., Chen, Y., Stawicki, S., Mukhyala, K., Wu, Y., Martin, F., Bazan, J. F., & Starovasnik, M. A. (2012). Structural basis for the dual recognition of helical cytokines IL-34 and CSF-1 by CSF-1R. *Structure*, 20, 676–687.
- Mabbott, N. A., Kenneth Baillie, J., Hume, D. A., & Freeman, T. C. (2010). Meta-analysis of lineage-specific gene expression signatures in mouse leukocyte populations. *Immunobiology*, 215, 724–736.
- MacDonald, K. P. A., Palmer, J. S., Cronau, S., Seppanen, E., Olver, S., Raffelt, N. C., Kuns, R., Pettit, A. R., Clouston, A., Wainwright, B., Branstetter, D., Smith, J., Paxton, R. J., Cerretti, D. P., Bonham, L., Hill, G. R., & Hume, D. A. (2010). An antibody against the colony-stimulating factor 1 receptor depletes the resident subset of monocytes and tissue- and tumor-associated macrophages but does not inhibit inflammation. *Blood*, 116, 3955–3963.
- Mack, K. D., Goetz, M. Von, Lin, M., Venegas, M., Barnhart, J., Lu, Y., Lamar, B., Stull, R., Silvin, C., Owings, P., Bih, F. Y., & Abo, A. (2005). Functional identification of kinases essential for T-cell activation through a genetic suppression screen. *Immunol. Letters*, 96, 129–145.
- Mackman, B. N., Brand, K., & Edgington, T. S. (1991). Lipopolysaccharide-mediated transcriptional activation of the human tissue factor gene in THP-1 monocytic cells requires both activator protein 1 and nuclear factor kB binding sites. *J Exp Med*, 174.
- Mackman, N., Morrissey, J. H., Fowler, B., & Edgington, T. S. (1989). Complete sequence of the human tissue factor gene, a highly regulated cellular receptor that initiates the coagulation protease cascade. *Biochemistry*, 28, 1755–1762.
- Madisen, L., Zwingman, T. A., Sunkin, S. M., Oh, S. W., Zariwala, H. A., Gu, H., Ng, L. L., Palmiter, R. D., Hawrylycz, M. J., Jones, A. R., Lein, E. S., & Zeng, H. (2010). A robust and high-throughput Cre reporting and characterization system for the whole mouse brain. *Nat. Neurosci.*, 13, 133–142.
- Mahajan, S., Decker, C. E., Yang, Z., Veis, D., Mellins, E. D., & Faccio, R. (2019). Plcy2/Tmem178 dependent pathway in myeloid cells modulates the pathogenesis of cytokine storm syndrome. *J. Autoimmun.*, 100, 62–74.
- Mahmoud, A. I., & Porrello, E. R. (2011). Turning back the cardiac regenerative clock : lessons from the neonate. *TCM*, 22, 128–133.
- Mahmoud, A. I., Porrello, E. R., Kimura, W., Olson, E. N., & Sadek, H. A. (2014). Surgical models for cardiac regeneration in neonatal mice. *Nat. Protoc.*, 9, 305–311. 21
- Makkar, R. R., Smith, R. R., Cheng, K., Malliaras, K., Thomson, L. E. J., Berman, D., Czer, L. S. C., Marbán, L., Mendizabal, A., Johnston, P. V, Russell, S. D., Schuleri, K. H., Lardo, A. C., Gerstenblith, G., & Marbán, E. (2012). Intracoronary cardiosphere-derived cells for heart regeneration after myocardial infarction (CADUCEUS): a prospective, randomised phase 1 trial. *Lancet.*, 379, 895–904.
- Malliaras, K., Ibrahim, A., Tseliou, E., Liu, W., Sun, B., Middleton, R. C., Seinfeld, J., Wang, L., Sharifi, B. G., & Marbán, E. (2014). Stimulation of endogenous cardioblasts by exogenous cell therapy after myocardial infarction. *EMBO Mol. Med.*, 6, 760–777.
- Malliaras, Zhang, Y., Seinfeld, J., Galang, G., Tseliou, E., Cheng, K., Sun, B., Aminzadeh, M., & Marbán, E. (2013). Cardiomyocyte proliferation and progenitor cell recruitment underlie therapeutic regeneration after myocardial infarction in the adult mouse heart. *EMBO Mol. Med.*, 5, 191–209.
- Mangi, A. A., Noiseux, N., Kong, D., He, H., Rezvani, M., Ingwall, J. S., & Dzau, V. J. (2003). Mesenchymal stem cells modified with Akt prevent remodeling and restore performance of infarcted hearts. *Nat. Med.*, 9, 1195–1201.

- Manrique-Acevedo, C., Chinnakotla, B., Padilla, J., Martinez-Lemus, L. A., & Gozal, D. (2020). Obesity and cardiovascular disease in women. *Int J Obes*, *44*, 1210–1226.
- Mantovani, A. (1999). The chemokine system: redundancy for robust outputs. *Immunol. Today*, *20*, 254–257.
- Mantovani, A., Locati, M., Vecchi, A., Sozzani, S., & Allavena, P. (2001). Decoy receptors: A strategy to regulate inflammatory cytokines and chemokines. *Trends Immunol.*, *22*, 328–336.
- Mantovani, A., Sica, A., Sozzani, S., Allavena, P., Vecchi, A., & Locati, M. (2004). The chemokine system in diverse forms of macrophage activation and polarization. *Trends Immunol.*, *25*, 677–686.
- Mantovani, A., Sozzani, S., Locati, M., Allavena, P., & Sica, A. (2002). Macrophage polarization: tumor-associated macrophages as a paradigm for polarized M2 mononuclear phagocytes. *Trends Immunol.*, *23*, 549–555.
- Marim, F. M., Silveira, T. N., Lima, D. S., & Zamboni, D. S. (2010). A method for generation of bone marrow-derived macrophages from cryopreserved mouse bone marrow cells. *PLoS ONE*, *5*, 1–8.
- Markousis-Mavrogenis, G., Tromp, J., Ouwerkerk, W., Devalaraja, M., Anker, S. D., Cleland, J. G., Dickstein, K., Filippatos, G. S., van der Harst, P., Lang, C. C., Metra, M., Ng, L. L., Ponikowski, P., Samani, N. J., Zannad, F., Zwinderman, A. H., Hillege, H. L., van Veldhuisen, D. J., Kakkor, R., van der Meer, P. (2019). The clinical significance of interleukin-6 in heart failure: results from the BIOSTAT-CHF study. *EJHF*, *21*, 965–973.
- Martin, C. M., Meeson, A. P., Robertson, S. M., Hawke, T. J., Richardson, J. A., Bates, S., Goetsch, S. C., Gallardo, T. D., & Garry, D. J. (2004). Persistent expression of the ATP-binding cassette transporter, *Abcg2*, identifies cardiac SP cells in the developing and adult heart. *Dev. Biol.*, *265*, 262–275.
- Martinez, F. O. (2011). Regulators of macrophage activation. *Eur. J Immunol.* *41*, 1531–1534.
- Martinez, F. O., & Gordon, S. (2014). The M1 and M2 paradigm of macrophage activation: time for reassessment. *F1000prime Reports*, *6*, 13.
- Martinez, F. O., Helming, L., & Gordon, S. (2008). Alternative Activation of Macrophages: An Immunologic Functional Perspective. *Annu. Rev. Immunol.*, *27*, 451–483.
- Martinez, F. O., Helming, L., Milde, R., Varin, A., Melgert, B. N., Draijer, C., Thomas, B., Fabbri, M., Crawshaw, A., Ho, L. P., Hacken, N. H. T., Jiménez, V. C., Kootstra, N. A., Hamann, J., Greaves, D. R., Locati, M., Mantovani, A., & Gordon, S. (2013). Genetic programs expressed in resting and IL-4 alternatively activated mouse and human macrophages: Similarities and differences. *Blood*, *121*, 57–69.
- Martini, E., Kunderfranco, P., Peano, C., Carullo, P., Cremonesi, M., Schorn, T., Carriero, R., Termanini, A., Colombo, F. S., Jachetti, E., Panico, C., Faggian, G., Fumero, A., Torracca, L., Molgora, M., Cibella, J., Pagiatakis, C., Brummelman, J., Alvisi, G., Kallikourdis, M. (2019). Single-cell sequencing of mouse heart immune infiltrate in pressure overload-driven heart failure reveals extent of immune activation. *Circulation*, *140*, 2089–2107.
- Masaoka, T., Shibata, H., Ohno, R., Katoh, S., Harada, M., Motoyoshi, K., Takaku, F., & Sakuma, A. (1990). Double-blind test of human urinary macrophage colony-stimulating factor for allogeneic and syngeneic bone marrow transplantation: effectiveness of treatment and 2-year follow-up for relapse of leukaemia. *Br. J. Haematol.*, *76*, 501–505.
- Mass, E., Ballesteros, I., Farlik, M., Halbritter, F., Günther, P., Crozet, L., Jacome-Galarza, C. E., Händler, K., Klughammer, J., Kobayashi, Y., Gomez-Perdiguero, E., Schultze, J. L., Beyer, M., Bock, C., & Geissmann, F. (2016). Specification of tissue-resident macrophages during organogenesis. *Science*, *353*(6304), 10–12. 8

- Massaia, A., Chaves, P., Samari, S., Meyer, K., Miragaia, R. J., Teichmann, S. A., & Nosedá, M. (2018). Single cell gene expression to understand the dynamic architecture of the heart. *Front. Cardiovasc. Med*, 5, 1–19.
- Matsunaga, T., Weihrauch, D. W., Moniz, M. C., Tessmer, J., Wartier, D. C., & Chilian, W. M. (2002). Angiostatin inhibits coronary angiogenesis during impaired production of nitric oxide. *Circulation*, 105, 2185–2191.
- Matsuura, K., Nagai, T., Nishigaki, N., Oyama, T., Nishi, J., Wada, H., Sano, M., Toko, H., Akazawa, H., Sato, T., Nakaya, H., Kasanuki, H., & Komuro, I. (2004). Adult cardiac sca-1-positive cells differentiate into beating cardiomyocytes. *JBC*, 279, 11384–11391.
- Matsuura, K., Nobuhisa, H., & Komuro, I. (2009). Transplantation of cardiac progenitor cells ameliorates cardiac dysfunction after myocardial infarction in mice. *J. Clin. Investig.*, 119, 2204–2217.
- McDavid, A., Finak, G., Chattopadhyay, P. K., Dominguez, M., Lamoreaux, L., Ma, S. S., Roederer, M., & Gottardo, R. (2013). Data exploration, quality control and testing in single-cell qPCR-based gene expression experiments. *Bioinformatics*, 29, 461–467.
- McLaren, J. E., Michael, D. R., Ashlin, T. G., & Ramji, D. P. (2011). Cytokines, macrophage lipid metabolism and foam cells: Implications for cardiovascular disease therapy. *Prog. Lipid Res*, 50, 331–347.
- Medbury, H. J., James, V., Ngo, J., Hitos, K., Wang, Y., Harris, D., & Fletcher, J. (2013). Differing association of macrophage subsets with atherosclerotic plaque stability. *Int Angiol.*, 32, 74–84.
- Mensah, G. A., Roth, G. A., Sampson, U. K. A., Moran, A. E., Feigin, V. L., Forouzanfar, M. H., Naghavi, M., & Murray, C. J. L. (2015). Mortality from cardiovascular diseases in sub-Saharan Africa, 1990–2013: a systematic analysis of data from the Global Burden of Disease Study 2013. *Cardiovasc. J. Afr*, 26, S6–S10.
- Mercola, M., Ruiz-Lozano, P., & Schneider, M. D. (2011). Cardiac muscle regeneration: lessons from development. *Genes*, 25, 299–309.
- Messina, E., De Angelis, L., Frati, G., Morrone, S., Chimenti, S., Fiordaliso, F., Salio, M., Battaglia, M., Latronico, M. V. G., Coletta, M., Vivarelli, E., Frati, L., Cossu, G., & Giacomello, A. (2004). Isolation and expansion of adult cardiac stem cells from human and murine heart. *Circ. Res.*, 95, 911–921.
- Meyer, G. P., Wollert, K. C., Lotz, J., Steffens, J., Lippolt, P., Fichtner, S., Hecker, H., Schaefer, A., Arseniev, L., Hertenstein, B., Ganser, A., & Drexler, H. (2006). Intracoronary bone marrow cell transfer after myocardial infarction: Eighteen months' follow-up data from the randomized, controlled BOOST (Bone marrow transfer to enhance ST-elevation infarct regeneration) trial. *Circulation*, 113, 1287–1294.
- Michalopoulos, G. K. (2007). Liver Regeneration. *J. Cell Physiol.*, 213, 286–300.
- Mills, C. D., Kincaid, K., Alt, J. M., Heilman, M. J., & Hill, A. M. (2000). M-1/M-2 macrophages and the Th1/Th2 paradigm. *J. Immunol. Res.*, 164, 6166–6173.
- Mohamed, T. M. A., Ang, Y. S., Radzinsky, E., Zhou, P., Huang, Y., Eifenbein, A., Foley, A., Magnitsky, S., & Srivastava, D. (2018). Regulation of cell cycle to stimulate adult cardiomyocyte proliferation and cardiac regeneration. *Cell*, 173, 104–116.e12.
- Molawi, K., Wolf, Y., Kandalla, P. K., Favret, J., Hagemeyer, N., Frenzel, K., Pinto, A. R., Klapproth, K., Henri, S., Malissen, B., Rodewald, H.-R., Rosenthal, N. A., Bajenoff, M., Prinz, M., Jung, S., & Sieweke, M. H. (2014). Progressive replacement of embryo-derived cardiac macrophages with age. *The J Exp Med*, 211, 2151–2158.
- Molenaar, B., Timmer, L. T., Droog, M., Perini, I., Versteeg, D., Kooijman, L., Monshouwer-Kloots, J., de Ruiter, H., Gladka, M. M., & van Rooij, E. (2021). Single-cell transcriptomics following ischemic injury identifies a role for B2M in cardiac repair. *Commun. Bio.*, 4, 1–15.

- Montanaro, F., Liadaki, K., Volinski, J., Flint, A., & Kunkel, L. M. (2003). Skeletal muscle engraftment potential of adult mouse skin side population cells. *PNAS*, *100*, 9336–9341.
- Moore, K. W., Malefyt, R. D. W., Co, R. L., & Garra, A. O. (2001). Interleukin-10 and the interleukin-10 receptor. *Annu Rev Immunol*, *19*, 683–765.
- Moran, A. E., Forouzanfar, M. H., Roth, G. A., Mensah, G. A., Ezzati, M., & Murray, C. J. L. (2014). The global burden of disease 2010 study. *Circulation*, *129*, 1483–1492.
- Moretti, A., Caron, L., Nakano, A., Lam, J. T., Bernshausen, A., Chen, Y., Qyang, Y., Bu, L., Sasaki, M., Martin-Puig, S., Sun, Y., Evans, S. M., Laugwitz, K. L., & Chien, K. R. (2006). Multipotent embryonic isl1+ progenitor cells lead to cardiac, smooth muscle, and endothelial cell diversification. *Cell*, *127*, 1151–1165.
- Morimoto, H., & Takahashi, M. (2007). Role of monocyte chemoattractant protein-1 in myocardial infarction. *IJBS*, *3*, 159–167.
- Morimoto, T., Sunagawa, Y., Kawamura, T., Takaya, T., Wada, H., Nagasawa, A., Komeda, M., Fujita, M., Shimatsu, A., Kita, T., & Hasegawa, K. (2008). The dietary compound curcumin inhibits p300 histone acetyltransferase activity and prevents heart failure in rats. *J. Clin. Investig.*, *118*, 868–878.
- Morris, L., Graham, C. F., & Gordon, S. (1991). Macrophages in haemopoietic and other tissues of the developing mouse detected by the monoclonal antibody F4/80. *Dev.* *112*, 517–526.
- Mosser, D. M. (2003). The many faces of macrophage activation. *J. Leukoc. Biol.*, *73*, 209–212.
- Mosser, D. M., & Karp, C. L. (1999). Receptor mediated subversion of macrophage cytokine production by intracellular pathogens. *Curr. Opin. Immunol*, *11*, 406–411.
- Mozaffarian, D. (2016). Dietary and policy priorities for cardiovascular disease, diabetes, and obesity. *Circulation*, *133*, 187–225.
- Mun, S. H., Park, P. S. U., & Park-Min, K. H. (2020). The M-CSF receptor in osteoclasts and beyond. *Exp. Mol. Med.*, *52*, 1239–1254.
- Munn, D. H., Garnick, M. B., & Cheung, N. K. V. (1990). Effects of parenteral recombinant human macrophage colony-stimulating factor on monocyte number, phenotype, and antitumor cytotoxicity in nonhuman primates. *Blood*, *75*, 2042–2048.
- Murayama, T., Yokode, M., Kataoka, H., Imabayashi, T., Yoshida, H., Sano, H., Nishikawa, S., Nishikawa, S. I., & Kita, T. (1999). Intraperitoneal administration of anti-c-fms monoclonal antibody prevents initial events of atherogenesis but does not reduce the size of advanced lesions in apolipoprotein E-deficient mice. *Circulation*, *99*, 1740–1746.
- Murray, P. J., Allen, J. E., Biswas, S. K., Fisher, E. A., Gilroy, D. W., Goerdt, S., Gordon, S., Hamilton, J. A., Ivashkiv, L. B., Lawrence, T., Locati, M., Mantovani, A., Martinez, F. O., Mege, J. L., Mosser, D. M., Natoli, G., Saeij, J. P., Schultze, J. L., Shirey, K. A., Wynn, T. A. (2014). Macrophage activation and polarization: nomenclature and experimental guidelines. *Immunity*, *41*, 14–20.
- Murray, P. J., & Wynn, T. A. (2011). Protective and pathogenic functions of macrophage subsets. *Nat. Rev. Immunol.*, *11*, 723–737.
- Murry, C. E., Soonpaa, M. H., Reinecke, H., Nakajima, H., Nakajima, H. O., Rubart, M., Pasumarthi, K. B. S., Virag, J. I., Bartelmez, S. H., Poppa, V., Bradford, G., Dowell, J. D., Williams, D. A., & Field, L. J. (2004). Haematopoietic stem cells do not transdifferentiate into cardiac myocytes in myocardial infarcts. *Nature*, *428*, 664–668.
- Na, Y. R., Jung, D., Gu, G. J., & Seok, S. H. (2016). GM-CSF grown bone marrow derived cells are composed of phenotypically different dendritic cells and macrophages. *Mol. Cells*, *39*, 734–741.

- Nadella, V., Wang, Z., Johnson, T. S., Griffin, M., & Devitt, A. (2015). Transglutaminase 2 interacts with syndecan-4 and CD44 at the surface of human macrophages to promote removal of apoptotic cells. *Biochim. Biophys. Acta - Mol. Cell Res* 1853, 201–212.
- Nahrendorf, M., & Swirski, F. K. (2013). Monocyte and macrophage heterogeneity in the heart. *Circ. Res.*, 112, 1624–1633.
- Nahrendorf, M., & Swirski, F. K. (2016). Abandoning M1/M2 for a Network Model of Macrophage Function. *Circ Res*, 118, 6072–6078.
- Nahrendorf, M., Swirski, F. K., Aikawa, E., Stangenberg, L., Wurdinger, T., Figueiredo, J.-L., Libby, P., Weissleder, R., & Pittet, M. J. (2007). The healing myocardium sequentially mobilizes two monocyte subsets with divergent and complementary functions. *J Exp Med*, 204, 3037–3047.
- Natori, T., Sata, M., Washida, M., Hirata, Y., Nagai, R., & Makuuchi, M. (2002). G-CSF stimulates angiogenesis and promotes tumor growth: Potential contribution of bone marrow-derived endothelial progenitor cells. *Biochem. Biophys. Res. Commun.*, 297, 1058–1061.
- Neidig, L., Weinberger, F., Palpant, N., Mignone, J., Martinson, A., Sorensen, D., Bender, I., Nemoto, N., Reinecke, H., Pabon, L., Molkentin, J., Murry, C., & van Berlo, J. (2018). Evidence for minimal cardiogenic potential of stem cell antigen 1–positive cells in the adult mouse heart. *Circulation*, 2960–2962.
- Nguyen, N. U. N., Canseco, D. C., Xiao, F., Nakada, Y., Li, S., Lam, N. T., Muralidhar, S. A., Savla, J. J., Hill, J. A., Le, V., Zidan, K. A., El-Feky, H. W., Wang, Z., Ahmed, M. S., Hubbi, M. E., Menendez-Montes, I., Moon, J., Ali, S. R., Le, V., Sadek, H. A. (2020). A calcineurin–Hoxb13 axis regulates growth mode of mammalian cardiomyocytes. *Nature*, 582, 271–276.
- Nguyen, P. K., Rhee, J., & Wu, J. C. (2016). Adult stem cell therapy and heart failure, 2000 to 2016: a systematic review. *JAMA Cardiol*, 1, 831–841.
- Nie, L., Cai, S.-Y., Shao, J.-Z., & Chen, J. (2018). Toll-like receptors, associated biological roles, and signaling networks in non-mammals. *Front. Immunol*, 9.
- Nie, S., Wang, X., Sivakumaran, P., Chong, M. M. W., Liu, X., Karnezis, T., Bandara, N., Takov, K., Nowell, C. J., Wilcox, S., Shambrook, M., Hill, A. F., Harris, N. C., Newcomb, A. E., Strappe, P., Shayan, R., Hernández, D., Clarke, J., Hanssen, E., Lim, S. Y. (2018). Biologically active constituents of the secretome of human W8B2 + cardiac stem cells. *Sci. Rep.*, 8, 1–12.
- Niebauer, J., Pflaum, C. D., Clark, A. L., Strasburger, C. J., Hooper, J., Poole-Wilson, P. A., Coats, A. J. S., & Anker, S. D. (1998). Deficient insulin-like growth factor I in chronic heart failure predicts altered body composition, anabolic deficiency, cytokine and neurohormonal activation. *J. Am. Coll. Cardiol.*, 32, 393–397.
- Nikolaos G Frangogiannis, M. (2014). The immune system and the remodeling infarcted heart: cell biological insights and therapeutic opportunities. *JCPT*, 63, 185–195.
- Nosedá, M., Abreu-Paiva, M., & Schneider, M. D. (2015). The quest for the adult cardiac stem cell. *Circ. J. CIRC J*, 79, 1422–1430.
- Nosedá, M., Harada, M., McSweeney, S., Leja, T., Belian, E., Stuckey, D. J., Paiva, M. S. A., Habib, J., Macaulay, I., de Smith, A. J., Al-Beidh, F., Sampson, R., Lumbers, R. T., Rao, P., Harding, S. E., Blakemore, A. I. F., Jacobsen, S. E., Barahona, M., Nosedá, M., & Schneider, M. D. (2015). PDGFR α demarcates the cardiogenic clonogenic Sca1⁺ stem/progenitor cell in adult murine myocardium. *Nat. Commun.*, 6, 1–16.
- Nowak, D. G., Woolard, J., Amin, E. M., Konopatskaya, O., Saleem, M. A., Churchill, A. J., Ladomery, M. R., Harper, S. J., & Bates, D. O. (2008). Expression of pro- and anti-angiogenic isoforms of VEGF is differentially regulated by splicing and growth factors. *J Cell Sci* 121, 3487–3495.

- Nowbar, A. N., Mielewicz, M., Cole, G. D., & Francis, D. P. (2014). Discrepancies in autologous bone marrow stem cell trials and enhancement of ejection fraction (DAMASCENE): weighted regression and meta-analysis. *BMJ* 2688, 1–9.
- Ogawa, K., Funaba, M., Chen, Y., & Tsujimoto, M. (2006). Activin a functions as a Th2 cytokine in the promotion of the alternative activation of macrophages. *J. Immunol. Res.*, 177, 6787–6794.
- Ogawa, K., Funaba, M., Mathews, L. S., & Mizutani, T. (2000). Activin A stimulates type iv collagenase (matrix metalloproteinase-2) production in mouse peritoneal macrophages. *J. Immunol. Res.*, 165, 2997–3003.
- Oh, H., Bradfute, S. B., Gallardo, T. D., Nakamura, T., Gaussin, V., Mishina, Y., Pocius, J., Michael, L. H., Behringer, R. R., Garry, D. J., Entman, M. L., & Schneider, M. D. (2003). Cardiac progenitor cells from adult myocardium: homing, differentiation, and fusion after infarction. *PNAS*, 100, 12313–12318.
- Oh, H., Chi, X., Bradfute, S. B., Mishina, Y., Pocius, J., Michael, L. H., Behringer, R. R., Schwartz, R. J., Entman, M. L., & Schneider, M. D. (2004). Cardiac muscle plasticity in adult and embryo by heart-derived progenitor cells. *Ann. N. Y. Acad. Sci.*, 1015, 182–189.
- Oh, Hidemasa, Wang, S. C., Prahash, A., Sano, M., Moravec, C. S., Taffet, G. E., Michael, L. H., Youker, K. a, Entman, M. L., & Schneider, M. D. (2003). Telomere attrition and Chk2 activation in human heart failure. *PNAS*, 100, 5378–5383.
- Ohmori, Y., & Hamilton, T. A. (2001). Requirement for STAT1 in LPS-induced gene expression in macrophages. *J. Leukoc. Biol.*, 69, 598–604.
- Ohtani, T., Ishihara, K., Atsumi, T., Nishida, K., Kaneko, Y., Miyata, T., Itoh, S., Narimatsu, M., Maeda, H., Fukada, T., Itoh, M., Okano, H., Hibi, M., & Hirano, T. (2000). Dissection of signaling cascades through gp130 in vivo: reciprocal roles for STAT3- and SHP2-mediated signals in immune responses. *Immunity*, 12, 95–105.
- Okamura, H., Shultz, L. D., Kunisada, T., Nishikawa, S.-I., Sudo, T., Ogawa, M., Yoshida, H., Hayashi, S.-I., & Nishikawa, S. (2003). The murine mutation osteopetrosis is in the coding region of the macrophage colony stimulating factor gene. *Nature*, 345, 442–444.
- Olingy, C. E., San Emeterio, C. L., Ogle, M. E., Krieger, J. R., Bruce, A. C., Pfau, D. D., Jordan, B. T., Peirce, S. M., & Botchwey, E. A. (2017). Non-classical monocytes are biased progenitors of wound healing macrophages during soft tissue injury. *Sci. Rep.*, 7, 1–16.
- Oliveira, L. Z., Arruda, R. P., Celeghini, E. C. C., de Andrade, A. F. C., Perini, A. P., Resende, M. V., Miguel, M. C. V., Lucio, A. C., & Hossepian de Lima, V. F. M. (2012). Effects of discontinuous Percoll gradient centrifugation on the quality of bovine spermatozoa evaluated with computer-assisted semen analysis and fluorescent probes association. *Andrologia*, 44, 9–15.
- Olson, E. (2006). Gene regulatory networks in the evolution and development of the heart. *Science*, 313, 1922–1928.
- Ong, Hernández-Reséndiz, S., Crespo-Avilan, G. E., Mukhametshina, R. T., Kwek, X. Y., Cabrera-Fuentes, H. A., & Hausenloy, D. J. (2018). Inflammation following acute myocardial infarction: Multiple players, dynamic roles, and novel therapeutic opportunities. *Pharmacol. Ther.*, 186, 73–87.
- Ong, S.-G., Huber, B. C., Lee, W. H., Kodo, K., Ebert, A. D., Ma, Y., Nguyen, P. K., Diecke, S., Chen, W.-Y., & Wu, J. C. (2015). Microfluidic single cell analysis of transplanted human induced pluripotent stem cell-derived cardiomyocytes following acute myocardial infarction. *Circulation*, 132, 762–771.
- Opie, L. H., Commerford, P. J., Gersh, B. J., & Pfeffer, M. A. (2006). Controversies in ventricular remodelling. *Lancet* 367,356-367.
- Orecchioni, M., Ghosheh, Y., Pramod, A. B., & Ley, K. (2019). Macrophage polarization: different gene signatures in M1(Lps+) vs. Classically and M2(LPS-) vs. alternatively activated macrophages. *Front. Immunol*, 10, 1–14.

- Orlic, D., Hill, J. M., & Arai, A. E. (2002). Stem cells for myocardial regeneration. *Circ. Res.*, *91*, 1092–1102.
- Osborne, G. W., Andersen, S. B., & Battye, F. L. (2015). Development of a novel cell sorting method that samples population diversity in flow cytometry. *Cytometry Part A*, *87*, 1047–1051.
- Oskouei, B., Lamirault, G., Joseph, C., Treuer, A., Landa, S., Da Silva, J., Hatzistergos, K., Daure, M., Balkan, W., McNiece, I., & Hare, J. (2012). Increased potency of cardiac stem cells compared with bone marrow mesenchymal stem cells in cardiac repair. *Stem Cells Transl Med.*, *1*, 116–124.
- Osterloh, A., Kalinke, U., Weiss, S., Fleischer, B., & Breloer, M. (2007). Synergistic and differential modulation of immune responses by Hsp60 and lipopolysaccharide. *JBC*, *282*, 4669–4680.
- Ovchinnikov, D. A., DeBats, C. E. E., Sester, D. P., Sweet, M. J., & Hume, D. A. (2010). A conserved distal segment of the mouse CSF-1 receptor promoter is required for maximal expression of a reporter gene in macrophages and osteoclasts of transgenic mice. *J. Leukoc. Biol.*, *87*, 815–822.
- Oyama, J. I., Blais, C., Liu, X., Pu, M., Kobzik, L., Kelly, R. a., Bourcier, T., Oyama, Blais, C., Liu, X., Pu, M., Kobzik, L., Kelly, R. a., & Bourcier, T. (2004). Reduced myocardial ischemia-reperfusion injury in toll-like receptor 4-deficient mice. *Circulation*, *109*, 784–789.
- Oyama, T., Nagai, T., Wada, H., Naito, A. T., Matsuura, K., Iwanaga, K., Takahashi, T., Goto, M., Mikami, Y., Yasuda, N., Akazawa, H., Uezumi, A., Takeda, S., & Komuro, I. (2007). Cardiac side population cells have a potential to migrate and differentiate into cardiomyocytes in vitro and in vivo. *JCB*, *176*, 329–341.
- Paik, D. T., Cho, S., Tian, L., Chang, H. Y., & Wu, J. C. (2020). Single-cell RNA sequencing in cardiovascular development, disease and medicine. *Nat. Rev. Cardiol.*, *17*, 457–473.
- Paine, R., Morris, S. B., Jin, H., Wilcoxon, S. E., Phare, S. M., Moore, B. B., Coffey, M. J., & Toews, G. B. (2001). Impaired functional activity of alveolar macrophages from GM-CSF-deficient mice. *Am. J. Physiol. - Lung Cell. Mol. Physiol.*, *281*, 1210–1218.
- Palis, J., Robertson, S., Kennedy, M., Wall, C., & Keller, G. (1999). Development of erythroid and myeloid progenitors in the yolk sac and embryo proper of the mouse. *Dev.*, *126*, 5073–5084.
- Palis, James, & Yoder, M. C. (2001). Yolk-sac hematopoiesis: the first blood cells of mouse and man. *Exp Hematol.*, *29*, 1–10.
- Parente, V., Balasso, S., Pompilio, G., Verduci, L., Colombo, G. I., Milano, G., Guerrini, U., Squadroni, L., Cotelli, F., Pozzoli, O., & Capogrossi, M. C. (2013). Hypoxia/reoxygenation cardiac injury and regeneration in zebrafish adult heart. *PLoS ONE*, *8*(1).
- Parisi, L., Gini, E., Baci, D., Tremolati, M., Fanuli, M., Bassani, B., Farronato, G., Bruno, A., & Mortara, L. (2018). Macrophage polarization in chronic inflammatory diseases: killers or builders? *J. Immunol. Research*, *2018*, 1–25.
- Park, B. S., Song, D. H., Kim, H. M., Choi, B.-S., Lee, H., & Lee, J.-O. (2009). The structural basis of lipopolysaccharide recognition by the TLR4-MD-2 complex. *Nature*, *458*, 1191–1195.
- Pauleau, A.-L., Rutschman, R., Lang, R., Pernis, A., Watowich, S. S., & Murray, P. J. (2004). Enhancer-mediated control of macrophage-specific arginase i expression. *J. Immunol. Res.*, *172*, 7565–7573.
- Peña, B., Laughter, M., Jett, S., Rowland, T. J., Taylor, M. R. G., Mestroni, L., & Park, D. (2018). Injectable hydrogels for cardiac tissue engineering. *Macromol. Biosci.*, *18*, 1–22.
- Penter, L., Dietze, K., Bullinger, L., Westermann, J., Rahn, H. P., & Hansmann, L. (2018). FACS single cell index sorting is highly reliable and determines immune phenotypes of clonally expanded T cells. *Eur. J Immunol.* *48*, 1248–1250.
- Perrier, P., Martinez, F. O., Locati, M., Bianchi, G., Nebuloni, M., Vago, G., Bazzoni, F., Sozzani, S., Allavena, P., & Mantovani, A. (2004). Distinct transcriptional programs activated by interleukin-10

- with or without lipopolysaccharide in dendritic cells: induction of the B cell-activating chemokine, CXC chemokine ligand 13. *J. Immunol. Res.*, 172, 7031–7042.
- Pesce, J. T., Ramalingam, T. R., Mentink-Kane, M. M., Wilson, M. S., Kasmi, K. C. E., Smith, A. M., Thompson, R. W., Cheever, A. W., Murray, P. J., & Wynn, T. A. (2009). Arginase-1-expressing macrophages suppress Th2 cytokine-driven inflammation and fibrosis. *PLoS Pathogens*, 5(4).
- Petty, R. H., & Todd, F. R. (1996). Integrins as promiscuous signal transduction devices. *Immunol.*, 17, 209–212.
- Pfefferli, C., & Jaźwińska, A. (2017). The careg element reveals a common regulation of regeneration in the zebrafish myocardium and fin. *Nat Commun*, 8.
- Pfister, O., Mouquet, F., Jain, M., Summer, R., Helmes, M., Fine, A., Colucci, W. S., & Liao, R. (2005). CD31-but not CD31+cardiac side population cells exhibit functional cardiomyogenic differentiation. *Circ. Res.*, 97, 52–61.
- Phillips, D. J., de Kretser, D. M., & Hedger, M. P. (2009). Activin and related praoteins in inflammation: not just interested bystandersac. *Cytokine Growth Factor Rev.*, 20, 153–164.
- Picelli, S., Björklund, Å. K., Faridani, O. R., Sagasser, S., Winberg, G., & Sandberg, R. (2013). Smart-seq2 for sensitive full-length transcriptome profiling in single cells. *Nat. Methods*, 10, 1096–1100.
- Pinto, A. R., Ilinykh, A., Ivey, M. J., Kuwabara, J. T., D'antoni, M. L., Debuque, R., Chandran, A., Wang, L., Arora, K., Rosenthal, N. A., & Tallquist, M. D. (2016). Revisiting cardiac cellular composition. *Circ. Res.*, 118, 400–409.
- Pinto, A. R., Paolicelli, R., Salimova, E., Gospocic, J., Slonimsky, E., Bilbao-Cortes, D., Godwin, J. W., & Rosenthal, N. A. (2012). An abundant tissue macrophage population in the adult murine heart with a distinct alternatively-activated macrophage profile. *PLoS ONE*, 7(5).
- Pixley, F. J., & Stanley, E. R. (2004). CSF-1 regulation of the wandering macrophage: complexity in action. *Trends Cell Biol.*, 14, 628–638.
- Pollard, Jeffery W., Bartocci, A., Arceci, R., Orlofsky, A., Ladner, M. B., & Stanley, E. R. (1987). Apparent role of the macrophage growth factor, CSF-1, in placental development. *Nature*, 330, 484–486.
- Pollard, Jeffrey W. (2009). Trophic macrophages in development and disease. *Nat. Rev. Immunol.*, 9, 259–270.
- Poltorak, a, He, X., Smirnova, I., Liu, M. Y., Van Huffel, C., Du, X., Birdwell, D., Alejos, E., Silva, M., Galanos, C., Freudenberg, M., Ricciardi-Castagnoli, P., Layton, B., & Beutler, B. (1998). Defective LPS signaling in C3H/HeJ and C57BL/10ScCr mice: mutations in Tlr4 gene. *Science*, 282, 2085–2088.
- Porcheray, F., Viaud, S., Rimaniol, A. C., Léone, C., Samah, B., Dereuddre-Bosquet, N., Dormont, D., & Gras, G. (2005). Macrophage activation switching: an asset for the resolution of inflammation. *Clin. Exp. Immunol.*, 142, 481–489.
- Porrello, E. R., Mahmoud, A. I., Simpson, E., Hill, J. a, James, A., Olson, E. N., & Sadek, H. a. (2011). Transient regeneration potential of the neonatal mouse heart. *Science*, 331, 1078–1080.
- Porrello, E. R., Mahmoud, A. I., Simpson, E., Johnson, B. A., Grinsfelder, D., Canseco, D., Mammen, P. P., Rothermel, B. A., Olson, E. N., & Sadek, H. A. (2013). Regulation of neonatal and adult mammalian heart regeneration by the miR-15 family. *PNAS*, 110, 187–192.
- Poss, K. D. (2002). Heart regeneration in zebrafish supplemental. *Science*, 298, 2188–2190.
- Power, C. A., & Proudfoot, A. E. I. (2001). The chemokine system: Novel broad-spectrum therapeutic targets. *COPHAR*, 1, 417–424.

- Prabhu, S. D. (2005). Post-infarction ventricular remodeling: an array of molecular events. *J. Mol. Cell. Cardiol.*, *38*, 547–550.
- Prabhu, S. D., & Frangogiannis, N. G. (2016). The biological basis for cardiac repair after myocardial infarction. *Circ. Res.*, *119*, 91–112.
- Preda, M. B., Rønningen, T., Burlacu, A., Simionescu, M., Moskaug, J. Ø., & Valen, G. (2014). Remote transplantation of mesenchymal stem cells protects the heart against ischemia-reperfusion injury. *Stem Cells*, *32*, 2123–2134.
- Priceman, S. J., Sung, J. L., Shaposhnik, Z., Burton, J. B., Torres-Collado, A. X., Moughon, D. L., Johnson, M., Lusic, A. J., Cohen, D. A., Iruela-Arispe, M. L., & Wu, L. (2010). Targeting distinct tumor-infiltrating myeloid cells by inhibiting CSF-1 receptor: combating tumor evasion of antiangiogenic therapy. *Blood*, *115*, 1461–1471.
- Ptaszek, L. M., Mansour, M., Ruskin, J. N., & Chien, K. R. (2012). Towards regenerative therapy for cardiac disease. *The Lancet*, *379*, 933–942.
- Pyonteck, S. M., Akkari, L., Schuhmacher, A. J., Bowman, R. L., Sevenich, L., Quail, D. F., Olson, O. C., Quick, M. L., Huse, J. T., Teijeiro, V., Setty, M., Leslie, C. S., Oei, Y., Pedraza, A., Brennan, C. W., Sutton, J. C., Holland, E. C., Daniel, D., & Joyce, J. A. (2014). CSF-1R inhibition alters macrophage polarization and blocks glioma progression. *Nat Med.*, *19*, 1264–1272.
- Qian, C., An, H., Yu, Y., Liu, S., & Cao, X. (2015). TLR agonists induce regulatory dendritic cells to recruit Th1 cells via preferential IP-10 secretion and inhibit Th1 proliferation. *Immunobiology*, *109*, 3308–3316.
- Radi, Z. A., Koza-Taylor, P. H., Bell, R. R., Obert, L. A., Runnels, H. A., Beebe, J. S., Lawton, M. P., & Sadis, S. (2011). Increased serum enzyme levels associated with Kupffer cell reduction with no signs of hepatic or skeletal muscle injury. *Am. J. Pathol.*, *179*, 240–247.
- Rae, F., Woods, K., Sasmono, T., Campanale, N., Taylor, D., Ovchinnikov, D. A., Grimmond, S. M., Hume, D. A., Ricardo, S. D., & Little, M. H. (2007). Characterisation and trophic functions of murine embryonic macrophages based upon the use of a Csf1r-EGFP transgene reporter. *Dev. Biol.*, *308*, 232–246.
- Rajavashisth, T. B., Andalibi, A., Territo, M. C., Berliner, J. A., Navab, M., Fogelman, A. M., & Lusic, A. J. (1990). Induction of endothelial cell expression of granulocyte and macrophage colony-stimulating factors by modified low-density lipoproteins. *Nature*, *344*, 254–257.
- Rajavashisth, T., Qiao, J. H., Tripathi, S., Tripathi, J., Mishra, N., Hua, M., Wang, X. P., Loussarian, A., Clinton, S., Libby, P., & Lusic, A. (1998). Heterozygous osteopetrotic (op) mutation reduces atherosclerosis in LDL receptor-deficient mice. *J. Clin. Investig.*, *101*, 2702–2710.
- Ramsköld, D., Luo, S., Wang, Y. C., Li, R., Deng, Q., Faridani, O. R., Daniels, G. A., Khrebtukova, I., Loring, J. F., Laurent, L. C., Schroth, G. P., & Sandberg, R. (2012). Full-length mRNA-Seq from single-cell levels of RNA and individual circulating tumor cells. *Nat. Biotechnol.*, *30*, 777–782.
- Ranganath, S., Levy, O., Inamdar, M., & Kar, J. (2012). Harnessing the MSC secretome for the treatment of cardiovascular disease. *Cell Stem Cell*, *10*, 244–258.
- Raschke, W. C., Baird, S., Raplh, P., & Nakoinz, I. (1978). Functional macrophage cell lines transformed by abelson leukemia virus. *Cell*, *15*, 251–267.
- Rath, M., Müller, I., Kropf, P., Closs, E. I., & Munder, M. (2014). Metabolism via arginase or nitric oxide synthase: two competing arginine pathways in macrophages. *Front. Immunol.*, *5*, 532.
- Raya, A., Koth, C. M., Scher, D. B., Kawakami, Y., Tohru Itoh, R. M. R., Sternik, G., Tsai, H.-J., Rodríguez-Esteban, C. n., & Belmonte, J. C. I. (2003). Activation of Notch signaling pathway precedes heart regeneration in zebrafish. *Proc Natl Acad Sci U S A.*, *60*, 45–49.

- Reddy, K. S. (2016). Global burden of disease study 2015 provides gps for global health 2030. *the Lancet*, *388*, 1448–1449.
- Reiss, K., Cheng, W., Pierzchalski, P., Kodali, S., Li, B., Wang, S., Liu, Y., & Anversa, P. (1997). Insulin-like growth factor-1 receptor and its ligand regulate the reentry of adult ventricular myocytes into the cell cycle. *ERC*, *235*, 198–209.
- Riabov, V., Gudima, A., Wang, N., Mickley, A., Orekhov, A., & Kzhyshkowska, J. (2014). Role of tumor associated macrophages in tumor angiogenesis and lymphangiogenesis. *Front. Physiol*, *5*, 1–13.
- Richmond, A. (2002). NF- κ B, chemokine gene transcription and tumour growth. *Nat. Rev. Immunol.*, *2*, 664–674.
- Ridker, P. M., Everett, B. M., Thuren, T., MacFadyen, J. G., Chang, W. H., Ballantyne, C., Fonseca, F., Nicolau, J., Koenig, W., Anker, S. D., Kastelein, J. J. P., Cornel, J. H., Pais, P., Pella, D., Genest, J., Cifkova, R., Lorenzatti, A., Forster, T., Kobalava, Z., CANTOS Trial Group. (2017). Antiinflammatory Therapy with Canakinumab for Atherosclerotic Disease. *NEJM*, *377*, 1119–1131.
- Rieser, B. C., Böck, G., Klocker, H., Bartsch, G., & Thurnher, M. (1997). Activate human dendritic cells : synergistic activation of interleukin 12 production. *J Exp. Med*, *186*, 1603–1608.
- Riley, J. K., Takeda, K., Akira, S., & Schreiber, R. D. (1999). Interleukin-10 receptor signaling through the JAK-STAT pathway. *JBC*, *274*, 16513–16521.
- Robbins, S. H., Walzer, T., Dembélé, D., Thibault, C., Defays, A., Bessou, G., Xu, H., Vivier, E., Sellars, M., Pierre, P., Sharp, F. R., Chan, S., Kastner, P., & Dalod, M. (2008). Novel insights into the relationships between dendritic cell subsets in human and mouse revealed by genome-wide expression profiling. *Genome Biol.*, *9*, 1–27.
- Robson, N. C., Phillips, D. J., McAlpine, T., Shin, A., Svobodova, S., Toy, T., Pillay, V., Kirkpatrick, N., Zanker, D., Wilson, K., Helling, I., Wei, H., Chen, W., Cebon, J., & Maraskovsky, E. (2008). Activin-A: a novel dendritic cell derived cytokine that potently attenuates CD40 ligand specific cytokine and chemokine production. *Blood*, *111*, 2733–2743.
- Rollins, B. J. (1997). Chemokines. *Blood*, *90*, 909–928.
- Root, R. K., & Dale, D. C. (1999). Granulocyte colony-stimulating factor and granulocyte-macrophage colony-stimulating factor: Comparisons and potential for use in the treatment of infections in nonneutropenic patients. *J. Infect. Dis.*, *179*, 342–352.
- Rosen, M. R., Myerburg, R. J., Francis, D. P., Cole, G. D., & Marbán, E. (2014). Translating stem cell research to cardiac disease therapies: Pitfalls and prospects for improvement. *J. Am. Coll. Cardiol.*, *64*, 922–937.
- Rosenblatt-Velin, N., Ogay, S., Felley, A., Stanford, W. L., & Pedrazzini, T. (2011). Cardiac dysfunction and impaired compensatory response to pressure overload in mice deficient in stem cell antigen-1. *FASEB J.*, *26*, 229–239.
- Rosenfeld, M. E., Yla-Herttuala, S., Lipton, B. A., Ord, V. A., Witztum, J. L., & Steinberg, D. (1992). Macrophage colony-stimulating factor mRNA and protein in atherosclerotic lesions of rabbits and humans. *Am. J. Pathol.*, *140*, 291–300.
- Rossini, A., Frati, C., Lagrasta, C., Graiani, G., Scopece, A., Cavalli, S., Musso, E., Baccarin, M., Di Segni, M., Fagnoni, F., Germani, A., Quaini, E., Mayr, M., Xu, Q., Barbuti, A., Diffrancesco, D., Pompilio, G., Quaini, F., Gaetano, C., & Capogrossi, M. C. (2011). Human cardiac and bone marrow stromal cells exhibit distinctive properties related to their origin. *Cardiovasc. Res.*, *89*, 650–660.
- Röszer, T., Menéndez-Gutiérrez, M. P., Lefterova, M. I., Alameda, D., Núñez, V., Lazar, M. A., Fischer, T., & Ricote, M. (2011). Autoimmune kidney disease and impaired engulfment of apoptotic cells in mice with macrophage peroxisome proliferator-activated receptor γ or retinoid x receptor α deficiency. *J. Immunol. Res.*, *186*, 621–631.

- Roth, G. A., Abate, D., Abate, K. H., Abay, S. M., Abbafati, C., Abbasi, N., Abbastabar, H., Abd-Allah, F., Abdela, J., Abdelalim, A., Abdollahpour, I., Abdulkader, R. S., Abebe, H. T., Abebe, M., Abebe, Z., Abeje, A. N., Abera, S. F., Abil, O. Z., Abraha, H. N., Murray, C. J. L. (2018). Global, regional, and national age-sex-specific mortality for 282 causes of death in 195 countries and territories, 1980–2017: a systematic analysis for the Global burden of disease study 2017. *The Lancet*, *392*, 1736–1788.
- Roth, G. A., Johnson, C., Abajobir, A., Abd-Allah, F., Abera, S. F., Abyu, G., Ahmed, M., Aksut, B., Alam, T., Alam, K., Alla, F., Alvis-Guzman, N., Amrock, S., Ansari, H., Ärnlöv, J., Asayesh, H., Atey, T. M., Avila-Burgos, L., Awasthi, A., Murray, C. (2017). Global, regional, and national burden of cardiovascular diseases for 10 causes, 1990 to 2015. *J. Am. Coll. Cardiol.*, *70*, 1–25.
- Roth, P., Bartocci, A., & Stanley, E. R. (1997). Lipopolysaccharide induces synthesis of mouse colony-stimulating factor-1 in vivo. *J Immunol*, *158*, 3874–3880.
- Rovida, E., & Sbarba, P. Dello. (2015). Colony-stimulating factor-1 receptor in the polarization of macrophages: a target for turning bad to good ones? *J. clin. cell. immunol.*, *06*.
- Ruckh, J. M., Zhao, J., Shadrach, J. L., Wijngaarden, P. Van, Rao, T. N., Wagers, A. J., & Franklin, R. J. M. (2012). Rejuvenation of regeneration in the aging central nervous system. *Cell Stem Cell*, *10*, 96–103.
- Ruifrok, W. P. T., de Boer, R. A., Iwakura, A., Silver, M., Kusano, K., Tio, R. A., & Losordo, D. W. (2009). Estradiol-induced, endothelial progenitor cell-mediated neovascularization in male mice with hind-limb ischemia. *Vasc. Med.*, *14*, 29–36.
- Rupert, C. E., & Coulombe, K. L. K. (2017). IGF1 and NRG1 enhance proliferation, metabolic maturity, and the force-frequency response in hESC-derived engineered cardiac tissues. *Stem Cells Internat.*, *2017*.
- Sadek, A. H., Martin, C. M., Latif, S. S., Garry, M. G., & Garry, D. J. (2009). Bone-marrow-derived side population cells for myocardial regeneration. *J Cardiovasc Transl Res*, *2*, 173–181.
- Sager, H. B., Heidt, T., Hulsmans, M., Dutta, P., Courties, G., Sebas, M., Wojtkiewicz, G. R., Tricot, B., Iwamoto, Y., Sun, Y., Weissleder, R., Libby, P., Swirski, F. K., & Nahrendorf, M. (2015). Targeting interleukin-1 β reduces leukocyte production after acute myocardial infarction. *Circulation*, *132*, 1880–1890.
- Sager, H. B., Hulsmans, M., Lavine, K. J., Moreira, M. B., Heidt, T., Courties, G., Sun, Y., Iwamoto, Y., Tricot, B., Khan, O. F., Dahlman, J. E., Borodovsky, A., Fitzgerald, K., Anderson, D. G., Weissleder, R., Libby, P., Swirski, F. K., & Nahrendorf, M. (2016). Proliferation and recruitment contribute to myocardial macrophage expansion in chronic heart failure. *Circ. Res.*, *119*, 853–864.
- Saleh, M., & Ambrose, J. A. (2018). Understanding myocardial infarction. *F1000Research*, *7*, 1–8.
- Saleh, R., Lee, M.-C., Khiew, S. H., Louis, C., Fleetwood, A. J., Achuthan, A., Förster, I., Cook, A. D., & Hamilton, J. A. (2018). CSF-1 in inflammatory and arthritic pain development. *J. Immunol. Res.*, *201*, 2042–2053.
- Sandler, H., & Stoecklin, G. (2008). Control of mRNA decay by phosphorylation of tristetraprolin. *Biochem. Soc. Trans.*, *36*, 491–496.
- Santini, M. P., Tsao, L., Monassier, L., Theodoropoulos, C., Carter, J., Lara-Pezzi, E., Slonimsky, E., Salimova, E., Delafontaine, P., Song, Y. H., Bergmann, M., Freund, C., Suzuki, K., & Rosenthal, N. (2007). Enhancing repair of the mammalian heart. *Circ. Res.*, *100*, 1732–1740.
- Sarmiento, J., Shumate, C., Suetomi, K., Ravindran, A., Villegas, L., Rajarathnam, K., & Navarro, J. (2011). Diverging mechanisms of activation of chemokine receptors revealed by novel chemokine agonists. *PLoS ONE*, *6*, 6–12.

- Sato, N., Beitz, J. G., Kato, J., Yamamoto, M., Clark, J. W., Calabresi, P., & Frackelton, A. R. (1993). Platelet-derived growth factor indirectly stimulates angiogenesis in vitro. *Am. J. Pathol.*, *142*, 1119–1130.
- Savill, J., Dransfield, I., Gregory, C., & Haslett, C. (2002). A blast from the past: clearance of apoptotic cells regulates immune responses. *Nat. Rev. Immunol.*, *2*, 965–975.
- Scarpellini, A., Germack, R., Lortat-Jacob, H., Muramatsu, T., Billett, E., Johnson, T., & Verderio, E. A. M. (2009). Heparan sulfate proteoglycans are receptors for the cell-surface trafficking and biological activity of transglutaminase-2. *JBC*, *284*, 18411–18423.
- Schafer, S., Viswanathan, S., Widjaja, A. A., Lim, W. W., Moreno-Moral, A., DeLaughter, D. M., Ng, B., Patone, G., Chow, K., Khin, E., Tan, J., Chothani, S. P., Ye, L., Rackham, O. J. L., Ko, N. S. J., Sahib, N. E., Pua, C. J., Zhen, N. T. G., Xie, C., Cook, S. A. (2017). IL-11 is a crucial determinant of cardiovascular fibrosis. *Nature*, *552*, 110–115.
- Schindelin, J., Arganda-Carreras, I., Frise, E., Kaynig, V., Longair, M., Pietzsch, T., Preibisch, S., Rueden, C., Saalfeld, S., Schmid, B., Tinevez, J.-Y., White, D. J., Hartenstein, V., Eliceiri, K., Tomancak, P., & Cardona, A. (2012). Fiji: an open-source platform for biological-image analysis. *Nat. Methods*, *9*, 676–682.
- Schioppa, T., Uranchimeg, B., Saccani, A., Biswas, S. K., Doni, A., Rapisarda, A., Bernasconi, S., Saccani, S., Nebuloni, M., Vago, L., Mantovani, A., Melillo, G., & Sica, A. (2003). Regulation of the chemokine receptor CXCR4 by hypoxia. *J Exp Med*, *198*, 1391–1402.
- Schmitz, J., Owyang, A., Oldham, E., Song, Y., Murphy, E., McClanahan, T. K., Zurawski, G., Moshrefi, M., Qin, J., Li, X., Gorman, D. M., Bazan, J. F., & Kastelein, R. A. (2005). IL-33, an interleukin-1-like cytokine that signals via the IL-1 receptor-related protein ST2 and induces T helper type 2-associated cytokines. *Immunity*, *23*, 479–490.
- Schneider, M. D. (2016). Heartbreak hotel: a convergence in cardiac regeneration. *Dev.*, *143*, 1435–1441.
- Schulte, R., Wilson, N. K., Prick, J. C. M., Cossetti, C., Maj, M. K., Gottgens, B., & Kent, D. G. (2015). Index sorting resolves heterogeneous murine hematopoietic stem cell populations. *Exp. Hematol.*, *43*, 803–811.
- Scotton, C. J., Martinez, F. O., Smelt, M. J., Sironi, M., Locati, M., Mantovani, A., & Sozzani, S. (2005). Transcriptional profiling reveals complex regulation of the monocyte IL-1 β system by IL-13. *J. Immunol. Res.*, *174*, 834–845.
- Segawa, M., Fukada, S., Ichiro, Yamamoto, Y., Yahagi, H., Kanematsu, M., Sato, M., Ito, T., Uezumi, A., Hayashi, S., Miyagoe-Suzuki, Y., Takeda, S., Tsujikawa, K., & Yamamoto, H. (2008). Suppression of macrophage functions impairs skeletal muscle regeneration with severe fibrosis. *Experim. Cell Res.*, *314*, 3232–3244.
- Segers, V. F. M., & Lee, R. T. (2008). Stem-cell therapy for cardiac disease. *Nature*, *451*, 937–942.
- Senyo, S. E., Steinhauser, M. L., Pizzimenti, C. L., Yang, V. K., Cai, L., Mei Wang, 5, Ting-Di Wu, 3, Jean-Luc Guerquin-Kern, 2, 3, Claude P. Lechene, 4, 5, & Lee, and R. T. (2013). Mammalian heart renewal by preexisting cardiomyocytes samuel. *Nature*, *15*, 34–48.
- Sevilla, L., Zaldumbide, A., Carlotti, F., Dayem, M. A., Pognonec, P., & Boulukos, K. E. (2001). Bcl-xL expression correlates with primary macrophage differentiation, activation of functional competence, and survival and results from synergistic transcriptional Activation by Ets2 and PU.1. *JBC*, *276*, 17800–17807.
- Shalek, A. K., Satija, R., Adiconis, X., Gertner, R. S., Gaublotme, J. T., Raychowdhury, R., Schwartz, S., Yosef, N., Malboeuf, C., Lu, D., Trombetta, J. J., Gennert, D., Gnirke, A., Goren, A., Hacohen, N., Levin, J. Z., Park, H., & Regev, A. (2013). Single-cell transcriptomics reveals bimodality in expression and splicing in immune cells. *Nature*, *498*, 236–240.

- Shaposhnik, Z., Wang, X., & Lusis, A. J. (2010). Arterial colony stimulating factor-1 influences atherosclerotic lesions by regulating monocyte migration and apoptosis. *J. Lipid Res.*, *51*, 1962–1970.
- Shen, C., Shi, L., Jin, X., Liu, L., Yin, G., Zhang, Y., Xiang, Y., Dong, J., & Lu, Y. (2018). Advanced glycation end products enhance murine monocyte proliferation in bone marrow and prime them into an inflammatory phenotype through MAPK signaling. *J. Diabetes Res*, *2018*, 1–10.
- Sherr, C. J., Matsushima, H., & Roussel, M. F. (1992). Regulation of CYL/Cyclin D genes by colony-stimulating factor 1. *Ciba Found Symp.*, *170*, 209–219.
- Sherr, C. J., Roussel, M. F., & Rettenmier, C. W. (1988). Colony-stimulating factor4 receptor (c-fms). *J Cell Biochem.*, *187*, 179–187.
- Shi, Y., Liu, C. H., Roberts, A. I., Das, J., Xu, G., Ren, G., Zhang, Y., Zhang, L., Zeng, R. Y., Tan, H. S. W., Das, G., & Devadas, S. (2006). Granulocyte-macrophage colony-stimulating factor (GM-CSF) and T-cell responses: what we do and don't know. *Cell Res*, *16*, 126–133.
- Shintani, Y., Yashiro, K., Ishida, H., Saba, R., Suzuki, K., Shiraishi, M., Yamaguchi, A., Adachi, H., & Shintani, Y. (2016). Alternatively activated macrophages determine repair of the infarcted adult murine heart. *J. Clin. Investig.*, *126*, 2151–2166.
- Shishido, T., Nozaki, N., Yamaguchi, S., Shibata, Y., Nitobe, J., Miyamoto, T., Takahashi, H., Arimoto, T., Maeda, K., Yamakawa, M., Takeuchi, O., Akira, S., Takeishi, Y., & Kubota, I. (2003). Toll-Like receptor-2 modulates ventricular remodeling after myocardial infarction. *Circulation*, *108*, 2905–2910.
- Sica, A., & Mantovani, A. (2012). Macrophage plasticity and polarization: in vivo veritas. *J. Clin. Investig.*, *122*, 787–795.
- Sica, A., Sacconi, A., Borsatti, A., Power, C. A., Wells, T. N. C., Luini, W., Polentarutti, N., Sozzani, S., & Mantovani, A. (1997). Bacterial lipopolysaccharide rapidly inhibits expression of C-C chemokine receptors in human monocytes. *J Exp Med*, *185*, 969–974.
- Sierra-Filardi, E., Puig-Kröger, A., Blanco, F. J., Nieto, C., Bragado, R., Palomero, M. I., Bernabéu, C., Vega, M. A., & Corbó, A. L. (2011). Activin A skews macrophage polarization by promoting a proinflammatory phenotype and inhibiting the acquisition of anti-inflammatory macrophage markers. *Blood*, *117*, 5092–5101.
- Silverstein, R. L., & Febbraio, M. (2009). CD36 a scavenger receptor ,nvolved in immunity metabolism angiogenesis and behavior 2009 article. *Sci Signal.*, *2*.
- Sjaarda, J., Gerstein, H., Chong, M., Yusuf, S., Meyre, D., Anand, S. S., Hess, S., & Paré, G. (2018). Blood CSF1 and CXCL12 as causal mediators of coronary artery disease. *J. Am. Coll. Cardiol.*, *72*, 300–310.
- Skelly, D. A., Squiers, G. T., McLellan, M. A., Bolisetty, M. T., Robson, P., Rosenthal, N. A., & Pinto, A. R. (2018). Single-cell transcriptional profiling reveals cellular diversity and intercommunication in the mouse heart. *Cell Rep.*, *22*, 600–610.
- Smart, N., Bollini, S., Dubé, K. N., Vieira, J. M., Zhou, B., Davidson, S., Yellon, D., Riegler, J., Price, A. N., Lythgoe, M. F., Pu, W. T., & Riley, P. R. (2011). De novo cardiomyocytes from within the activated adult heart after injury. *Nature*, *474*, 640–644.
- Smart, N., Mojet, M. H., Latchman, D. S., Marber, M. S., Duchon, M. R., & Heads, R. J. (2006). IL-6 induces PI 3-kinase and nitric oxide-dependent protection and preserves mitochondrial function in cardiomyocytes. *Cardiovasc. Res.*, *69*, 164–177.
- Smith, R. R., Barile, L., Cho, H. C. P., Leppo, M. K., Hare, J.M., Messina, E., Giacomello, A., Abraham, M. R., Marbán, E. (2017). Regenerative potential of cardiosphere-derived cells expanded from percutaneous endomyocardial biopsy specimens. *Circulation*, *95*(3), 154–162.

- Smith, W., Feldmann, M., & Londei, M. (1998). Human macrophages induced in vitro by macrophage colony-stimulating factor are deficient in IL-12 production. *Eur. J Immunol.* *28*, 2498–2507.
- Song, E., Ouyang, N., Hörbelt, M., Antus, B., Wang, M., & Exton, M. S. (2000). Influence of alternatively and classically activated macrophages on fibrogenic activities of human fibroblasts. *Cell. Immunol.*, *204*, 19–28.
- Soonpaa, M. H., Lafontant, P. J., Reuter, S., Scherschel, J. A., Srour, E. F., Zaruba, M.-M., Rubart-von Der Lohe, M., & Field, L. J. (2018). Absence of cardiomyocyte differentiation following transplantation of adult cardiac-resident Sca-1+ cells into infarcted mouse hearts. *Circulation*, 2963–2966.
- Sozzani, B. S., Ghezzi, S., Iannolo, G., Luini, W., Borsatti, A., Polentarutti, N., Sica, A., Locati, M., Mackay, C., Wells, T. N. C., Biswas, P., Vicenzi, E., Poli, G., Mantovani, A., Unit, I., & Raffaele, S. (1998). Interleukin 10 Increases CCR5 Expression and HIV infection in human monocytes. *J Exp Med.*, *187*, 439–444.
- Spiller, K. L., Anfang, R. R., Spiller, K. J., Ng, J., Nakazawa, K. R., Daulton, J. W., & Vunjak-Novakovic, G. (2014). The role of macrophage phenotype in vascularization of tissue engineering scaffolds. *Biomaterials*, *35*, 4477–4488.
- Spinale, F. G. (2007). Myocardial matrix remodeling and the matrix metalloproteinases: Influence on cardiac form and function. *Physiol. Rev.*, *87*, 1285–1342.
- Stamatovic, S. M., Keep, R. F., Mostarica-Stojkovic, M., & Andjelkovic, A. V. (2006). CCL2 regulates angiogenesis via activation of Ets-1 transcription factor. *J. Immunol. Res.*, *177*, 2651–2661.
- Stanford, W. L., Haque, S., Alexander, R., Liu, X., Latour, A. M., Snodgrass, H. R., Koller, B. H., & Flood, P. M. (1997). Altered proliferative response by T lymphocytes of Ly-6A (Sca-1) Null Mice. *J Exp Med*, *186*, 705–717.
- Stanley, E. R., Chen, D. M., & Lin, H. S. (1978). Induction of macrophage production and proliferation by a purified colony stimulating factor. *Nature*, *274*, 168–170.
- Stanley, E. Richard, & Chitu, V. (2014). CSF-1 receptor signaling in myeloid cells. *Cold Spring Harb. perspect. biol.* *6*, 1–21.
- Steffel, J., Lüscher, T. F., & Tanner, F. C. (2006). Tissue factor in cardiovascular diseases: molecular mechanisms and clinical implications. *Circulation*, *113*, 722–731.
- Stein, M., Keshav, S., Harris, N., & Gordon, S. (1992). Interleukin 4 potently enhances murine macrophage mannose receptor activity: a marker of alternative immunologic macrophage activation. *J. Exp. Med.*, *176*, 287–292.
- Steinhauser, M. L., Bailey, A. P., Senyo, S. E., Guillermier, C., Perlstein, T. S., Gould, A. P., Lee, R. T., & Lechene, C. P. (2012). Multi-isotope imaging mass spectrometry quantifies stem cell division and metabolism. *Nature*, *481*, 516–519.
- Stevens, S. M., von Gise, A., VanDusen, N., Zhou, B., & Pu, W. T. (2016). Epicardium is required for cardiac seeding by yolk sac macrophages, precursors of resident macrophages of the adult heart. *Dev. Biol.* , *413*, 153–159.
- Stewart, M., Thiel, M., & Hogg, N. (1995). Leukocyte integrins. *Curr. Opin. Cell Biol*, *7*, 690–696.
- Stockmann, C., Kirmse, S., Helfrich, I., Weidemann, A., Takeda, N., Doedens, A., & Johnson, R. S. (2011). A wound size-dependent effect of myeloid cell-derived vascular endothelial growth factor on wound healing. *JID* *131*, 797–801.
- Stone, G. W., Selker, H. P., Thiele, H., Patel, M. R., Udelson, J. E., Ohman, E. M., Maehara, A., Eitel, I., Granger, C. B., Jenkins, P. L., Nichols, M., & Ben-Yehuda, O. (2016). Relationship between infarct size and outcomes following primary pci patient-level analysis from 10 randomized trials. *J. Am. Coll. Cardiol.*, *67*, 1674–1683.

- Stoudemire, J. B., & Garnick, M. B. (1991). Effects of recombinant human macrophage colony-stimulating factor on plasma cholesterol levels. *Blood*, *77*, 750–755.
- Strassmann, G., Patil-Koota, V., Finkelman, F., Fong, M., & Kambayashi, T. (1994). Evidence for the involvement of interleukin 10 in the differential deactivation of murine peritoneal macrophages by prostaglandin E2. *J Exp Med*, *180*, 2365–2370.
- Strauer, B. E., Brehm, M., Zeus, T., Köstering, M., Hernandez, A., Sorg, R. V., Kögler, G., & Wernet, P. (2002). Repair of infarcted myocardium by autologous intracoronary mononuclear bone marrow cell transplantation in humans. *Circulation*, *106*, 1913–1918.
- Stremmel, C., Schuchert, R., Wagner, F., Thaler, R., Weinberger, T., Pick, R., Mass, E., Ishikawa-Ankerhold, H. C., Margraf, A., Hutter, S., Vagnozzi, R., Klapproth, S., Frampton, J., Yona, S., Scheiermann, C., Molkentin, J. D., Jeschke, U., Moser, M., Sperandio, M., Schulz, C. (2018). Yolk sac macrophage progenitors traffic to the embryo during defined stages of development. *Nat Commun*, *9*(1).
- Su, H., Lei, C. T., & Zhang, C. (2017). Interleukin-6 signaling pathway and its role in kidney disease: An update. *Front. Immunol*, *8*, 1–10.
- Sudo, T., Nishikawa, S., Ogawa, M., Kataoka, H., Ohno, N., Izawa, A., Hayashi, S. I., & Nishikawa, S. I. (1995). Functional hierarchy of c-kit and c-fms in intramarrow production of CFU-M. *Oncogene*, *11*, 2468–2476.
- Suh, H., Zhao, M., Derico, L., Choi, N., & Lee, S. C. (2013). Insulin-like growth factor 1 and 2 (IGF1, IGF2) expression in human microglia: differential regulation by inflammatory mediators. *J Neuroinflamm.*, *10*, 1.
- Summer, R., Kotton, D. N., Sun, X., Ma, B., Fitzsimmons, K., & Fine, A. (2003). Side population cells and Bcrp1 expression in lung. *Am J Physiol Lung Cell Mol Physiol*, *285*, L97–L104.
- Sunderkötter, C., Goebeler, M., Schulze-Osthoff, K., Bhardwaj, R., & Sorg, C. (1991). Macrophage-derived angiogenesis factors. *Pharmacol. Ther.*, *51*, 195–216.
- Sunderkötter, C., Steinbrink, K., Goebeler, M., Bhardwaj, R., & Sorg, C. (1994). Macrophages and angiogenesis. *J. Leukoc. Biol.*, *55*, 410–422.
- Sutton, Mgs. G., & Sharpe, N. (2000). Left ventricular remodeling after myocardial infarction: pathophysiology and therapy. *Circulation*, *101*, 2981–2988.
- Svensson-Arelund, J., Mehta, R. B., Lindau, R., Mirrasekhian, E., Rodriguez-Martinez, H., Berg, G., Lash, G. E., Jenmalm, M. C., & Ernerudh, J. (2015). The human fetal placenta promotes tolerance against the semiallogeneic fetus by inducing regulatory T cells and homeostatic M2 macrophages. *J. Immunol. Res.*, *194*, 1534–1544.
- Swirski, F. K. (2009). Identification of Splenic Reservoir. *Science*, *325*, 612–616.
- Szentes, V., Gazdag, M., Szokodi, I., & Dézsi, C. A. (2018). The role of CXCR3 and associated chemokines in the development of atherosclerosis and during myocardial infarction. *Front. Immunol*, *9*, 1932.
- Tabeta, K., Georgel, P., Janssen, E., Du, X., Hoebe, K., Crozat, K., Mudd, S., Shamel, L., Sovath, S., Goode, J., Alexopoulou, L., Flavell, R. A., & Beutler, B. (2004). Toll-like receptors 9 and 3 as essential components of innate immune defense against mouse cytomegalovirus infection. *PNAS*, *101*, 3516–3521.
- Tachibana, A., Santoso, M. R., Mahmoudi, M., Shukla, P., Wang, L., Bennett, M., Goldstone, A. B., Wang, M., Fukushi, M., Ebert, A. D., Woo, Y. J., Rulifson, E., & Yang, P. C. (2017). Paracrine effects of the pluripotent stem cell-derived cardiac myocytes salvage the injured myocardium. *Circ. Res.*, *121*, e22–e36. 3

- Takayama, J., Koyamada, N., Abe, T., Hatsugai, K., Usuda, M., Ohkohchi, N., & Satomi, S. (2000). Macrophage depletion prevents accelerated rejection and results in long-term survival in hamster to rat cardiac xenotransplantation. *Transplant. Proc.*, *32*, 1016.
- Takehara, N., Ogata, T., Nakata, M., Kami, D., Nakamura, T., Matoba, S., Gojo, S., Sawada, T., Yaku, H., & Kyoto, H. M. (2012). The ALCADIA (autologous human cardiac-derived stem cell to treat ischemic cardiomyopathy) trial. *Circulation*, *126*, 2783.
- Tang, F., Barbacioru, C., Bao, S., Lee, C., Nordman, E., Wang, X., Lao, K., & Surani, M. A. (2010). Tracing the derivation of embryonic stem cells from the inner cell mass by single-cell RNA-seq analysis. *Cell Stem Cell*, *6*, 468–478.
- Tang, F., Barbacioru, C., Wang, Y., Nordman, E., Lee, C., Xu, N., Wang, X., Bodeau, J., Tuch, B. B., Siddiqui, A., Lao, K., & Surani, M. A. (2009). mRNA-Seq whole-transcriptome analysis of a single cell. *Nat. Methods*, *6*, 377–382.
- Tang, J., Li, Y., Huang, X., He, L., Zhang, L., Wang, H., Yu, W., Pu, W., Tian, X., Nie, Y., Shengshou, H., Wang, Q.-D., Lui, K. O., & Zhou, B. (2018). Fate mapping of Sca1+ cardiac progenitor cells in the adult mouse heart. *Circulation*, 2967–2969.
- Tang, X.-L., Li, Q., Rokosh, G., Sanganalmath, Santosh K. Chen, N., Ou, Q., Stowers, H., Hunt, G. and, & Bolli, R. (2016). Long-term outcome of administration of c-kitpos cardiac progenitor cells after acute myocardial infarction. *Circ Res*, *118*, 1091–1105.
- Tannenbaum, C. S., Tubbs, R., Armstrong, D., Finke, J. H., Bukowski, R. M., & Hamilton, T. A. (1998). The CXC chemokines IP-10 and Mig are necessary for IL-12-mediated regression of the mouse RENCA tumor. *J. Immunol.*, *161*, 927–932.
- Tarzami, S. T., Calderon, T. M., Deguzman, A., Lopez, L., Kitsis, R. N., & Berman, J. W. (2005). MCP-1/CCL2 protects cardiac myocytes from hypoxia-induced apoptosis by a Gai-independent pathway. *Biochem. Biophys. Res. Commun.*, *335*, 1008–1016.
- Telci, D., Wang, Z., Li, X., Verderio, E. A. M., Humphries, M. J., Baccarini, M., Basaga, H., & Griffin, M. (2008). Fibronectin-tissue transglutaminase matrix rescues RGD-impaired cell adhesion through syndecan-4 and β 1 integrin co-signaling. *JBC*, *283*, 20937–20947.
- Thomas-Ecker, S., Lindecke, A., Hatzmann, W., Kaltschmidt, C., Za, K. S., & Dittmar, T. (2007). Alteration in the gene expression pattern of primary monocytes after adhesion to endothelial cells. *PNAS*, *104*, 5539–5544.
- Timmers, L., Pasterkamp, G., De Hoog, V. C., Arslan, F., Appelman, Y., & De Kleijn, D. P. V. (2012). The innate immune response in reperfused myocardium. *Cardiovasc. Res.*, *94*, 276–283.
- Timmers, L., Sluijter, J., & Keulen, J. Van. (2008). Toll-like receptor 4 mediates maladaptive left ventricular remodeling and impairs cardiac function after myocardial infarction. In *Circ. Res.*, *102*, 257–264.
- Titos, E., Rius, B., González-Pérez, A., López-Vicario, C., Morán-Salvador, E., Martínez-Clemente, M., Arroyo, V., & Clària, J. (2011). Resolvin D1 and its precursor docosahexaenoic acid promote resolution of adipose tissue inflammation by eliciting macrophage polarization toward an M2-like phenotype. *J. Immunol. Res.*, *187*, 5408–5418.
- Tober, J. M., Koniski, A. D., Vemishetti, R., Emerson, R. L., McGrath, K. E., Waugh, R., & Palis. (2006). The megakaryocyte lineage originates from hemangioblast precursors during gastrulation and is an integral component of primitive and definitive hematopoiesis. *Dev. Biol.* , *295*, 461.
- Torella, D., Rota, M., Nurzynska, D., Musso, E., Monsen, A., Shiraishi, I., Zias, E., Walsh, K., Rosenzweig, A., Sussman, M. A., Urbanek, K., Nadal-Ginard, B., Kajstura, J., Anversa, P., & Leri, A. (2004). Cardiac stem cell and myocyte aging, heart failure, and insulin-like growth factor-1 overexpression. *Circ. Res.*, *94*, 514–524.

- Tous, E., Purcell, B., Ifkovits, J. L., & Burdick, J. A. (2011). Injectable acellular hydrogels for cardiac repair. *J. Cardiovasc. Transl. Res.*, *4*, 528–542.
- Townsend, N., Nichols, M., Scarborough, P., & Rayner, M. (2016). Cardiovascular disease in Europe - Epidemiological update 2015. *Eur Heart J*, *36*, 2696–2705.
- Treutlein, B., Brownfield, D. G., Wu, A. R., Neff, N. F., Mantalas, G. L., Espinoza, F. H., Desai, T. J., Krasnow, M. A., & Quake, S. R. (2014). Reconstructing lineage hierarchies of the distal lung epithelium using single-cell RNA-seq. *Nature*, *509*, 371–375.
- Troidl, C., Möllmann, H., Nef, H., Masseli, F., Voss, S., Szardien, S., Willmer, M., Rolf, A., Rixe, J., Troidl, K., Kostin, S., Hamm, C., & Elsässer, A. (2009). Classically and alternatively activated macrophages contribute to tissue remodelling after myocardial infarction. *J Cell Mol Med*, *13*, 3485–3496.
- Troncoso, R., Ibarra, C., Vicencio, J. M., Jaimovich, E., & Lavandero, S. (2014). New insights into IGF-1 signaling in the heart. *Trends Endocrinol. Metab.*, *25*, 128–137.
- Tsonis, P. A., & Fox, T. P. (2009). Regeneration according to Spallanzani. *Dev. Dyn.*, *238*, 2357–2363.
- Tsutamoto, T., Hisanaga, T., Wada, A., Maeda, K., Ohnishi, M., Fukai, D., Mabuchi, N., Sawaki, M., & Kinoshita, M. (1998). Interleukin-6 spillover in the peripheral circulation increases with the severity of heart failure, and the high plasma level of interleukin-6 is an important prognostic predictor in patients with congestive heart failure. *J. Am. Coll. Cardiol.*, *31*, 391–398.
- Tura, O., Crawford, J., Barclay, G. R., Samuel, K., Hadoke, P. W. F., Roddie, H., Davis, J., & Turner, M. L. (2010). Granulocyte colony-stimulating factor (G-CSF) depresses angiogenesis in vivo and in vitro: implications for sourcing cells for vascular regeneration therapy. *J Thromb Haemost.*, *8*, 1614–1623.
- Turner, L., Scotton, C., Negus, R., & Balkwill, F. (1999). Hypoxia inhibits macrophage migration. *Eur. J Immunol.* *29*, 2280–2287.
- Tushinski, R. J., & Stanley, E. R. (1985). The regulation of mononuclear phagocyte entry into S phase by the colony stimulating factor CSF-1. *J. Cell. Physiol.*, *122*, 221–228.
- Uchida, S., De Gaspari, P., Kostin, S., Jenniches, K., Kilic, A., Izumiya, Y., Shiojima, I., Grosse Kreymborg, K., Renz, H., Walsh, K., & Braun, T. (2013). Sca1-derived cells are a source of myocardial renewal in the murine adult heart. *Stem Cell Rep.*, *1*, 397–410.
- Ulich, T. R., Del Castillo, J., Watson, L. R., Yin, S., & Garnick, M. B. (1990). In vivo hematologic effects of recombinant human macrophage colony-stimulating factor. *Blood*, *75*, 846–850.
- Uygun, A., & Lee, R. T. (2016). Mechanisms of Cardiac Regeneration. *Dev. Cell*, *36*, 362–374.
- Vagnozzi, R. J., Sargent, M. A., Lin, S.-C. J., Palpant, N. J., Murry, C. E., & Molkentin, J. D. (2018). Genetic lineage tracing of Sca-1+ cells reveals endothelial but not myogenic contribution to the murine heart. *Circulation*, *1*.
- Van Amerongen, M. J., Harmsen, M. C., Van Rooijen, N., Petersen, A. H., & Van Luyn, M. J. A. (2007). Macrophage depletion impairs wound healing and increases left ventricular remodeling after myocardial injury in mice. *Am. J. Pathol.*, *170*, 818–829.
- Van Berlo, J. H., Kanisicak, O., Maillet, M., Vagnozzi, R. J., Karch, J., Lin, S. C. J., Middleton, R. C., Marbán, E., & Molkentin, J. D. (2014). C-kit+ cells minimally contribute cardiomyocytes to the heart. *Nature*, *509*, 337–341.
- van der Pouw Kraan, T. C. T. M., Boeijs, L. C. M., Smeenk, R. J. T., Wijdenes, J., & Aarden, L. A. (1995). Prostaglandin-e2 is a potent inhibitor of human interleukin 12 production. *J Exp Med*, *181*, 775–779.

- Van Ramshorst, J., Bax, J. J., Beeres, S. L. M. A., Dibbets-Schneider, P., Roes, S. D., Stokkel, M. P. M., De Roos, A., Fibbe, W. E., Zwaginga, J. J., Boersma, E., Schalij, M. J., & Atsma, D. E. (2009). Intramyocardial bone marrow cell injection for chronic myocardial ischemia: A randomized controlled trial. *JAMA*, *301*, 1997–2004.
- Verreck, F. A. W., de Boer, T., Langenberg, D. M. L., Hoeve, M. A., Kramer, M., Vaisberg, E., Kastelein, R., Kolk, A., de Waal-Malefyt, R., & Ottenhoff, T. H. M. (2004). Human IL-23-producing type 1 macrophages promote but IL-10-producing type 2 macrophages subvert immunity to (myco)bacteria. *PNAS*, *101*, 4560–4565.
- Vigen, R., Maddox, T. M., & Allen, L. A. (2012). Aging of the united states population: Impact on heart failure. *Curr. Heart Fail. Rep.*, *9*, 369–374.
- Voronov, E., Shouval, D. S., Krelin, Y., Cagnano, E., Benharroch, D., Iwakura, Y., Dinarello, C. A., & Apte, R. N. (2003). IL-1 is required for tumor invasiveness and angiogenesis. *PNAS*, *100*, 2645–2650.
- Walsh, S., Pontén, A., Fleischmann, B. K., & Jovinge, S. (2010). Cardiomyocyte cell cycle control and growth estimation in vivo—An analysis based on cardiomyocyte nuclei. *Cardiovasc. Res.*, *86*, 365–373.
- Wan, E., Yeap, X. Y., Dehn, S., Terry, R., Novak, M., Zhang, S., Iwata, S., Han, X., Homma, S., Drosatos, K., Lomasney, J., Engman, D. M., Miller, S. D., Vaughan, D. E., Morrow, J. P., Kishore, R., & Thorp, E. B. (2013). Enhanced efferocytosis of apoptotic cardiomyocytes through myeloid-epithelial-reproductive tyrosine kinase links acute inflammation resolution to cardiac repair after infarction. *Circ. Res.*, *113*, 1004–1012.
- Wang, F., Li, Z., Khan, M., Tamama, K., Kuppusamy, P., Wagner, W. R., Sen, C. K., & Guan, J. (2010). Injectable, rapid gelling and highly flexible hydrogel composites as growth factor and cell carriers. *Acta Biomaterialia*, *6*, 1978–1991.
- Wang, X., Hu, Q., Nakamura, Y., Lee, J., Zhang, G., From, A. H. L., & Zhang, J. (2006). The Role of the Sca-1⁺/CD31[−] cardiac progenitor cell population in postinfarction left ventricular remodeling. *Stem Cells*, *24*, 1779–1788.
- Wang, Z., Collighan, R. J., Gross, S. R., Danen, E. H. J., Orend, G., Telci, D., & Griffin, M. (2010). RGD-independent cell adhesion via a tissue transglutaminase-fibronectin matrix promotes fibronectin fibril deposition and requires syndecan-4/2 and $\alpha 5\beta 1$ integrin co-signaling. *JBC*, *285*, 40212–40229.
- Wang, Z., Collighan, R. J., Pytel, K., Rathbone, D. L., Li, X., & Griffin, M. (2012). Characterization of heparin-binding site of tissue transglutaminase: Its importance in cell surface targeting, matrix deposition, and cell signaling. *JBC*, *287*, 13063–13083.
- Wang, Z., & Griffin, M. (2012). TG2, a novel extracellular protein with multiple functions. *Amino Acids*, *42*, 939–949.
- Warren, L. A., Rossi, D. J., Schiebinger, G. R., Weissman, I. L., Kim, S. K., & Quake, S. R. (2007). Transcriptional instability is not a universal attribute of aging. *Aging Cell*, *6*, 775–782.
- Watari, K., Shibata, T., Kawahara, A., Sata, K. I., Nabeshima, H., Shinoda, A., Abe, H., Azuma, K., Murakami, Y., Izumi, H., Takahashi, T., Kage, M., Kuwano, M., & Ono, M. (2014). Tumor-derived interleukin-1 promotes lymphangiogenesis and lymph node metastasis through M2-type macrophages. *PLoS ONE*, *9*, 1–15.
- Wei, S., Lightwood, D., Ladyman, H., Cross, S., Neale, H., Griffiths, M., Adams, R., Marshall, D., Lawson, A., McKnight, A. J., & Stanley, E. R. (2005). Modulation of CSF-1-regulated post-natal development with anti-CSF-1 antibody. *Immunobiology*, *210*, 109–119.
- Wei, S., Nandi, S., Chitu, V., Yeung, Y.-G., Yu, W., Huang, M., Williams, L. T., Lin, H., & Stanley, E. R. (2010). Functional overlap but differential expression of CSF-1 and IL-34 in their CSF-1 receptor-mediated regulation of myeloid cells. *J. Leukoc. Biol.*, *88*, 495–505.

- Weichhart, T., & Säemann, M. D. (2008). The PI3K/Akt/mTOR pathway in innate immune cells: Emerging therapeutic applications. *ARD*, *67*, 70–74.
- Weisser, S. B., Mclarren, K. W., Voglmaier, N., van Netten-Thomas, C. J., Antov, A., Flavell, R. A., & Sly, L. M. (2011). Alternative activation of macrophages by IL-4 requires SHIP degradation. *Eur. J Immunol.* *41*, 1742–1753.
- White, H. D., & Chew, D. P. (2008). Acute myocardial infarction. *Lancet*, *372*, 570–584.
- Wiktor-Jedrzejczak, W., Bartocci, A., Ferrante, A. W., Ahmed-Ansari, A., Sell, K. W., Pollard, J. W., & Stanley, E. R. (1990). Total absence of colony-stimulating factor 1 in the macrophage-deficient osteopetrotic (op/op) mouse. *PNAS*, *87*, 4828–4832.
- Wilcox, J. N., Smith, K. M., Schwartz, S. M., & Gordon, D. (1989). Localization of tissue factor in the normal vessel wall and in the atherosclerotic plaque. *PNAS*, *86*, 2839–2843.
- Wilkins E., Wilson I., Wickramasinghe K., Bhatnagar P., Leal J., Luengo-Fernandez R., Burns R., Rayner M., & Townsend N. (2017). European cardiovascular disease statistics 2017 edition. *EHN*, 192.
- Willenborg, S., Lucas, T., Van Loo, G., Knipper, J. A., Krieg, T., Haase, I., Brachvogel, B., Hammerschmidt, M., Nagy, A., Ferrara, N., Pasparakis, M., & Eming, S. A. (2012). CCR2 recruits an inflammatory macrophage subpopulation critical for angiogenesis in tissue repair. *Blood*, *120*, 613–625.
- Williams, A. R., & Hare, J. M. (2011). Mesenchymal stem cells: Biology, pathophysiology, translational findings, and therapeutic implications for cardiac disease. *Circ. Res.*, *109*, 923–940.
- Williams, J. W., Giannarelli, C., Rahman, A., Randolph, G. J., & Kovacic, J. C. (2018). Macrophage biology, classification, and phenotype in cardiovascular disease: JACC macrophage in CVD series (Part 1). *J. Am. Coll. Cardiol.* , *72*, 2166–2180.
- Wilson, N. K., Kent, D. G., Buettner, F., Shehata, M., Macaulay, I. C., Calero-Nieto, F. J., Sánchez Castillo, M., Oedekoven, C. A., Diamanti, E., Schulte, R., Ponting, C. P., Voet, T., Caldas, C., Stingl, J., Green, A. R., Theis, F. J., & Göttgens, B. (2015). Combined Single-cell functional and gene expression analysis resolves heterogeneity within stem cell populations. *Cell Stem Cell*, *16*, 712–724.
- Winkels, H., Ehinger, E., Vassallo, M., Buscher, K., Dinh, H. Q., Kobiyama, K., Hamers, A. A. J., Cochain, C., Vafadarnejad, E., Saliba, A. E., Zernecke, A., Pramod, A. B., Ghosh, A. K., Michel, N. A., Hoppe, N., Hilgendorf, I., Zirlík, A., Hedrick, C. C., Ley, K., & Wolf, D. (2018). Atlas of the immune cell repertoire in mouse atherosclerosis defined by single-cell RNA-sequencing and mass cytometry. *Circ. Res.*, *122*, 1675–1688.
- Wollert, Kai C., Taga, T., Saito, M., Narazaki, M., Kishimoto, T., Glembofski, C. C., Vernallis, A. B., Heath, J. K., Pennica, D., Wood, W. I., & Chien, K. R. (1996). Cardiotrophin-1 activates a distinct form of cardiac muscle cell hypertrophy. *JBC*, *271*, 9535–9545.
- Wollert, Kal C., & Drexler, H. (2010). Cell therapy for the treatment of coronary heart disease: A critical appraisal. *Nat. Rev. Cardiol.*, *7*, 204–215.
- Wong, G. G., Temple, P. A., Leary, A. C., Witek-Giannotti, J. A. S., Yang, Y. C., Ciarletta, A. B., Chung, M., Murtha, P., Kriz, R., Kaufman, R. J., Ferenz, C. R., Sibley, B. S., Turner, K. J., Hewick, R. M., Clark, S. C., Yanai, N., Yokota, H., Yamada, M., Saito, M., Takaku, F. (1987). Human CSF-1: Molecular cloning and expression of 4-kb cDNA encoding the human urinary protein. *Science*, *235*, 1504–1508.
- Wu, W. K., Llewellyn, O. P. C., Bates, D. O., Nicholson, L. B., & Dick, A. D. (2010). IL-10 regulation of macrophage VEGF production is dependent on macrophage polarisation and hypoxia. *Immunobiology*, *215*, 796–803.

- Wulf, G. G., Luo, K.-L., Jackson, K. A., Brenner, M. K., & Goodell, M. A. (2003). Cells of the hepatic side population contribute to liver regeneration and can be replenished by bone marrow stem cells. *Hematologica*, *88*, 368-378.
- Wysoczynski, M., Yiru, G., Joseph B., Moore IV Senthilkumar, M., Qianhong, L., Marjan, N., Hong, L., Yibing, N., Wenjian, W., Alex A., T., Xiaoping, Z., Gregory, H., Anna, M. G., Michael J., B., Abdur, K., Xian-Liang, T., & Roberto, B. (2017). Myocardial reparative properties of cardiac mesenchymal cells isolated on the basis of adherence. *J Am Coll Cardiol.*, *69*, 1824–1838.
- Xie, M., Zhang, D., Dyck, J. R. B., Li, Y., Zhang, H., Morishima, M., Mann, D. L., Taffet, G. E., Baldini, A., Khoury, D. S., & Schneider, M. D. (2006). A pivotal role for endogenous TGF-beta-activated kinase-1 in the LKB1/AMP-activated protein kinase energy-sensor pathway. *PNAS*, *103*, 17378–17383.
- Xin, M., Kim, Y., Sutherland, L. B., Murakami, M., Qi, X., McAnally, J., Porrello, E. R., Mahmoud, A. I., Tan, W., Shelton, J. M., Richardson, J. A., Sadek, H. A., Bassel-Duby, R., & Olson, E. N. (2013). Hippo pathway effector Yap promotes cardiac regeneration. *PNAS*, *110*, 13839–13844.
- Xu, J., Kimball, T. R., Lorenz, J. N., Brown, D. A., Bauskin, A. R., Klevitsky, R., Hewett, T. E., Breit, S. N., & Molkentin, J. D. (2006). GDF15/MIC-1 functions as a protective and antihypertrophic factor released from the myocardium in association. *Circ. Res.*, *98*, 342–350.
- Xu, Y., Zhan, Y., Lew, A. M., Naik, S. H., & Kershaw, M. H. (2007). Differential development of murine dendritic cells by GM-CSF versus Flt3 ligand has implications for inflammation and trafficking. *J. Immunol. Res.*, *179*, 7577–7584.
- Xue, J., Schmidt, S. V., Sander, J., Draffehn, A., Krebs, W., Quester, I., DeNardo, D., Gohel, T. D., Emde, M., Schmidleithner, L., Ganesan, H., Nino-Castro, A., Mallmann, M. R., Labzin, L., Theis, H., Kraut, M., Beyer, M., Latz, E., Freeman, T. C., Schultze, J. L. (2014). Transcriptome-based network analysis reveals a spectrum model of human macrophage activation. *Immunity*, *40*, 274–288.
- Yacoub, M. (2015). Cardiac donation after circulatory death: a time to reflect. *The Lancet*, *385*, 2554–2556.
- Yamada, S., & Nomura, S. (2020). Review of single-cell RNA sequencing in the heart. *Int. J. Mol. Sci.*, *21*, 1–15.
- Ye, J., Boyle, A., Shih, H., Sievers, R. E., Zhang, Y., Prasad, M., Su, H., Zhou, Y., Grossman, W., Bernstein, H. S., & Yeghiazarians, Y. (2012). Sca-1 + cardiosphere-derived cells are enriched for isl1-expressing cardiac precursors and improve cardiac function after myocardial injury. *PLoS ONE*, *7*.
- Yeh, R. W., Sidney, S., Chandra, M., Sorel, M., Selby, J. V., & Go, and A. S. (2010). Population trends in the incidence and outcomes of acute myocardial infarction. *NEJM*, 2155–2165.
- Yin, V. P., & Poss, K. D. (2008). New regulators of vertebrate appendage regeneration. *Curr. Opin. Genet. Dev.* *18*, 381–386.
- Yona, S., Kim, K., Wolf, Y., Mildner, A., Varol, D., Breker, M., Strauss-Ayali, D., Viukov, S., Guilliams, M., Misharin, A., Hume, D., Perlman, H., Malissen, B., Zelzer, E., & Jung, S. (2013). Fate mapping reveals origins and dynamics of monocytes and tissue macrophages under homeostasis. *Immunity*, *38*, 79–91.
- Zeyda, M., Farmer, D., Todoric, J., Aszmann, O., Speiser, M., Györi, G., Zlabinger, G. J., & Stulnig, T. M. (2007). Human adipose tissue macrophages are of an anti-inflammatory phenotype but capable of excessive pro-inflammatory mediator production. *Int J Obes*, *31*, 1420–1428.
- Zhang, B., Zhang, J., Zhu, D., & Kong, Y. (2019). Mesenchymal stem cells rejuvenate cardiac muscle after ischemic injury. *Aging*, *11*, 63–72.

- Zhang, D. S., Piazza, V., Perrin, B. J., Rzadzinska, A. K., Poczatek, J. C., Wang, M., Prosser, H. M., Ervasti, J. M., Corey, D. P., & Lechene, C. P. (2012). Multi-isotope imaging mass spectrometry reveals slow protein turnover in hair-cell stereocilia. *Nature*, *481*, 520–524.
- Zhang, J.-M., & An, J. (2007). Cytokines, inflammation and pain. *Int Anesthesiol Clin.*, *45*, 27–37.
- Zhang, L., Sultana, N., Yan, J., Yang, F., Chen, F., Chepurko, E., Yang, F.-C., Du, Q., Zangi, L., Xu, M., Bu, L., & Cai, C.-L. (2018). Cardiac Sca-1+ cells are not intrinsic stem cells for myocardial development, renewal, and repair. *Circulation*, 2919–2930.
- Zhang, Xia, Goncalves, R., & Mosser, D. M. (2008). The isolation and characterization of murine macrophages. *Curr Protoc Immunol*, *9*, 177–180.
- Zhang, Xiaodong, Heckmann, B. L., Campbell, L. E., & Liu, J. (2017). G0S2: A small giant controller of lipolysis and adipose-liver fatty acid flux. *Biochim. Biophys. Acta - Mol. Cell Biol. Lipids*, *1862*, 1146–1154.
- Zhang, Yu, Cao, N., Huang, Y., Spencer, C. I., Fu, J. D., Yu, C., Liu, K., Nie, B., Xu, T., Li, K., Xu, S., Bruneau, B. G., Srivastava, D., & Ding, S. (2016). Expandable cardiovascular progenitor cells reprogrammed from fibroblasts. *Cell Stem Cell*, *18*, 368–381.
- Zhang, Yuelin, Liang, X., Liao, S., Wang, W., Wang, J., Li, X., Ding, Y., Liang, Y., Gao, F., Yang, M., Fu, Q., Xu, A., Chai, Y. H., He, J., Tse, H. F., & Lian, Q. (2015). Potent paracrine effects of human induced pluripotent stem cell-derived mesenchymal stem cells attenuate doxorubicin-induced cardiomyopathy. *Sci. Rep.*, *5*, 1–17.
- Zhang, Z., Egaña, J. T., Reckhenrich, A. K., Schenck, T. L., Lohmeyer, J. A., Schantz, J. T., MacHens, H. G., & Schilling, A. F. (2012). Cell-based resorption assays for bone graft substitutes. *Acta Biomater.*, *8*, 13–19.
- Zheng, S. X., Weng, Y. L., Zhou, C. Q., Wen, Z. Z., Huang, H., Wu, W., Wang, J. F., & Wang, T. (2013). Comparison of cardiac stem cells and mesenchymal stem cells transplantation on the cardiac electrophysiology in rats with myocardial infarction. *SCRR*, *9*, 339–349.
- Zheng, W., Nurmi, H., Appak, S., Sabine, A., Bovay, E., Korhonen, E. A., Orsenigo, F., Lohela, M., D'Amico, G., Holopainen, T., Leow, C. C., Dejana, E., Petrova, T. V., Augustin, H. G., & Alitalo, K. (2014). Angiopoietin 2 regulates the transformation and integrity of lymphatic endothelial cell junctions. *Genes Dev.*, *28*, 1592–1603.

Appendix

Table A1 Summary of the key findings of the Sca1 fate-mapping papers

Mouse Model	Experimental design	Key findings and comments	Reference
Research articles			
Sca1 ^{H2B;TdT/+} Nkx2.5 ^{H2B;GFP/+}	Early cardiogenic marker Nkx2.5 tested by FACS: P30-P180 (15- to 30-day intervals between stages)	No double-positive cells were found	(Zhang et al., 2018)
Sca1 ^{H2B;TdT/+} cTnT ^{H2B;GFP/+}	Differentiated CMs cTnT tested by FACS: P30-P180 (15- to 30-day intervals between stages)	No double-positive cells were found	
Sca1 ^{nLacZ;H2B;GFP/+} Tie2 ^{Cre}	Tie2, endothelial-specific mice; co-localisation with CD31 ⁺ cells. Immunostaining.	Sca1 ⁺ cells were purely Tie2 endothelial lineage.	
Sca1 ^{mCm/+} cTnT ^{nLacZ;H2B;GFP/+} ROSA26R ^{TdT/+}	Post-injury: LAD ligation. Immunostaining.	Ten cells (=0.001% of total CMs) were found in the heart at 30, 60, 120 dps	
Sca1 ^{nLacZ;H2B;GFP/+} Tie2 ^{Cre}	Post-injury: LAD ligation. Immunostaining.	Sca1 ⁺ cells were distributed in the border zone and infarct area at 3 to 30 dps. Sca1 ⁺ cells maintained endothelial features after injury.	
Ly6a ^{+Cre} R26 ^{TdT}	Developmental. Postnatal day 1 (P1) versus 1.5 months. Immunostaining.	Sca1 ⁺ cells generated cardiac vasculature. The vast majority of TdT ⁺ cells were vascular endothelial CD31 ⁺ .	(Vagnozzi et al., 2018)
	Ageing: 3 months. FACS.	70% of Sca1 ⁺ were CD31 ⁺ TdT ⁺ ; 8-9% of Sca1 ⁺ were CD31 ⁻ TdT ⁺ . CMs: 0.0003%	
Ly6a ^{+mCm} R26 ^{eGFP}	Ageing/Post-MI remodelling analysis by immunohistochemistry: 3 months	Percentage of eGFP ⁺ cells were 80% in Sca ⁺ CD31 ⁺ and 10% in Sca ⁺ CD31 ⁻ cells. CMs: 0.002%.	
	Ageing/Post-MI remodelling analysis by immunohistochemistry: Post-MI	Mostly CD31 ⁺ endothelial cells were eGFP ⁺ .	

Research Letters			
Sca1 ^{mCm} R26 ^{TdT}	MI performed after seven days of Tam treatment: 6 months. Immunostaining.	Very low Sca1 ⁺ cell-derived CMs were detected (TdT ⁺ CMs found: 0.0002% at base line; 0.007% post-MI), compared to the higher number of Sca1 ⁺ cell-derived endothelial cells	(Neidig et al., 2018)
Sca1 ^{2A} -CreER	Pulse Tam-induction. Self-cleaving peptide sequence between endogenous Sca1 and inducible Cre-recombinase. Heart collection within 48hrs. FACS, immunostaining, and Z-stack confocal images.	95% of TdT ⁺ were VEcad ⁺ cells. 67% of VEcad ⁺ TdT ⁺ cells were Sca1 ⁺ cells. Sca1 ⁺ cells were VEcad ⁺ EC.	(Tang et al., 2018)
	Homeostasis.	60% of EC were TdT ⁺ . 95% of them were CD31 ⁺ .	
	1,4, 6 weeks post-MI.	Sca1 ⁺ cells differentiated into EC and fibroblast, but not cardiomyocytes. No TdT ⁺ CMs (TNNI3 ⁺). 65% VEcad ⁺ cells were TdT ⁺ . 91% of TdT ⁺ cells were VEcad ⁺ . TdT ⁺ PDGFR α ⁺ cells in: infarct (7%), border (5%), remote regions (2%).	
ACT ^{egGFP} MHC ^{nLac}	100,000 Sca1 ⁺ EGFP ⁺ Lin ⁻ cells were isolated via FACS and injected into the infarct border zone of nontransgenic mice post-MI. Immunostaining.	In 30 engrafted hearts, 88,062 EGFP ⁺ donor cells were tested, and no CMs arose from transplanted Sca1 ⁺ cells.	(Soonpaa et al., 2018)

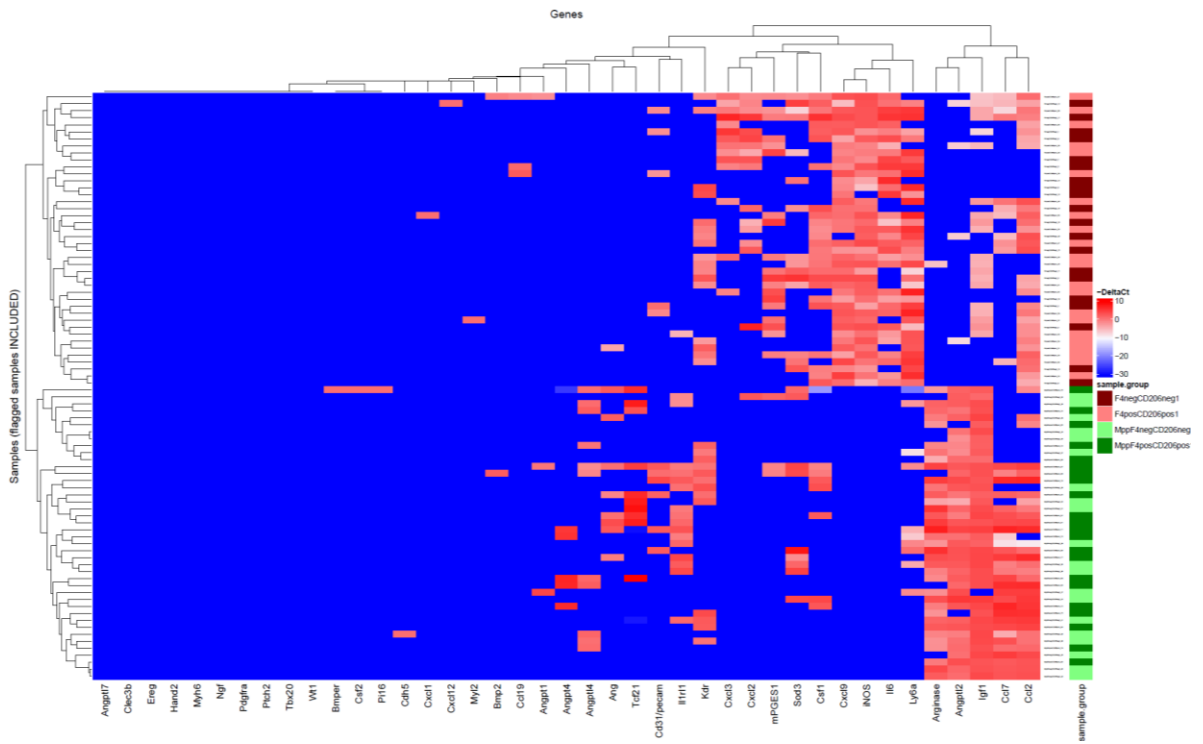


Figure A1. Result I: Full heatmap.

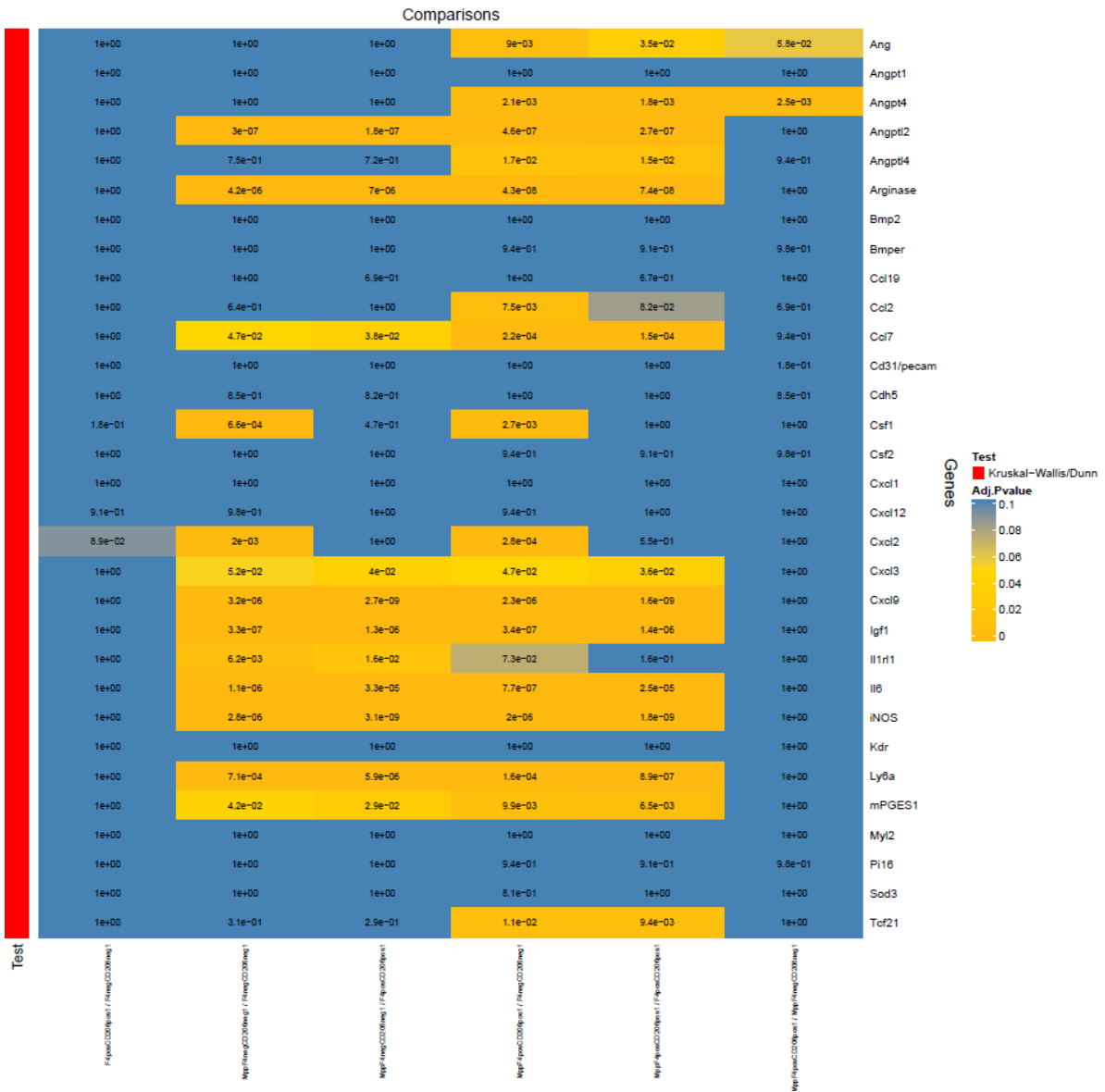


Figure A2. Result I: p-values heatmap.